Prostate cancer targeting using replication-selective adenoviruses in combination with phytochemicals

Adam, Virginie Sarah

Prostate cancer targeting using replication-selective adenoviruses in combination with phytochemicals

Virginie Sarah Adam

A thesis submitted for the degree of Doctor of Philosophy

July 2009

Viral Gene Therapy Group
Centre for Molecular Oncology and Imaging
Institute of Cancer
Barts and The London School of Medicine and Dentistry
Queen Mary, University of London
Charterhouse Square
London
United Kingdom

Declaration

The work presented in this thesis was done by the author, Virginie Sarah Adam, at the Centre for Molecular Oncology and Imaging, Institute of Cancer, Barts and The London School of Medicine and Denistry, Queen Mary, University of London. All external sources have been properly acknowledged.

Acknowledgements

I would like to express my appreciation and heartfelt gratitude to the people who supported me during my PhD, because without them I would not have gotten very far…

I would like to thank the members of Gunnel's team, past and present, and in particular Dr Siew Chiat Cheong, who taught me so many precious things, always with patience and inspiration, and Katrina Sweeney and Enrique Miranda, for being there to help me in (and out of) the lab. I would like to thank Dr Daniel Öberg for his time and endless supply of encouragement, ideas and advice, I really appreciate it. I am also grateful to Sabari Vallath, for helping me with flow cytometry and confocal microscopy, and especially for his friendship. Thanks to Chris Binny, Ginevra Botta, Dr Gioia Cherubini and Lynda Coughlan for interesting and stimulating scientific discussions. I have also had the privilege of supervising two graduate students, Alan Holford and Latifa Sultana, who produced great data and were lovely to work with. Thank you.

I am very thankful to Professor Nick Lemoine for the opportunity to work in such a fantastic institute with such fantastic people; thank you to all my colleagues from Molecular Oncology and Tumour Biology, it has been a pleasure working with you and getting to know you.

I am extremely grateful to my family, who always believed in me and helped me in every way they could. Special thanks also to my friends for their support and understanding, particularly during my final year.

Finally, I would like to thank my supervisor, Dr. Gunnel Halldén, who gave me priceless counsel, provided with equal measures of honesty, enthusiasm and laughter. Through her guidance, I gained confidence in my scientific capabilities and judgment, and this has shaped me into the scientist I am now. I will always remember my time as her PhD student with pleasure and I am deeply indebted to her.

Abstract

Oncolytic adenoviral mutants have demonstrated good safety profiles but, despite some encouraging clinical results, efficacy as a single agent was limited. Combinations with conventional chemo- or radiotherapy significantly enhanced the anti-tumour effect.

We investigated the possibility of enhancing prostate cancer (PCa) cell killing using adenovirus type 5 (Ad5) with phytochemicals. Phytochemicals are chemopreventive and can modulate intracellular signalling pathways, including the mitogen-activated protein kinase (MAPK) pathway which regulates the expression of the coxsackie-adenovirus receptor (CAR).

Equol and resveratrol synergistically enhanced cell death in both androgen receptor (AR)-positive and AR-negative PCa cell lines. On the other hand, curcumin, epigallocatechin-gallate (EGCG) and genistein had either synergistic and antagonistic responses with Ad5, depending on the dose and timing of addition. We therefore decided not to pursue the use of these compounds.

Although we found that equol and resveratrol increased adenoviral receptor expression and viral uptake, this was not paralleled by enhanced viral replication. Treatment of DU145 and PC-3 cells with equol or resveratrol decreased viral titres, but did not block cell cycle progression. E1A expression in these cells was lower at 18h post-infection, but levels were normal by 72h. The exact mechanism behind the repression of adenovirus replication remains unclear.

Equol and resveratrol induced moderate apoptotic responses. Mitochondrial membrane depolarization and caspase-3 activation were further increased by the addition of Ad5 in DU145 and PC-3 cells, but was reduced in 22Rv-1 cells. Caspase inhibition could not prevent sensitisation of 22Rv-1 cells to combination-induced cell death. The involvement of additional cell death mechanisms was therefore considered. Equol and resveratrol triggered autophagy while Ad5 acted as an autophagy repressor. Modulation of autophagy using pharmacological inducers and repressors indicates that autophagy may play a protective role in AR-negative cell lines.

Abbreviations

3-MA: 3-methyladenine

5-FC: 5-fluorocytosine

5-FU: 5-fluorouracil

Ab: antibody

Abs: absorbance

Ad5: adenovirus type 5

ADP: adenovirus death protein

AR: androgen receptor

ARE: androgen-responsive element

ATCC: American Type Tissue Culture Collection

BSA: bovine serum albumin

BP: binding protein

CAB: combined androgen blockade

CAR: coxsackie and adenovirus receptor

CCI-779: an ester of rapamycin

CD: cytosine deaminase

CDK: cyclin-dependent kinase

CI: combination index

CMV: cytomegalovirus promoter

Cox-2: cyclooxygenase 2

CPE: cytopathic effect

CR: conserved region

CtBP: C-terminal binding protein

CTL: cytotoxic T-lymphocyte

DES: diethylstilbestrol

DHT: dihydrotestosterone

DMEM: Dulbecco's modified Eagle's medium

DNA: deoxyribonucleic acid

EC_{50}: effective concentration required to kill 50% of cells

ECM: extracellular matrix

EGCG: epigallocatechin-gallate

EGFR: epithelial growth factor receptor

eIF: eukaryotic initiation factor

ER: estrogen receptor

ERK: extracellular-regulated kinase

FCS: foetal calf serum

GFP: green fluorescent protein

GnRH: gonadotrophin releasing hormone

h: hours

HDAC: histone deacetylase

HIV: human immunodeficiency virus

HRPC: homone-refractory prostate cancer

HS-GAG: heparan sulfate glycosaminoglycans

i.p.: intra-peritoneal

i.t.: intra-tumoural

i.v.: intra-venous

ITR: inverted terminal repeat

kD: kiloDalton

LHRH: luteinising hormone releasing hormone

MAPK: mitogen-activated protein kinase

MEC: Multiethnic Cohort Study

MEK: MAPK kinase

min: minutes

MMP: matrix metalloprotease

MOI: multiplicity of infection

mRNA: messanger RNA

MTOC: microtubule organising centre

mTOR: mammalian target of rapamycin

N: number of times an experiment was repeated

NAD: nicotinamide adenine dinucleotide

NFκB: nuclear factor κB

NK: natural killer cells

NPC: nuclear pore complex

OD: optical density

orf: open reading frame

PCa: prostate cancer

PCD: programmed cell death

PCR: polymerase chain reaction

pfu: plaque-forming units

PI3K: phosphoinositide-3 kinases

PKR: protein kinase R

ppc: particles per cell

pRb: retinoblastoma protein

PSA: prostate specific antigen

PTEN: phosphatase and tensin homologue protein

qPCR: quantitative PCR

RAD001: a chemotherapeutic analogue of rapamycin, also known as Everolimus

Rheb: Ras homolog enriched in brain protein

RIP1: receptor interactive protein 1

RGD: arginine-glycine-aspartic acid motif

RTK: receptor tyrosine kinase

RNA: ribonucleic acid

ROS: reactive oxygen species

rpm: revolutions per minute

s: seconds

SD: standard deviation

SDS: sodium dodecyl sulphate

SIR2: silent information regulator-2

Sirt1: the human homologue of SIR2

SRC-1: steroid receptor coactivator-1

$TCID_{50}$: tissue culture inhibitory dose 50%

TF: transcription factor

tk: thymidine kinase

TMRE: tetramethylrhodamine

TNF: tumour necrosis factor

TNF-R: tumour necrosis factor receptor

TRAIL: TNF-related apoptosis-inducing ligand

TRAMP: transgenic adenocarcinoma of the mouse prostate

TSC: tuberous sclerosis complex proteins

UV: ultraviolet

VA: virus associated RNA

wt: wild type

Contents

1 Introduction

1.1 Prostate cancer

1.1.1 Etiology

Prostate cancer (PCa) is the most common cancer in men worldwide after lung cancer (Ferley *et al.*, 2004). Around 30,000 cases are diagnosed in the UK each year and a third of all patients die from it. Prostate cancer incidence increases with age. Prevalence among men in their 50's is 30% but this increases to 80% among those in their 70's (Breslow *et al.*, 1977). Prostate cancer can often be detected by autopsy in elderly men having died of other causes. This reflects the disease's slow progression and demonstrates its high prevalence in Western countries.

The incidence and mortality for prostate cancer vary widely across different regions of the world (Damber & Aus, 2008). Incidence is lowest in Asia, whereas it is high in Europe and North America. Autopsy studies have revealed that the incidence of 'latent' carcinoma does not differ significantly from country to country. Although the frequency and accuracy of diagnosis may vary across the globe, it is thought that the differences in PCa incidence do not reflect differences in initiation but rather differences in exposure to environmental factors that affect the conversion of histopathologically apparent lesions to clinically-relevant tumours (Dewailly *et al.*, 2003). The worldwide variation in PCa incidence is also linked to individual genetic background that render men more or less susceptible to protective or risk factors. The Multiethnic Cohort (MEC) Study found that the risk of PCa is approximately double in African-American men compared to their Caucasian counterparts (Kolonel *et al.*, 2004). Prostate cancer susceptibility has recently been linked to genetic variants on chromosome 8q24, although the genes encoded by this region are currently unknown (Gudmundsson *et al.*, 2007).

Apart from age and ethnic background, the only other well-established risk factor for PCa is family history. Almost a quarter of prostate cancers occurs in family clusters, so men with a first degree relative affected by prostate cancer are twice to three times as likely to suffer from the disease. About 9% PCa cases can be attributed to hereditary PCa and segregation analyses suggest that this is at least partly due to the inheritance of an autosomal dominant susceptibility trait (Shand & Gelmann, 2006). Genetic polymorphisms have also been reported in several genes such as those encoding the androgen receptor (AR), 5α-reductase and steroid hydroxylase, which are involved in androgen metabolism.

Environmental factors also contribute to PCa initiation. This is supported by the observation that Japanese men living in the USA have a higher risk of developing PCa compared to their counterparts living in Japan, a country which traditionally has very low rates of PCa, although the numbers are increasing as lifestyles become more 'Westernised' (Sim & Cheng, 2005). A high intake of saturated fats has been correlated with an increased risk of PCa, which may account for the high incidence in Western countries, where people consume more food products rich in saturated fats. Other risk factors are vitamin D deficiency and high plasma levels of insulin-like growth factor-1 (IGF-1). Protective habits include a high soy intake, which is part of the traditional Asian diet, and a diet rich in tomatoes, which are a source of lycopene (Kurahashi *et al.*, 2007; Sonn *et al.*, 2005).

1.1.2 Diagnosis

In many Western countries, including the USA, screening programmes are in place for men above 50 to detect PCa at the earliest possible stage. Screening is usually done by determining serum levels of prostate-specific antigen (PSA), which is a biomarker for PCa progression. In the UK, patients with a family history of PCa can be offered a PSA test, and symptomatic patients can also be diagnosed by digital rectal examination (DRE) to determine local staging (T staging) and enable estimation of the presence of extracapsular extension of the tumour.

Following a positive PSA test (usually PSA > 4ng/ml), patients may be advised to undergo a biopsy to evaluate the cancer grade (Damber & Aus, 2008). The most commonly used system is the Gleason score. The score of a tumour is the sum of the two most common histological patterns (grades 1-5) of tumour growth and can range from 2 (least aggressive) to 10 (most aggressive).

If the patient does not suffer from additional symptoms and is in the 'low risk' group (PSA <10ng/ml, Gleason score < 5, disease stage T1c-2a) or if the patient's natural life expectancy <10 years, the recommended cancer management strategy is commonly 'active surveillance'. This simply involves close monitoring for any further increases in PSA levels or prostate size, as, at this stage, the risks of surgery or radiation out-weigh the benefits.

1.1.3 Treatment of locally-restricted PCa

Men with poorly differentiated tumours and short PSA doubling-time, especially those with a longer life expectancy, are offered treatment with a curative intent. Prostatectomy is highly effective for locally restricted cancer and reduces PSA to non-detectable levels. Alternatively,

radiotherapy is also effective in reducing PSA levels. Novel delivery routes have been developed to minimise damage to surrounding tissue, including Intensity-Modulated Radiation Therapy (IMRT), Image-Guided Radiation Therapy (IGRT) and brachytherapy.

Patients with extracapsular extensions of the tumour can be offered high-dose radiotherapy, often in combination with hormonal therapy, but are less likely to benefit from radical prostatectomy due to the difficulties in obtaining a disease-free margin of resection.

1.1.4 Treatment of advanced hormone-responsive PCa

If the cancer is not detected during its early stage, it commonly metastasizes to the lymph nodes and then to the vertebrae, pelvis or ribs, causing acute bone pain, requiring second-line treatment. Therapy for advanced, metastatic PCa initially involves hormonal treatment, followed by combinations of radiotherapy and/or chemotherapy. Patients whose PSA levels continue to rise after primary surgery and/or radiotherapy are also give hormone therapy, although if there are no symptoms and the rise in PSA occurs more than a year after initiation of treatment with a long PSA doubling-time, providing that the cancer was not aggressive on presentation (Gleason score < 8), active surveillance may offer the best quality of life. All treatments cause significant side effects and choice of therapy therefore depends on prognosis, patient life expectancy and their general health.

Effective treatment for metastatic cancer by ‘chemical castration’ was developed in the 1950s by Charles Huggins, using the xenoestrogen diethylstilbestrol (DES) to inhibit the synthesis of androgens via inhibition of the hypothalmamic-pituitary axis.

The theory behind hormonal treatment is based on the requirement of prostate cells for androgen stimulation via the androgen receptor (AR), without which these cells stop proliferating and die. Androgens are secreted by the testes, the adrenal glands and the prostate itself. The main androgen hormone is testosterone, which can be converted by 5-α-reductase to dihydrotestosterone (DHT) in prostate cells. DHT has a higher affinity for the AR than testosterone and is more potent.

Androgen production is regulated by endocrine stimulation from the hypothalamus via the pituitary gland (Figure 1). Gonadotrophin releasing hormone (GnRH) is normally released in pulses from the hypothalamus, stimulating pulsatile release of follicle-stimulating hormone (FSH) and luteinising hormone (LH), the latter stimulating production of testosterone by the Leydig cells in the testes.

In order to abort prostate cancer growth, GnRH agonists (eg: goserelin, leuprolide) can be used to inhibit downstream stimulation of testosterone production (Hellerstedt & Pienta, 2002; Miyamoto *et al.*, 2004). These drugs initially trigger a surge in FSH and LH (the 'flare effect'), but the long-term result is a down-regulation of the GnRH receptor in the pituitary, reduced FSH and LH, and a concomitant decrease in testosterone production. The flare effect can be avoided using GnRH antagonists (eg: abarelix) to directly inhibit GnRH. The hormonal loop can also be interrupted with nonsteroidal antiandrogens (eg: flutamide, bicalutamide) which interact directly with the AR and competitively inhibit binding by androgens. However, 10% of circulating testosterone remains if antiandrogens are used as monotherapy, due to the conversion of adrenal steroids to testosterone. It is therefore common to treat patients with combined androgen blockade (CAB) with a GnRH agonist plus a nonsteroidal antiandrogen, although this is associated with more significant side-effects. If the patient experiences spinal cord compression and bone pain, they may be offered orchidectomy to abolish circulating testosterone levels as quickly as possible. Androgen ablation therapy may also be prescribed before (neoadjuvant) or after (adjuvant) prostatectomy or radiotherapy (Miller *et al.*, 2009).

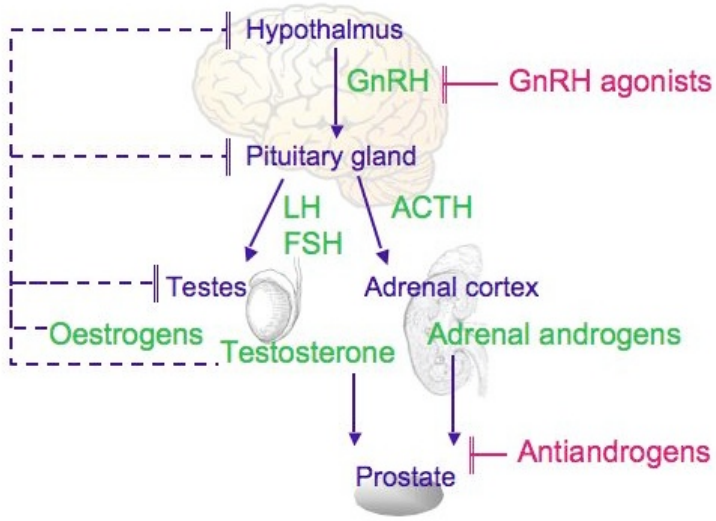

Figure 1 Androgen hormonal feedback

Stimulation shown by arrows, negative feedback represented by dashed lines. Hormones shown in green, gonadotrophin releasing-hormone (GnRH), luteinising hormone (LH), follicle-stimulating hormone (FSH), adrenocorticotrophic hormone (ACTH). Hormone ablation drugs shown in pink.

Hormone ablation therapy causes various side-effects including loss of libido, cardiovascular events, hot flushes, osteoporosis, impotence, gynecomastia, weight gain, fatigue, anaemia, muscle atrophy and loss of cognitive function (Hellerstedt & Pienta, 2002). The combination of an oestrogen with a GnRH agonist may reduce these effects. Antiandrogens are associated

with rare but occasionally fatal hepatotoxicity and patients with pre-existing liver conditions should therefore be carefully monitored.

1.1.5 Progression to androgen-resistance

In around 15% of patients, mostly those with high-grade metastatic tumours, hormone ablation therapy does not produce any clinically meaningful response (Hamdy & Thomas, 2001). In responsive patients, androgen blockade results in a rapid inhibition of growth, followed by tumour regression. Serum PSA levels are rapidly reduced and cancer-related symptoms are decreased. However, the selection pressure of androgen starvation results in clonal expansion of androgen resistant cells from the initial heterogenous cancer cell population (Craft *et al.*, 1999; Tso *et al.*, 2000). This inevitable progression to hormone-refractory prostate cancer (HRPC) occurs within 18 – 24 months after beginning hormone therapy.

The most common hypothesis postulated to explain this is that a pre-existing abnormal AR is clonally selected. An equally valid hypothesis is that cancer treatments create conditions favouring the development of AR mutations which provide a survival advantage to the PCa cells, allowing their propagation. These explanations are not mutually exclusive. In addition, PCa cells develop AR-independent stimulatory pathways involving stimulation by growth factors and anti-apoptotic feedback, weaning the cells off the need for androgen stimulation (Figure 2).

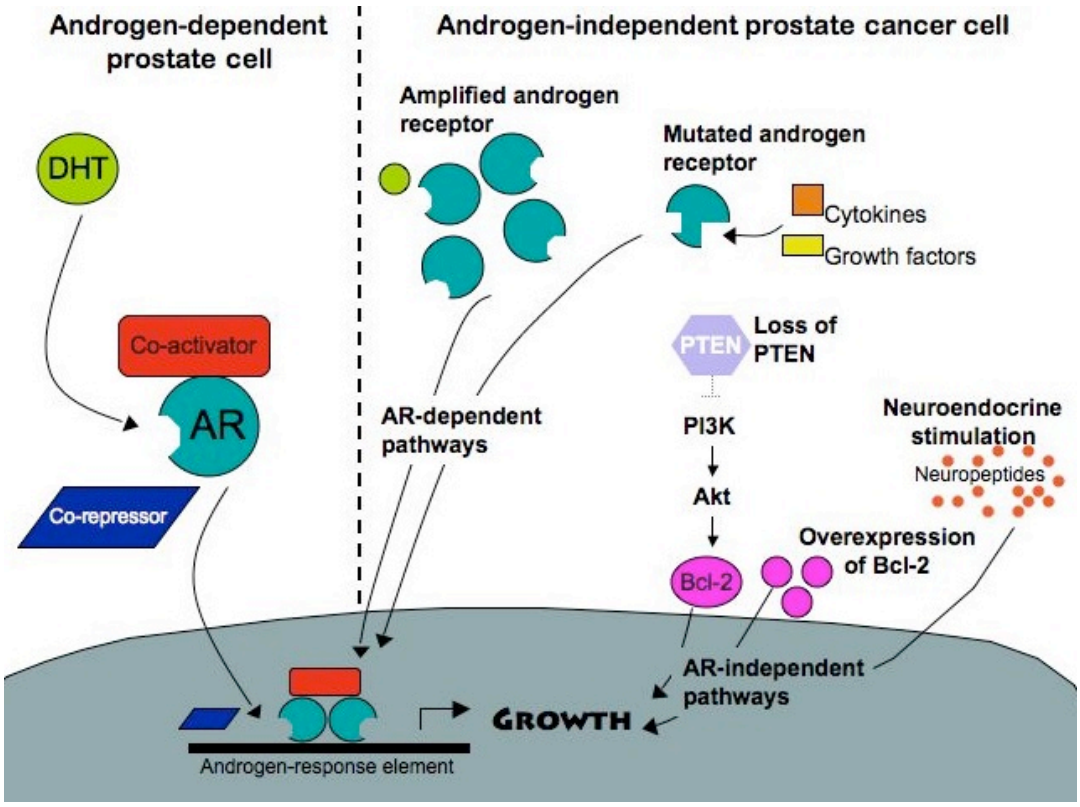

Figure 2 Androgen-dependent and –independent pathways involved in PCa progression

In androgen-dependent PCa, the tumour cells depend on androgen stimulation for growth. At this stage, androgen deprivation and hormonal treatment are therefore effective. However, androgen-resistance develops as the cells acquire growth stimulation from abnormal AR signalling and other pathways bypassing the AR.

The androgen receptor is a transcription factor belonging to the nuclear receptor superfamily. Although it normally resides in the cytoplasm, it homodimerises and translocates to the nucleus upon ligand binding. There, it mediates transcription of target genes containing androgen-response elements (ARE). Activation of the AR in the cytoplasm is kept in check by phosphorylating kinases and its transcriptional effect in the nucleus is modulated by coregulators (Heinlein & Chang, 2002).

A proposed mechanism for AR hyperactivation is AR gene amplification. This has been observed in a third of androgen-independent tumours (Linja *et al.*, 2001; Visakorpi *et al.*, 1995). In these studies, none of the samples collected prior to hormone ablation therapy from the same patients showed AR gene amplification. This implies the androgen blockade has a causative role.

Other studies have found that 50% of advanced PCa samples exhibit mutations in the AR gene (Marcelli *et al.*, 2000a; Suzuki *et al.*, 1993; Taplin *et al.*, 1999). Most mutations appear in the ligand-binding domain of the receptor, causing decreased receptor affinity and sensitivity. This

results in a 'promiscuous' receptor that can be activated by non-specific ligands such as estrogens, progestins and even anti-androgens. The growth of prostate cells is thus triggered by inappropriate stimuli. Mutations may also render the AR constitutively active and androgen-independent.

Another abnormality detected in androgen-resistant prostate cancer tissue samples is the overexpression of AR coactivators, such as steroid receptor coactivator-1 (SRC-1) and transcriptional intermediary factor-2 (TIF-2) (Fujimoto *et al.*, 2001; Gregory *et al.*, 2001). Receptor coactivators function by enhancing the transcriptional activity of activated AR, or by lowering the AR activation threshold.

AR activity can also be deregulated by the abnormal functioning of AR corepressors. Corepressors are proteins that reduce target gene transcription without altering basal transcription rates. For example, Hey1 is a downstream mediator of Notch signalling that directly interacts with SRC1 and AR to specifically repress transcription from AR-dependent promoters. Immunohistochemical analysis of cancer samples has demonstrated that Hey1 is often excluded from the nucleus in PCa (Belandia *et al.*, 2005).

Mutations in other genes, such as the tumour suppressor Phosphatase and Tensin Homologue (PTEN), can also affect AR activity. PTEN is a tumour suppressor which interrupts PI3K activation of Akt, thereby decreasing the overall flux through the PI3K pathway. PTEN has been shown to repress the transcriptional activity of AR (Li *et al.*, 2001). It is often lost in advanced PCa and this correlates with higher Gleason score and clinical stage (Cairns *et al.*, 1997).

In addition to abnormalities involving the AR, other growth-stimulating mechanisms may play a role in androgen-resistant PCa. For example, survival proteins are often abnormally active due to over-expression or mutations. The insulin-like growth factor (IGF) pathway is commonly hyperactive in androgen-independent tumours. In normal cells, the pathway is 'off' as IGF-1 is bound by insulin-like growth factor binding protein -3 (IGFBP-3). However, in PCa, IGFBP-3 is down-regulated such that unbound IGF-1 triggers downstream Mitogen-Activated Protein Kinase (MAPK) and phosphatidyl-inositol-3-OH kinase (PI3K) pathways, preventing apoptosis and promoting survival (Meinbach & Lokeshwar, 2006). IGF signalling has also been shown to affect AR cellular localization and stimulate transcriptional activity (Wu *et al.*, 2006).

Similarly, fibroblast growth factors (FGFs) and their receptors (FGFR) have been found to be overexpressed in prostate tumours with high Gleason grade (Gowardhan *et al.*, 2005). Fibroblast growth factor signalling induces the MAPK pathway, enabling cell survival, proliferation and angiogenesis. Also, increased expression of the epidermal growth factor receptor ErbB1 has recently been correlated with progression to androgen resistance (Shah *et al.*, 2006).

Advanced PCa also exhibit deregulated apoptotic responses that arise in response to hormone ablation treatment. Bcl2 inhibits cell death and contributes to hormone ablation resistance (Raffo *et al.*, 1995). The overexpression of the anti-apoptotic protein Bcl-x_L correlates with onset of androgen-resistance and is associated with higher Gleason scores (Castilla *et al.*, 2006). Bcl-x_L exerts its anti-apoptotic effect by binding to and inhibiting the effect of the pro-apoptotic protein Bax. Another anti-apoptotic protein, clusterin, has also been show to be instrumental in androgen resistance and many efforts are being made to develop a therapeutic anti-sense oligonucleotide targeting this protein (Miyake *et al.*, 2006). Heat shock protein-27 (Hsp27) modulates Signal Transducer and Activator of Transcription-3 (STAT-3)-mediated apoptosis after metastasis and is another potential therapeutic target (Rocchi *et al.*, 2005).

Finally, neuroendocrine differentiation (NED) provides PCa cells with another source of growth stimulatory signals. The normal benign epithelial prostate compartment includes neuron-like neuroendocrine (NE) cells. In high grade and high stage tumours, the number of these cells increases, especially in hormonally-treated, androgen-independent tumours. The NE cells secrete neuropeptides, such as chromogranin, which act in a paracrine fashion on neighbouring non-NE tumour cells to stimulate their survival and proliferation. The PI3K-Akt-mTOR pathway has recently been shown to be critically involved in NED (Wu & Huang, 2006).

1.1.6 Management of androgen resistant cancers

PCa is considered androgen-resistant when patients have >25% increase in PSA levels to a value of ≥ 5ng/ml despite castration levels of testosterone (<50ng/ml). The estimated median survival ranges from 24 – 68 months, depending on the presence of skeletal metastases which is associated with poor prognosis (Oefelein *et al.*, 2004).

Patients with HRPC have limited treatment options beyond the addition of other antiandrogens. Chemotherapy has generally been ineffective in providing a survival advantage or in alleviating symptoms, so HRPC is usually considered a chemoresistant disease.

Mitoxantrone and docetaxel are now commonly used because, although survival benefits of monotherapy are not significant, the chemotherapeutic drugs can reduce the duration and intensity of pain associated with HRPC. A number of clinical trials have shown stabilization of disease and decreased PSA levels by combinations of docetaxel or mitoxantrone with estramustine, prednisolone, dexamethasone (Chang & Kibel, 2009). Novel targeted therapeutics currently in clinical trials include calcitriol (the biologically active form of vitamin D), bevacizumab (an anti-angiogenic monoclonal antibody against vascular endothelial growth factor) and thalidomide (an anti-angiogenic agent which inhibits platelet-derived growth factor and TNF).

In conclusion, androgen deprivation is usually initially a very successful treatment that leads to tumour size reduction. However, PCa inevitably progresses to androgen-independence via the acquisition of various abnormal characteristics including mutations of the AR, co-regulators, tumour suppressors, growth factors and survival factors. Androgen-insensitive cancers are currently incurable since resistance to other treatments such as chemotherapy and radiotherapy also develops. Consequently, innovative therapies need to be developed to treat patients suffering from advanced, androgen-independent, and metastatic forms of the disease. Novel treatments curtailing cancer progression to the androgen-resistant state, or reversing the process, would also be of immense value. These goals require greater in-depth understanding of the mechanisms of PCa in order to design targeted therapies.

1.2 Adenovirus type 5

1.2.1 Adenovirus structure

Adenoviruses (Ad) are icosahedral, double-stranded DNA viruses first isolated in 1953 which can infect humans and animals (Shenk, 2001). With a diameter of 60-90nm, they are the largest non-enveloped viruses able to infect cells via the endosome, and not requiring membrane fusion. Adenoviral particles consist of the viral genome encapsulated by a protein shell (Figure 3). The main components of the capsid are the 240 hexon homotrimers and 12 pentameric penton bases at the apices (Russell, 2009). Trimeric fibres, consisting of a tail, shaft and knob region, extend from each penton. Penton is also associated with five copies of polypeptide IIIa at its base. Proteins VI and VIII are minor capsid proteins which bind hexon on the inner side of the capsid, while IX is located externally and acts to 'cement' and stabilise the capsid. The 36kb linear viral genome is contained within the capsid together with the viral protease, and is packaged by the core proteins, mu, IVa2, V and VII, which ensure its availability for transcription and subsequent packaging. The 5' DNA termini are bound by two terminal proteins (pTPs) which act as protein primers during replication.

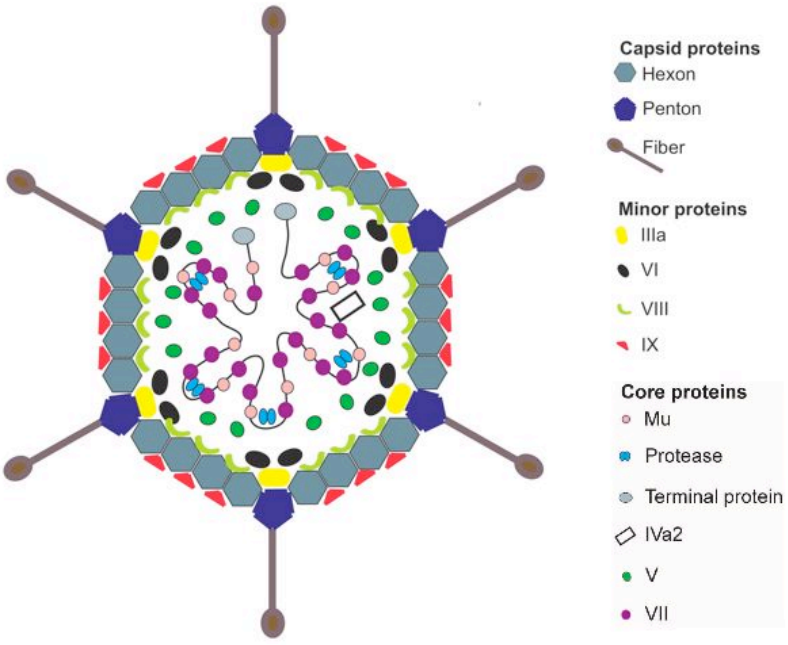

Figure 3 Adenovirus structure

Adenoviral structure has been studied by electron microscopy and crystallography. The locations of capsid and minor components have been determined but the disposition of core proteins is unknown. Not to scale. Based on a figure shown in (Russell, 2009).

1.2.2 Adenovirus classification

Adenoviruses are classified into six groups (A-F) based on their ability to agglutinate red blood cells and their biological and DNA sequence similarities (Table 1). There are 51 serotypes of human adenoviruses which were originally classified based on their expression of antigens and their neutralising-susceptibility to specific animal antisera.

Only a third of adenoviral serotypes cause symptomatic infections in humans (Lenaerts *et al.*, 2008). Usually, these are limited to a mild, self-resolving infection with flu-like symptoms. Some serotypes are responsible for viral gasteroenteritis which affects young children, acute respiratory disease (ARD), for example, among military recruits who live in crowded and physically challenging conditions, and keratoconjunctivitis which can have long-term consequences. Additional population groups at risk of serious consequences from adenoviral infection are immunocompromised individuals, such as those who are HIV-positive, or organ transplant recipients on immunosuppressive therapy. The most widely studied adenoviruses are the Group C serotypes 2 and 5 (Ad2, Ad5) which cause only mild, self-limited respiratory symptoms.

Table 1 Classification of human adenoviral serotypes

Group	Serotypes	Tropism	Diseases
A	12, 18, 31	Intestine	Mainly asymptomatic
B	3, 7, 11, 14, 16, 21, 34, 35, 50	Lung, urinary tract	Respiratory and ocular diseases
C	1, 2, 5, 6	Upper respiratory tract, (liver)	Respiratory diseases
D	8, 9, 10, 13, 15, 17, 19, 20, 22-30, 32, 33, 36-39, 42-49, 51	Eye, (intestine)	Ocular diseases
E	4	Respiratory tract	Respiratory and ocular diseases
F	40, 41	Intestine	Gasteroenteritis

Human adenovirus serotypes are classified based on biological and physiochemical properties which generally coincide with viral tropism and the diseases they can cause. In brackets are sites of infection which may affect immunocompromised individuals.

1.2.3 Adenovirus lifecycle

1.2.3.1 Attachment

The lifecycle of adenoviruses begins with the infection of target cells (Figure 4). Group C adenoviruses are transmitted between host organisms via aerosol droplets. The tropism of adenoviruses is mainly the epithelia of the airways and gastro-intestinal tract that express the Coxsackie and Adenovirus Receptor (CAR), although Group B adenoviruses and Ad37 (Group D) instead use CD46, CD80 or CD86 as cellular receptors. Ad37 has been reported to use sialic acid (Burmeister *et al.*, 2004).

CAR is bound by the virus via the AB surface loop on the side of the fibre knob protein (Bergelson *et al.*, 1997; Bewley *et al.*, 1999). One fibre molecule interacts with three CAR proteins, resulting in a high affinity interaction that allows viral docking to the cell. The AB loop is conserved amongst adenoviral serotypes which use CAR as a receptor while it is absent in serotypes which use alternative receptors.

It has been shown that docking of some serotypes onto host cells can take place in the absence of CAR via heparan sulphate glycosaminoglycans (HS-GAGs) which are widely expressed on cell surfaces and within the extracellular matrix (ECM) (Dechecchi *et al.*, 2000; Zhang & Bergelson, 2005). Binding to HS-GAGs requires a lysine-lysine-threonine-lysine (KKTK) motif on the fibre shaft and is thought to allow viral access to high affinity receptors, CAR or CD46, HS-GAGs thus acting as co-receptors (Tuve *et al.*, 2008).

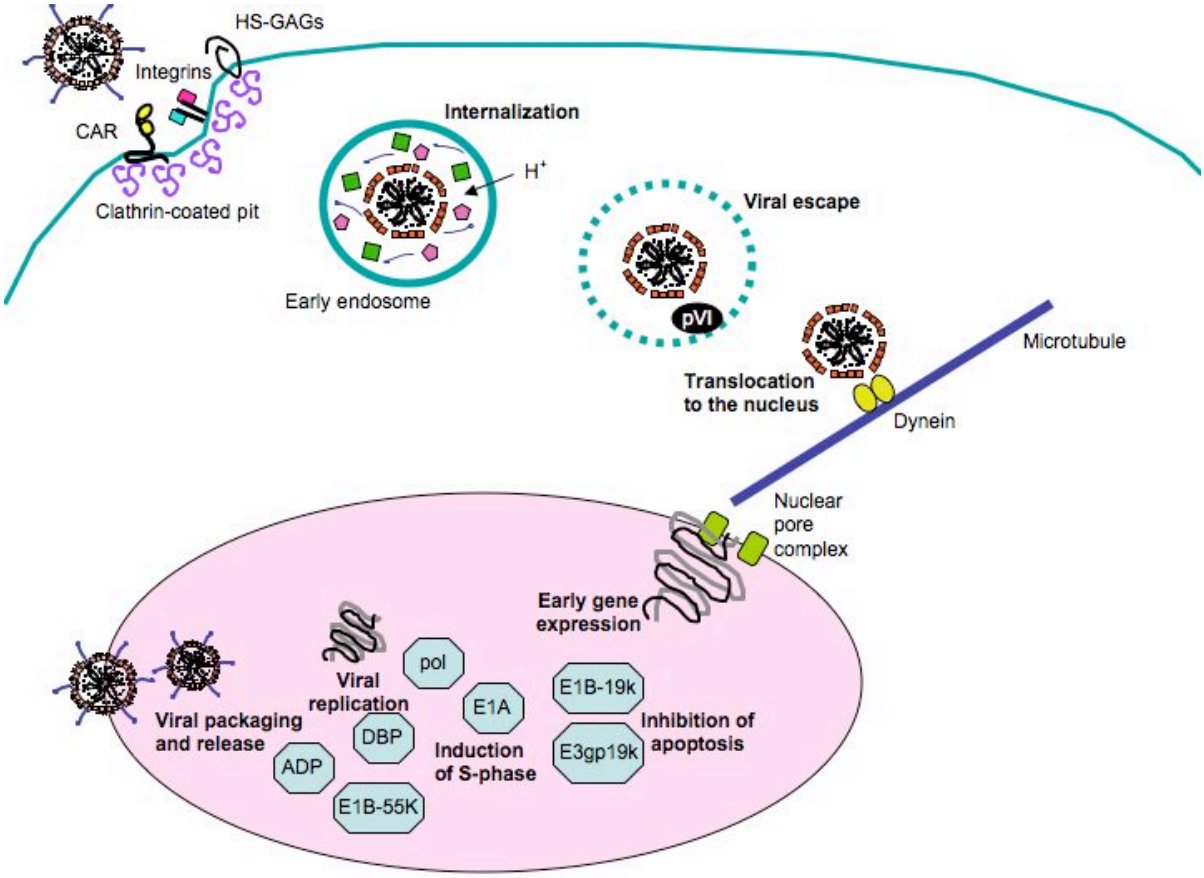

Figure 4 Schematic of the adenoviral lifecycle

Ad5 attaches to host cells via the coxsackie adenovirus receptor (CAR), or alternatively, via heparan sulfate glycoproteins (HS-GAGs). Internalization is mediated by an interaction with integrins $\alpha_V\beta_3$ and $\alpha_V\beta_5$ which induces endocytosis. The viral capsid is partly dismantled in the endosome, from which the virus escapes before the environment becomes too acidic. The viral protein VI is key in this process. Ad5 binds to dynein motors which facilitate viral translocation along microtubule tracks to the nucleus. Here Ad5 docks with the nuclear pore complex and the viral genome enters the nucleus. Transcription of the viral genome begins from the constitutively-active E1A promoter. E1A transactivates other viral genes whose products cooperate to establish a favourable enviroment for viral replication. The viral genome is replicated by the viral polymerase in association with the DNA-binding protein (DBP). Genome copies are packaged into newly-assembled caspid shells. Virions accumulate, eventually causing cell lysis, releasing progeny virus particles in the extracellular matrix and allowing a new replication cycle to begin.

1.2.3.2 Internalization

After attachment, internalization is initiated by the binding of viral penton protein to integrins $\alpha_V\beta_3$ or $\alpha_V\beta_5$ in a quick and efficient process that is completed within 15min (Wickham *et al.*, 1993). Integrins are heterodimeric cell membrane proteins involved in cell adhesion, cell migration, differentation and proliferation. The penton base protein contains a consensus arginine-glycine-aspartic acid (RGD) motif on five flexible surface loops which fit into the groove between the α_V and β integrin subunits. Structural models have shown that the arrangement of the loops on the penton base and the position of the fibre prevent binding by

neutralising antibodies, whilst enabling clustering of integrins in a ring pattern around the penton base (Nemerow *et al.*, 2009).

Binding to integrins via the RGD penton motif triggers down-stream intracellular signalling and endocytosis via clathrin-coated vesicles. Viral uptake requires and induces activation of the PI3K pathway, which, in turn, stimulates downstream targets including rac1 and cdc42 GTPase (Li *et al.*, 1998; Nemerow & Stewart, 1999). These events catalyses actin polymerization and facilitate endosomal vesicular trafficking and functioning.

The endosome matures as proton pumping causes the environment within it to become acidic. At pH 6.0, conformational changes enable the virus to escape into the cytoplasm before the formation of a lysosome. It is thought that free fibre protein, released by viral protease, might act as a pH sensor, thus coordinating the timing of viral exit from the endosome. Vertex components of the capsid, including the fibre, penton base, peripentonal hexons, polypeptides IIIa2 and VI are released. The latter protein has recently been shown to possess lytic activity, enabling disruption of the endosomal membrane (Wiethoff *et al.*, 2005).

1.2.3.3 Intracellular trafficking

Having entered the cell and escaped the endosome successfully, the virus then encounters the viscous, crowded cytoplasm through which passive diffusion to the nucleus is not possible. The adenoviral capsid must be translocated to the nucleus along microtubule tracks by dynein motors (Kelkar *et al.*, 2004). The exact mechanism behind this interaction remains unknown but it is thought that adenoviral translocation uses the same mechanism as adeno-associated virus (AAV), since trafficking of these two viruses is mutually exclusive (Kelkar *et al.*, 2006). Adenovirus traffic can also be interrupted by microtubule depolymerisation and function-inhibiting antibodies against dynein (Leopold *et al.*, 2000).

The movement of viral particles towards the nucleus is induced by the protein kinase A pathway, which is activated by integrin binding (Suomalainen *et al.*, 2001). Movement towards the periphery of the cell is inhibited by p38/MAPK signalling such that the net speed of adenovirus towards the nucleus is around 0.6μm/s (Leopold *et al.*, 1998; Suomalainen *et al.*, 2001).

The viral particles are unloaded at the microtubule organizing center (MTOC) located next to the nucleus by the nuclear export factor CRM1 (Strunze *et al.*, 2005). The partially dismantled adenoviral capsid binds to the CAN/Nup214 protein of the nuclear pore complexes (NPC), and

possibly also interacts with nuclear histone H1 (Campbell & Hope, 2005). The capsid components are sequentially dismantled before transit of the viral genome, complexed with protein VII, through the NPC.

1.2.3.4 Initiation of viral gene expression

Upon entry in the cell nucleus, *E1A* is the first gene to be transcribed from its constitutively active promoter (Figure 5) (Berk, 2005). E1A induces the transcription of the other viral genes, which leads to the expression of various adenoviral proteins (Table 2). Alternative RNA splicing yields two main E1A proteins: 12S (243 residues) and 13S (289 residues). The larger protein is produced during the early stages of infection after which there is a switch in splice selection such that the smaller E1A protein in produced during the late phase. Three additional E1A mRNA species also accumulate during the late stage of the infection.

Comparison of E1A amino acid sequences from different adenoviral serotypes revealed the presence of four conserved regions (CR1-4) in E1A. These and the N-terminal region of E1A are the interaction sites for most E1A-interacting proteins.

E1A-CR3 is present only in the larger 13S and binds proteins involved in transcriptional activation, including the TATA binding protein, Mediator 23 (Med23) and transcription factors. This promotes the assembly of preinitiation complexes (PICs) with RNA polymerase II to the early adenovirus promoters, trans-initiating transcription of the other viral genes. E1A-CR3 interaction with Med23 also enables sufficienctly high rates of transcription reinitiation to support viral replication.

Another role of E1A is to induce cellular progression to S phase to enable viral genome replication. The ability of E1A to counter senescence is often referred to as its 'immortalization' function, as E1A with viral E1B or activated Ras can transform mammalian cells to an oncogenic phenotype. E1A-CR2 binds to Rb family proteins (pRb, p107 and p130) on a motif which is also the binding site for E2F transcription factors. This frees E2F, enabling its activation of genes required for entry into S phase, such as those coding for CDK2 and cyclins E and A.

E1A-CR1 also functions to induce cell cycle progression by interacting with cellular proteins involved in the control of chromatin structure (Frisch & Mymryk, 2002). Most notably, E1A-CR1 binds to and inhibits the activity of the structurally related proteins p300 and CREB-binding protein (CBP). Both are multidomain proteins which function as histone-

acetyltransferases (HATs). CBP and p300 activate transcription by acetylating histone tails or target lysines in transcription factors which control cellular differentiation and the cell cycle. Depletion of p300 allows the activation of cyclin E and A and leads to the expression of c-*myc* and c-*jun*.

E1A-CR4 competitively binds and inhibits a cellular transcriptional corepressor, C-terminal binding protein (CtBP), which is recruited to promoters where it engages histone deacetylases (HDACs) and heterochromatin-interacting protein Polycomb-2. Target genes of CtBP include pro-apoptotic and genes involved in differentiation.

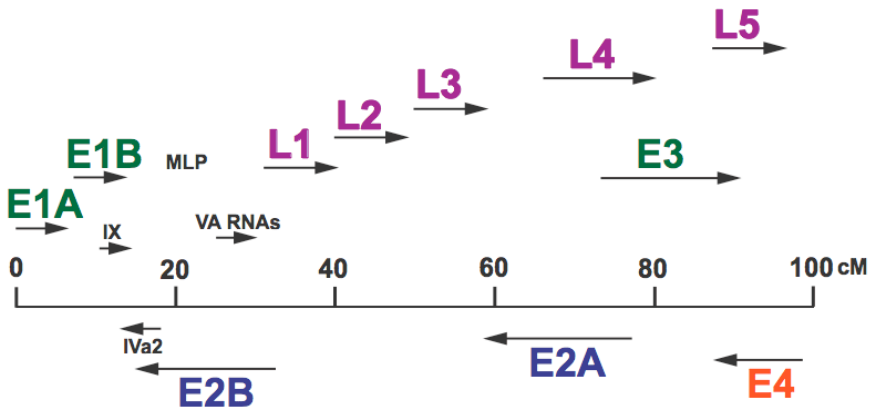

Figure 5 Simplified transcriptional organisation of the adenoviral genome

Transcription begins from the constitutively-active promoter of E1A. E1A transactivates transcription of the other early (E1B, E2A, E2B, E3 and E4) genes. The late genes (L1-5) are transcribed from the Major Late Promoter (MLP). Proteins IX and IVa2 have their own promoter. VA RNAs are transcribed but not translated. The functions of the proteins transcribed from these regions are described in Table 2. Not to scale. cM: centimorgans. Based on a figure in (Akusjärvi, 1986)

Table 2 The products of Ad5 genes and their functions

Gene	Product	Function
E1A	12S and 13S	Transactivators of other viral genes. Bind to cellular pRb, TBP, p300/CPB. Activate p53.
E1B	19kD	Bcl-2 homolog. Inhibits apoptotis by sequestering proapoptotic Bak and Bax.
	55kD	Inhibits apoptosis by binding to p53 and preventing its activity. Blocks cellular but enables viral mRNA accumulation, with E4-orf6.
E2A	Polymerase	Contains 5'-3' polymerase and 3'-5' exonuclease activity.
	DNA-binding protein (DBP)	Binds DNA and separates strands, allowing replication.

E2B	Pre-terminal protein (pTP)	Core protein covalently bound to 5' ends of the viral genome. Acts as a primer for viral transcription.
E3	Adenovirus death protein (11.6K)	Accumulates in the cell during the late stage of infection. Triggers cell death.
	10.4, 14.5, 14.7K (E3B proteins)	Inhibit activation of phospholipase A2, preventing TNFα-induced cytolysis. Block proapoptotic activities of FAS and FIP proteins.
	gp19K	Inhibits antigen processing and recognition of infected cells by cytotoxic T lymphocytes by binding MHC class I molecules and sequestering them in the endoplasmic reticulum.
E4	orf4	Stimulates release of viral progeny during the late stage of infection. Binds protein phosphatates 2A.
	orf6/7	Cooperates with E1B-55k in the nuclear export of viral mRNAs. Shuts off cellular mRNA processing.
L1	IIIa	Structural protein interacting with penton and bridging the core and capsid.
L2	III	Structural protein associating pentamers to form the penton base.
	V	Core protein associated with VI, VII and viral DNA. Bridges core and capsid.
	VII	Abundant histone-like core protein around which viral DNA is wrapped.
L3	II	Associates in trimers to form the hexon capsomere.
	Protease	Processes structural proteins to produce mature proteins. Cleaves cytokeratin component of the cytoskeleton at the end of infection to aid cell lysis
	VI	Structural protein located on the inner side of the capsid beneath hexon. Instrumental in viral escape from the endosome.
L4	100k	Stimulates late viral gene transcription.
	VIII	Structural protein stabilising hexon-hexon interactions.
L5	IV	Fibre protein which associates in trimers. Mediates attachment to the host cell via primary receptors.
VA RNA	VA1 and VA2	Virus-associated RNAs. Protect the cell from interferon-α and -β.
IX		Structural protein on the external side of the capsid, confers stability.
Mu (protein X)		Core protein.
Delayed early gene IVa2		Structural protein involved in encapsidation and regulation of late transcription.

Based on information in (Berk, 2005; Russell, 2009; Shenk, 2001)

1.2.3.5 Counteracting the induction of apoptosis

The natural host response to viral induction of S phase is cellular apoptosis mediated by activation of p53, which is stabilised by E1A. E1A expression also results in the proteosomal degradation of anti-apoptotic Bcl-2 family member Myeloid Cell Leukaemia (MCL)-1, which usually binds to and represses proapoptotic Bak. The DNA-damage response is also triggered by the presence of foreign DNA.

In order to prevent apoptosis-induced degradation of both cellular and viral DNA and premature cell death, which would limit viral replication, adenoviruses possess antiapoptotic proteins (Berk, 2005). These are mainly transcribed from *E1B*. E1B-19K is a Bcl-2 homolog which sequesters Bak and Bax (Cuconati *et al.*, 2002). This interaction represses their ability to form a mitochondrial transmembrane pore which would otherwise lead to the leakage of cytochrome *c* and the activation of downstream effectors such as caspases -9 and -3. E1B-55K blocks p53 activity by binding to its activation domain, acting as a repression domain, and causes p53 to aggregate at the microtubule organising centres (MTOCs) before being degraded by proteosomes. Furthermore, E1B-55K and E4-orf6 form a ubiquitin ligase complex which targets p53 and the cellular MRE11-RAD50-NBS-1 (MRN) complex for degradation. MRN initiates non-homologous end-joining DNA double-stranded break repair which results in the concatanation of viral DNA if allowed to proceed and would consequently prevent viral DNA replication.

1.2.3.6 Countering the cellular immune response to Ad5

The host response to adenoviral infection is a rapid induction of both arms of the immune system. The innate response to adenoviral infection involves upregulation of the transcription factor NFκB, which regulates the expression of immunomodulatory genes, and the production of interferons. The immune response efficiently eliminates transduced cells, thus limiting viral spread. Adenoviruses have therefore evolved strategies to avoid immune recognition and counteract pro-inflammatory signalling.

E3-10.4K and -14.5K, also known as the receptor internalisation and degradation (RID)-α/β complex, prevent tumour necrosis factor (TNF) and Fas-induced cell death by triggering the internalization and degradation of death domain receptors via the lysosome, blocking arachidonic acid release and inhibiting phospholipase A2 translocation to the cellular membrane (Braithwaite & Russell, 2001; Horwitz, 2004; Zhao *et al.*, 2007). Fas-induced apoptosis is also prevented by the interaction of E3-14.7K with FLICE (caspase-8) and other

pro-apoptotic proteins. The activity of NFκB, which is induced by Toll-Like Receptors (TLR) or TNF signalling, is also inhibited by E3-10.4K/14.5K which blocks its nuclear import and inactivates Iκ-kinase (IKK). This downregulates chemokine expression and pro-inflammatory stimuli. Pro-apoptotic signals that are triggered by NFκB or TNF-related apoptosis-inducing ligand (TRAIL) are inhibited by E1B-19K with E3gp19K. The latter protein also prevents the presentation of viral antigens to cytotoxic T-lymphocytes (CTLs) by inhibiting the transport of viral antigens from the endoplasmic reticulum (ER) to the cell membrane with the class I major histocompatibility complex (MHC).

1.2.3.7 Viral genome replication

Having established optimal conditions, replication of the viral genome can proceed. This requires E2-encoded viral polymerase, DNA-binding protein (DBP) and terminal protein (pTP) (Shenk, 2001). Synthesis is initiated from one strand at either terminus of the viral DNA. The viral polymerase contains 5'-3'-polymerase activity and 3'-5'-exonuclease proof-reading ability and uses pTP as a primer. The pTP-polymerase complex is stabilised by cellular nuclear factors (NF) I and II. NFII also cooperates with the viral DBP to allow chain elongation and to maintain strand separation.

1.2.3.8 Virion assembly and release

After the initiation of viral DNA replication, gene expression is initiated from the major late promoter (MLP) which controls transcription of the late genes, *L1-L5*. These genes code for structural proteins (fibre, hexon etc.) involved in assembly of the capsids and packaging of replicated viral DNA into these shells.

During viral replication, E1B-55K and E4orf6 block cytoplasmic accumulation of cellular mRNA whilst enabling efficient cytoplasmic export of viral mRNAs. E1B-55K has an intrinsic RNA binding ability and binds E4orf6 which contains a nuclear export sequence and shuttles between the nucleus and the cytoplasm. The complex also interacts with cellular transport partners, redirecting them to viral transcription centres.

In the cytoplasm, viral mRNAs are preferentially translated over host mRNAs. Viral antagonist (VA) RNAs inhibit protein kinase R (PKR) which would otherwise phosphorylate eukaryotic initiation factor (eIF)-2α and block translation. The L4 100K protein (L4-100K) also inhibits eIF-4E phosphorylation and activation, preventing cellular cap-dependent mRNA

translation. Late viral mRNAs are exempt from this block because they contain a non-coding 5' tripartite leader sequence which enables them to be translated by ribosome shunting. This method allows loading of the small ribosomal subunit (40S) to the capped 5' end of viral mRNAs followed by direct translocation to the downsteam initiation site, directed by the tripartite leader 'shunting elements'. L4-100K contains an RNA-binding domain and a tripartite-specific mRNA binding domain which enables it to promote the initiation of translation by ribosome shunting (Xi *et al.*, 2005).

Assembly begins with the formation of the capsid, starting with hexon capsomeres, followed by penton bases and trimeric fibres, L4-100K functioning as a scaffold. Once formed, the viral genome enters the empty capsid. This requires the packaging sequence located on the 5' end of the viral genome to mediate the DNA-capsid interaction. The particles are then rendered infectious by processing of VI, VII, VIII and pTP by the L3 protease (Ostapchuk & Hearing, 2005).

The viral protease is also instrumental in viral exit from the cell, as it cleaves cytokeratins K18 and K7 which are components of the cellular intermediate filament network. Coupled with the inhibition of protein translation, the cell is unable to replace degraded subunits of the cytoskeleton, resulting in compromised structural integrity and the characteristic phenotype of viral cytopathic effect (CPE): cell rounding, clumping and detachment (Zhang & Schneider, 1994). This, together with initiation of cell death by the adenovirus death protein (ADP), causes cell lysis and releases progeny virions, completing the viral cycle (Tollefson *et al.*, 1996).

1.3 Optimization of adenoviruses for oncolytic therapy

Oncolytic viruses were first considered for use in cancer therapy in the 1950s when doctors noticed that cancer patients suffering from non-related viral infections or those having been recently administered with a virus-based vaccine had better outcomes. With the advent of genetic engineering, many oncolytic viruses have been designed in the past 15 years.

Ad5 is an attractive vector for use in cancer therapy as it is a human pathogen that naturally only causes minor illness. Ad5 is a well-studied virus and the functions of the majority of its genes are known. The virus can easily be genetically modified for tumour-selectivity or armed with suicide genes. Non-essential genes can be deleted from the genome to accommodate desired genes or modulate the specificity of the virus. The natural genome size (36kD) can be exceeded by up to 5% without hampering genome packaging. Furthermore, Ad5 does not integrate in the human genome, avoiding problems associated with insertional mutagenesis. It can infect and replicate in non-cycling epithelial cells and has a rapid lytic lifecycle that is completed within 18-24h. The viral load is amplified 1000 to 10,000-fold in a single replicative cycle, increasing the potency of the viral load delivered to the tumour, and it can be produced to high titres of up to 10^{12} particles (pt)/ml in the laboratory.

1.3.1 Tumour selectivity

Initially, only replication-deficient adenoviruses were designed for clinical evaluation due to safety concerns. However, it was soon apparent that the cancer-killing ability of these viruses was not potent enough (McCormick, 2001). The expression level of tumour suppressor genes inserted into the adenoviral genome was limited due to low viral transduction of tumour cells. Cancer growth still exceeded cell death so the overall anti-cancer effect was not sufficient to eradicate the cancer. Research therefore turned to the design of replication-selective viruses in order to benefit from dose amplification by viral replication and intratumoural spread.

Since adenoviruses target most epithelial cells and not only cancer cells, tumour selectivity needs to be engineered for their use as an oncolytic virus. The most common method to engineer tumour-selectivity into oncolytic adenoviruses is to delete viral genes that are expendable in tumour cells but not in normal cells (Figure 6). Since cellular processes such as the cell cycle and apoptosis are often deregulated in cancer, adenoviral proteins subverting these mechanisms are not necessary in tumour cells. The viral genes encoding these proteins can be deleted without preventing viral replication in cancer cells. However, in normal cells

where the pathways function normally, viral replication will be restricted. 'Complementation mutations' can thus render viruses tumour-selective.

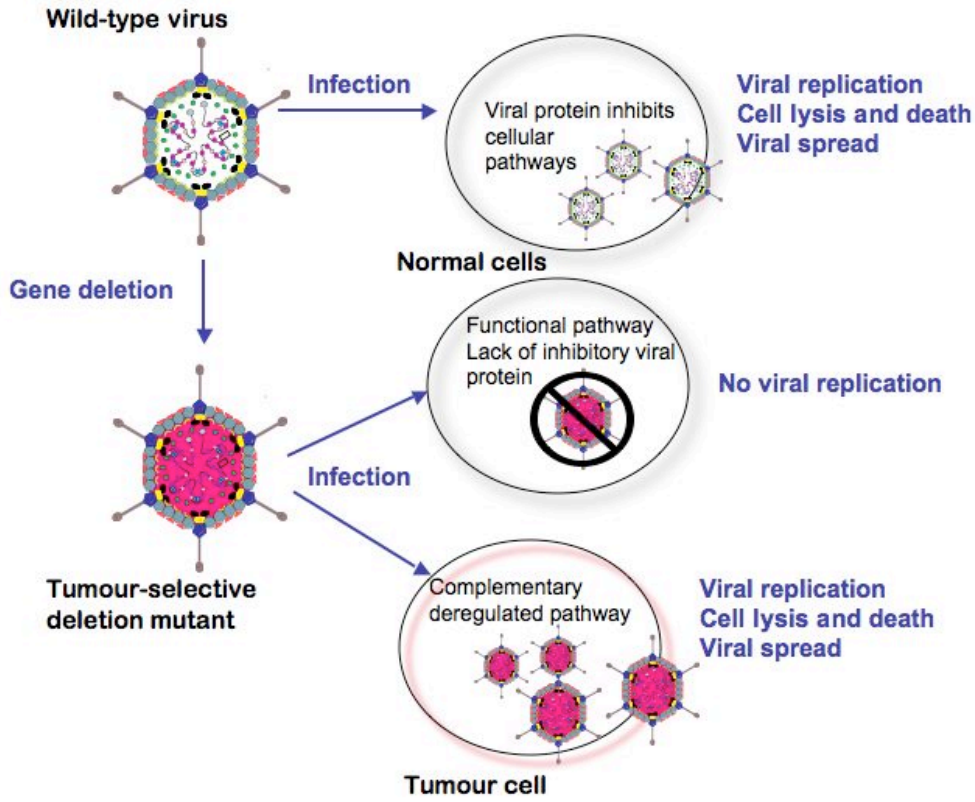

Figure 6 Tumour selectivity of viral mutants

Conditionally-replicating viral muatants contain gene deletions that restrict their replication to tumour cells, although both normal and cancer cells can be infected by the mutant. The infection of normal cells by the tumour-selective mutant is non-productive as it lacks essential complementation proteins. However, in the tumour cell, replication of the viral mutant is facilitated by deregulated apoptotic and cell cycle pathways which complement the gene deletion, enabling progeny production and further viral spread within the tumour.

The first Ad5 complementation mutant to be genetically engineered was Onyx-015 (also known as *dl*1520) (Bischoff *et al.*, 1996). This modified adenovirus lacks the *E1B-55K* gene whose protein product binds p53 to prevent apoptosis, as described in Section 1.2.3.5. Onyx-015 was predicted to be tumour-selective due to the inactivation of the p53 pathway in most cancer cells, which would allow viral replication to proceed unchecked. However, in normal cells functional p53 is present and would trigger apoptosis before Onyx-015 could replicate and spread.

Clinical studies showed variability in patient response to Onyx-015 treatment. It was later shown that the tumour-selectivity of Onyx-015 was not only dependent on non-functional p53 status but also on the cellular host-protein shut-off and mRNA export functions mediated by

E1B-55K and the L4-100K viral protein(Geoerger *et al.*, 2002; O'Shea *et al.*, 2004). Tumour cells which support Onyx-015 replication can complement the absence of these E1B-55K-mediated late functions. However, not all tumour cells have this ability, so overall Onyx-015 replication is severely attenuated.

Non-permissive tumour cells can be induced to support Onyx-015 replication by triggering a heat-shock response which mimics the effect of E1B-55K (O'Shea *et al.*, 2005b). During heat shock, molecular chaperone heat-shock proteins, such as Hsp70, are selectively exported from the nucleus and translated in the endoplasmic reticulum, while expression of other cellular proteins is repressed (to prevent aggregation of mis-folded proteins). This selectivity is mediated by the special 5'-UTR of heat shock protein mRNAs which distinguishes them from other cellular mRNAs. The 5'UTR of *100K* bears homology with the 5'UTR region of *Hsp70*, suggesting that both mRNAs might be translated via the same mechanism. Heat shock proteins are commonly over-expressed and deregulated in tumours (Jolly & Morimoto, 2000), while normal cells cannot be rendered sensitive to Onyx-015 even by heat shock induction. This is thought to be due to a differential heat shock response in primary cells. Details of the exact mechanism behind this are of high interest but remain to be elucidated.

Currently, deletion mutants with improved cancer selectivity are being constructed and evaluated preclinically. These mutants have small regions of *E1A* deleted, whilst the essential functions for viral replication are preserved. This renders the mutants selective for tumour cells which can complement the deleted function of E1A. For example, the *dl*922-947 mutant has a seven amino-acid deletion in the CR2 domain of E1A which impairs binding to pRb (Heise *et al.*, 2000a). This mutant therefore has a reduced ability to induce S-phase such that its replication is severely attenuated in non-proliferating cells.

Another approach to achieve tumour selectivity is to place the *E1A* gene under the control of a tumour- or tissue-specific promoter, instead of its native promoter. For example, in CV706, which has the PSA promoter upstream of *E1A*, viral replication can only take place in prostate cells (DeWeese *et al.*, 2001). Similarly, CV787 has the *E1A* gene under the control of the prostate-specific probasin promoter and the *E1B* gene under the control of the human prostate-specific antigen enhancer promoter (PSE), conferring high prostate selectivity to the virus (Yu *et al.*, 1999).

Metastatic PCa has also been targeted using the conditionally replicating Ad-OC-E1A mutant (Matsubara *et al.*, 2001). This virus has the bone matrix protein osteocalcin (OC) promoter driving *E1A*. This restricts viral replication to OC-expressing cells such as the tumour

epithelia, prostate and bone stroma. This strategy has the advantage of targeting both the PCa cells and the stromal compartment which support the primary tumour and metastases to the bone. OC is normally expressed in maturing osteoblasts during bone mineralization where it negatively regulates bone formation. Transgenic OC knockout mice exhibit increased bone mass rather than any damage to the skeleton.

1.3.2 Improving viral potency

1.3.2.1 Arming vectors with suicide genes

Another method to augment the cancer-killing capacity of replication-selective adenoviruses is to insert a gene coding for a non-mammalian pro-drug converting enzyme into the viral genome (Greco & Dachs, 2001; Kirn *et al.*, 2002). The patients receive the virus which selectively infects and expresses the enzyme in tumour cells. The non-toxic pro-drug is then administered and, although it is taken up by all cells, it is only converted to its cytotoxic form by the enzyme in infected cancer cells, thus achieving tumour selectivity. The toxic metabolite kills the infected cell and diffuses throughout the tumour via gap junctions. This is known as the 'bystander effect' and is a major advantage of 'suicide' gene therapy propagated by viral vectors. The potency of antitumour effects by suicide virotherapies varies in different systems. It is thought that differences may be due to differing levels of enzyme within tumours. Crucial factors affecting this are viral uptake efficiency, suicide gene expression and the numbers of gap junctions in different tissues (Elshami *et al.*, 1996).

A phase I/II trial has been conducted to evaluate the replication-selective mutant Ad-OC-TK for metastatic PCa treatment (Hinata *et al.*, 2006). This virus carries the herpes simplex virus (HSV) enzyme thymidine kinase (tk) under the control of the OC promoter. Expression is induced in OC-expressing cells, where HSV-tk converts the prodrug ganciclovir (GCV), or structurally-related prodrugs such as valaciclovir, to cytotoxic deoxyguanosine triphosphate (dGTP) analogues. This nucleotide becomes incorporated in DNA, terminating elongation and resulting in cell death. None of the three patients suffered serious adverse events and one showed partial response to the therapy. Further trials are ongoing with higher doses of the virus.

The Ad5-CD/*TKrep* provides another suicide gene therapy approach (Freytag *et al.*, 1998). This mutant has wild type E1A, so it is replication-competent, and it has a pro-drug enzyme expression cassette under the control of the CMV promoter in the E1B region. It is rendered replication-selective by the mutation of *E1B-55K* although it expresses E1B-19K. Ad5-

CD/*TKrep* expresses a fusion protein composed of the *Escherichia coli* cytosine deaminase (CD) enzyme as well as the HSV-tk enzyme described above. Cytosine deaminase converts the prodrug 5-fluorocytosine (5-FC) to the cytotoxic analog 5-fluorouracil (5-FU). This product is further metabolized by cellular enzymes to analogues that inhibit thymidylate synthase, resulting in double-stranded DNA breaks, cell cycle redistribution and cell death. These cytotoxic analogues also become incorporated into DNA and RNA strands, inhibiting nucleotide synthesis as well as DNA repair (Aghi *et al.*, 2000).

Initial studies showed that combining Ad5-CD/*TKrep* with suicide therapy was associated with low toxicity and PSA declined in half of the patients (Freytag *et al.*, 2002). A five-year follow-up of the trial demonstrated that PSA doubling time (PSADT) increased significantly and resulted in an average delay to hormone therapy initiation of two years (Freytag *et al.*, 2007). The investigators suggest that selected patients can benefit from this type of treatment, while those with a PSADT of less than six months, who are more likely to have subclinical metastases and die from PCa, should be offered more aggressive therapies such as hormone ablation treatment in combination with chemotherapy and/or gene therapy.

1.3.2.2 Combination therapies

Despite transient, local tumour killing, adenoviruses as single agent therapies have limitations, particularly insufficient infection of target cells, restricted viral spread and rapid elimination from the body (Chu *et al.*, 2004; Kirn, 2001). However, a combination of treatment types that target different cellular mechanisms can prevent the development of resistance to chemotherapeutic drugs and radiotherapy and enhances the adenoviral anti-cancer effect.

Initial *in vitro* and *in vivo* studies of oncolytic viruses with chemotherapeutic drugs demonstrated the efficiency of combination strategies. The overall effects of combination treatments targeting cancer may be dependent upon the sequence of administration of each agent and the dose. *In vivo* experiments showed that administration of Onyx-015 prior to, or simultaneously with, chemotherapy caused superior killing of xenograft tumours to chemotherapy followed by Onxy-015 (Heise *et al.*, 2000b). Premature dosing with cytotoxic drug induces early cell death, curtailing viral replication and spread, and so does not benefit combination therapies with adenoviral mutants. *In vitro* and *in vivo* evaluation of CV787 showed that subtoxic doses of paclitaxel or docetaxel acted synergistically to kill LNCaP cells (Yu *et al.*, 2001).

The exact mechanism underlying the synergy between chemotherapeutic agents and oncolytic viruses remains unknown. Hypotheses include enhancement of viral replication by the chemotherapeutic drugs, altered structure of tumours due to chemotherapeutic drug treatment, allowing greater diffusion and infection of tumour cells, or viral potentiation of drug-induced cytotoxicity, perhaps due to sensatisation of cells to apoptosis by E1A (Kruyt & Curiel, 2002).

Combinations of radiotherapy with adenoviruses have also shown promising results. For example, combination of the prostate-specific CV706 with 10Gy radiation resulted in greater cell killing *in vitro* and synergistic inhibition of tumour growth *in vivo* with increased necrosis and apoptosis and decreased tumour blood supply (Chen *et al.*, 2001). Crucially, the toxic effect *in vivo* was no higher than radiation alone, and viral replication was actually increased when combined with radiation treatment, possibly due to the activation of the cellular DNA synthesis machinery caused by irradiation damage. Combination of double suicide therapy of Ad5-CD/TK*rep* with radiotherapy for PCa has demonstrated promising results without exacerbating toxic side effects (Freytag *et al.*, 2003).

1.3.2.3 Delivery of viral vectors

The safety of Onyx-015 has been tested in around 15 clinical trials involving more than 250 patients (Kirn, 2001). In 2006, an E1B-55K-deleted mutant known as H101 (the equivalent of Onyx-015) was approved for use in head and neck cancer patients by China's State Food and Drug Administration (Garber, 2006; Xia *et al.*, 2004). Despite this success, therapeutic adenoviruses face a number of hurdles *in vivo* which reduce their potency.

In a staged clinical research and development approach, safety was first evaluated in clinical trials with the intra-tumoral (i.t.) delivery of Onyx-015 in patients suffering from recurrent head and neck carcinomas (Kirn, 2001). These patients benefited from the palliative effect of the virus and some had prolonged survival without the maximum tolerated doses being reached. Intra-peritoneal (i.p.) administration in ovarian cancer patients caused only mild side effects (local swelling and flu-like symptoms) with feasible doses up to 10^{13} particles. However, no objective responses could be demonstrated. Complete regression of tumours was observed, although rarely (Nemunaitis *et al.*, 2000). The limited efficacy in these trials was probably due to insufficient viral transduction of tumour cells, such that tumour growth exceeded tumour cell killing.

Investigators began to consider intravenous (i.v.) delivery in order to reach inoperable sites and target metastases. However, use of the i.v. route has been met with some obstacles and

concerns particularly over significant transient increases in liver transaminases which indicate liver damage (Reid *et al.*, 2002). The toxicity to the liver is due to viral transduction of liver parenchymal cells and Kupffer cells. Kuffer cells are liver-specific macrophages of the reticuloendothelial system which break down erythrocytes by phagocytosis. Ad5 has recently been shown to bind human red blood cells via CAR and complement receptor (CR)-1, as well as blood coagulation factors, especially Factor X (Baker *et al.*, 2007; Carlisle *et al.*, 2009; Parker *et al.*, 2006; Waddington *et al.*, 2008). It would appear that humans have therefore evolved a very efficient protective mechanism for sequestering Ad5 in the blood and clearing the virus by the liver. This effect is detrimental in gene therapy as it reduces the circulating viral dose and therefore requires high viral doses to target tumour cells.

Despite the challenges of viral delivery, clinical trials did demonstrate the feasibility of adenoviral cancer therapy (Lin & Nemunaitis, 2004). Evidence of viral replication was obtained from continuous detection of viral elements by qPCR 15 days after i.p. injection of Onyx-015 in advanced ovarian cancer patients. Onyx-015 was found to be present at metastatic sites in two trials following i.v. delivery, although no significant tumour regression was observed (Kirn, 2001). No sign of replication nor toxicity was found in normal tissue. Clinical evaluation of i.t. delivery of *dl*1520 with cisplatin and 5-fluorouracil or gemcitabine showed no additional toxicity and higher response rates in tumours supporting viral replication (head and neck, and colorectal), but not in those resistant to viral replication (pancreatic).

1.3.2.4 Retargeting adenoviral vectors

A novel strategy to improve infection rates of tumour cells involves the modification of adenoviral envelope proteins to 'retarget' the virus. For example, in AdΔ24-RGD, the integrin-binding arginine-glycine-aspartate (RGD) motif has been engineered into the HI-loop of the fibre protein of Ad5 with the E1A gene lacking the pRb-binding site (CR2). This mutant binds primarily to the widely expressed integrins, instead of CAR which is often downregulated in cancer cells, confering an amplified tropism to the virus and enhancing its oncolytic potency (Cripe *et al.*, 2001).

Another possibility is the substitution of fibre protein on Ad5 with those of other Ad serotypes. For example, Ad5/3 carries the Ad3 fibre knob, and displays targeting to the Ad3 receptors CD80 and CD86 (Kawakami *et al.*, 2003; Short *et al.*, 2004). This tropism is beneficial for ovarian cancer cells which express these proteins to higher densities than CAR. Furthermore, Kawakami *et al.* showed that not only are Ad5/3 infection rates superior, but also additional steps in the viral lifecycle, including nuclear translocation, *E1A* transcription, transgene

expression and oncolysis. Another mutant, Ad5.Ad3.SH.luc1, carries the Ad3 fibre shaft and the Ad5 fibre knob and exhibited much lower liver tropism *in vivo* (Breidenbach *et al.*, 2004).

In order to reduce interactions of Ad5 with blood components, 'stealth' viruses have been designed by shielding the viral capsid with a polymer coat such as poly-ethylene glycol (PEG) or poly-N-(2-hydroxypropyl) methacrylamide (HPMA) (Green *et al.*, 2008; Subr *et al.*, 2009). Additional ligands can also be covalently attached to the polymer coat to redirect the virus to tumour cells. These cloaked viruses have shown promising results in murine models and *in vitro* with human blood components (Kreppel & Kochanek, 2008).

1.4 Phytochemicals

Phytochemicals are chemical compounds found in plants commonly consumed by humans. Phytochemicals can be classified according to their sources and chemical structures (Table 3). These natural substances are not considered 'nutrients' as such because their deficiency does not directly cause adverse effects, although they are beneficial to human health. For example, they can affect the immune system, promote good functioning of various organs and prevent cancerous and cardiovascular diseases. This has traditionally been attributed to their antioxidant properties since they can act as free radical scavengers using their hydroxyl groups to donate hydrogens/electrons. Increased production of reactive oxygen species (ROS) had been linked to PCa initiation and progression (Kumar *et al.*, 2008). Exogenous ROS can result from exposure to UV, radiation, chemotherapeutic drugs, environmental toxins and cytokines. ROS are also produced intracellularly by cytosolic NADPH oxidases and by complex III in the mitochondria (Finkel & Holbrook, 2000). Premature 'leakage' from the electron transport chain can cause the production of superoxide anions (O_2^-), hydrogen peroxide (H_2O_2) and hydroxyl radicals (-OH). ROS can damage DNA, proteins and lipids, requiring the maintenance of homeostasis by cellular enzymes which prevent the excessive formation and accumulation of ROS. These enzymes include superoxide dismutase (SOD), catalase, glutathione peroxidase and glutathione S-transferases. Oxidative stress can also be neutralised by antioxidant metabolites synthesised by the cell, such as glutathione, or obtained from the diet.

Phytochemicals have attracted attention in recent years as scientists and clinicians realise the grossly untapped pharmaceutical potential of these compounds. This is especially true in light of the shortcomings of 'conventional' drugs which are commonly associated with dose-limiting side-effects. Phytochemicals have been consumed by humans since the beginning of time, demonstrating their inherent lack of toxicity (at least to dermal and oral exposure). As the incidence and significance of resistance against conventional therapies increase, therapeutic use of phytochemicals will probably become even more attractive. Resistance to phytochemicals is less likely to develop since, in contrast to traditional drugs, these bioactive compounds have multiple molecular targets and function via more than one mechanism.

Nearly 30 years ago, an average of 35% cancer mortality was estimated to be attributable to diet (Doll & Peto, 1981). Since then, epidemiological data and some clinical studies have supported the notion that the consumption of fruits and vegetables containing phytochemicals is beneficial and may be cancer-preventive (Research, 2007; Surh, 2003; Wiseman, 2008).

Amongst others, soya and soy products have been shown to protect against stomach and prostate cancer. This could explain, perhaps at least in part, the low PCa incidence in Asian countries where soy consumption is high. Foods containing lycopene and selenium have also been found to decrease the risk of prostate cancer (Nelson & Montgomery, 2003).

Some discrepancies between epidemiological observations, the results of in *vitro* experiments and clinical trials has been attributed in part to the extensive metabolism that phytochemicals undergo in the human body (Russo, 2007). Polyphenols are usually present in the gut as glycosyl-derivatives. The sugar moiety is removed by glycosidases before the compounds can be absorbed through the small intestine, resulting in an aglycone, which can subsequently be conjugated by methylation and/or sulfation, glucuronidation. Compounds which reach target cells may therefore be quite different structurally from their parent compound and may thus have different effects. Another possible explanation for discrepancies could also be the phytochemical concentration range used *in vitro* which is often higher than measured plasma and tissue concentrations. Additionally, while epidemiological studies indicate beneficial food intakes, phytochemicals in clinical trials are usually evaluated as single agents, not as interacting mixtures of compounds which may act synergistically (Meyskens & Szabo, 2005). These problems are of course quite complex, and, furthermore, since mouse and human metabolism differ greatly, the insights to be gained from animal experiments remain limited.

Table 3 The major classes of phytochemicals with biological activity

Phytochemical class	Chemical structure	Examples and plant sources
Carotenoids	40-carbon skeleton of isoprene units. Responsible for the colours of plants, fruits, flowers, etc.	β-carotene (carrots), lycopene (tomatoes)
Organosulphur compounds	Organic compounds containing sulphur. Often give off potent smells/taste.	Diallyl sulphide (garlic), isothiocyanate (mustard oil), sulfopharane (broccoli)
Polyphenols	Compounds containing one or more benzene rings. Includes phenylpropanoids, tannins, flavonoids.	Catechins (tea), quercetin (capers, apples, berries)

Based on information in (Liu, 2004)

In the first stage of this project, a literature review was conducted and five polyphenolic phytochemicals were selected for study with Ad5. Some of the effects of these phytochemicals are shown in Table 4 and they are described in Sections 1.4.1 and 1.4.2. The rationale for their use with Ad5 is discussed in Section 1.4.3.

Table 4 Effects of five selected polyphenolic phytochemicals

	Curcumin	EGCG	Equol	Gensitein	Resveratrol
Source	Turmeric in curry	Green tea	Intestinal metabolite of daidzein from soy	Soy	Grapes, mulberries, etc.
Effect on hormonal pathways	↓ *AR*	↓ AR expression	× 5α-reductase × DHT ERα agonist ERβ affinity ¼ genistein's	↓ AR × 5α-reductase SERM ↓ ERα, ERβ ERβ agonist	↓ AR via Raf/MEK/ERK.
Effect on GF pathways	✖ EGFR ✖ ERK1/2 ✖ JNK, IκK, NF-κB	✖ VEGFR1/2 ✖ EGFR ✖ IGF ✖ Akt ✖ ERK	× NF-κB ↓ TNFα	× EGFR ✖ IGF-1R × ERK, p38 MAPK × IκB , NF-κB ↑ PTEN ✖ AP-1	✖ ERK ✓ p38 MAPK ✖ NF-κB, AP-1, Egr-1
Effect on cell cycle	Arrest in G2/M ✓ p53 ↓ Cyclin A and E ↑ $p21^{WAF1/CIP1}$ ↑ $p27^{Kip1}$ ↓ CDK1	Arrest in G1 ✖ pRb ↓ Cyclin D and E ↑ $p16^{INK4A}$ ↑ $p21^{WAF1/CIP1}$ ↑ $p27^{Kip1}$	Arrest in G0/G1	Arrest in G_2/M (LNCaP cells arrested in G0/G1) ↓ c-fos ↓ Cyclin B ↑ $p21^{WAF1/CIP1}$ ↑ $p27^{Kip1}$ ↓ cdc25C ↓ cdc2	Arrest in S phase ✓ p53 ✖ cyclin D and E ✖ CDK2 ↑ $p21^{WAF1/CIP1}$ ↑ $p27^{Kip1}$ ✓ Sir2
Effect on apoptosis	✓ caspase-3, -7, -8, -9 ↓ Ψ_M ✖ Cox2, P450	✓ caspase-3,-8, -9 ✖ Cox2	Unknown	✓ caspase-3 × topoisomerase II ↑ Bax ↓ Bcl-2, Bcl-X_L	↑ Bax × Cox-2 ↓ Bcl-2
Effect on metastasis and angiogenesis	↓ MMP-9, MMP-2	↓ MMP-2, -9 ↓ HIF-1α ↓ VEGF, ↓VEGFR1/2 ↓ uPA	✖ MDA cell invasion *in vivo*	↓ MMP-2, -9, ↓ uPA ↓ VEGF ↓ HIF-1α	↓ VEGF ↓ FGF
Synergy with other therapies	Radiation, TRAIL, doxorubicin, cisplatin, genistein.	5-FU, taxol, tamoxifen, curcumin	Unknown	TSA, tamoxifen, 5-FU, radiation	Cisplatin, doxorubicin.

↑ upregulation ↓ downregulation × inhibition ✓ activation. Abbreviations see page 4.

References: general (Dorai & Aggarwal, 2004; Meeran & Katiyar, 2008; Ramos, 2008; Russo, 2007); curcumin (Chendil *et al.*, 2004; Deeb *et al.*, 2004; Mukhopadhyay *et al.*, 2001); EGCG (Siddiqui *et al.*, 2006; Yang *et al.*, 2006); equol (Hedlund *et al.*, 2003; Setchell *et al.*, 2002), genistein (Banerjee *et al.*, 2008; Gao *et al.*, 2004; Huang *et al.*, 2005; Takahashi *et al.*, 2006; Wang *et al.*, 2006); resveratrol (Kundu & Surh, 2004; Signorelli & Ghidoni, 2005; Ulrich *et al.*, 2005).

1.4.1 Phytochemicals selected for initial study

1.4.1.1 Curcumin

Curcumin is the principal curcuminoid present in turmeric (*Curcuma longa*) (Figure 7). It is widely used in Indian cuisine, giving curries their distinctive colour and taste. Turmeric is used in Chinese medicine and is also known as jiang huang. Curcumin is a strong antioxidant, with an oxygen-scavenging activity comparable to vitamin C and E. It is also a potent immunomodulatory compound and has been shown to decrease the production of pro-inflammatory cytokines Tumour Necrosis Factor (TNF)-α and IL-1β (Maheshwari *et al.*, 2006). Curcumin has been shown to induce apoptosis in DU145 and LNCaP cells by

suppressing NFκB and AP-1 growth-promoting transcription factors (Mukhopadhyay *et al.*, 2001). Another reported target of curcumin is Toll-Like Receptor (TLR)-4 which is involved in the innate immune response to bacterial pathogens (Youn *et al.*, 2006).

Curcumin has recently been evaluated in Phase II clinical trials as a chemopreventive agent for colorectal and pancreatic cancers (Dhillon *et al.*, 2008; Thomasset *et al.*, 2007). A number of patients showed positive responses and stable disease, despite its limited absorption.

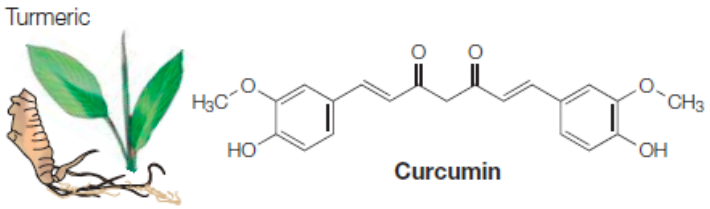

Figure 7 The chemical structure of curcumin
Curcumin is composed of two aromatic rings connected by a diketone.

1.4.1.2 Epigallocatechin-gallate (EGCG)

EGCG is a polyphenol found in the leaves of minimally oxidised *Camellia sinensis* (green tea) (Figure 8). EGCG has been observed to inhibit cancer growth in multiple *in vitro* and *in vivo* models. It inhibited Insulin-like Growth Factor (IGF) signalling and the PI3K/Akt pathway in both androgen-responsive and -nonresponsive cell lines, resulting in apoptosis (Khan *et al.*, 2006). In Transgenic Adenocarcinoma of the Mouse Prostate (TRAMP) mice, EGCG prevented carcinogenesis and prolonged survival. The molecular mechanism behind these effects could be linked to the irreversible arrest of cells in G_1 via increased protein expression of p21 (Gupta *et al.*, 2003). Several studies have also shown IκK and NFκB inactivation by EGCG.

Numerous clinical trials have been conducted to determine the benefits of EGCG in humans. A phase II trial in patients with prostate intra-epithelial neoplasia showed decreased progression of the disease, although another trial did not find any improvements in patients with advanced hormone-independent PCa (Thomasset *et al.*, 2007).

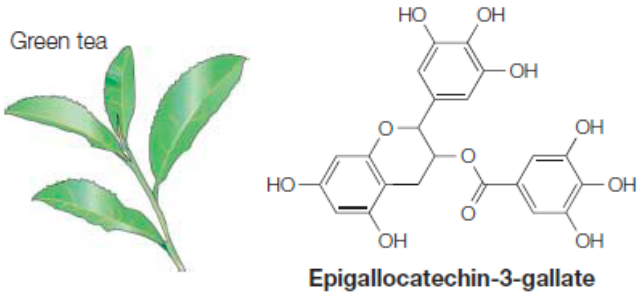

Figure 8 The chemical structure of epigallocatechin-gallate (EGCG)

EGCG is contains a galloyl group linked to a skeleton of two benzene rings linked by a heterocyclic pyrane ring.

1.4.1.3 Genistein

Genistein is the most abundant isoflavone derived from soy (*Glycine max*). It occurs naturally as a glucosidic conjugate, genistin, and is hydrolysed to the active aglycone form, genistein, by intestinal enzymes. The structure of genistein contains two benzene rings linked by a heterocyclic pyrane ring (Figure 9). Genistein has structural similarity to oestrogen (Figure 14), and has a strong binding affinity for estrogen receptor (ER)-β (Kuiper *et al.*, 1998). In addition to its hormonal effects, genistein can modulate various intracellular signalling pathways involved in proliferation, apoptosis and cell cycle progression via the inhibition of DNA topoisomerases and tyrosine kinases (Table 4).

Two chemopreventive phase II clinical trials with genistein have been conducted for breast and pancreatic cancer. A phase II clinical trial in PCa patients showed that soy supplementation containing genistein could inhibit PSA increases in both androgen-sensitive and -insensitive patient populations (Banerjee *et al.*, 2008).

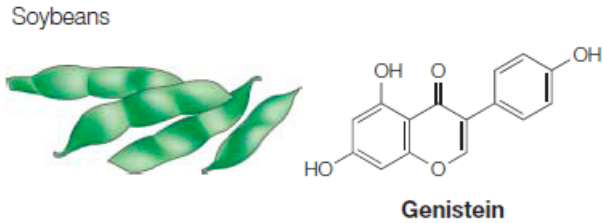

Figure 9 The chemical structure of genistein

Genistein is composed of two benzene rings linked by a heterocyclic pyrane ring

1.4.2 Additional phytochemicals selected for in-depth study

1.4.2.1 Equol

Equol is not strictly a phytochemical as it exists exclusively as an intestinal metabolite of daidzein which is present in soy. Equol is optically active due to its unique chiral centre and exists in R- and S-forms. Metabolism of daidzein by the intestinal bacterial flora results in the formation of the S-enantiomer. Two bacterial species, *Adlercreutzia equolifaciens* and *Slackia isoflavoniconvertens*, have recently been identified for their ability to convert daidzein to equol (Maruo *et al.*, 2008; Matthies *et al.*, 2009). Only about 30-50% of soy-consuming adults have the ability to produce equol, depending on their intestinal microflora (Yuan *et al.*, 2007). The ability to produce equol is thought to be closely related to the lower incidence of PCa. Plasma and prostatic fluid concentrations of equol are higher in men from Hong Kong, who traditionally consume higher quantities of soy-based foods, compared to men from the UK or Portugal, whose diets do not usually include soy.

Fewer studies have been conducted with equol due to its high cost and limited availability, although it has attracted more attention since it was shown to be more biologically active than its parent compound, daidzein, in terms of antioxidant and antiproliferative effects. Equol, like genistein, is a phytoestrogen. Equol has a high binding affinity for ERβ while genistein is less potent, with only a modest affinity for ERβ and little or no affinity for ERα (Setchell *et al.*, 2005). Equol inhibited cell growth in PCa cell lines by inducing cell cycle arrest in G_1 (Hedlund *et al.*, 2003). The antiproliferative effect has been shown to hold true also *in vivo* (Lund *et al.*, 2004). Equol's anti-PCa effects are most probably due to its ability to act as a potent androgen antagonist, thus preventing growth stimulation through the AR (Lund *et al.*, 2004).

Equol is typically present at concentrated levels in prostatic fluid compared to plasma levels, although the mechanism for its concentration has not been described (Hedlund *et al.*, 2005). Equol is currently being assessed in a phase I and II clinical trial for the prevention of recurrent cancer in patients who have undergone surgery for stage II PCa.

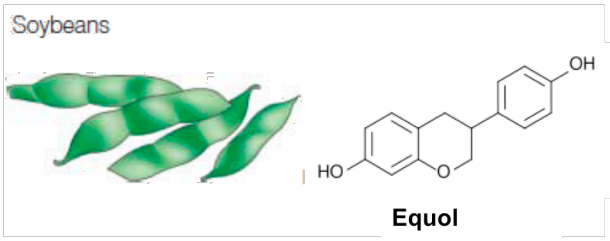

Figure 10 The chemical structure of equol

Equol is structurally similar to genistein but it lacks a hydroxyl and an oxygen group.

1.4.2.2 Resveratrol

Resveratrol (3,4',5-tri-hydroxystilbene) is a polyphenol comprising two aromatic rings connected by an ethylene bridge (Figure 11). Resveratrol is a phytoalexin produced by various plants, including grapes (*Vitis vinifera*) and berries of the *Vaccinium* species, in response to fungal infection (de la Lastra & Villegas, 2005). The resveratrol concentration of red wine is double that of grape juice as resveratrol is released by the wine-making process. Resveratrol content of wines varies with the grape cultivar and its exposure to fungal infection, geographical origin and fermentation time.

Resveratrol was first isolated in 1940, but therapeutic interest only developed after 1992 when resveratrol was postulated to explain some of the cardioprotective effects of red wine and the so-called 'French paradox' (the low incidence of heart disease in France, despite diets high in saturated fats) (Fitzpatrick *et al.*, 1993). Resveratrol can decrease platelet aggregation and lipid peroxidation, promote vasorelaxation and improve serum cholesterol and triglycerides concentrations (Baur & Sinclair, 2006).

In 1997, a study showing the anticancer effects of resveratrol promoted the possibility of using the compound for chemoprevention and cancer therapy (Jang *et al.*, 1997). Since then, there have been numerous reports of the anticancer effects of resveratrol in different models including PCa (Athar *et al.*, 2007). Resveratrol in the diet decreased cancer progression in TRAMP mice and inhibited IGF-1 and ERK signalling (Harper *et al.*, 2007).

More recently, resveratrol has attracted attention as it has been shown to extend the lifespan of flies, worms, small vertebrate fish and even mice (Baur *et al.*, 2006). This effect is thought to be due to resveratrol's ability to enhance the activity of the nictotinamide adenine dinucleotide $(NAD)^{+}$-dependent deacetylase silent information regulator-2 (SIR2) and the human homolog Sirt1 which belong to the sirtuin class III histone deacetylase family (Brown *et al.*, 2009;

Howitz *et al.*, 2003). These proteins are evolutionarily conserved and are thought to play a role in genomic stability, DNA repair and ageing (Michishita *et al.*, 2005; Wang *et al.*, 2008a).

The pharmacokinetics of resveratrol have been investigated in a phase I clinical trial which demonstrated that oral doses up to 5g of resveratrol could be taken without any significant side-effects (Udenigwe *et al.*, 2008). Resveratrol in the body has a short half-life and is rapidly converted to metabolites which remain present for much longer and may retain biological activity. The chemopreventive potential of resveratrol for colon cancer is being tested in a phase I clinical trial and its therapeutic efficiency is being tested in phase I-II trials for colorectal cancers.

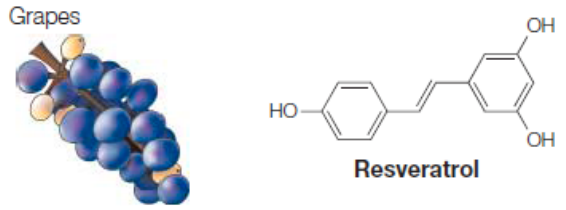

Figure 11 The chemical structure of resveratrol

Resveratrol is composed of two benzene rings linked by a styrene double bond.

1.4.3 Rationale for combining phytochemicals with Ad5

1.4.3.1 Enhancing Ad5 infectability

Many studies have shown that oncolytic efficiency can be enhanced by combining viral treatment with chemotherapy (see Section 1.2.3.3). Phytochemicals have been found to affect various signalling pathways and they could therefore also act in synergy with viruses.

The five phytochemicals were selected based on their modulatory effects on the MAPK pathway which has been implicated in the regulation of the adenoviral receptor CAR (Anders *et al.*, 2003a). The cell surface expression levels of adenoviral receptors on target cells are crucial for efficient adenoviral-mediated oncolysis. The susceptibility of cells with low cell surface expression of CAR to Ad5 infection can be improved by ectopic expression of CAR (Douglas *et al.*, 2001; Kaner *et al.*, 1999). Thus, if phytochemicals could increase CAR expression levels, adenoviral potency might be enhanced.

Adenoviral transgene expression has previously been shown to be increased by treatment of cells with agents such as etoposide, topotecan and FR901228, and that this correlated with

enhanced CAR expression (Hemminki *et al.*, 2003). Adenoviral transgene expression was increased *in vivo*, up to 11.2-fold by FR901228. A modified version of the TRAMP mouse which expressed CAR under the control of the PSA promoter also demonstrated enhanced expression of an adenoviral reporter transgene (Bao *et al.*, 2005).

CAR is a 46kDa transmembrane immunoglobulin-like protein which localizes to basolateral cell-cell adhesions and tight junctions of epithelial cells (Cohen *et al.*, 2001). CAR co-localises with zonula occludens-1 (ZO-1), a protein central to tight juction structure which serves not only as a scaffold protein but also mediates downstream intracellular signalling (Coyne & Bergelson, 2005). CAR is most highly expressed in the heart, brain and pancreas, with significant expression in the testis and prostate (Tomko *et al.*, 1997).

Although human adult prostate cells have moderate levels of CAR, it is often decreased in PCa (Rauen *et al.*, 2002). Forced expression of CAR in ovarian, cervical and PCa cell lines prevented cell migration so it is thought that CAR could act as a tumour inhibitor at this stage (Bruning & Runnebaum, 2004; Okegawa *et al.*, 2000). Similarly, in gastric cancer cell lines, RNAi-mediated knock-down of CAR increased proliferation, migration and invasion, whereas ectopic expression of CAR had the opposite effect (Anders *et al.*, 2009). Loss of CAR was also correlated with decreased tumour differentiation, the presence of distant metastases and reduced survival.

It has also been shown that the spatial distribution of CAR within the cell is important in determining cellular susceptibility to adenoviral infection (Anders *et al.*, 2003b). In normal human breast tissue, CAR was expressed at the cell membrane, particularly at the lateral cell surface where tight junctions are located. When CAR is participating in cell-cell adhesion complexes, it seems to be physically inaccessible and unavailable for binding by Ad5, rendering normal cells in intact tissue resistant to adenoviral infection. Early stage ductal carcinoma *in situ* (DCIS) samples exhibited even expression of CAR at the membrane and low cytoplasmic expression and their equivalent cell line in 3D culture lacked polarity and tissue organisation. This was associated with enhanced CAR expression and good infectability by Ad5. In contrast, infiltrating breast cancer samples showed weak, diffuse cytoplasmic staining or complete loss of CAR expression.

Surprisingly, after metastasis, PCa cells have been found to re-express CAR to levels comparable to those found in normal tissue (Rauen *et al.*, 2002). At this stage, CAR might act as an oncogene, enabling the attachment of metastatic cells to new sites or mediates survival signals that enhance proliferation.

Epigenetic studies of *CAR* have shown that CAR is transcribed from three exons downstream of a 5'-regulatory region containing potential binding sites for transcription factors including E2F, Sp1, Ets and c-Jun (Pong *et al.*, 2003). The number of methylated CpG islands did not differ between CAR-positive and CAR-negative urogenital cancer cell lines, indicating that methylation does not regulate the *CAR* gene promoter. However, histone acetylation seems to play a role in the modulation of CAR expression as the chromatin structure surrounding the *CAR* gene promoter was maintained in an "open" conformation by the association with acetylated histone H4 and this was enhanced by the histone deacetylase (HDAC) inhibitor FR901228 which increased viral uptake. Other studies have also described *CAR* gene transcription up-regulation by HDAC inhibitors (Hemminki *et al.*, 2003; Kitazono *et al.*, 2001; Pong *et al.*, 2003; Sachs *et al.*, 2004). A recent study demonstrated that genistein can synergistically enhance the inhibition of HDAC activity and the level of acetylated H4 on the *CAR* promoter induced by FR901228, although genistein alone did not inhibit HDAC activity (Pong *et al.*, 2006).

Various signalling pathways have been implicated in CAR regulation. TGF-β treatment of pancreatic Panc-1 cells induced a mesenchymal phenotype, accompanied by loss of cell surface CAR, which could be reversed by the TGF-β inhibitor LY2109761 (Lacher *et al.*, 2006). TGF-β and the anti-inflammatory drug dexamethasone also decreased CAR expression in ovarian cancer cells, and pre-treatment with either agent reduced adenoviral gene transfer efficiencies (Bruning & Runnebaum, 2003).

CAR has also been shown to be upregulated by the inhibition of the Raf-MEK-ERK pathway (Anders *et al.*, 2003a). Inhibition of MEK in SW480, a colon cancer cell line, increased CAR at the mRNA level as well as the protein level, but that the inhibition of the PI3K pathway, which is also downstream of Ras, caused the opposite effect and decreased CAR expression. This might indicate that the level of CAR expression in a given cell line may be dictated by the balance between PI3K and MAPK signalling activities.

1.4.3.2 Enhancing Ad5-induced tumour cell death

As mentioned previously (Section 1.3.2.2), adenoviruses have been reported to increase the anti-cancer effects of a number of conventional chemotherapeutic drugs. This is thought to be mediated via the enhancement of viral replication and/or the induction of apoptosis by E1A. We hypothesised that, in addition to possible effects on viral uptake, the phytochemicals might also enhance cell death in combination with Ad5. Phytochemicals have been reported to

induce apoptotic and non-apoptotic cell death in various different models (Choi *et al.*, 2009; Gatz & Wiesmuller, 2008; Li *et al.*, 2007; Siddiqui *et al.*, 2006; Singletary & Milner, 2008; Trincheri *et al.*, 2008). We therefore sought to harness the ability of the phytochemicals to modulate signalling cascades synergistically to induce cell death with Ad5, whilst benefiting from their low systemic toxicity profiles.

1.4.3.2.1 Apoptosis

Apoptosis is a form of programmed cell death (PCD) during which the cell is dismantled by executioner cysteine proteases (caspases), resulting in the controlled fragmentation of DNA and the formation of apoptotic bodies which are engulfed and cleared up by macrophages (Taylor *et al.*, 2008). Apoptosis can be induced extrinsically, via death receptor signalling and caspase-8, or intrinsically via pro-apoptoic proteins, such as Bad and Bid, and caspase-9 (Figure 12).

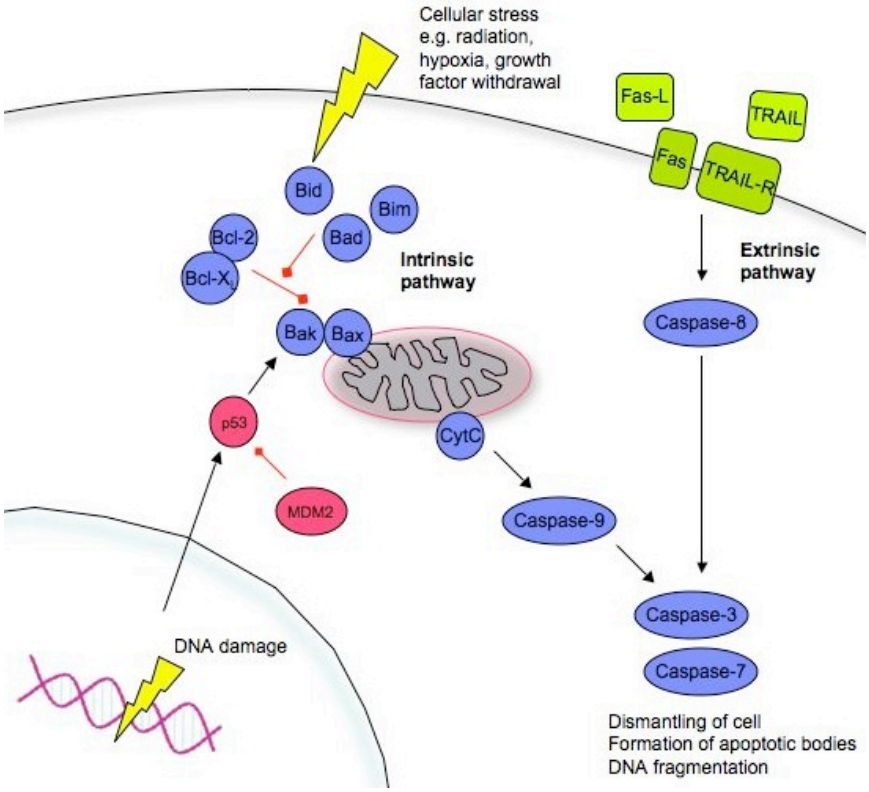

Figure 12 Apoptosis signalling

Apoptosis can be induced by the binding of extracellular death ligands, such as TRAIL, to transmembrane death recptors, which induce downstream activation of caspase-8. Alternatively, apoptosis can be induced by the intrinsic pathway where cell stress or damage activate pro-apoptotic proteins such as Bid, Bim and Bad. These proteins promote the assembly of Bak-Bax in the mitochondrial outer membrane. This causes the release of cytochrome *c* into the cytosol, triggering caspase-9 activation. The extrinsic and intrinsic pathways converge at the activation of effector caspases-3 and -7 which mediate proteolysis and controlled dismantling of the cell into apoptotic bodies. These are subsequently engulfed by phagocytes. Based on figures in (Taylor *et al.*, 2008).

High doses of phytochemicals have been reported to induce apoptosis and also sensitise cells to cytotoxic agents. Curcumin has been shown to be pro-apoptotic by downregulating anti-apoptotic genes such as *Bcl-X_L* and *c-myc* (Mukhopadhyay *et al.*, 2001). This effect is mediated by its inhibition of IκB phosphorylation which prevents translocation of the transcription factor NFκB to the nucleus, so anti-apoptotic genes under its control are not transcribed. Curcumin sensitised PCa cells to TRAIL-, TNF- and radiation-induced cell death via this pathway (Chendil *et al.*, 2004; Deeb *et al.*, 2004). EGCG arrests PCa cells in G_1, resulting in apoptosis, by modulating p21/WAF1, Bax and Bcl-2 (Hastak *et al.*, 2003). Genistein is capable of inducing apoptosis by inhibiting DNA topoisomerase II (Markovits *et al.*, 1989; Salti *et al.*, 2000). Genistein was also found to synergistically enhance cell death with cisplatin, docetaxel and doxorubicin via the inhibition of NFκB (Li *et al.*, 2005). Fewer studies have been conducted with equol, but it has been reported to induce cytochrome *c* release in breast cancer cells and trigger apoptosis via caspase-9 (Choi *et al.*, 2009). Resveratrol can induce apoptosis in PCa cells directly and can sensitise these cells to apoptosis induced by death receptor-mediated apoptosis by TRAIL, Fas and TNFα (Gill *et al.*, 2007; Shankar *et al.*, 2007).

It is possible that by combining phytochemicals with Ad5 cell death could be enhanced by decreasing the apoptotic threshold of cells. The adenoviral protein E1A can sensitise infected cells to TNFα-, TRAIL- and radiation-induced apoptosis (Brader *et al.*, 1997; Sanchez-Prieto *et al.*, 1996). The apoptotic-inducing effect of E1A can be enhanced by the deletion of E1B-19K which is a Bcl-2 homolog and functions to block apoptosis (see Section 1.2.3.5) (White *et al.*, 1991). We have recently shown that a replication-competent, E1B-19K-deleted adenoviral mutant enhances cell death in pancreatic cancer cells in combination with the DNA damage-inducing chemotherapeutic drug gemcitabine (Leitner *et al.*, 2009).

1.4.3.2.2 Autophagy

Although individual adenoviral proteins can induce apoptosis, adenovirus-mediated cell death is generally recognised to be non-apoptotic. The exact mechanism is still unknown but has been observed to be a 'necrosis-like' form of PCD (Abou El Hassan *et al.*, 2004). A replication-selective mutant containing E1A under the control of the human telomerase reverse transcriptase promoter (hTERT-Ad) has also been shown to induce autophagic cell death of malignant glioma cell lines *in vitro* and *in vivo* (Ito *et al.*, 2006). Similarly, Δ24-RGD (an adenoviral mutant deleted in E1A-CR2 with enhanced infectability via additional RGD motif in the fibre HI loop) also induces autophagy in glioma cells (Alonso *et al.*, 2008). This type of

cell death may be cell type-specific, since infected ovarian cancer cells showed induced autophagy but it was not required for cell death (Baird *et al.*, 2008).

Autophagy is an evolutionarily conserved cellular process by which long-lived proteins and bulk cytosplasmic material are sequestered within a double-membrane vesicle, known as the autophagosome, and delivered to the lysosome for degradation and recycling of amino acids (Degterev & Yuan, 2008). Autophagy occurs at a basal rate as a 'quality-control' mechanism to eliminate damaged or aggregated proteins and maintaining cellular homeostasis. Misfunctioning of the pathway been implicated in a number of pathological conditions including Alzheimer's and Crohn's diseases (Levine & Kroemer, 2008).

Autophagy is increased in response to nutrient starvation, withdrawal of growth factors, and external triggers such as infection or radiation. Under these types of stressful conditions, autophagy allows cells to recycle nutrients, maintaining protein synthesis and energy production. Autophagy therefore gives cells time to adapt and survive, or it can eventually lead to type II (autophagic) PCD, although this has yet to be demonstrated in mammals *in vivo* (Scarlatti *et al.*, 2009).

The main modulator of autophagy is the mammalian target of rapamycin (mTOR) which integrates growth-factor induced signals and represses autophagy (Figure 13) (Pattingre *et al.*, 2008). mTOR negatively regulates the induction of autophagy by phosphorylating autophagy protein-13 (Atg13). Atg13 complexes with Atg1 and Atg17 and initiates autophagosome formation by activating vacuolar protein sorting-34 (Vps34), a class III PI3K. Vps34 usually exists in its inactive form as it is repressed by leucine, the principal indicator of amino acid supply in mammalian cells. Upon stimulation, Vps34 complexes with Beclin-1 and stimulates the formation of the autophagosome.

Autophagy induction is controlled by upstream sensors that detect the nutritional status and stress levels of the cell. Class I PI3K signalling is enhanced by nitrogen sources and amino acids, acting as a sensor of the nutritional status of the cell (Codogno & Meijer, 2005). Active Class I PI3K negatively regulates autophagy via the serine threonine kinase Akt, which activates mTOR and downstream protein translation regulators p70S6K and eukaryotic initiation factor 4E (eIF-4E)-binding protein 1. Autophagy can also be inhibited by PTEN, which blocks Class I PI3K signalling and is often lost in advanced PCa. Conversely, oncogenic Ras downregulates autophagy via activation of Class I PI3K. The level of activation of the different branches of the PI3K pathway, as well as Ras status, affects the sensitivity of cell lines to the modulation of autophagy. The PI3K/Akt/mTOR signalling cascade is often

hyperactive in tumour cells and has been implicated in PCa progression (Gao *et al.*, 2003; Murillo *et al.*, 2001; Wu & Huang, 2006). Another important modulator of autophagy is the anti-apoptotic protein Bcl-2 which inhibits autophagy by binding to Beclin-1 (Pattingre *et al.*, 2005). This blocks the interaction of Beclin-1 and Vps34, inhibiting the assembly of the autophagosome, providing a link between apoptosis and autophagy.

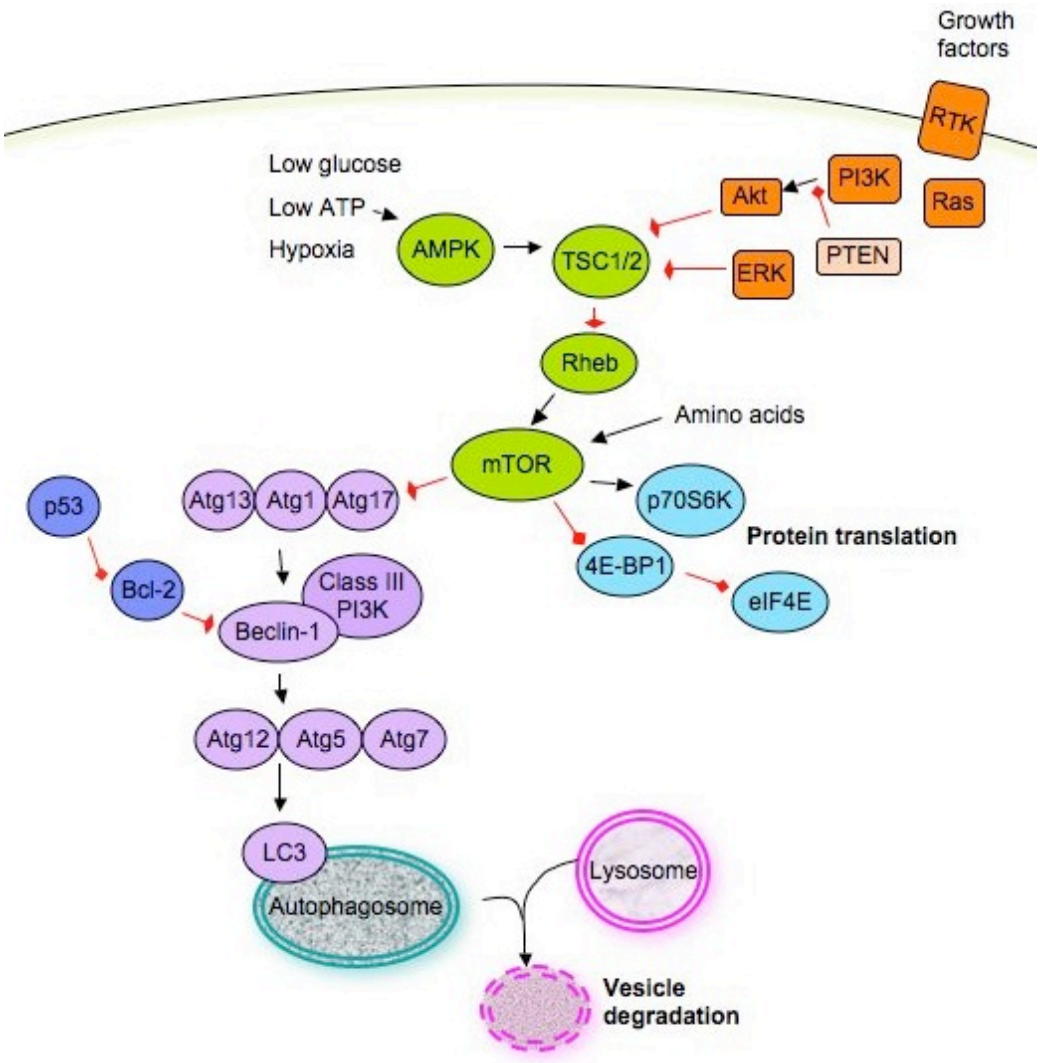

Figure 13 Autophagy signalling

Autophagy is induced by nutrient starvation via the energy sensor AMPK and mTOR. mTOR also regulates protein translation by inducing p70S6K and inhibiting 4E-BP1. Inactivation of mTOR allows the formation of the Atg13-Atg1-Atg17 complex which stimulates Beclin-1 binding with the class III PI3K, Vps34 protein. In turn, this stimulates downstream Atg proteins and initiates authophagosome formation. The LC3 protein is a component of the double membrane of the autophagosome. The autophagosome eventually fuses with the lysosome, allowing degradation of proteins and recycling of amino acids. Growth factor stimulus signals through class I PI3K and negatively regulates autophagy. Cross-talk between autophagy and apoptosis occurs via Bcl-2 which blocks autophagy.

Autophagy defects and gene mutations have been detected in mouse models of breast, ovarian and prostate cancer (Kang *et al.*, 2009; Qu *et al.*, 2003). However, understanding whether the therapeutic goal should be to induce or repress autophagy is complicated by several observations indicating that autophagy might play differing roles depending on the stage of cancer progression (Kondo *et al.*, 2005). Autophagy seems to act as a tumour suppressive mechanism during the development of cancer, but later it can provide a survival advantage to oxygen-restricted and nutrient-starved tumour cells. Autophagy may also function as a resistance mechanism against chemotherapeutic drug treatment, although, on the other hand, autophagy has been shown to crosstalk with, and in some cases be required for, apoptosis and other forms of cell death (Mathew *et al.*, 2007).

A number of chemotherapeutic agents have been shown to induce autophagic cell death. The antiestrogen tamoxifen induces autophagic cell death via downregulation of Akt and ceramide-dependent induced expression of Beclin-1 in breast cancer cells (Bursch *et al.*, 1996; Scarlatti *et al.*, 2004). Temozolomide, a DNA alkylating agent, caused type II cell death in glioma cells and its anticancer effect was enhanced by inhibition of autophagy, depending on where in the autophagy pathway the inhibitor acted (Kanzawa *et al.*, 2004). The Class III PI3K inhibitor 3-methyladenine (3-MA) prevented temozolomide-induced cell death, while bafilomycin-A1, which prevents the fusion of autophagosomes with lysosomes, increased cell death and activated caspase-3. Radiotherapy has also been shown to induce autophagy in malignant breast, colon and prostate cells. Derivatives of the mTOR inhibitor and autophagy inducer rapamycin, CCI-779 and RAD001, are currently being developed as anticancer agents. These agents may have increased anti-tumour efficacy in combination with γ-irradiation therapy or chemotherapeutic agents (Kondo *et al.*, 2005).

Genistein has been reported to induce autophagy in ovarian cancer cells, by inhibiting glucose uptake and Akt phosphorylation (Gossner *et al.*, 2007). Similarly, resveratrol downregulated glycolysis and blocked Akt phosphorylation and downstream signalling in ovarian cancer cells via mTOR and p70S6K which was proposed to explain the induction of autophagy (Kueck *et al.*, 2007). Ovarian cancers have increased glycolytic activity and often over-express the Glut1 glucose transporter, and may therefore be more sensitive to the restriction of glucose metabolism. Resveratrol has also been shown to induce autophagy in colorectal cancer cells (Trincheri *et al.*, 2008). This effect was reversible but lead to apoptosis if allowed to proceed. Both the genetic inactivation of autophagy and the pharmacological inhibition of apoptosis prevented resveratrol-induced cytotoxicity. Interestingly, these examples demonstrate that autophagy and apoptosis are not mutually exclusive. Indeed, the cross-talk between the two pathways is beginning to emerge (Maiuri *et al.*, 2007).

1.4.3.3 Restricting cancer growth-promoting pathways

The inhibition of growth factor signalling pathways by phytochemicals could also break the endocrine loop in PCa required for androgen-resistant growth. The ERK1/2 signalling cascade has been implicated in PCa progression (Oka *et al.*, 2005; Papatsoris *et al.*, 2007). Hormone-responsiveness could be restored by the phytochemicals. Genistein has a biphasic effect on human prostate epithelial cell proliferation: at low concentrations, believed to be physiologically achievable by soy-rich diets (<12.5μM), genistein decreases cell proliferation and ERK1/2 and MEK activity (Wang *et al.*, 2006). At concentrations of 50-100μM, genistein has the opposite effect. Cell proliferation induced by low doses could be inhibited by the MEK1 inhibitor PD098059 and the antioestrogen ICI 182,780, indicating that the effect of genistein may be mediated via ER-dependent pathways.

Genistein has been been shown to downregulate AR in LNCaP cells at the transcriptional level using doses as low as 0.1-1.0μM and this occurs via ERβ (Bektic *et al.*, 2004). Equol and genistein are known as 'phytoestrogens' as they are structurally similar to 17β-oestradiol although they possess much lower estrogenic activity (Rosenberg Zand *et al.*, 2002). Equol and genistein have higher affinity for ERβ than ERα, the former isoform being the predominant ER in the adult prostate gland (Kuiper *et al.*, 1998; Prins & Korach, 2008). Ligand bound ERβ has been shown to protect against PCa while signalling through ERα is associated with increased hyperplasia and squamous cell metaplasia of the prostate. Equol and genistein also share common chemical features with other steroid hormones, such as testosterone and progesterone, and synthetic inhibitors including tamoxifen (Figure 14). They have been classified as natural selective ER modulators (SERMs) as they can act as estrogen agonists or antagonists in different tissues, depending on the concentrations of endogenous estrogen and the distribution of ER (Hwang *et al.*, 2006).

Resveratrol is also structurally related to oestrodiol. Resveratrol has been shown to compete for ER binding, leading to the expression of estrogen-responsive genes, and that this effect can be inhibited by estrogen antagonists (Gehm *et al.*, 1997). In addition, resveratrol can decrease AR and PSA expression levels in LNCaP cells (Mitchell *et al.*, 1999)

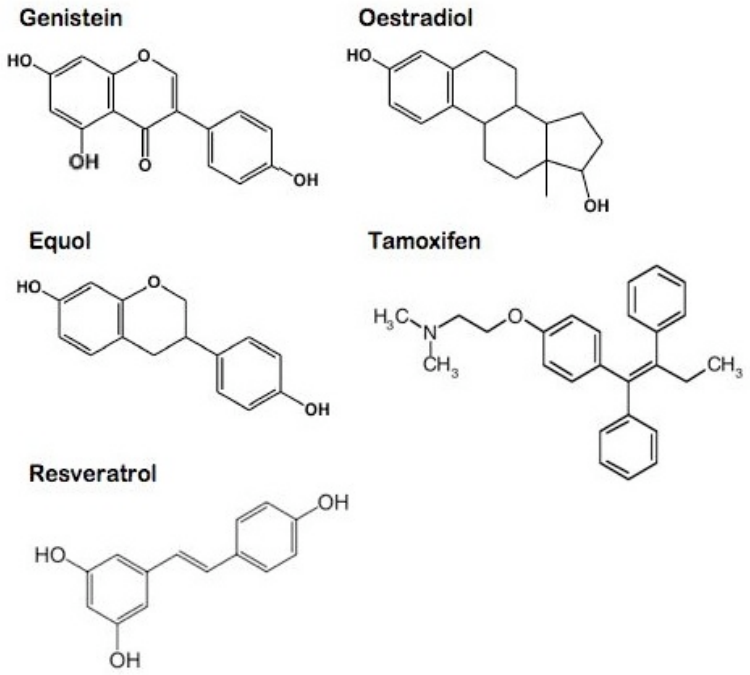

Figure 14 Structure of isoflavone phytoestrogens and related compounds

Adapted from (Dixon & Ferreira, 2002)

1.5 Project aims

- To identify phytochemicals that interact synergistically on cell death with Ad5 in PCa cell lines.
- To select the most promising phytochemicals for in-depth study.
- To determine the optimal sequence of administration of each combination of phytochemical and Ad5.
- To determine the effects of equol and resveratrol on the viral lifecycle
    - Effects on the infectability of PCa cell lines
    - Effects on viral replication.
- To determine the effects of equol and resveratrol on cellular processes with and without Ad5 on
    - Cell cycle progression
    - Apoptosis induction
    - Autophagy induction.
- To confirm the synergistic enhancement of cell death by equol and resveratrol with replication-selective Ad5 mutants designed in our lab.

2 Methods

2.1 Reagents

Curcumin and epigallocatechin gallate (EGCG) were obtained from Merck Biosciences (Nottingham, UK). Equol and genistein were from Apin Chemicals (Adington, UK). Resveratrol, 3-methyladenine (3-MA), rapamycin and bafilomycin-A1 were from Sigma (St. Louis, MO, USA). The phytochemicals were reconstituted in dimethyl sulphoxide (DMSO) (Fisher Scientific, Loughborough, UK) to give a stock concentration of 50mM. Bafilomycin-A1, rapamycin and the pan-caspase inhibitor zVAD-FMK (Calbiochem, La Jolla, CA, USA) were also dissolved in DMSO to stocks of 5μM, 100μM and 5mM respectively. 3-methyladenine (3-MA) was diluted in sterile distilled water to a stock concentration of 100mM. Trichostatin-A was obtained from Calbiochem and diluted in DMSO to 1mM. All chemicals were aliquoted and stored at -20°C for use up to a year after reconstitution as it was noted that EC_{50} values for the phytochemicals decreased over time after storage for around 8 months under these conditions.

2.2 Cell culture

The PCa cell lines 22Rv-1, LNCaP, DU145 and PC-3 were obtained from Cancer Research UK Cell Services (Clare Hall, Middlesex, UK). Characteristics of the cell lines are shown in Table 5. JH293 cells used for $TCID_{50}$ assays are a sub-clone of the E1-transformed human embryonic kidney (HEK) 293 cell line, both obtained from Cancer Research UK Cell Services, as well as A549 human lung carcinoma cells used for primary viral expansions. Cells were cultured in Dulbecco's modified Eagle medium (DMEM) supplemented with 10% fetal calf serum (FCS), 100 units/ml penicillin, 100mg/L streptomycin and 584mg/L L-glutamine. Viral infections were done in 0% FCS DMEM medium for 2h and 2% FCS DMEM medium was used for culturing cells in 96- or 6-well plates. All experiments were done with cells between passages 5-25. Cells were subcultured every 3-4 days using 0.25% trypsin in versene to detach monolayers and generate single cells. Cells were incubated at 37°C in a humidified atmosphere with 5% CO_2. Aliquots of 1×10^6 cells/ml were frozen in 10% DMSO, 20% FCS DMEM and stored in liquid nitrogen. All cell culture reagents were obtained from Cancer Research UK Cell Services.

Table 5 Characteristics of human PCa cell lines used in this project

Characteristic	22Rv-1	DU145	LNCaP	PC-3
Year established	1999	1977	1980	1978
Origin	Primary tumour from CRW22Rv xenograft serially-passaged in mice.	Carcinoma brain metastasis.	Carcinoma supraclavicular lymph node metastasis.	Grade IV adenocarcinoma bone metastasis.
Androgen dependency	Mutated androgen receptor. Androgen independent but responsive.	Independent (no androgen receptor protein nor mRNA).	Androgen responsive, promiscuous androgen receptor binding.	Androgen independent (no androgen receptor protein nor mRNA).
p53 status	Wild type	Mutated	+	-
PTEN status	+	+	-	-
Bcl-2 status	++	-	+	+

(Skjoth & Issinger, 2006; Webber *et al.*, 1997)

2.3 Viruses

2.3.1 Adenoviral mutants

The majority of the experiments described in this thesis were done using wild-type adenovirus type 5 (Ad5). Synergy assays were also carried out using adenoviral mutants constructed in our laboratory based on the Ad5 backbone (Table 6). The identity of the viral mutants was confirmed by PCR using specific primers described in Section 2.3.5.

Table 6 Adenoviral vectors and their deletions

Virus	Deletion	Insertions	Reference
Ad5	–	–	
*dl*312	ΔE1A, ΔE3B	–	(Jones & Shenk, 1979)
Ad5-Hey1	ΔE1, ΔE3	Hey1 under the control of the CMV promoter replacing E1A	S. Cheong (manuscript in preparation)
AdE1A-12S	ΔE1, ΔE3	E1A-12S under the control of the CMV promoter replacing E1A	E. Miranda (manuscript in preparation)
Ad5-GFP	ΔE1	GFP under the control of the CMV promoter replacing E1A	Prof. Nick Lemoine's lab
Ad5-GFP REP	ΔE3	GFP under the control of the Major Late Promoter region	(Jin *et al.*, 2005)
Ad5tg	None (wild type Ad5 generated from pTG3602)		(Chartier *et al.*, 1996)
AdΔΔ	ΔE1A-CR2, ΔE1B-19K	–	D. Oberg (submitted)
AdΔE1B-19K	ΔE1B-19K	–	(Leitner *et al.*, 2009)
AdΔCR2	ΔE1A-CR2	–	D. Oberg (submitted)

2.3.2 Viral production

Viruses were produced and characterised by Jennelle Francis and Katrina Sweeney (scientific officers, Viral Gene Therapy group, Centre for Molecular Oncology and Imaging). Primary viral expansions were made using 30μl viral stock to infect a subconfluent T175 culture flask of A549 cells in 30ml 2% FSC medium. Cells and medium were harvested after the appearance of cytopathic effect (CPE) 48-72h post-infection, freeze-thawed three times and stored at -80°C. The primary expansion was used to infect HEK293 cells grown to 80% confluency in 10% FCS medium in ten-layer cell factories (CF-10, Fisher Scientific) in 2% FCS medium for 72h or until signs of CPE and detachment were observed, followed by routine viral isolation procedures (Wold, 1998). Briefly, cells and media were collected and centrifuged for 10min at 2000rpm at 4°C in a Sigma 6K15 centrifuge (Sigma, Germany). Cells were resuspended in 15ml cold PBS, centrifuged for 10min at 1000rpm and finally resuspended in 12ml cold 10mM Tris-HCl (pH8). Viral suspensions were freeze-thawed three times to release viral particles and centrifuged for 10min at 6000rpm. The supernatants were layered onto CsCl gradients prepared in 3.5" ultracentrifuge tubes (Beckman, UK) with 10ml 1.25g/ml CsCl underlayed with 7.6ml 1.4g/ml CsCl solution. The virus preparation was centrifuged for 2h at 25,000rpm at 15°C in a Beckman SW28 swing-out rotor in an Optima LE-80K ultracentrifuge. After centrifugation, using a 19G needle, the bottom band of virus was extracted in a minimum amount of CsCl, discarding the top band of cell debris and the second band of empty viral particles. The virus suspension was layered onto 2.5ml 1.35g/ml CsCl solution in 2" ultracentrifuge tubes (Beckman) and centrifuged for 15h at 40,000rpm at 15°C in a Beckman SW55Ti swing-out rotor in an Optima LE-80K ultracentrifuge. The purified virus band was collected using a 19G needle and the volume made up to 12ml with

TSG buffer containing 96mM NaCl, 0.5mM Na_2HPO_4, 2.8mM KCl, 0.3mM $MgCl_2$, 0.5mM $CaCl_2$ and 30% (v/v) glycerol adjusted to pH7.5. The suspension was dialysed using a 3-12ml Slide-a-Lyser (Pierce Biotechnology, Rockford, IL, USA) against a buffer containing 10mM Tris-HCl (pH7.5), 1mM $MgCl_2$, 150mM NaCl and 10% (v/v) glycerol for 24h at 4°C. The purified virus was removed from the dialysis chamber, aliquoted and stored at −80°C. An aliquot was used to determine viral particle and plaque-forming unit (pfu) titres as described below.

2.3.3 Determination of viral particle titres

To determine the particle count of purified virus, two viral samples were prepared:

Sample 1. 100µl virus + 100µl dialysis buffer + 200µl lysis buffer
Sample 2. 200µl virus + 200µl lysis buffer.

The dialysis buffer was prepared as described in Section 2.3.2 and the lysis buffer contained 1% SDS, 0.04M Tris-HCl in ddH_2O. The samples were vortexed and heated for 10min at 56°C, vortexed, allowed to cool for 10min and made up to 1ml with sterile H_2O. The absorbance of each sample was measured at 260nm (OD_{260}) with a Beckman DU520 spectrophotometer. The viral particle count for each sample was determined according to Equation 1.

Equation 1 Determination of viral particle counts by optical density

Viral particles (vp)/ml = OD_{260} × dilution factor × extinction coefficient at 260nm wavelength (ε_{260})
Where the dilution factor for Sample 1 = 10 and for Sample 2 = 5
And purified adenovirus $\varepsilon_{260} = 1.12\times10^{12}$ vp/absorbance unit

ε_{260} is the molar extinction coefficient of one vp/ml/absorbance unit, based on the assumption that 87% total dry weight of Ad5 is protein and that the molecular mass of a viral particle is 2.3×10^7 Da (Maizel *et al.*, 1968; Mittereder *et al.*, 1996).

Alternatively, viral particles were measured by determining DNA content using the Quanti-iT Pico Green dsDNA Assay Kit (Invitrogen, OR, USA). Viral stocks were diluted 1:6 and 1:10 in Tris-EDTA (TE) buffer containing 10mM Tris-HCl (pH8), 1mM EDTA and 1% SDS and assayed in triplicate in 96-well plates. The Pico Green reagent was diluted 200-fold and 100µl added to each well. A standard curve was made using Lambda DNA (provided with the kit).

Emission was read at 535nm after excitation at 485nm using Magellan Software version 6.3 and a Tecan Infinite F200 plate-reader (Mannedorf, Switzerland). Viral particles/ml were calculated from the standard curve, assuming that 2.7×10^{10} viral particles contain 1μg DNA.

2.3.4 Determination of viral activity

Viral replication was determined by limiting dilution tissue culture infectious dose $(TCID)_{50}$ assay. JH293 cells were seeded in 96-well plates at a density of 1×10^{4}cells/well in 200μl/well in 10% FCS medium. The following day, purified virus was diluted to 1×10^{-7} and used to infect the top row of duplicate or triplicate plates (20μl/well) and serially diluted down the plate by transferring 22μl/well from each row down to the following row, leaving the last row uninfected as controls. Plates were incubated for 10 days after which each well was scored for signs of cytopathic effect (CPE). Wells where the monolayer had plaques of clear areas or where cells were rounded up were counted as positive. The titre of each sample was calculated in plaque-forming units (pfu)/ml using the Reed and Muench method (O'Reilly *et al.*, 1994) (Equation 2). All viruses used in this thesis had a particle/pfu ratio between 10-50.

Equation 2 Calculation to determine viral replication units

$TCID_{50} = 10^{\,L - d\,(s - 0.5)}$
$TCID_{50}/ml = TCID_{50} \times v$

L = lowest dilution with CPE
d = log difference between dilution steps
s = Σ proportion of CPE-positive wells in each row
v = infection volume = 0.02ml

$pfu/ml = \text{Log } TCID_{50} \times \mu$
Where $\mu = -\ln p = 0.69$

According to the Poisson distribution:
μ is the mean concentration of infectious particles at a given dose
p is the proportion of cultures remaining uninfected, = 0.5

2.3.5 Confirmation of viral identity

The identity of each viral mutant was confirmed by PCR using specific primers. Viral DNA was extracted from 200μl dialysed virus using purification columns from a DNA Blood Mini Kit (Qiagen, West Sussex, UK) following the manufacturer's protocol. PCR reactions were set up with 8 primer sets shown in Table 7 using the Advantage 2 PCR Kit (Clontech, CA, USA). Each reaction contained 50ng purified viral DNA, 1μl of forward and reverse primers (10μM), 3μl 10X PCR buffer, 1μl dNTP (10mM), 1μl DNA mix and 20μl dH_2O to make a final volume

of 30µl. DNA was amplified by 35 cycles (94°C 40s, 62°C 60s, 72°C 90s) in a Gene Amp PCR System 9700 (Applied Biosystems, CA, USA). PCR samples were separated on a 1.5% agarose gel with a DNA Hyper ladder IV (Bioline, UK) to determine the size of amplified DNA fragments. The expected sizes were calculated from known sizes of each sequence and the deletions made (Table 8). An example of a typical PCR identity gel is shown in Figure 15.

Table 7 PCR primers used to determine viral identity

Primer set	Direction	Sequence
1	5' forward	CCCGGTGAGATTCCTCAAGAGGCCAC
	3' reverse	CCGGACCCAAGGCTCTCTGCTCTCCGGCTGCTCGGGC
2	5' forward	GTAATGTTGGCGGTGCAGGAAGGGATTG
	3' reverse	GGGTCCCCCGTATTCCTCCGGTGATAATGAC
3	5' forward	GTGTTCGCTTTGCTATATGAGGACCTGTGGC
	3' reverse	CCTCGATACATTCCACAGCCTGGCGACGCCCACC
4	5' forward	CCTGTGATTGCGTGTGTGG
	3' reverse	GACAACAGTAGCAGGCGATTC
5	5' forward	GCATCTGTGGAGAGCGGTTGTGAGACAC
	3' reverse	GCGCCAGCAGATCAAGCTCATTAGCGC
6	5' forward	GCTTAATGACCAGACACCGTCCTGAGTG
	3' reverse	GCACCAAGTGATCGGGCCTCAGCTCC
7	5' forward	CACCCTCACGCTCATCTGCAGCCTCATCACTGTGG
	3' reverse	CTTCAGACGGTCTTGCGCGCTTCATCTGC
8	5' forward	CGCTGGGGTCGCCACCCAAGATGATTAGG
	3' reverse	GAGTAGGGTACAGACCAAAGCGAGCACTG

Table 8 Expected size of DNA fragments generated by PCR primer sets

Primer set	5' binding site	3' binding site	Target sequence	Expected Ad5 size (bp)
1	476	853	E1A start	377
2	767	1029	E1A-CR2	262
3	1069	1453	E1A end	384
4	1554	2086	E1B-19K	532
5	2073	2440	E1B-55K	367
6	2383	3434	E1B-55K	1051
7	29915	31038	E3B	1123
8	28715	29135	E3-gp19K	420

5' and 3' binding sites refer to the Ad5 genome sequence base pairs (NCBI Reference Sequence: AC_000008.1) (Chroboczek *et al.*, 1992)

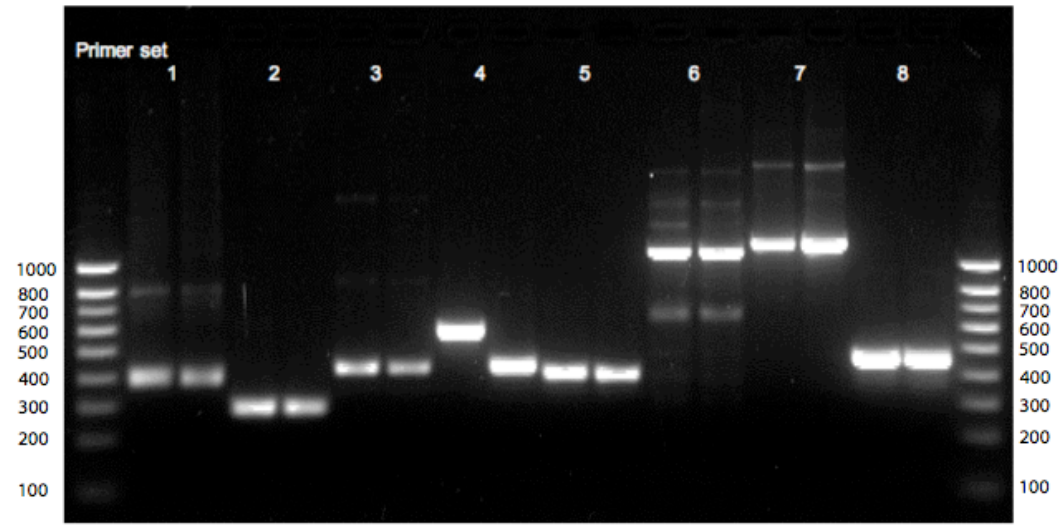

Figure 15 Verification of viral identity for Ad5ΔE1B-19K

The sizes of 8 regions of the viral genome were determined by PCR using primer sets shown in Table 7 as detailed in Methods Section 2.3.5. The first lane in each set represents amplified DNA from Ad5 wild-type, the second lanes are from the mutant, Ad5ΔE1B-19K in this case. Fragment sizes were estimated using the DNA ladders on either side of the gel, and compared to expected sizes (Table 8). Primer set 4, detecting E1B-19K, amplified a smaller (390bp) DNA region in the Ad5Δ19K mutant (right lane) compared to wild type Ad5 (left lane) which shows amplification of the full-length 532bp region.

2.4 Cell viability and synergy

2.4.1 MTS assay

Cells were seeded in 96-well plates in 200μl/well of 10% FCS medium at a density of 1×10^4cells/well (DU145, PC-3) or 2×10^4 cells/well (22Rv-1 and LNCaP) in triplicate plates. After allowing cells to adhere overnight, the seeding medium was replaced with 2% FCS medium to a total volume of 100μl/well. Ad5 and phytochemicals were diluted in serum-free medium and added to the wells at 10-fold higher concentration after serial dilution (5-fold dilutions, 10μl/well). Viability was assessed 6 days post-treatment (7 days after seeding) using the MTS viability assay performed according to the manufacturer's instructions (Promega, WI, USA). The tetrazolium salt MTS (3-(4,5-dimethylthiazol-2-yl)-5(3-carboxymethoxyphenyl)-2-(4-sulphophenyl)-2H-tetrazolium) is converted by mitochondrial dehydrogenases in metabolically active cells to a soluble formazan compound which absorbs light at 490nm. The product of the reaction is directly proportional to the relative number of live cells. After incubation at 37°C for 3h (DU145 and PC-3), 4h (LNCaP) or 7h (22Rv-1), the plates were read using a microplate reader (Opsys MR, Dynex Technologies) at a wavelength of 495nm. Values were corrected against the blank wells containing media without cells and expressed as

percentage cell death compared to untreated control cells. Sigmoidal dose-response curves were generated by non-linear regression analysis using GraphPad Prism version 4.0c for Macintosh (GraphPad Software, San Diego California, USA) to determine the effective concentration $(EC)_{50}$ values (dose required to kill 50% cells) for each agent or combination of agents in each cell line.

2.4.2 Synergistic interactions between Ad5 and phytochemicals

Drug combinations have been used empirically since the earliest days to cure diseases and alleviate symptoms. For example, Chinese herbal medicine is based on the interaction of mixtures of plant-based compounds. A number of stategies to evaluate these interactions mathematically have been proposed. This is of particular interest in oncolytic drug development where the mechanisms of action of drugs might suggest therapeutic benefits when used in combination. It can also be of value when a drug being developed is to be used in combination with an exisiting drug as part of a treatment regime.

Evaluating the interactions between drugs is challenging, not least due to the complexitiy of biological systems. A review by Greco *et al.* categorized thirteen different approaches to model and evluate drug combinations (Greco *et al.*, 1995). The most commonly used stategies and those employed in this study will be considered here. The various models and their limitations have most recently been presented in a complete review by Chou who has developed this field for the past 35 years (Chou, 2006).

2.4.2.1 Summation method

This basic evaluation of the interaction between two agents involves simply comparing the sum of the inhibitory effects of each drug alone to the observed effect. If the observed effect is greater than the expect sum of the effects of each drug alone, the drugs are considered to act synergistically (Equation 3). The limitations of this method can immediately be seen when considering drugs with high effects alone.

Equation 3 Summation of effects

$$E(d_a d_b) = E(d_a) + E(d_b)$$

For example :

$E(d_a d_b) = 30\% + 30\% = 60\%$

But $E(d_a d_b) = 60\% + 60\%$ cannot equal 120%

$E(d_a)$ = effect of drug a alone at dose d

$E(d_b)$ = effect of drug b alone at dose d

$E(d_a d_b)$ = effect of the combination of drugs a and b

2.4.2.2 Fractional product method

An alternative to the summation method first described by Webb (Webb, 1963) is known as the fractional product or the survival fraction method (Chou & Talalay, 1984). It takes into account the potency of each drug alone (Equation 4), avoiding the problem of fractional inhibition which occurs in the evaluation of synergy by the summation of effects (Equation 3). However, it is only valid when the drugs assessed have hyperbolic curves (i.e. simple Michaelis-Menten kinetics). This is typically the case for simple systems such as enzymatic inhibition, but complex systems involving cellular or in vivo models more commonly have sigmoidal curves (Figure 16). Furthermore, it requires that the mechanisms of the drugs are mutually nonexclusive (i.e. that they act totally independently).

Equation 4 Fractional product effect

$$S(d_a d_b) = [1 - F(d_a)][1 - F(d_b)]$$
$$F(d_a d_b) = 1 - S(d_a d_b)$$

For example :

$(1 - 0.4)(1 - 0.4) = 0.36$

$1 - 0.36 = 0.64$

$F(d_a)$ = fractional effect of drug a alone at dose d

$F(d_b)$ = fractional effect of drug b alone at dose d

$S(d_a d_b)$ = surviving fraction of the combination of drugs a and b

$F(d_a d_b)$ = fractional effect of the combination of drugs a and b

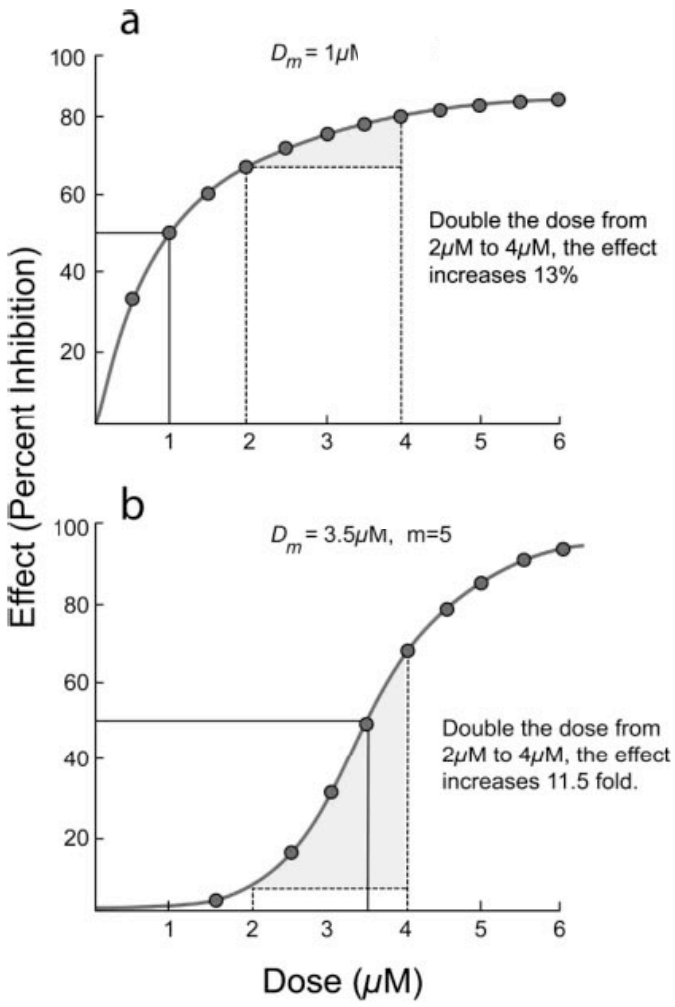

Figure 16 Dose-response curves for two drugs with differing kinetics

Examples of dose-response curves for two drugs. A: drug with a hyperbolic curve and an EC_{50} (D_m) value of 1μM. B: drug with a sigmoidal curve and an EC_{50} (Dm) value of 3.5μM. The effect of doubling the doses varies greatly between the two drugs due to their differing kinetics, highlighting the difficulty of estimating the 'additive effect' of the two drugs (Chou, 2006).

2.4.2.3 Combination index and isobologram method

The combination index (CI) and isobologram method is based on the concept that synergy is characterized by two agents 'working together', as opposed to antagonism where the agents 'work against' each other. This implies the existence of a middle state where there is no interaction. This is referred to as the zone of 'additivity' or 'zero interaction'.

The region of zero interaction can be respresented graphically by an isobole joining points of isoeffective doses of the combination on a graph with axes for doses of each agent (Figure 17). At these doses, CI equals 1 (Equation 5). Synergistic combinations have a CI < 1 and map below the line of additivity while antagonistic combinations have a CI > 1 and are located above the isoeffective isobole. The classic isobologram method was introduced by Loewe in

1928, and later refined by Chou and Talalay (Chou, 2006). Isobolograms representing Effective concentrations (EC) rather than percentages of inhibition effect are most commonly used to offer a more complete overview of the interaction between two agents (Figure 18).

Equation 5 Combination index

$$CI = \frac{E(c_a)}{E(d_a)} + \frac{E(c_b)}{E(d_b)}$$

CI = combination index
$E(c_a)$ = effect for drug a in combination
$E(c_b)$ = effect for drug b in combination
$E(d_a)$ = effect of drug a alone
$E(d_b)$ = effect of drug b alone

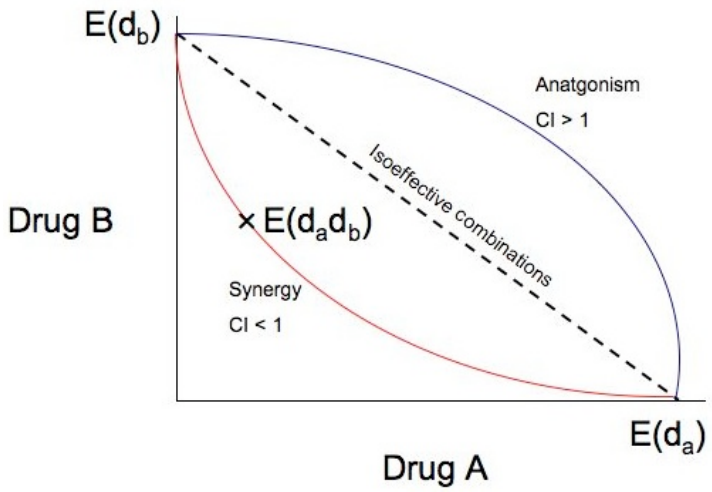

Figure 17 A classic isobologram

Isobolograms showing interactions between drug A and drug B. The dashed line indicates the zero interaction isobole i.e. the loci of combinations that would produce this effect if there was no interaction between the drugs. Combinations are plotted, e.g. $E(d_a d_b)$ at ×. Combinations that plot below the line of additivity are synergistic (CI<1, concave isobole, red line). Those that fall above the isoeffective line are antagonistic (CI>1, convex isobole, blue line). Based on figures in (Berenbaum, 1989).

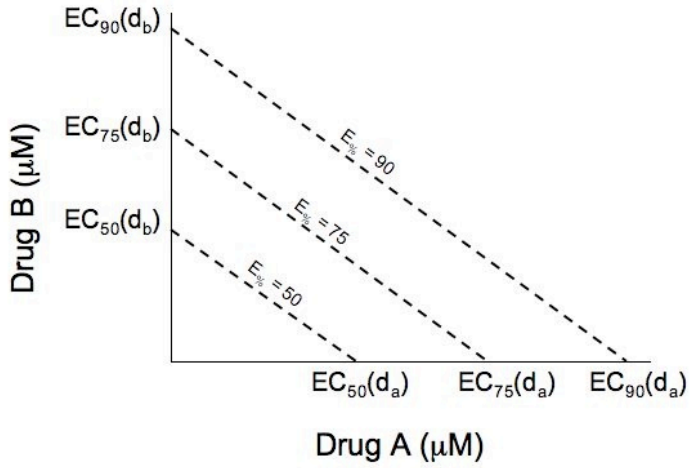

Figure 18 Isoeffective isoboles at varying effect levels

Isoboles can be constructed for differing levels of effectiveness. Each dashed line represents zones of zero interaction at different effect levels (EC_x) for drugs A and B. Based on a figure in (Chou, 2006).

CIs calculated for varying levels of inhibition ($EC_{\%}$) can be plotted on a graph of CI against effect level, as the response for the same drugs can vary according to the doses and inhibition level (Figure 19). For infectious diseases and cancer therapies, synergy at high effect levels such as $EC_{90\text{-}99}$ may be more therapeutically relevant than low levels. Although initially it is recommended to begin synergy studies with equipotent ratios (e.g. EC_{50} D_a:EC_{50} D_b) so that the contribution of each drug can be expected to be equal. However, this is not essential and indeed the ratios can be varied according to the requirements for particular drugs. For instance, the contribution of an agent may be deemphasized if it is known to induce severe toxiticity, has a narrow dose range, or if it exhibits limited availability due to source, price or solubility.

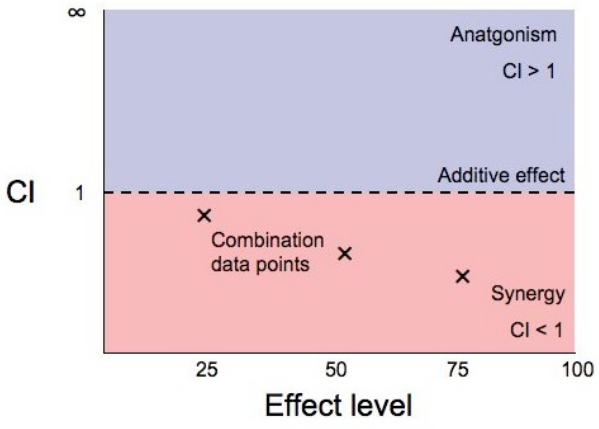

Figure 19 Combination index plot

Combination indices are calculated for each drug combination at varying inhibitory effect levels, according to Equation 5. Drugs typically demonstrate better synergy at higher effect levels. Based on a figure in (Chou, 2006).

2.4.2.4 Theoretical considerations for selecting an appropriate model

The isobole method is generally considered the most valid as it is independent of the mechanism of action of the agents and their dose-response kinetics (Berenbaum, 1989). Computer software has been developed to simplify isobologram analyses. These include CalcuSyn and CompuSyn, the latter being the most recent (Chou, 1997; 2005). This program can handle data analysis of large scale drug combination studies and present data in publication-quality graphics with statistics.

The use of other stategies will sometimes give different answers for the same drugs. For example, if two drugs give 50% inhibition alone, and 90% inhibition when combined, the summation method classifies this as antagonistic (100% inhibition expected) while using the fractional method it is synergistic (75% inhibition expected). However, the choice of analysis depends on the drugs to be investigated, as well as the time and resources available. Nevertheless, it is useful to bear the limitations of each method in mind when considering results reported in the literature.

We chose to assess the interactions between Ad5 and phytochemicals by generating isobolograms and CIs (see Section 2.4.3), since this is the most robust method to determine synergy between two agents. Having established the occurance of synergy between Ad5 and selected phytochemicals at specific ratios, we went on to use the simpler combination assay to conduct a wider screening study with five phytochemicals (as detailed in Method Section 2.4.4, see also Results Sections 3.1.3 and 3.1.4). Synergy between equol and resveratrol with Ad5 mutants was established using the isobologram and CI method using optimised ratios detailed in Section 2.4.3 (see also Results Section 3.5).

2.4.3 Determination of synergy between Ad5 and phytochemicals

Synergy assays were performed by combining 5-fold serially diluted phytochemicals (0.001-500μM) and wild type or mutant Ad5 (0.004-100,000 particles per cell (ppc)) according to Chou and Talalay's combination index method (see Section 2.4.2.3) (Chou & Talalay, 1984). Cells in 96-well plates were treated in triplicate with different fixed ratios of virus and phytochemical. The ratios tested for equol and genistein in the first study with wild-type Ad5 were 1ppc:5nM, 1ppc:1nM, 1ppc:0.2nM and 1ppc:0.04nM (DU145 and 22Rv-1) or 1ppc:10nM, 1ppc:2nM, 1ppc:0.4nM and 1ppc:0.08nM (LNCaP) (see Results Section 3.1.2). These ratios were based on effective ratios used previously in our lab to test for synergy

between Ad5 and chemotherapeutic drugs. In the second study of equol and resveratrol with adenoviral mutants, the ratios tested were lowered to emphasize the contribution of phytochemicals and take into account their low cytotoxicity. The ratios used in this study were 1ppc:125nM, 1ppc:625nM, 1ppc:3125nM, 1ppc:15625nM (DU145 and PC-3) or 1ppc:250nM, 1:1250nM, 1ppc:6250 and 1ppc:31250nM (22Rv-1) (see Results Section 3.5). Cellular viability was determined 6-days post-infection by MTS assay as described in Section 2.4.1.

Dose-response data for each agent alone were compared to dose-response data for combinations at fixed concentration ratios (Figure 20 A and B). By plotting doses of each single agent which killed 50% of cells and connecting these two points by a straight line (Figure 20 C) representing theoretical additive effects, experimental results from combination dose-response EC_{50} values were plotted as coordinates on the isobologram. Data points below the line indicate a synergistic interaction between the agents at the respective combination ratio and those above the line indicate a subadditive/antagonistic effect. Synergistic interactions were also evaluated by determining combination indexes (CIs, Figure 20 D) according to Equation 6 and following a conservative version of Chou's suggested CI ranges for categorizing interactions as synergistic, additive or antagonistic (Chou, 2006; Hallden *et al.*, 2004).

Equation 6 Combination index calculation

$$CI = \frac{EC_{50}V_c}{EC_{50}V_a} + \frac{EC_{50}D_c}{EC_{50}D_a}$$

$EC_{50}V_a$ = EC_{50} for the virus alone

$EC_{50}V_c$ = EC_{50} for the virus in combination

$EC_{50}D_a$ = EC_{50} for the drug alone

$EC_{50}D_b$ = EC_{50} for the drug in combination

CI ≥ 1.2 sub-additive effect (antagonism)

0.8 < CI < 1.2 additive effect

CI ≤ 0.8 supra-additive effect (synergy)

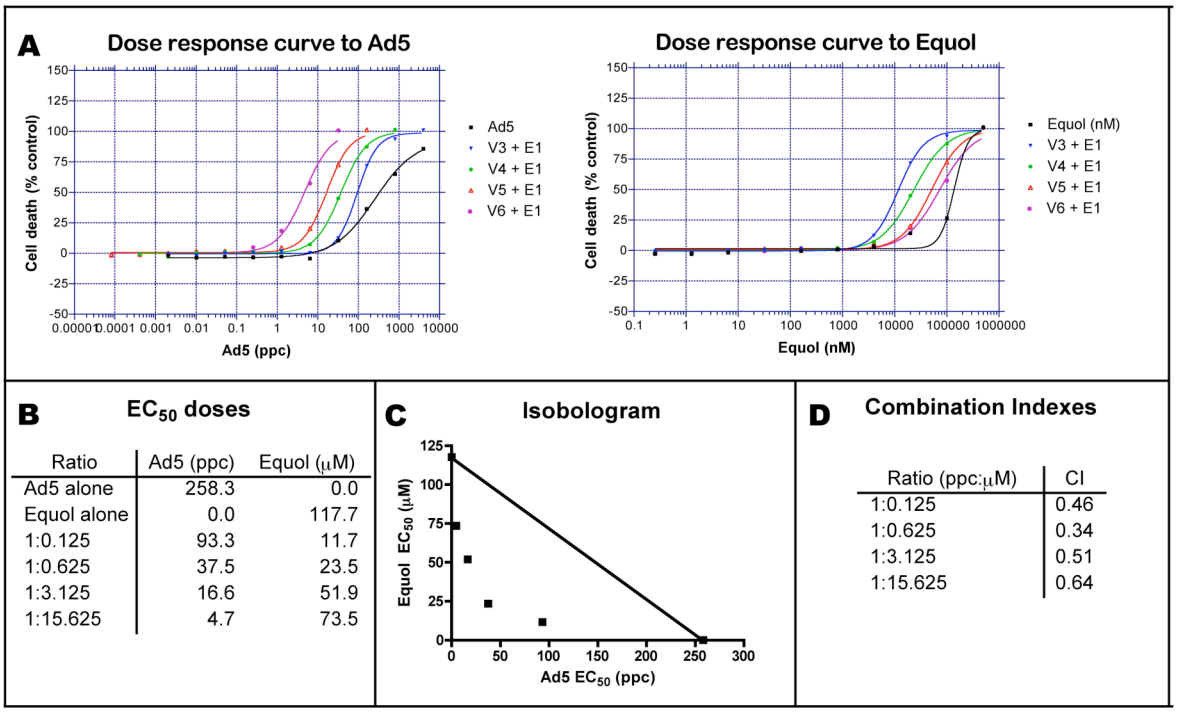

Ratio	Ad5 (ppc)	Equol (μM)
Ad5 alone	258.3	0.0
Equol alone	0.0	117.7
1:0.125	93.3	11.7
1:0.625	37.5	23.5
1:3.125	16.6	51.9
1:15.625	4.7	73.5

Ratio (ppc:μM)	CI
1:0.125	0.46
1:0.625	0.34
1:3.125	0.51
1:15.625	0.64

Figure 20 Example of isobologram analysis of synergy

PC-3 cells were treated with Ad5 and equol at four fixed combination ratios as detailed in Methods Section 2.4.3. Cell viability was determined 6 days post-infection by MTS assay. The isobologram analysis was performed as described above using Excel and Prism softwares to obtain combination indexes (CI) for each ratio.

2.4.4 Combination assays

Combination assays were performed by combining three fixed concentrations of phytochemicals with 5-fold serially diluted wild type Ad5 to generate Ad5 dose-response curves. The combinations selected were based on the dose-response curves and EC_{50} values in each cell line so that <40% of cells were killed by the phytochemicals alone. In the first study, Ad5 was serially-diluted ten times from 1×10^{-1}-2×10^{5}ppc (PC-3) or 1×10^{-1}-1×10^{5}ppc (22Rv-1). The concentrations of phytochemicals used were 5μM, 10μM, 30μM (PC-3) or 40μM (22Rv-1) for curcumin, 1μM (PC-3), 5μM, 10μM, 25μM (22Rv-1) for EGCG, 5μM, 50μM, 100μM for equol, 5μM, 50μM, 70μM (22Rv-1), 100μM and 150μM (PC-3) for genistein, 1μM, 10μM and 50μM for resveratrol. In the second study, equol was used at 10μM, 50μM and 100μM, resveratrol at 5μM, 10μM and 15μM with 5-6 serial dilutions of Ad5 (22Rv-1: 1×10^{-1}-6.4×10^{1}ppc; DU145: 2.56×10^{-1}-1.6×10^{2}ppc; PC-3: 1.28×10^{-1}-4×10^{3}ppc). Cells in 96-well plates were treated in triplicate and read by MTS assay 6-days post-treatments as described in Section 2.4.1.

2.5 Flow cytometry

2.5.1 Infectability

Cells were plated in 24-well plates at a density of 1×10^5 cells in 1ml/well. Cells were pre-treated with equol (100μM) or resveratrol (10μM) or normal 10% FCS medium. After 24h the cells were infected in duplicate in 0% FCS medium (500μl/well) with a non-replicating Ad5-GFP (22Rv-1: 25 ppc; DU145: 50 ppc, PC-3: 300ppc). Infection was allowed to proceed for 2h, after which the infection medium was removed and replaced with normal or phytochemical-containing 2% FCS medium (1ml/well). Uninfected and untreated infected cells were used as controls. Cells were incubated at 37°C until harvesting for flow cytometry by trypsinisation. The cells were washed once with 3ml/sample of cold FACS buffer containing 1mM EDTA (Cancer Research UK Cell Services) and 0.1% BSA (Sigma) in PBS (Cancer Research UK Cell Services). Cells were spun at 1700rpm for 3min and resuspended in 400-800μl FACS buffer. Cells were kept on ice and 2.5μg/ml propidium iodide (PI, Invitrogen) in PBS was added 5min before analysis by flow cytometry. Ten thousand events were acquired by flow cytometry on a FACScalibur cytometer (Becton Dickinson Immunocytometry Systems, Belgium) with CellQuest Pro Software version 4.0.2. The data was analysed by gating live cells on a PI (FL-3) vs. forward scatter (FSC) plot and then quantifying GFP+ cells on a plot of green fluorescence (FL-1) vs FSC and setting the marker to encompass <1% cells on the uninfected, untreated control.

2.5.2 Surface expression levels of Ad5 receptors

Cells (2×10^5 cells/well) were seeded in 6-well plates and allowed to adhere overnight. The following day, the medium was replaced with medium containing equol (100μM) or resveratrol (10μM) or no phytochemical. Cells were treated in duplicate wells. Following 24h incubation, cell surface receptors were detected using mouse monoclonal primary antibodies against CAR (American Type Cell Collection, Manassas, VA, USA, diluted 1:500), $\alpha_V\beta_3$ integrin (Chemicon, USA, diluted 1:400) or $\alpha_V\beta_5$ integrin (Cancer Research UK Mab Services, diluted 1:520). Cells were incubated with the primary antibody in 5% goat serum (DakoCytomation, Glostrup, Denmark) at 4°C for 1h. The cells were then washed and incubated in the dark at 4°C for 1h with a secondary goat anti-mouse $F(ab')_2$ fluorescein isothiocyanate (FITC)-conjugated antibody (Dakocytomation, 1:30 dilution). All dilutions and washes were performed using 3ml/sample cold FACS buffer (composition detailed in Section 2.5.1). To control for background fluorescence, cells were incubated without the primary

antibody but labelled with the secondary antibody. Flow cytometry acquisition and analysis were performed as described in Section 2.5.1.

2.5.3 Cell Cycle analysis

Cells were seeded 24h before treatments in 6-well plates at a density of 2×10^5cells/well. Cells were infected in duplicate with Ad5 (100ppc) or mock infected. After 2h the infection medium was removed and replaced with 2% FCS medium with or without phytochemicals (equol 100μM or resveratrol 10μM). At 24h and 48h after treatments, the cells were harvested by trypsinisation and fixed in 1ml 70% ethanol (Fisher Scientific, Loughborough, UK). To analyse DNA contents of the cells, the samples were washed twice with PBS (3ml/sample) and then stained with 10μg PI and 5μg RNase (Sigma, St. Louis, MO, USA) in a final volume of 500μl PBS. Flow cytometry acquisition was performed as described in Section 2.5.1. A primary gate on forward scatter (FSC) vs. right angle side scatter (SSC) dot plot was used to exclude cell debris. A second gate on a dot plot of pulse-area (FL2-A) vs. pulse-width (FL2-W) was used to exclude doublets. PI fluorescence (FL3-H) was then plotted against cell counts on a linear scale to distinguish between the different phases of the cell cycle. The G_1 marker was set around the first peak at 2N DNA content, and the G_2/S marker was set to encompass the second peak at 4N DNA content. The S phase marker included cells between 2N and 4N DNA content, while the sub-G_1 marker counted cells with ≤2N DNA.

2.5.4 Mitochondrial membrane potential depolarization

Tetramethylrhodamine ethyl ester perchlorate (TMRE, 40nM) is a red fluorescent lipid cation which accumulates rapidly and reversibly in living cells. Loss of fluorescence intensity indicates mitochondrial membrane depolarization which is characteristic of apoptotic cells. Fluorescence can therefore be used as a measure of the mitochondrial potential difference ($\Delta\varphi_m$)

Cells were seeded 24h before treatments in 6-well plates at a density of $1\text{-}2\times10^5$cells/well. Cells were infected in duplicate with Ad5 (22Rv-1 and DU145: 100ppc, PC-3: 300ppc) for 2h and incubated with normal 2% FCS medium or phytochemical-containing medium. Treatment for 24h with the apoptosis-inducer staurosporine at 1μM/well (Calbiochem) was used as a positive control. Cells and media were harvested after 24-96h by trypsinisation, washed once with PBS (3ml/sample), then stained with TMRE (Invitrogen) by adding 40μL 1μM TMRE working stock to cells resuspended in 500μL PBS. Cells were incubated for 20min at 37°C in

the dark. Cells were washed with PBS, stained with 50µl 1µg DAPI (Polysciences, PA, USA) and flow cytometry performed as described in Section 2.5.1. The data were analysed by gating live cells on the FSC vs. SSC dot plot and then plotting DAPI fluorescence (FL-4) vs. TMRE fluorescence (FL-2). Results were shown as the percentage of cells that retained TMRE staining i.e. intact, active mitochondria but were negative for DAPI i.e. intact cellular membrane.

2.5.5 Annexin-V detection of phosphatidylserine externalisation

Cells were seeded and harvested as described in Section 2.5.4. Cells were stained for 30min at 4°C in the dark with Alexa Fluor 488-conjugated Annexin-V in dH_2O containing 10mM HEPES, 140mM NaCl and 2.5mM $CaCl_2$. Cells were washed with PBS, stained with PI and flow cytometry performed as described in Section 2.5.1. The data were analysed by gating live cells on an FSC vs. SSC dot plot. Gated cells were then plotted on a PI fluorescence (FL-3) vs. Alexa 488-Annexin-V fluorescence (FL-1) graph with a quadrant to distinguish between live (PI-negative/Annexin-V-negative), apoptosing (PI-negative/Annexin-V-positive) and dead (PI-positive/Annexin-V-positive) cells.

2.5.6 Active caspase-3 detection

Cells were seeded in 6-well plates at a density of 2×10^5cells/well. The following day, cells were infected with 100ppc Ad5 in serum-free medium. After 2h, the infection medium was aspirated and replaced with 2% FCS medium with or without equol (100µM) or resveratrol (10µM). At 48-96h post-infection, cells and media were harvested by trypsinisation, washed with PBS (3ml/sample) and labelled with a FITC-conjugated anti-active caspase-3 antibody according the the manufacturers' instructions (Active caspase-3 FITC Mab apoptosis kit 1, BD Biosciences Pharmingen, San Diego, CA, USA). Cells were washed with PBS, stained with PI and flow cytometry performed as described in Section 2.5.1. The data were analysed by gating live cells on a PI (FL-3) vs. forward scatter (FSC) plot and then quantifying FITC+ cells on a plot of green fluorescence (FL-1) vs FSC and setting the marker to encompass <1% cells on the uninfected, untreated control.

2.6 Viral replication

2.6.1 Burst assay

Viral replication was determined by performing burst assays in PCa cell lines followed by limiting dilution tissue culture infectious dose $(TCID)_{50}$ assays in JH293 as described in Section 2.3.4. For the burst assay, cells were seeded at a density of 2×10^5 cells/well in 6-well plates. The following day, cells were infected with 100ppc of Ad5 in serum-free medium for 2h. The infection medium was aspirated and replaced with 2% FCS media containing equol (100μM) or resveratrol (10μM) or no phytochemicals, each treatment in duplicate. At 24h, 48h and 72h post-infection, cells were detached by scraping and collected together with the media and stored at -80°C. Burst assay samples were freeze-thawed three times, diluted 100-1000-fold and assayed by $TCID_{50}$ as described in Section 2.3.4.

2.6.2 Quantitative PCR

Viral genome copies were quantified as an indirect measurement of viral replication. Cells were seeded in 6-well plates at a density of $2\text{-}4\times10^5$ cells/well. After adhering overnight, cells were infected in duplicate with 100ppc of Ad5 in 1ml/well serum-free medium for two hours. The infection medium was then removed and replaced with 2ml/well 2% FCS media containing equol (100μM) or resveratrol (10μM) or no phytochemicals. Samples were harvested at 3h, 24h, 48h and 72h post-infection by scraping cells into 200μl/well of PBS. DNA was extracted by adding 20μl/sample of proteinase K (Qiagen, UK) and using purification columns from the DNA Blood Mini Kit (Qiagen) following the manufacturer's protocol. DNA concentrations were determined by Nanodrop (ThermoScientific) and adjusted to 5ng/μl with autoclaved ddH_2O.

Gene copy numbers of hexon were determined for each sample in triplicate using 0.6μl each of 10μM forward and 10μM reverse primers (Table 9) with 10μl Power SYBR Green PCR MasterMix (Applied Biosystems, Warrington, Cheshire, UK) for 2μl DNA template with a total reaction volume of 20μl. The reactions were run on an ABI 7500 RealTime PCR System (Applied Biosystems).

Gene copy numbers were determined as increase in SYBR-Green fluorescence and quantified against a standard curve generated by using Ad5 DNA 10-fold serially diluted from 5×10^8 particles (V_1) in ten steps. One Ad5 particle has a mass of 3.9×10^{-5}pg, and consequently, the mass of the starting dilution of 5×10^8 viral genomes is equal to ≈9.8ng. The starting dilution to

make the standard curve can then be calculated as shown in Equation 7. The analysis was performed using the Sequence Detector Software version 1.9.1 (Applied Biosystems).

Table 9 Hexon DNA primers

Primer	Sequence
Forward	5'-GGACAGGCCTACCCTGCTAAC-3'
Reverse	5'-TGCTGTCAACTGCGGTCTTG-3'

Equation 7 Calculations to generate Ad5 standard curve

Ad5 genome size × average base pair mass = mass of Ad5 genome
$35938bp \times 1.096\times10^{-21} g/bp = 3.94\times10^{-5} pg/genome$

To make $V_1 = 5\times10^8$ genome copies:
Mass of 5×10^8 genome copies = 5×10^8 genomes × 3.94×10^{-5}pg/genome = 19694pg
qPCR reaction volume: 2μl
∴ 19694 ÷ 2 = 9847.012pg/μl

To make 25μL of V_1: (9847.012pg/μl × 25μl) ÷ stock DNA pg/μL = volume of stock DNA to use (μl) + (25μL –answer) dH_2O

2.7 Protein expression levels

2.7.1 Preparation of protein lysates

Cells were lysed in 1× Radio Immuno Precipitation Assay (RIPA) buffer containing protease inhibitor cocktail (Roche Diagnostics, Mannheim, Germany). RIPA buffer was made five-fold concentrated in dH_2O with 0.75M NaCl, 5% NP40, 2.5% deoxycholic acid, 0.5% SDS and 0.25M Tris pH8. One tablet of protease inhibitor cocktail containing inhibitors of serine-, cysteine- and metallo-proteases was used for 10ml 1× lysis buffer. Protein concentrations were determined by Bradford assay according to the manufacturer's instructions (Bio-Rad, Philadelphia, PA, USA) using bovine serum albumin (BSA, Sigma) stock at 1μg/μl to make a standard curve from 0 to 5μg. Protein lysates were diluted to 1μg/μl in loading buffer and stored at -80°C. Loading buffer was made up five-fold concentrated in dH_2O with 2% SDS, 250mM Tris-HCl pH7.5, 5mM EDTA in 50% glycerol, bromophenol blue (0.25% w/v). β-mercaptoethanol was added fresh (5% v/v) before diluting the samples.

2.7.2 Western blotting

Equal amounts of total protein (10-20μg) from the cell lysates were loaded onto 10-15% SDS reducing polyacrylamide gels made using the Hoefer SE-400 Western blot system (Amersham

Biosciences, UK). A PageRuler Prestained protein ladder (Fermentas, UK) was used to evaluate protein size. The samples and the ladder were separated by electrophoresis at 130V in a reducing running buffer containing 25mM Tris, 250mM glycine and 0.1% SDS. After 90min or until the bromophenol blue reached the bottom of the gel. The proteins were transferred from the gel onto polyvinylidene fluoride membranes (Invitrogen) using the iBlot transfer method according the manufacturer's instructions (Invitrogen). Membranes were blocked with 5% (w/v) dry milk (Marvel, Dublin, Ireland) in Tris-buffered saline Tween-20 buffer (TBS-T) containing 20mM Tris-HCl pH 7.4, 500mM NaCl and 0.05% Tween-20. The membranes were incubated overnight at 4°C with primary antibodies (Table 10) in 1.5% BSA (Sigma) in TBS-T, washed and incubated with secondary antibodies conjugated to horseradish peroxidase (DakoCytomation) in TBS-T for 1h at room temperature. The membranes were washed three times for 10min with TBS-T after each antibody incubation. Protein bands were visualised on X-ray film (FujiFilm, Düsseldorf, Germany) using ECL Western Blot Detection Reagent (GE Healthcare, UK).

Table 10 Primary antibodies used for Western blotting

Protein	Antibody	Reference	Company	Dilution
Actin	Goat polyclonal	sc1615	Santa Cruz	1:1000
AR	Rabbit polyclonal	sc816	Santa Cruz	1:1000
β-tubulin	Mouse monoclonal	T4026	Sigma	1:20,000
Beclin-1	Rabbit polyclonal	ab16998	Abcam	1:2000
Active and pro caspase-3	Mouse monoclonal	ab13585	Abcam	1:500
Ad2/5 E1A (13S-5)	Rabbit polyclonal	sc430	Santa Cruz	1:1000
LC3B	Rabbit polyclonal	ab51520	Abcam	1:2000
Ad5 Hexon	Rabbit polyclonal	LF-PA0099	Autogen Bioclear	1:2000
p53	Mouse monoclonal	sc126	Santa Cruz	1:1000

2.8 Visualisation of LC-3 cellular localization

2.8.1 Creation of LC-3-GFP Stably transfected cell lines

22Rv-1, DU145 and PC-3 cells were seeded in 6-well plates at a density of 2×10^5 cells/well and allowed to adhere overnight. The following day, cells were transfected with the pGFP-LC3 plasmid constructed and kindly donated by Prof. Tamotsu Yoshimori (Osaka University, Japan) (Kabeya *et al.*, 2000). The transfection was performed using JetPEI-RGD PolyPlus transfection reagent (Autogen Bioclear, Calne, UK) according to the manufacturer's instructions by adding 2μg DNA in 100μl 150mM NaCl solution to 6μl JetPEI-RGD

transfection reagent in 100µl 150mM NaCl solution to each well. The transfection medium was removed after 24h and replaced with normal 10% FCS medium. Selection was started three days post-transfection using geneticin (Gibco, Paisley, UK) as a selection agent. A previous titration of geneticin (0.4-1.5mg/ml) identified the lowest concentrations of geneticin that killed non-resistant cells in each PCa cell line (Table 11). Medium with geneticin at these concentrations was replaced every 48-72h while transfected and geneticin-resistant cells grew out clonally for approximately 3 weeks. Cells were passaged to larger flasks and frozen stocks of 22Rv-1-GFP-LC3 and DU145-GFP-LC3 cells were made. The transfection efficiency in PC-3 cells was very low and cells did not retain GFP-LC3 expression, so no clones could be expanded, despite selective pressure.

Table 11 Optimal concentrations of geneticin for selecting transfected cells

Cell line	Geneticin (mg/ml)
22Rv-1	1.0
DU145	0.5
PC-3	0.8

Cells were seeded in 24-well plates at a density of 10^5cells/well and exposed to increasing concentrations of geneticin (0.4-1.5mg/ml) in 10% FCS medium. Cells were observed for cell death every day for a week. The concentration selected was the lowest that killed the cells.

2.8.2 Confocal microscopy

Stably transfected 22Rv-1-GFP-LC3 or DU145-GFP-LC3 cells were seeded in 6-well plates with at least one glass coverslip per well at a density of 2×10^5 cells/well. The following day, cells were infected with Ad5 (100ppc) in 1ml/well for two hours or mock infected, incubated in 2ml/well with equol (100µM), resveratrol (10µM) or rapamycin (400nM) in 2% FCS medium, 0% FCS medium or normal 2% FCS medium for 3-48h. Cells were fixed with 1ml/well 3.7% formalin in PBS (Sigma) for 10min at room temperature and permeabilised with 1ml/well 0.5% Triton-X (Sigma) at 4°C for 5min. Cells were washed once with 1ml/well PBS in between each step. Coverslips were mounted onto glass slides with ProLong Gold antifade with DAPI mounting medium (Invitrogen). Coverslips were allowed to dry at room temperature in the dark overnight before storage at 4°C. Cells were viewed using a confocal laser scanning microscope (LSM510 META, Carl Zeiss, Inc., Germany) with a 63×/1.4 NA Plan-Apochromat oil immersion objective. DAPI was excited with a 405nm blue diode laser and GFP with the 488nm line of an Argon laser. High quality (12bit, 1024 pixels) images were acquired using LSM 5 Software, version 3.2.

2.9 Experimental design

The research described in this thesis was carried out following the four steps of the scientific method: formulation of the hypothesis, planning of the experiment, observing and collecting data and interpreting the results. One variable was investigated whilst keeping all others constant. Negative controls, including mock and vehicle controls, were used to ensure the relevance of the effects observed (minimizing false positives). Positive controls were included where possible to confirm the procedure was effective in observing the expected effect, thus minimizing false negatives.

Experimental conditions were set up in duplicates or triplicates to reduce intra-experimental variability. Experiments were repeated wherever possible (at least twice but as indicated) to minimize inter-experimental variance and ensure reproducibility. Quantitative data were analysed statistically as described in Section 2.10. Representative studies are presented for qualitative data, as indicated in figure legends.

2.10 Statistics

Mean values were obtained from from at least two independent experiments in duplicates (i.e. a minimum of four sample data values). The scatter was estimated by calculating standard deviations which are represented on graphs by error bars (Equation 8). The standard error of the sample mean was calculated to determine how precisely the population mean is estimated from the sample mean (Equation 9). Approximately 95% of the values in this theortical sampling distribution of sample means lie within two standard errors of the population mean. The 95% confidence interval of a data set was estimated to evaluate the spread of the samples compared to the mean (Equation 10). These analyses were performed using GraphPad Prism version 4.0c for Macintosh (GraphPad Software, San Diego California, USA).

Equation 8 Standard deviation to determine variability

$$s.d. = \sqrt{\frac{\sum (x_i - \bar{x})^2}{n-1}}$$

$s.d.$ = standard deviation
$\sum$ = sum of
x_i = each sample
$\bar{x}$ = mean of the sample data set
n = number of values in the data set

Equation 9 Standard error of the mean

$$s\mathcal{e}. = \frac{s\mathcal{d}.}{\sqrt{n}}$$

$s\mathcal{d}.$ = standard deviation
n = number of values in the data set

Equation 10 95% confidence intervals

$$CI = \bar{x} - (t' \times s\mathcal{e}.) \text{ to } \bar{x} + (t' \times s\mathcal{e}.)$$

$\bar{x}$ = mean of the sample data set
t' = the 5% percentage point of the *t* distribution for the appropriate degrees of freedom
$s\mathcal{e}.$ = standard error of the mean

Statistical difference between data sets was evaluated for data obtained from at least two independent experiments with duplicates. Two-tailed unpaired *t*-tests and p-values were calculated to test the Null Hypothesis (H_0), stating that any observed difference between sample means is due to sample variation (Equation 11). The Null Hypothesis was rejected when the *t*-value obtained was higher than the tabulated value for the percentage points of the *t* distribution for the corresponding degrees of freedom. This analysis was performed using GraphPad Prism version 4.0c for Macintosh (GraphPad Software, San Diego California, USA). Results were considered statistically significant when $p < 0.05$.

Equation 11 *t*-test for statistical significance

$$t = \frac{x_1 - x_2}{s\mathcal{e}.}$$

$$s\mathcal{e}. = \sqrt{\left[\frac{(n_1 - 1)s_1^2 + (n_2 - 1)s_2^2}{(n_1 + n_2 - 2)}\right]}$$

t = *t*-value
x_1 = mean of data set 1
x_2 = mean of data set 2
s.e. = standard error of the differences
s_1^2 = s.d. for data set 1
s_2^2 = s.d. for data set 2
n_1 = number of data values in set 1
n_2 = number of data values in set 2

3 Results

3.1 Synergistic interactions between Ad5 and phytochemicals

3.1.1 Sensitivity of prostate cancer cell lines to Ad5 and five phytochemicals as single agents

To determine whether phytochemicals might enhance antitumour efficiacy in combination with oncolytic adenoviruses in the treatment of PCa, we first assessed the cytotoxicity of five selected phytochemicals and Ad5 as single agents in two AR-positive (22Rv-1 and LNCaP) and two AR-negative (DU145 and PC-3) cell lines (Figure 21). The percentages of cell death were assessed six days post-infection and used to construct dose-response curves and determine the dose required to kill 50% of cells (Effective Concentration, EC_{50}).

All four human PCa cell lines were sensitive to Ad5-induced cell death to varying degrees. The AR-positive cell lines 22Rv-1 and LNCaP were the most sensitive, with EC_{50} values of 5.6±4.3ppc and 11±2.8ppc respectively (Table 12). DU145 cells were moderately sensitive with an EC_{50} value of 14.1±6.3ppc and PC-3 cells were the least sensitive, with an EC_{50} value of 430±182ppc.

Phytochemicals from soy (equol and genistein) were the least cytotoxic to the PCa cell lines, while curcumin and EGCG had a more potent effect, especially in the androgen-independent cell lines DU145 and PC-3. Equol had an EC_{50} between 139μM (PC-3) and 157μM (DU145) but 22Rv-1 cells were more resistant and had an EC_{50} of 182μM (Table 13). Resveratrol was less cytotoxic than curcumin and EGCG in AR-positive cell lines (22Rv-1 EC_{50} = 110μM, LNCaP EC_{50} = 95μM) whereas in androgen-independent cell lines it had a more significant effect (DU145 EC_{50} = 16μM, PC-3 EC_{50} = 41μM).

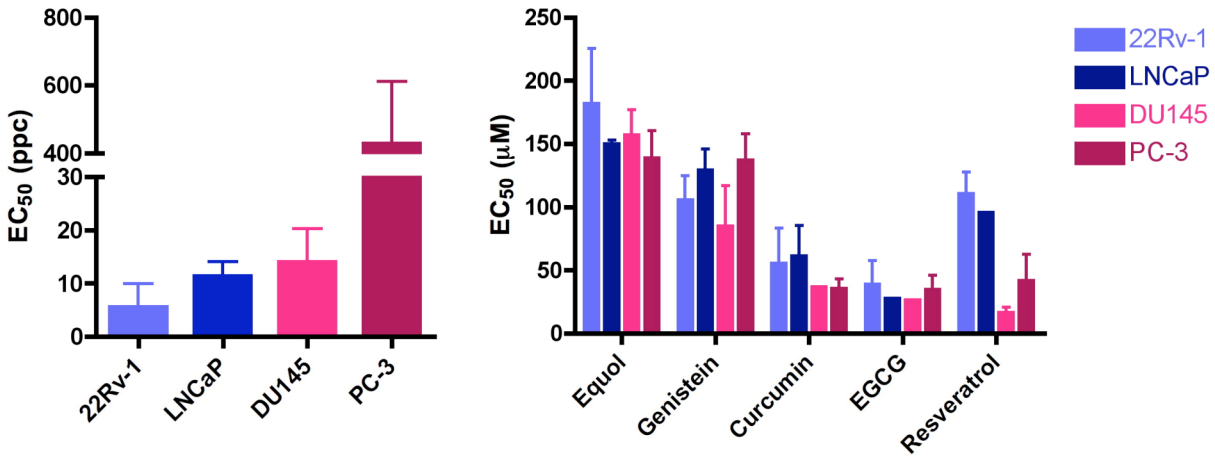

Figure 21 Sensitivity of PCa cell lines to Ad5 and phytochemicals

Dose-response curves were generated by treating cells in triplicate wells with five-fold serially diluted phytochemicals (2.56×10^{-4}–500μM) or Ad5 (1×10^{-2}–2×10^{4}ppc). Results were obtained six days post-infection by MTS cell viability assay. Results are shown as averages (±SD) from ≥2 experiments except for EGCG in LNCaP and DU145 cells, and resveratrol in LNCaP cells where N=1.

Table 12 Effective concentrations killing 50% cells (EC_{50}; ppc) for Ad5 in PCa cell lines

22Rv-1			LNCaP			DU145			PC-3		
Mean	SD	N	Mean	SD	N	Mean	SD	N	Mean	SD	N
5.60	4.30	16	11.40	2.80	2	14.05	6.27	8	440.74	216.83	15

Dose-response curves were generated by treating cells in triplicates with five-fold serial dilutions of Ad5 (1×10^{-2}–2×10^{4}ppc). Results were obtained 6 days post-infection by MTS cell viability assay.

Table 13 Effective concentrations killing 50% cells (EC_{50}, μM) for phytochemicals in PCa cell lines

	22Rv-1			LNCaP			DU145			PC-3		
	Mean	SD	N	Mean	SD	N	Mean	SD	N	Mean	SD	N
Equol	219.9	75.9	11	149.5	3.5	2	156.8	20.2	6	138.7	21.9	9
Genistein	105.2	19.7	4	128.9	17.0	3	84.7	32.3	4	136.8	21.1	4
Curcumin	55.4	27.9	4	61.2	24.4	2	36.4	0.6	2	35.1	7.8	5
EGCG	38.6	18.9	5	27.4	0.0	1	25.9	0.0	1	34.3	11.5	4
Resveratrol	110.3	17.6	5	95.3	0.0	1	16.1	4.8	4	41.4	21.2	7

Dose-response curves were generated by treating cells in triplicates with five-fold serially diluted phytochemicals (2.56×10^{-4}-500μM). Results were obtained six days post-infection by MTS cell viability assay.

3.1.2 Synergistic effects on cell death by combination treatments of Ad5 and phytochemicals at fixed ratios

To determine whether cell killing could be improved by combining Ad5 with phytochemicals, synergy studies were conducted in cell lines most sensitive to Ad5 (22Rv-1, DU145 and LNCaP). The two phytochemicals from soy, equol and genistein, were initially selected for testing as they were the least cytotoxic alone to PCa cell lines, despite their effects on a number of signalling pathways reported in the literature (Setchell *et al.*, 2002; Surh, 2003). The EC_{50} values obtained for Ad5 alone in 22Rv-1 and DU145 cells for these two synergy experiments were much higher than the averages (Table 12). This may be due to the specific batch of cells and virus used.

While the EC_{50} values for equol and genistein were decreased to very low levels at all combination ratios of Ad5, the changes in Ad5 EC_{50} values varied depending on the ratio (Figure 22 and Figure 23). The lowest combination ratios (22Rv-1 and DU145, 1ppc:5nM and LNCaP, 1 ppc:10nM) produced the lowest combination indexes (CI) with both equol and genistein in all three cell-lines, except equol in DU145 cells where this ratio produced a CI of 1.83, indicating antagonism. In this cell line a 25ppc:1nM ratio of Ad5 to equol was synergistic (CI = 0.61), although this ratio was only additive in other cell lines (CI = 1.06 in 22Rv-1 and 1.02 in LNCaP). Genistein also synergised with Ad5 at the lowest combination ratios in each cell line, and at a second ratio (1ppc:1nM, CI = 0.43) in DU145 cells. However, genistein also produced antagonistic effects at three ratios in 22Rv-1 cells (CI≥2), and at two ratios in LNCaP cells (1ppc:2nM, CI = 1.22 and 5 ppc:2nM, CI = 1.85).

These experiments showed that phytochemicals could act synergistically with Ad5, indicating that the concept had potential. However, the study also highlighted the fact that the interactions could also be antagonistic at certain combination ratios. Therefore we next sought a method of screening the five selected phytochemicals over a range of concentrations and conditions.

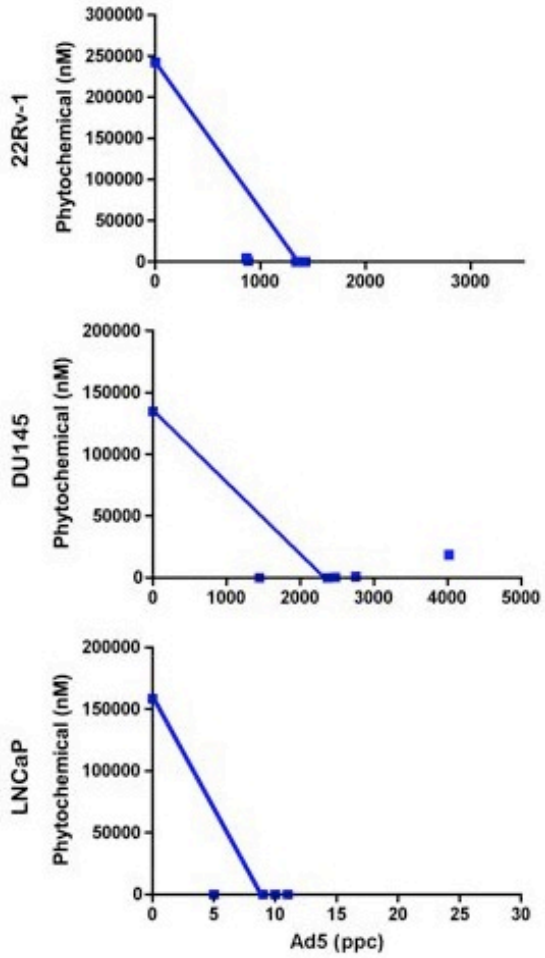

Ratio (ppc:nM)	EC50 Ad5 (ppc)	EC50 phyt (nM)	CI
Ad5 alone	1343	0	
Phyt alone	0	242406	
1:5	867	4352	0.66
1:1	882	930	0.66
5:1	1337	267	1.00
25:1	1426	57	1.06

Ratio (ppc:nM)	EC50 Ad5 (ppc)	EC50 phyt (nM)	CI
Ad5 alone	2369	0	
Phyt alone	0	134791	
1:5	4014	18617	1.83
1:1	2755	996	1.17
5:1	2475	495	1.05
25:1	1448	58	0.61

Ratio (ppc:nM)	EC50 Ad5 (ppc)	EC50 phyt (nM)	CI
Ad5 alone	9	0	
Phyt alone	0	158657	
1:10	5	25	0.53
1:2	9	9	0.96
5:2	11	2	1.13
25:2	10	0	1.02

Figure 22 Isobolograms and combination indexes for Ad5 with equol

Cells were treated with four fixed combination ratios of Ad5 and equol and cell viability determined by MTS assay six days post-infection. Dose-response curves and EC_{50} values were used to construct isobolograms and calculate combination indexes (CI) for each ratio. Ratios are expressed as virus (ppc) to phytochemical (nM). A line is drawn connecting the EC_{50} values of the virus and phytochemical as a single agent. A ratio producing a CI≤0.8 is considered synergistic (CIs in green, below the line), CIs between 0.8-1.2 additive (black, on or near the line) and CI≥1.2 antagonistic (in red, above the line). One experiment shown as a representative of two.

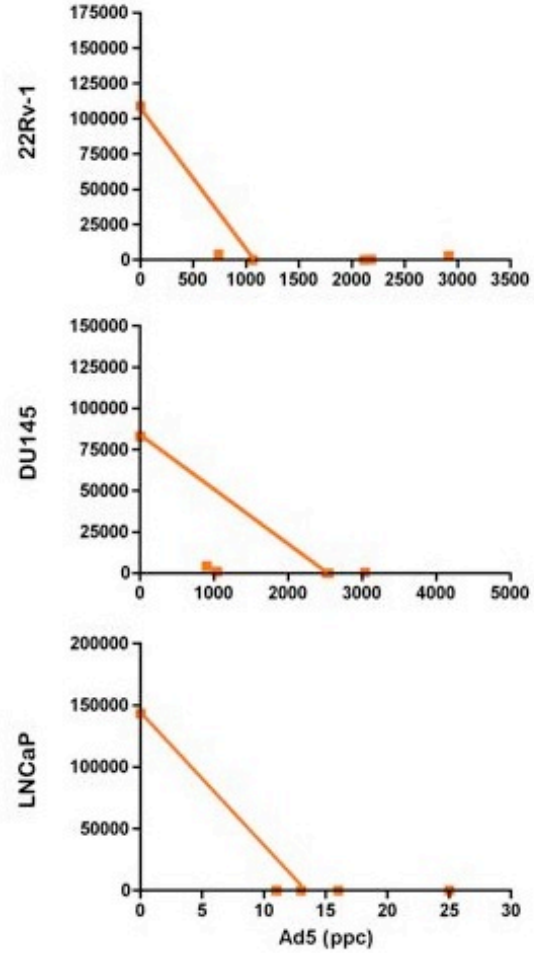

Ratio (ppc:nM)	EC50 Ad5 (ppc)	EC50 phyt (nM)	CI
Ad5 alone	1061	0	
Phyt alone	0	109029	
1:5	740	3907	0.73
1:1	2914	2914	2.77
5:1	2182	437	2.06
25:1	2116	85	2.00

Ratio (ppc:nM)	EC50 Ad5 (ppc)	EC50 phyt (nM)	CI
Ad5 alone	2517	0	
Phyt alone	0	83229	
1:5	897	4485	0.41
1:1	1041	1019	0.43
5:1	3036	607	1.20
25:1	2544	102	1.01

Ratio (ppc:nM)	EC50 Ad5 (ppc)	EC50 phyt (nM)	CI
Ad5 alone	13	0	
Phyt alone	0	143538	
1:10	11	54	0.81
1:2	16	16	1.22
5:2	25	5	1.85
25:2	13	1	0.94

Figure 23 Isobolograms and combination indexes for Ad5 with genistein

Cells were treated with four fixed combination ratios of Ad5 and genistein and cell viability determined by MTS assay six days post-infection. Dose-response curves and EC_{50} values were used to construct isobolograms and calculate combination indexes (CI) for each ratio. Ratios are expressed as virus (ppc) to phytochemical (nM). A line is drawn connecting the EC_{50} values of the virus and phytochemical as a single agent. A ratio producing a CI≤0.8 is considered synergistic (CIs in green, below the line), CIs between 0.8-1.2 additive (black, on or near the line) and CI≥1.2 antagonistic (in red, above the line). One experiment shown as a representative of two.

3.1.3 Fixed concentrations of phytochemicals decrease Ad5 EC_{50} values

The phytochemicals were also screened for synergistic interactions with Ad5 on cell death by combining a fixed dose of phytochemical with a complete dose-response curve for Ad5. This method was chosen over synergy assays because it is easier and faster to perform, therefore allowing more reproducible data to be produced in less time. 22Rv-1 and PC-3 cells were selected for these experiments due to their differing androgen receptor status and sensitivities to Ad5-induced cell death.

Based on the EC_{50} values and dose-response curves for the phytochemicals, three doses of each phytochemical were selected to span a range of concentrations that killed <50% cells (as single agents) (Table 13). Control cells treated only with phytochemical were also included in each experiment to determine the proportion of cell death due to each agent alone. Dose-response curves for Ad5 were corrected using these controls when cell death >10% (Table 14). Typically, this was required only for the highest doses of phytochemicals, except curcumin and equol which usually resulted in <10% cell death even at the highest concentrations used.

Table 14 Cell death (%) induced by phytochemicals alone for combination assays

	22Rv-1			PC-3		
Dose	**low**	**medium**	**high**	**low**	**medium**	**high**
Curcumin	-	-	-	-	-	-
Equol	-	-	5.5	-	-	10
EGCG	-	-	50	-	3.8	25
Genistein	-	8	40	-	-	18
Resveratrol	-	-	32	-	-	37

Dose-response curves for the combination assays were adjusted to account for any significant level of cell death (>10%) induced by the phytochemicals alone after 6 days of treatment. Doses: curcumin: 5μM (low), 10μM (medium), 30μM (high, PC-3); EGCG: 1μM (low, PC-3), 5μM (low, 22Rv-1), 5μM (medium, PC-3), 10μM (medium, 22Rv-1; high, PC-3), 25μM (high, 22Rv-1); equol: 5μM (low), 50μM (medium), 100μM (high); genistein: 50μM (medium), 100μM (high); resveratrol: 1μM (low), 5μM (medium), 50μM (high). –, no adjustment was necessary as cell death was <10%. Cell death percentages shown are from one experiment. Results of the combination assays are shown in Figure 24.

The combination treatments were generally beneficial, with twenty-two out of twenty-eight combinations decreasing the Ad5 EC_{50} value (Figure 24). Genistein (50μM) reduced the Ad5 EC_{50} value by more than 50% in both cell lines but, at a higher dose, genistein increased the Ad5 EC_{50} value (Figure 24). This correlates with the results from the synergy assay in 22Rv-1 cells with genistein where one ratio was synergistic, but the other three were antagonistic (Figure 22).

Curcumin and EGCG reduced Ad5 EC_{50} values at all concentrations in 22Rv-1 cells and at some concentrations in PC-3 cells (Figure 24). However, the decrease was moderate (maximum 40% decrease in 22Rv-1 by both curcumin and EGCG) and the responses were not dose-dependent over the concentrations tested. The greatest decreases in Ad5 EC_{50} value in both cell lines were observed in combinations with equol and resveratrol (Figure 24). In combination with 100μM equol, the Ad5 EC_{50} value was reduced to 8% (22Rv-1 cells) and 40% (PC-3 cells). With 50μM resveratrol, the Ad5 EC_{50} value was reduced to 18% (22Rv-1) and 38% (PC-3).

These effective reductions in Ad5 doses by the addition of equol and resveratrol can clearly be seen by the dose-response curves (Figure 25). The addition of increasing doses of equol and

resveratrol to serially-diluted Ad5 shifted the viral dose-response curves to the left, indicating lower Ad5 EC_{50} values. The exposure of cells to equol or resveratrol caused higher percentages of cell death compared to the same viral dose without phytochemicals. For example, in DU145 cells, 6.4ppc Ad5 alone killed 16.5% cells, but in combination with 10μM, 50μM and 100μM equol, the percentages of cell death increased to 55%, 78% and 90.4% respectively. Similarly, 6.4ppc Ad5 in combination with resveratrol increased cell death in this cell line from 32.3% to 59% (5μM), 83% (10μM) and 89% (15μM), respectively. Equol and resveratrol alone induced <10% cell death in these experiments.

At the lowest doses, equol and resveratrol had no effect in 22Rv-1 cells (99% of the Ad5 EC_{50} value with equol 5μM and 108% of the Ad5 EC_{50} value with resveratrol 1μM), and the interaction was slightly antagonistic in PC-3 cells (133% Ad5 EC_{50}, resveratrol 1μM) (Figure 24). The dose response curve for this combination was shifted to the right, compared to the dose-response for Ad5 alone, indicating a protective effect on cell death by resveratrol in PC-3 cells under these conditions (Figure 25).

These results showed that it was possible to significantly reduce the dose of Ad5 required to kill 50% cells by combining Ad5 with phytochemicals. Equol and resveratrol showed the greatest reductions in Ad5 EC_{50} at concentrations of 50μM (resveratrol) and 100μM (equol). At these concentrations, equol alone killed less than 10% cells and resveratrol alone killed 32% (22Rv-1) to 37% (PC-3) cells (Table 15).

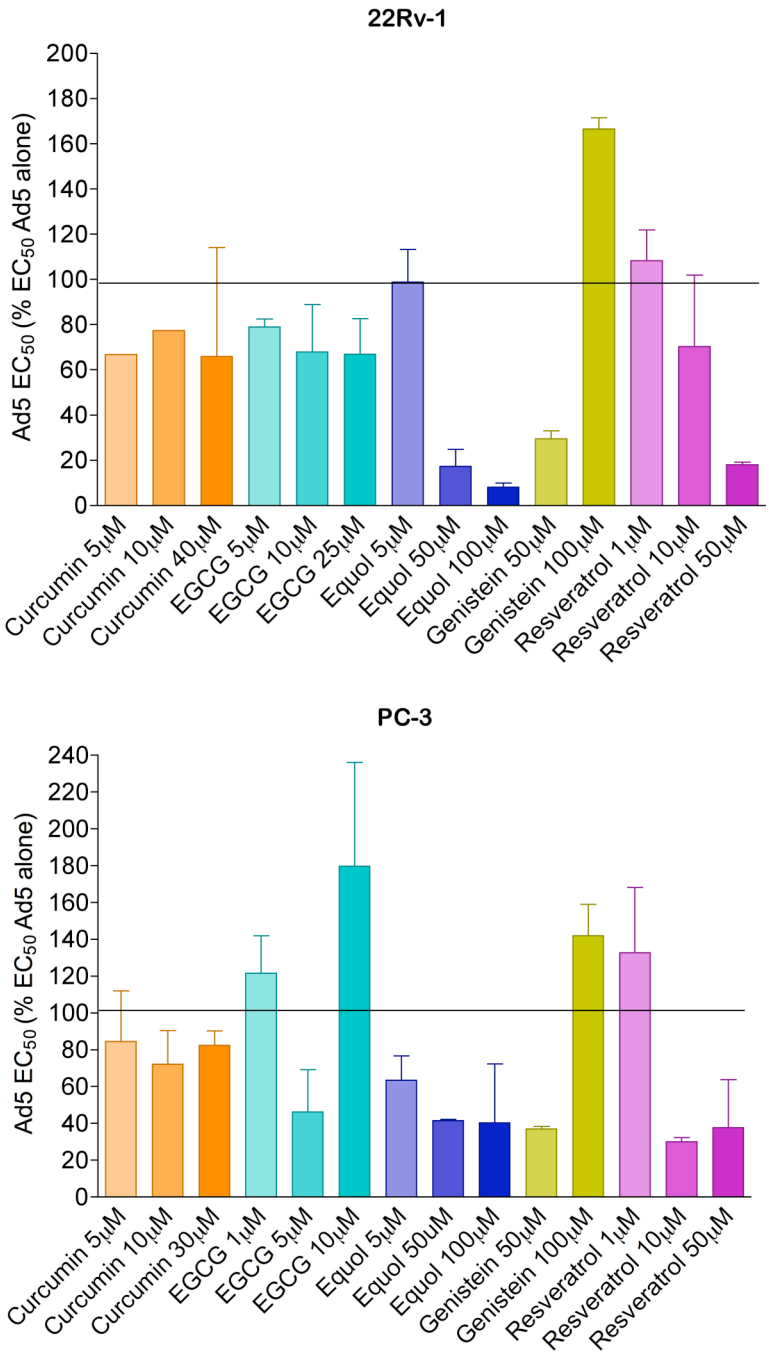

Figure 24 Changes in sensitivity to Ad5-induced cell death in cells treated with phytochemicals

Dose-response curves to Ad5 with and without three doses of phytochemicals were generated by determining cell death 6 days post-infection by MTS assay. Ad5 EC_{50} values were calculated for virus alone and in combination with each respective agent. When cell death due to phytochemical alone was >10%, cell death percentages were corrected as shown in Table 14. Data is expressed as the Ad5 EC_{50} for each combination divided by the EC_{50} for Ad5 alone × 100%. Ad5 EC_{50} percentages below 100% indicate that 50% cells were killed by a lower dose of Ad5 in combination with phytochemical. Results shown as mean of at least two experiments ± SD.

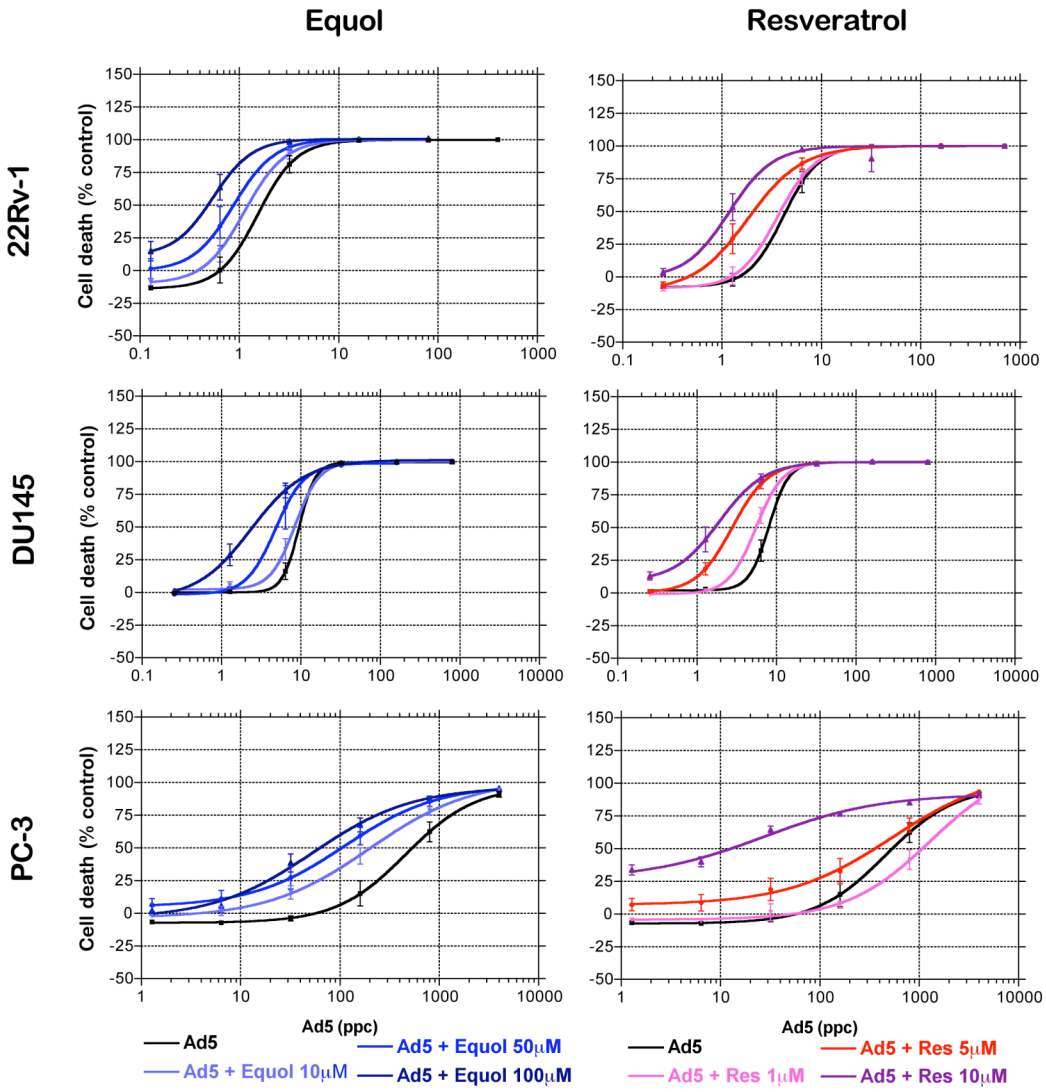

Figure 25 Simultaneous addition of equol or resveratrol reduced Ad5 EC50 independently of AR status of PCa cell lines.

Cells were infected with five-fold serially diluted Ad5 (black) with or without equol or resveratrol at three constant concentrations. Equol 10μM (light blue), 50μM (medium blue), 100μM (dark blue); resveratrol 5μM (pink), 10μM (red), 15μM (purple). Cell death was assayed 6 days post-infection by MTS assay and is expressed as percentage relative to uninfected controls ± SEM. Cell death due to the phytochemicals alone was <10%, except in 22Rv-1 cells treated with 100μM equol (14% cell death) and PC-3 cells treated with 15μM resveratrol (26.7% cell death). N= 3.

Table 15 Reductions in Ad5 EC_{50} values by equol and resveratrol

	22Rv-1		DU145		PC-3	
	Ad5 EC_{50} (ppc)	**Fold decrease**	**Ad5 EC_{50} (ppc)**	**Fold decrease**	**Ad5 EC_{50} (ppc)**	**Fold decrease**
Ad5	**1.41**		**9.58**		**461.00**	
Ad5 + equol 10μM	0.97	1.45	5.74	1.67	197.70	2.33
Ad5 + equol 50μM	0.55	2.54	2.35	4.07	111.30	4.14
Ad5 + equol 100μM	0.25	5.63	1.95	4.90	53.25	8.66
Ad5	**4.15**		**8.04**		**461.00**	
Ad5 + resveratrol 5μM	3.62	1.15	5.50	1.46	583.70	0.79
Ad5 + resveratrol 10μM	1.85	2.24	2.79	2.89	535.10	0.86
Ad5 + resveratrol 15μM	1.26	3.30	1.07	7.51	27.30	16.89

Ad5 EC_{50} doses from the dose-response curves shown in Figure 21. Fold decreases were calculated by dividing the Ad5 EC_{50} value as a single agent by the EC_{50} value of each combination.

3.1.4 The timing of addition of phytochemicals affected virus-induced cell death

To determine whether the order of addition of each agent could further enhance cell death, PCa cells were treated with phytochemicals 24h prior to or after infection with Ad5. In 22Rv-1 cells, pre-treatment for 24h with any of the phytochemicals did not further decrease the EC_{50} values for Ad5 (Figure 26 and Table 16) compared to simultaneous addition for any of the five phytochemicals (Figure 24). In PC-3 cells, pre-treatment with equol, genistein and resveratrol decreased Ad5 EC_{50} values further, compared to simultaneous addition (Figure 24 and Figure 26). However, in PC-3 cells pre-treated with curcumin and EGCG, Ad5 EC_{50} values were much higher than the EC_{50} for Ad5 alone. Under these conditions, exposure to low doses of curcumin and EGCG was actually protecting cells from Ad5-induced cell death rather than sensitising them.

When PC-3 cells were treated with curcumin 24h after infection, no decrease in Ad5 EC_{50} was observed (Ad5 EC_{50} values around 110%). However, the delay in treatment with EGCG was beneficial in both cell lines, indicating that this phytochemical may inhibit the viral lifecycle at an early step but may enhance a later stage.

The greatest increases in cell death for both cell lines were with equol and resveratrol. PC-3 cells were more sensitised when pre-treated for 24h with these phytochemicals, compared to simultaneous addition. In 22Rv-1 cells, simultaneous addition produced the largest decreases in Ad5 EC_{50} with equol and resveratrol, except at the lowest dose of resveratrol where treatment with the phytochemical 24h post-infection further improved the effect on cell death.

Genistein at an intermediate dose also invariably reduced the Ad5 EC_{50} value to around 40% of the EC_{50} for Ad5 alone in both cell lines. This response was not significantly affected by the sequence of addition of the agents, suggesting that a highly specific interaction between the virus and this dose of genistein might be occuring, which inevitably leads to cell death. This effect disappeared at higher doses of genistein.

In summary, each of the five phytochemicals was able to enhance Ad5-induced cell death under certain conditions. Out of the five phytochemicals tested, equol and resveratrol caused the largest decreases in Ad5 EC_{50} values without inducing high cytotoxicity at these doses when given alone. These synergistic effects were consistently observed at different sequences of addition although some cell line-dependent variability occurred with regard to the timing of phytochemical treatment relative to infection. Equol and resveratrol were selected for further study as the most promising phytochemicals in combination with Ad5. The largest decreases in Ad5 EC_{50} values with these phytochemicals were observed in simultaneously treated 22Rv-1 cells and pre-treated PC-3 cells.

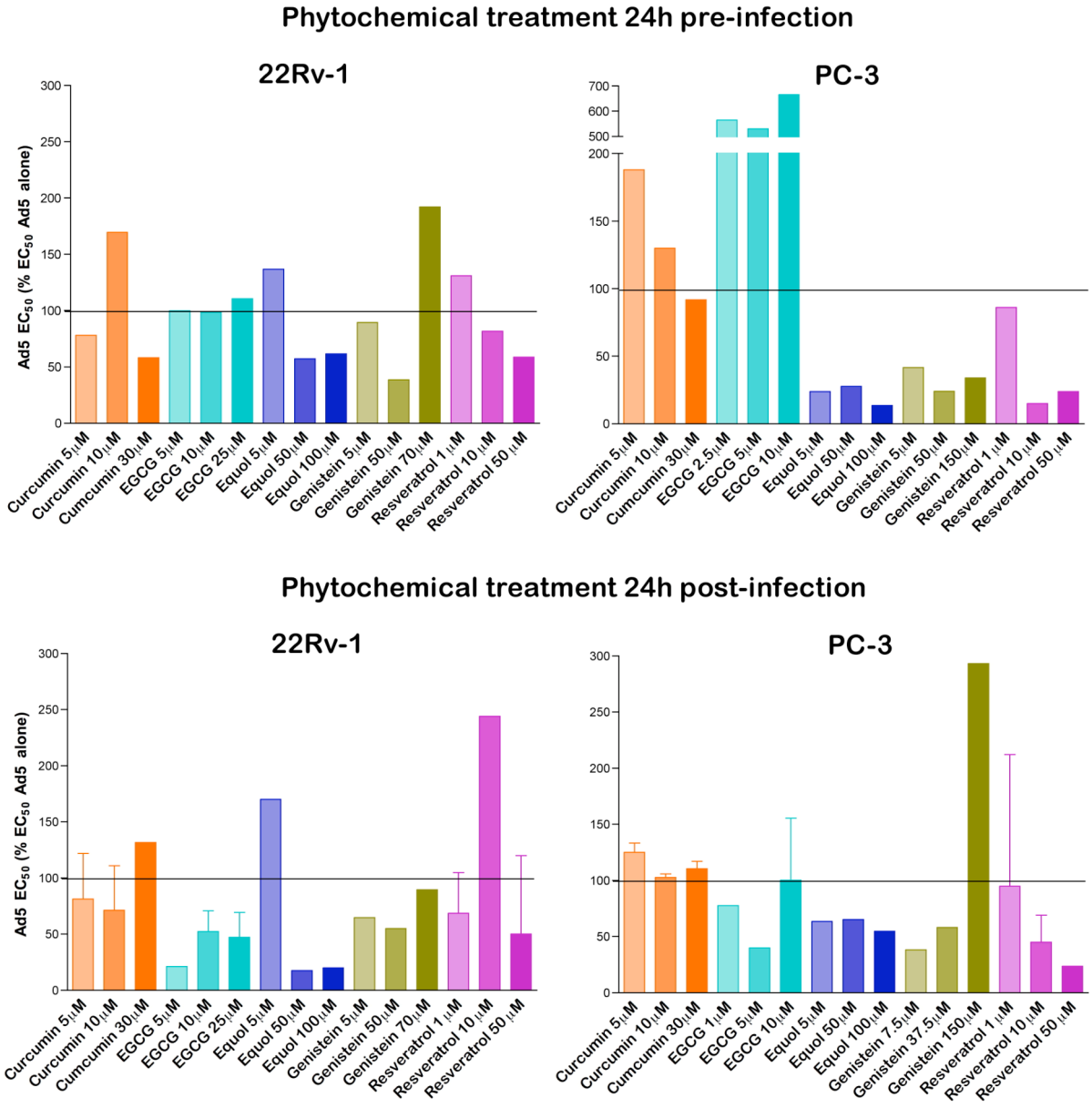

Figure 26 Changes in sensitivity to Ad5-induced cell death in cells treated with phytochemicals 24h pre-infection or 24h post-infection.

Cells were infected with 5-fold serially diluted Ad5 with or without phytochemicals. Cell death was assayed 6 days post-infection by MTS assay. Combination Ad5 EC_{50} values were obtained from dose-response curves and expressed as percentages relative to Ad5 EC_{50} values in untreated cells, percentages below 100% indicate that 50% of cells were killed by a lower dose of Ad5 in combination with phytochemical. Results are shown as averages from 1-2 experiments ± SD.

Table 16 Percentage change in Ad5 EC_{50} values by the addition of phytochemicals at different time-points

	Phytochemical		Ad5 EC50 (%, relative to Ad5 alone)		
Cell line		Concentration (μM)	24h pre-	Simultaneous	24h post-
22Rv-1	Curcumin	5	78.0	66.8	81.4
		10	169.5	77.4	71.3
		30	58.2	65.95 (40μM)	131.7
	EGCG	5	99.9	78.9	21.1
		10	98.6	67.8	52.3
		25	110.6	66.9	47.4
	Equol	5	136.9	98.8	170.2
		50	57.3	17.3	17.5
		100	61.6	8.2	20.1
	Genistein	5	99.5	-	64.9
		50	38.6	29.5	55.0
		70	192.2	166.5	89.6
	Resveratrol	1	130.9	108.3	68.8
		10	81.8	70.3	244.2
		50	58.8	18.0	50.3
PC-3	Curcumin	5	188.0	84.5	125.0
		10	130.0	72.0	102.8
		30	91.8	82.5	110.6
	EGCG	2.5	565.0	121.5	77.7 (1μM)
		5	530.0	46.3	39.9
		10	666.2	179.8	100.3
	Equol	5	24.0	63.4	63.5
		50	27.6	41.5	65.1
		100	13.7	40.3	54.9
	Genistein	5	41.8	-	38.3 (7.5μM)
		50	24.1	37.0	58.3 (37.5μM)
		150	33.9	142.0	293 (150μM)
	Resveratrol	1	86.2	132.7	94.8
		10	14.9	30.0	45.3
		50	23.9	37.7	23.7

Data from Figure 25 and Figure 26 with the percentage change in Ad5 EC_{50} for each combination compared to Ad5 alone. Reductions in Ad5 EC_{50} indicating a synergistic interaction (Ad5 EC_{50} < 60%) are highlighted in green. Antagonistic effects (Ad5 EC_{50} > 110%) are shown in red. - : not done.

3.2 The effects of equol and resveratrol on the adenoviral lifecycle

3.2.1 Equol and resveratrol increased the infectability of PCa cells

Combination assays with Ad5 demonstrated a potent enhancement of cell death by the addition of equol or resveratrol. Since the phytochemicals alone caused cytotoxicity only at the higher concentrations tested, it seemed likely that the phytochemicals might be sensitising the cells to Ad5-mediated cell death. To understand the mechanism behind these interactions, the effects of the phytochemicals on various steps of the viral lifecycle were investigated. The first challenge the virus has to overcome during viral infection *in vitro* is entry into the host cell. As discussed in Section 1.2.3, the infectability of different cell lines is dependent on the cellular expression levels of adenoviral receptors, such as CAR which mediates viral docking to the cell. The possibility that the phytochemicals might be increasing cellular infectability via an upregulation of Ad5 receptors was considered.

The infectability of four PCa cell lines was first determined in untreated cells using a non-replicating GFP-expressing Ad5 mutant. PC-3 cells were the least infectible, with less than 1% infected after 48h infection with 100ppc (Figure 27). The most infectible cell line was 22Rv-1, with more than 50% cells infected by a dose of 100ppc. DU145 and LNCaP cells were of intermediate sensitivity to adenoviral infection. This pattern of infectability paralleled the observed sensitivity to Ad5-induced cell death (Figure 21).

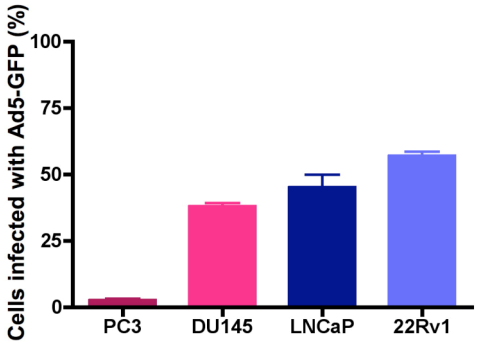

Figure 27 Infectability of PCa cell lines

Cells were infected with Ad5-GFP (100ppc) for two hours. Cells were then incubated with normal 2% FCS medium for a further 48h, after which cells were harvested by trypsinisation and analysed by flow cytometry. Cells positive for GFP above background level were considered infected. Results shown are averages of duplicates from one experiment ± SD.

The effect of phytochemical treatment on infectability was determined in 22Rv-1, DU145 and PC-3 cells at concentrations shown to act synergistically with Ad5 (Figure 25). After infection with Ad5-GFP, both equol and resveratrol increased the percentage of GFP-positive cells in all three cell lines, indicating a greater proportion of infected cells (Figure 28, upper graphs). Resveratrol was slightly more potent than equol, except in PC-3 cells where equol induced a greater proportion of infected cells than resveratrol, although this trend was not statistically significant compared to untreated control cells (Figure 28, upper right graph).

Median GFP fluorescence was also increased by both phytochemicals (Figure 28, lower graphs). The median GFP fluorescence represents the average viral load per cell. Equol was more potent than resveratrol and more than doubled the average viral load per cell in 22Rv-1 and PC-3 cells.

The increased Ad5-GFP uptake in response to treatment with equol and resveratrol was comparable to that observed in cells treated with trichostatin A (TSA, Figure 29). TSA is a well-known enhancer of adenoviral infectability via the upregulation of CAR expression in target cells (Hemminki *et al.*, 2003).

Increased viral uptake was also observed by measuring viral genome copies 3h post-infection with Ad5 (Figure 30). Equol doubled infectability in 22Rv-1 and DU145 cells, and increased the viral load in PC-3 cells from 72 to 96 viral copies/5ng DNA. Resveratrol doubled infectability in 22Rv-1 and PC-3 cells and increased the viral load in DU145 cells from 152 to 215 viral copies/5ng DNA.

Taken together, these results indicate that equol may sensitise a proportion of cells to Ad5, and that these cells become highly permissible to viral infection, resulting in a doubling of the average viral load per cell. On the other hand, exposure of cells to resveratrol enables a greater proportion of cells to become infected, although the average viral load per cell does not reach the levels achieved by treatment with equol.

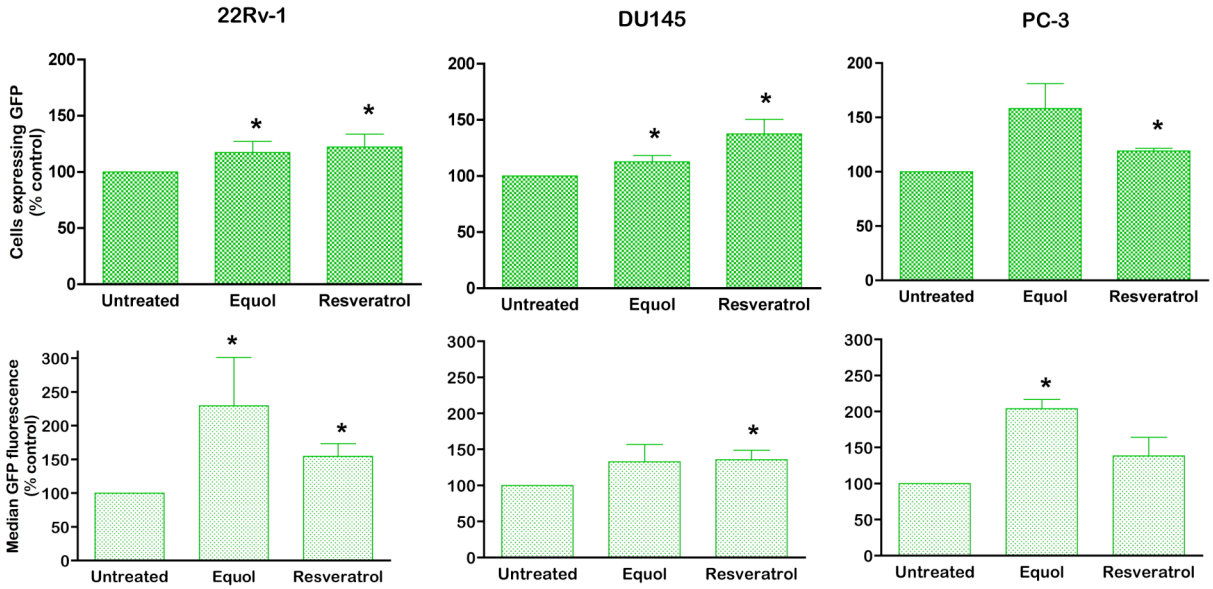

Figure 28 The infectability of cells treated with phytochemicals

Cells were incubated with equol (100μM) or resveratrol (10μM) or normal medium alone. After 24h exposure to the phytochemicals, the cells were infected with a non-replicating Ad5-GFP virus at doses determined to achieve around 30% infected cells (22Rv-1: 25 ppc; DU145: 50 ppc, PC-3: 300ppc). Infection was allowed to proceed for 2h, after which the infection medium was removed and replaced with normal or phytochemical-containing 2% FCS medium. Flow cytometry was performed 48h post-infection. Upper panels show the proportion of GFP-positive cells. The lower panel represents the average viral load per cell, as measured by median GFP fluorescence. Results are presented as a mean of duplicates in at least two experiments ± SD. * = $p < 0.05$.

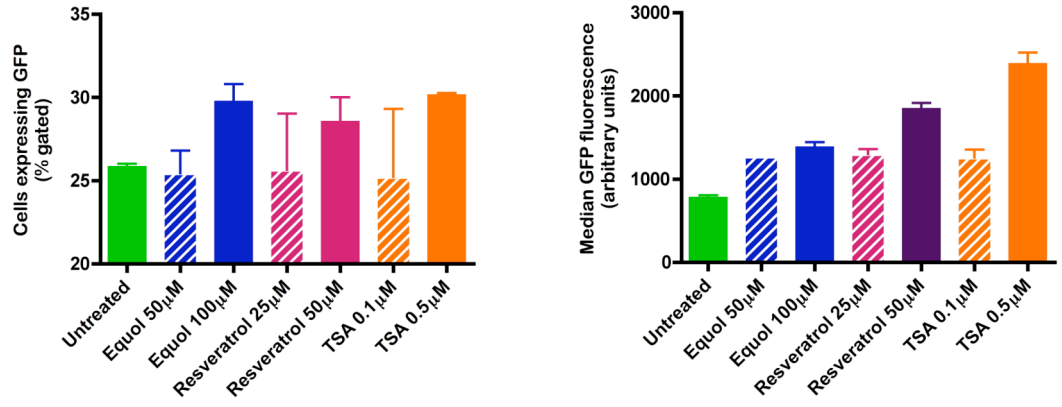

Figure 29 The infectability of 22Rv-1 cells treated with equol, resveratrol or trichostatin A (TSA)

22Rv-1 cells were infected with a non-replicating Ad5-GFP virus (30ppc) for 2h, after which the medium was removed and replaced with 2% FCS medium containing equol (50μM or 100μM), resveratrol (25μM or 50μM) or TSA (0.1μM or 0.5μM). Cells were harvested 48h post-infection and analysed by flow cytometry. The left panel show the percentage of GFP-positive cells. The right panel represents the average viral load per cell, as measured by median GFP fluorescence (arbitrary units). Results are expressed as the average of duplicates from one experiment ± SD.

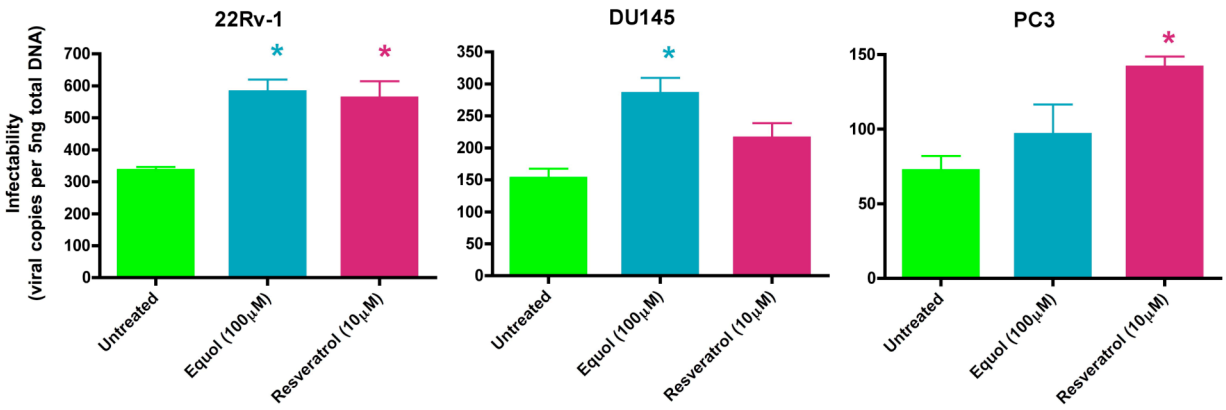

Figure 30 Infectability of PCa cells detect by qPCR

Cells were infected with Ad5 (22Rv-1 and DU145: 100ppc, PC-3: 300ppc) for 2h, after which the infection medium was removed and replaced with normal or phyochemical-containing (equol 100μM or resveratrol 10μM) 2% FCS medium. Cells were harvested 3h after the beginning of the infection (i.e. the cells were exposed to phytochemicals for 1h). DNA was extracted, quantified and hexon gene copy numbers were determined in duplicate for each sample by qPCR as described in Methods Section 2.6.2. Results are shown as mean of one experiment ± SD. * = $p < 0.05$ compared to untreated cells.

3.2.2 Equol and resveratrol enhanced the cellular expression of adenoviral receptors

To determine whether the higher infectability observed in the presence of equol and resveratrol might be due to increased levels of cell surface receptors, the expression of three known adenoviral receptors, the integrins $\alpha_V\beta_3$ and $\alpha_V\beta_5$ and the Coxsackie Adenovirus Receptor (CAR), was analysed by flow cytometry. This was done in 22Rv-1, DU145 and PC-3 cells to support the infectability data, and LNCaP cells were also included.

Untreated PC-3 cells expressed very low levels of all three adenoviral receptors. Integrins $\alpha_V\beta_3$, $\alpha_V\beta_5$ and CAR were present on only 4.8%, 6.5% and 2.9% of cells (Figure 31). This is likely to have contributed to the low infectability of this cell line (Figure 27) and has been previously described (Okegawa *et al.*, 2000). DU145 cells expressed moderate to high levels of all three receptors with CAR present on 99% cells, 44% of cells expressing $\alpha_V\beta_3$ integrins and 11% of cells expressing $\alpha_V\beta_5$ integrins. In contrast, 22Rv-1 and LNCaP cells did not appear to express either class of integrin (<3% cells), although 66% (22Rv-1) and 88% (LNCaP) cells expressed CAR.

The proportion of DU145 cells expressing $\alpha_V\beta_3$ integrins was increased from 44% to 58% by equol and to 67% by resveratrol. In PC-3 cells $\alpha_V\beta_3$ integrins were expressed on 4.8% cells and this was increased to 9% by equol and 13.3% by resveratrol. The proportion of cells expressing $\alpha_V\beta_5$ integrins was also increased in DU145 cells by equol from 11% baseline to

13.7% cells and by resveratrol to 29.3% cells. However, in PC-3 cells, equol caused a slight decrease in $\alpha_V\beta_5$ integrin expression from 6.5% to 4.6%, although resveratrol induced expression in 11.2% cells. Neither of the phytochemicals induced expression of these integrins in 22Rv-1 cells.

CAR expression was already maximal in DU145 cells, so no increase was detectable in response to phytochemical exposure. However, phytochemical treatment increased the percentage of 22Rv-1 cells expressing CAR from 66% to 71% by equol and 73% by resveratrol. This effect was not seen in PC-3 cells where CAR expression remained <4%. In LNCaP cells, the percentage cells expressing CAR was decreased by equol from 88% to 63% while resveratrol had no effect.

Considering the level of expression of all three adenoviral receptors, DU145 cells would be predicted to be the most, and PC-3 cells the least permissive cell line to Ad5 infection, since very few of those cells express any of the receptors. PC-3 cells were indeed the most resistant to Ad5 infection (Figure 27). However, the most infectible cell line was not DU145 but 22Rv-1 cells. This may indicate that additional factors, such as unidentified adenoviral receptors, could be involved in the infection process. Alternatively, this could be due to differences in transcription efficiency from the CMV promoter which controls GFP expression.

In summary, both equol and resveratrol increased the expression of one or more of the three known adenoviral receptors in three PCa cell lines, 22Rv-1, DU145 and PC-3 cells, but not in LNCaP cells.

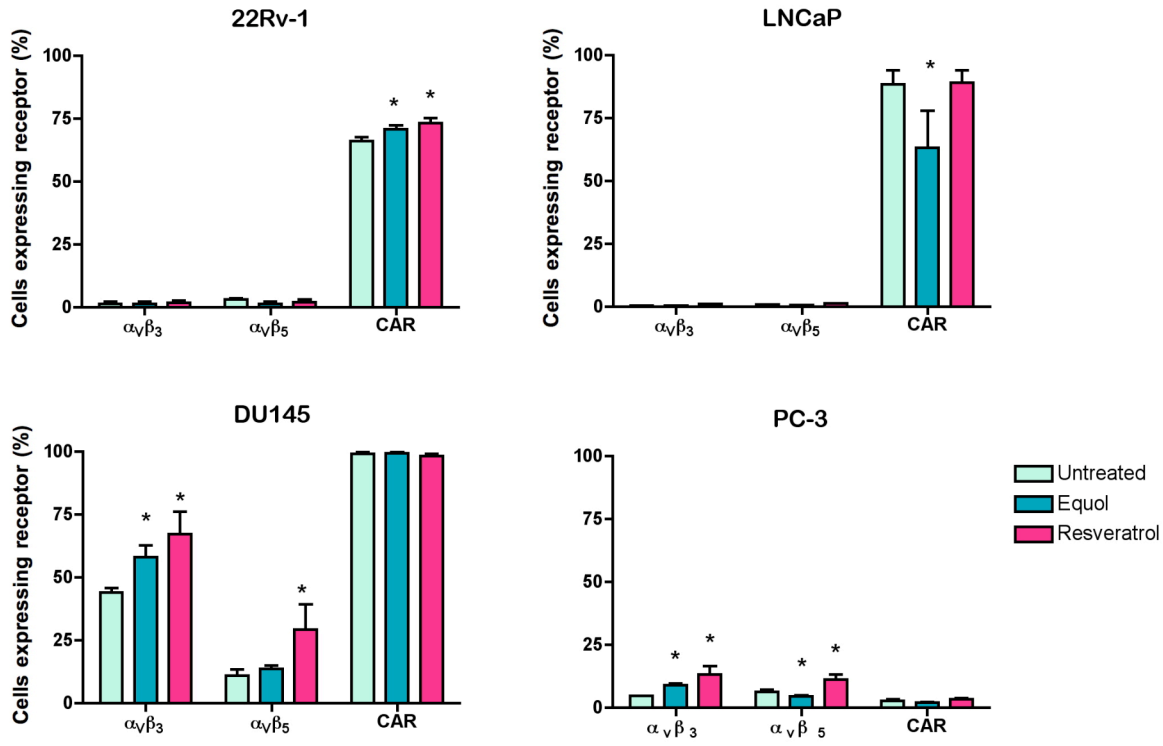

Figure 31 Cellular surface expression levels of three Ad5 receptors, CAR and the integrins $\alpha_v\beta_3$ and $\alpha_v\beta_5$

Cells were treated with equol (100μM) or resveratrol (10μM) or left untreated. After 24h, the proportion of receptor-positive cells was determined by flow cytometry. Results are presented as a mean of duplicates in two experiments ± SD. * = $p < 0.05$ compared to untreated cells.

3.2.3 The effect of phytochemicals on viral replication

To determine whether the increased infectability of cells treated with phytochemicals was paralleled by enhanced viral replication, viral titres were determined in cells treated with equol or resveratrol. These experiments were performed in 22Rv-1, DU145 and PC-3 cells to follow up on the data obtained from the infectability experiments described in Results Section 3.2.1.

In all three cell lines, viral titres increased up to 48h and plateaued at 72h (Figure 32). DU145 cells supported the highest levels of replication, with $1.57\times10^4\pm5.3\times10^3$ pfu/cell after 72h. Despite the higher infectability of 22Rv-1 cells, viral replication in this cell line was significantly lower than in DU145, with $1.9\times10^3\pm7.1\times10^2$ pfu/cell at 72h. PC-3 cells supported the lowest levels of viral replication, with titres of $1.1\times10^3\pm4.1\times10^2$ pfu/cell, which was also significantly lower than in DU145 cells. The levels of replication at 72h in 22Rv-1 and PC-3 cells were not statistically different ($p = 0.06$).

Viral replication in DU145 and PC-3 cells treated with equol or resveratrol was significantly reduced from 24h to 72h post-infection. Resveratrol reduced viral titres in both cell lines 10-fold. A smaller decrease was detected in resveratrol-treated 22Rv-1 cells which was statistically significant at 72h post-infection.

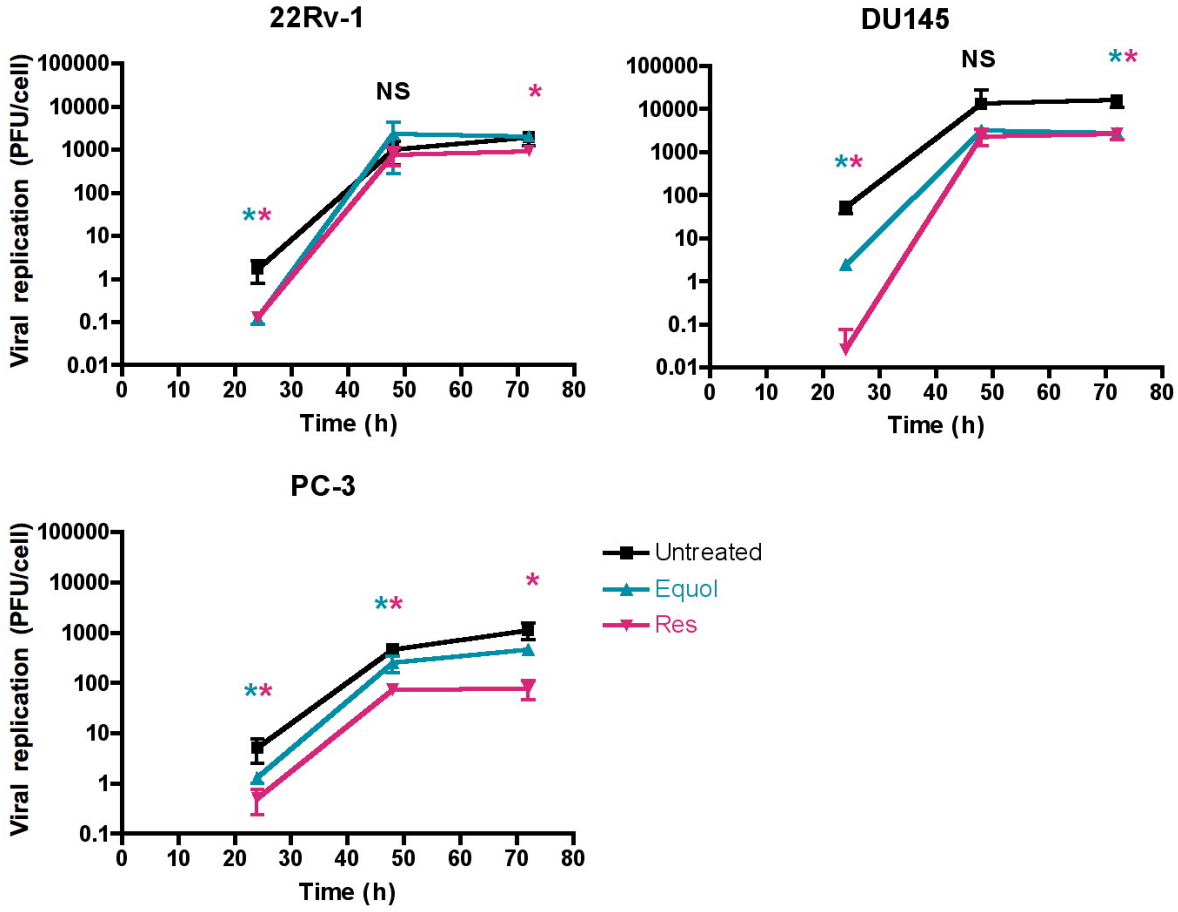

Figure 32 Viral replication over time determined by $TCID_{50}$ assay

Cells were infected with Ad5 (100ppc) and cultured in medium without (black lines) or with equol (100μM, blue) or resveratrol (10μM, pink). Cells and media were harvested at 24h, 48h and 72h post-infection and viral titres were determined by $TCID_{50}$ assay as described in Methods Section 2.6.1. One experiment, representative of 2-3. Results shown as mean of triplicates ± SD. * = $p < 0.05$ for viral titres in phytochemical-treated cells compared to untreated cells. NS = not statistically significant ($p > 0.05$) for treated cells compared to untreated cells.

To verify that the decreased viral titres were not simply due to a reduction in the proportion of viable cells, cell death under the conditions tested in the $TCID_{50}$ assay was determined over time (Figure 33 and Table 17). At 72h, there was a significant amount of cell death in cells treated with combinations, although virus alone did not induce any cytotoxicity. At this time-point, Ad5 and 100μM equol killed nearly 70% DU145 cells and 15% PC-3 cells, while Ad5

with 10μM resveratrol killed around 50% DU145 cells and 32% PC-3 cells. However, there was less than 6% cell death under all conditions up to 48h in all three cell lines.

This demonstrates that the observed reductions in viral titres up to 48h were likely due to inhibitory effects on replication by the phytochemicals. At 72h, the high levels of cell death in response to combination treatments probably also contributed to the reduced replication in DU145 and PC-3 cells. The decreased replication due to resveratrol in 22Rv-1 cells after 72h may also be due to a reduced viability of the cells (14% cell death under these conditions).

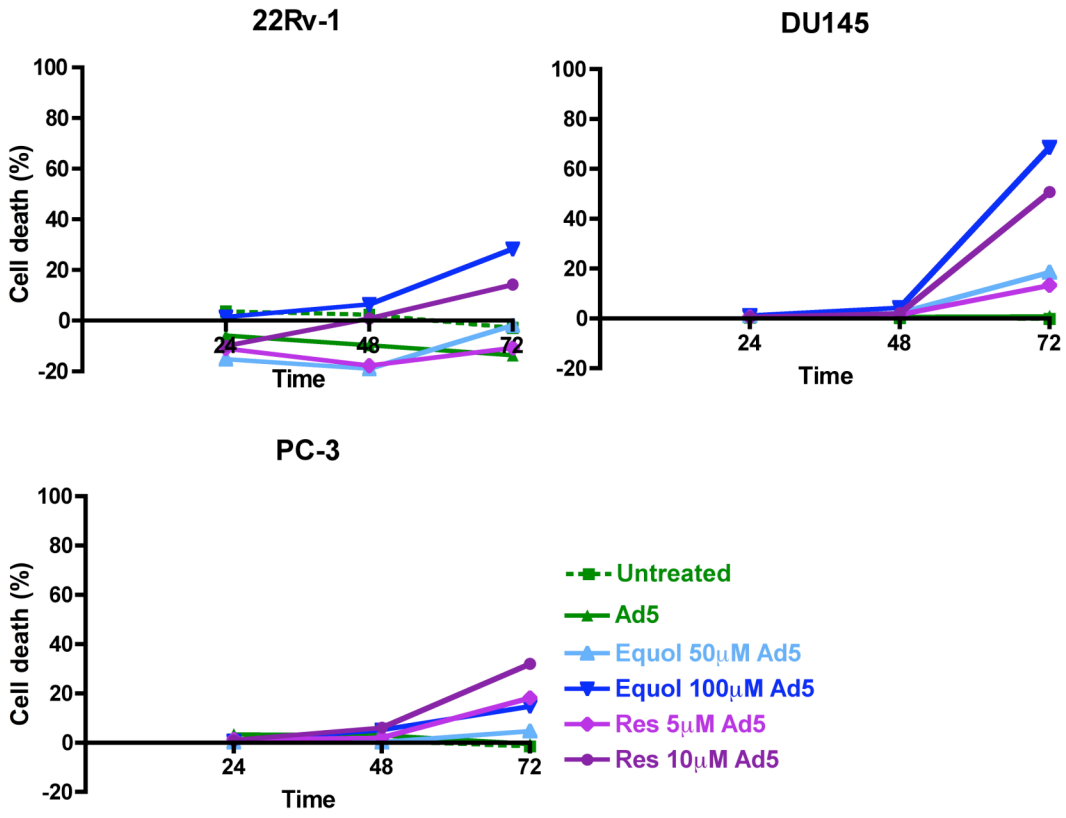

Figure 33 Cell death due to combination treatments under the conditions used for viral replication assays

Cells were seeded in 96-well plates and infected in triplicate with 100ppc (22Rv-1 and DU145) or 300ppc (PC-3) in 50μl serum-free medium. After 2h, the infection medium was replaced with normal or phytochemical-containing 2% FCS medium. Cell viability was assessed 24h, 48h and 72h post-infection by MTS assay. N=1.

Table 17 Cell death due to combination treatments under the conditions used for viral replication assays

	Time (h)	Untreated	Equol 50μM	Equol 100μM	Res 5μM	Res 10μM
22Rv-1	24	3.63	-8.52	8.68	0.83	2.29
	48	2.37	-17.67	**16.36**	-0.83	**15.61**
	72	-2.87	-0.39	**35.49**	6.37	**36.65**
	168	2.04	**38.27**	**65.7**	**43.13**	
	Time (h)	Ad5	Equol 50μM Ad5	Equol 100μM Ad5	Res 5μM Ad5	Res 10μM Ad5
	24	-5.83	-15.11	1.43	-10.99	-9.97
	48	-9.66	-18.98	6.45	-17.77	0.85
	72	-13.63	-1.81	**28.37**	-10.71	**14.29**
	168	**80.6**	**97.37**	**98.09**	**95.85**	**82.54**
DU145	Time (h)	Untreated	Equol 50μM	Equol 100μM	Res 5μM	Res 10μM
	24	0.33	0.8	0.71	0.09	-0.1
	48	0.23	1.41	3.25	1.09	1.42
	72	-0.17	6.87	**55.51**	5.49	**30.98**
	168	-0.04	**14.57**	**83.95**	**98.3**	
	Time (h)	Ad5	Equol 50μM Ad5	Equol 100μM Ad5	Res 5μM Ad5	Res 10μM Ad5
	24	0.6	1.16	1.17	0.53	0.63
	48	0.66	2.25	4.39	1.58	2.16
	72	0.94	**18.53**	**68.61**	**13.38**	**50.71**
	168	**95.65**	**98.71**	**99.07**	**98.97**	**96.44**
PC-3	Time (h)	Untreated	Equol 50μM	Equol 100μM	Res 5μM	Res 10μM
	24	1.36	-1.28	-0.59	-0.92	-0.77
	48	0.61	-1.7	2.89	-0.64	3.3
	72	-1.44	1.97	8.63	**14.7**	**24.67**
	168	-0.61	**22.31**	**54.85**	**34.3**	
	Time (h)	Ad5	Equol 50μM Ad5	Equol 100μM Ad5	Res 5μM Ad5	Res 10μM Ad5
	24	3.41	0.28	0.73	1.4	1.09
	48	3.04	0.24	5.29	2.04	6.1
	72	-0.53	4.71	**14.86**	**18.26**	**32.09**
	168	5.46	**69.29**	**84.83**	**68.51**	

Data from Figure 33 with percentage cell death (% compared to untreated and uninfected control cells) at each condition for each time-point. In red are the combination treatments of Ad5 with phytochemicals after 48h and 72h. Those causing significant levels of cell death are highlighted in bold.

Viral replication was also assayed by flow cytometry using a replicating adenovirus expressing GFP (Figure 34). Replication as detected by FACS appeared to increase steadily over 24-72h. By 72h resveratrol caused a statistically significant reduction in the proportion GFP-positive cells in both DU145 and PC-3 cells. These findings are in agreement with the $TCID_{50}$ assay results (Figure 32).

However, in contrast to the $TCID_{50}$ assay results, resveratrol increased the percentage of GFP-positive 22Rv-1 cells at 72h. As expected from the $TCID_{50}$ assays, equol increased viral replication in 22Rv-1, but surprisingly, also in PC-3 cells. The higher infection load used for PC-3 for FACS (300ppc, three times the dose used in the $TCID_{50}$ assay) could have had an impact on the results, the high dose overcoming inhibition by equol but not by resveratrol.

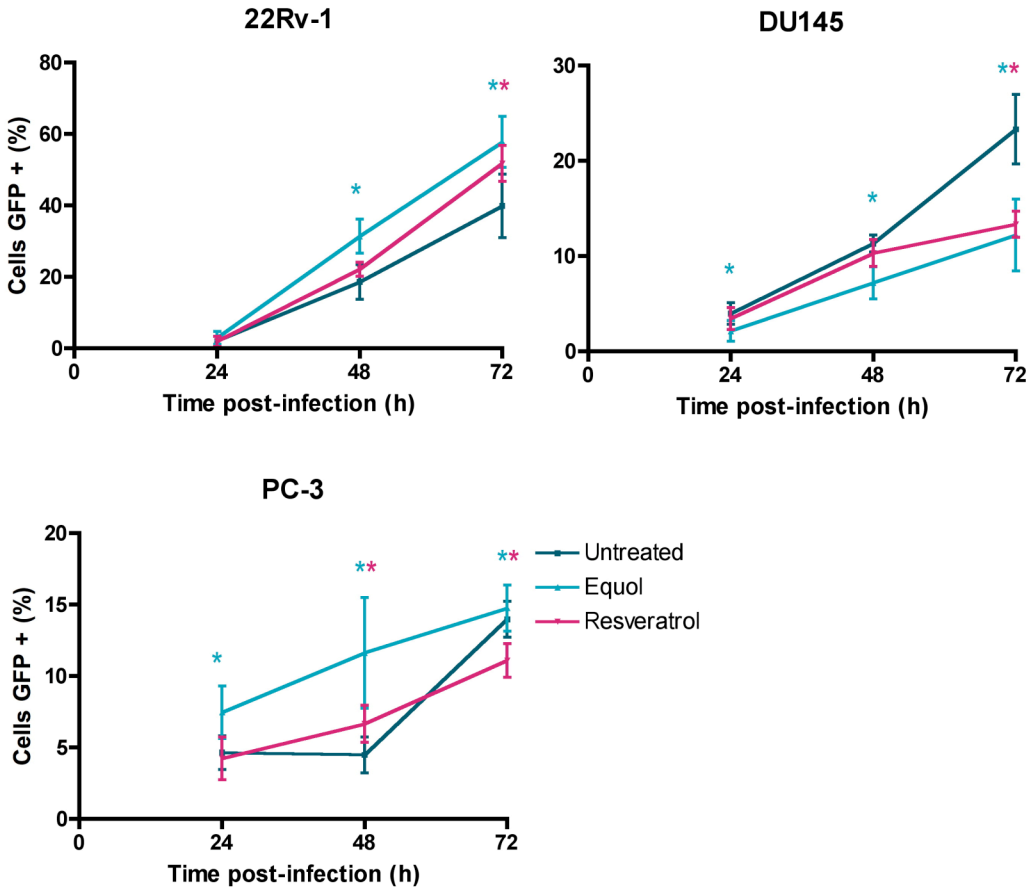

Figure 34 Flow cytometric detection of a replication-competent GFP-expressing Ad5 in phytochemical-treated cells

After 24h pre-treatment with equol (100μM) or resveratrol (10μM), cells were infected with a replicating Ad5-GFP virus (22Rv-1: 25ppc, DU145: 50ppc, PC-3: 300ppc). After 2h, the infection medium was removed and replaced with normal or phytochemical-containing (equol 100μM, resveratrol 10μM) 2% FCS medium. Cells were analysed by flow cytometry at 24h, 48h and 72h post-infection. Results are shown as mean of three experiments ± SD. * = $p < 0.05$ compared to untreated cells.

To resolve the differences between the results obtained from the $TCID_{50}$ assay with those from the data obtained by flow cytometry on cells infected with the replicating Ad5-GFP virus, viral genome amplification was assessed by qPCR under the same conditions.

Resveratrol significantly reduced hexon gene copy numbers in all three cell lines, although the effect was minor in 22Rv-1 cells (Figure 35). Gene copy numbers were also greatly reduced by equol in DU145 and PC-3 cells. However, 22Rv-1 cells treated with equol showed an increase in genome copy numbers, although the trend was not statistically significant at 72h. This may be due to reduced cell viability at this later time point (28% cell death at 72h., Table 17). Quantification of hexon gene amplification by qPCR therefore confirmed the trends shown by the $TCID_{50}$ assays (Figure 32).

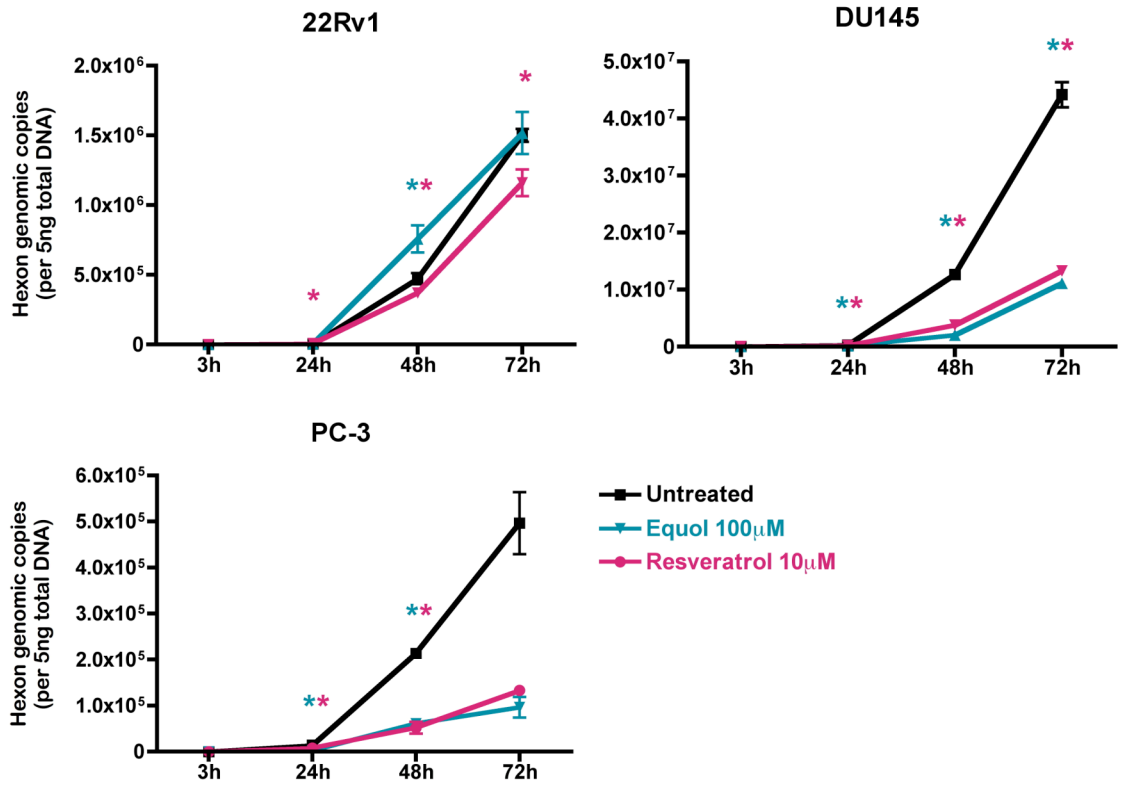

Figure 35 Ad5 DNA amplification measured by quantification of hexon gene copy numbers by qPCR

Cells were infected with Ad5 100ppc for 2h, after which the infection medium was removed and replaced with normal or phyochemical-containing (equol 100μM or resveratrol 10μM) 2% FCS medium. Cells were harvested at 3h, 24h, 48h and 72h post-infection. DNA was extracted, quantified and hexon gene copy numbers were determined in duplicate for each sample by qPCR as described in Methods Section 2.6.2. Results shown as means from one experiment ± SD. * = $p < 0.05$ compared to untreated cells.

Since E1A is essential for the initiation of viral replication, the expression levels of this protein in phytochemical-treated cells were also assessed to verify the replication data. Western blots showed that E1A expression in 22Rv-1 cells was affected by neither equol nor by resveratrol (Figure 36). However, in DU145 cells, there was a decrease in E1A protein levels in cells treated with resveratrol for 18-24h. By 48h, E1A expression in resveratrol-treated cells had recovered to levels similar to those observed in untreated cells. Equol had no effect in DU145 cells. In PC-3 cells, treatment with resveratrol decreased E1A expression at 24h and 48h and equol caused a slight decrease. These results indicate that equol had no effect on E1A expression levels, while resveratrol caused a decrease in E1A expression in DU145 and PC-3 cells. This paralleled the decrease in viral replication. E1A expression in 22Rv-1 cells appeared to be unaffected by phytochemical treatment which supports the replication data showing that the phytochemicals do not have significant effects on viral replication in this cell line.

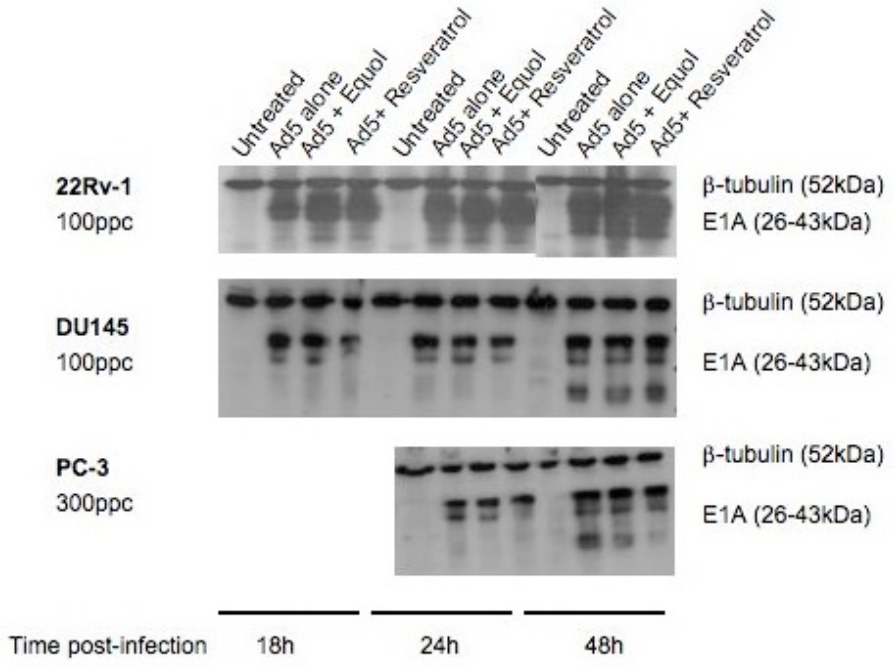

Figure 36 E1A expression in phytochemical-treated PCa cells

Cells were infected with Ad5 (22Rv-1 and DU145: 100ppc, PC-3: 300ppc). After 2h, the infection medium was removed and replaced with phytochemical-containing medium (equol 100μM or resveratrol 10μM). Cell lysates were harvested at the indicated times and used to blot for E1A as described in Methods section 2.7. One blot representative of three independent experiments.

Taken together, these results indicate that the effects of phytochemical treatment on viral replication were cell line dependent. Equol and resveratrol reduced viral replication in the AR-negative cell lines, particularly in DU145 cells. Ad5 replication in 22Rv-1 cells seemed relatively unaffected and titres were possibly increased by treatment with equol at 48h post-treatment, but not with resveratrol.

3.2.4 Effect of phytochemicals on cell cycle progression

The main function of the early viral proteins is to induce S phase to enable viral DNA synthesis and amplification. The cell cycle was analysed to determine whether treatment with phytochemicals might induce changes that could explain the synergistic interaction with Ad5 and/or the different responses of the cell lines in terms of viral replication.

Cell cycle progression was monitored by flow cytometry for 72h after treatment and infection (Figure 37, Figure 38, Figure 39). The distribution of cells was similar between 24h and 48h. Resveratrol treatment caused an increase in the proportion of cells in S phase (Figure 40). This effect was detected in all three cell lines and at both time points. Infection with Ad5 also stimulated S phase in 22Rv-1 and DU145 cells. Viral-induced S phase was not detected in

PC-3 cells at this dose of Ad5 (100ppc), probably due to the lower infectability of this cell line (Figure 27). Exposure of infected cells to resveratrol increased the proportion of cycling cells above the level induced by Ad5 (Figure 40). By 72h, phytochemical treatment increased the proportion of cells in sub-G_1, indicating the possible induction of apoptosis (Figure 41). This pattern was further enhanced by infection with Ad5. Equol slightly increased the proportion of PC-3 cells in G_2/M, while it increased the proportion of DU145 cells in S phase and had little effect in 22Rv-1 cells. There was an increase in sub-G_1 cells by 72h in 22Rv-1 and DU145 cells treated with equol (Figure 41 and Table 18). The increased viral replication in equol-treated 22Rv-1 cells and the decrease in equol- or resveratrol-treated DU145 and PC-3 cells therefore could not be explained by differences in cell cycle progression. The induction of S phase is presumably beneficial for viral replication, so resveratrol must interfere at a later step to attenuate replication.

Untreated DU145 cells had the highest proportion of cells going through S phase, reflecting the high proliferative index of this cell line. This might explain why this cell-line supported the highest levels of viral replication (Figure 32). In contrast, both slow-growing cells, 22Rv-1 and PC-3 cells, had fewer cells undergoing S phase, which correlates with the lower viral titres produced by these cell lines.

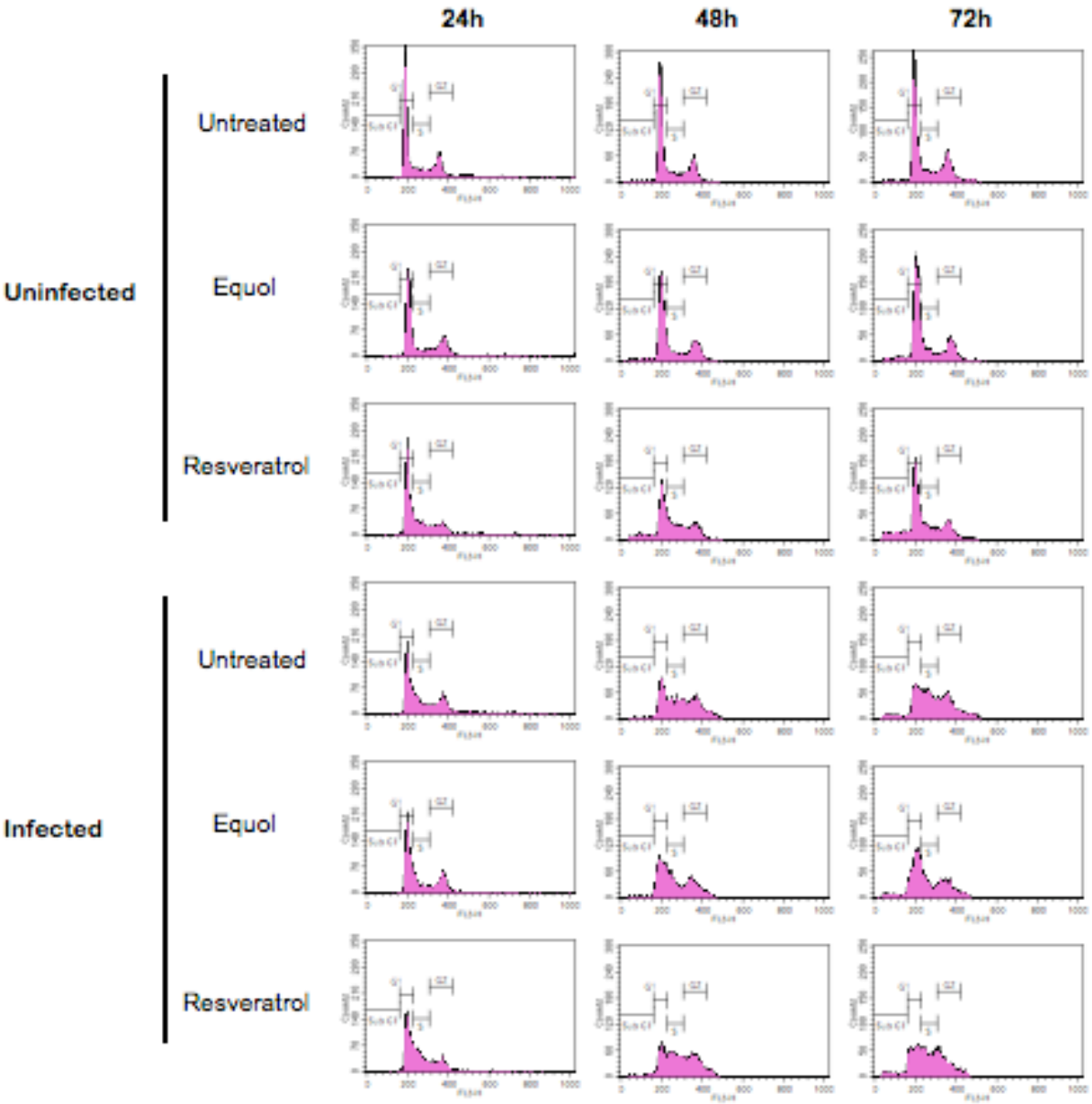

Figure 37 The effect of equol and resveratrol on cell cycle progression in 22Rv-1 cells

Cells were infected with Ad5 (100ppc) or mock infected. After 2h the infection medium was removed and replaced with 2% FCS medium with or without phytochemicals (equol, 100μM or resveratrol, 10μM). Cell cycle analysis was performed at 24-72h post-infection by flow cytometry. One experiment representative of two.

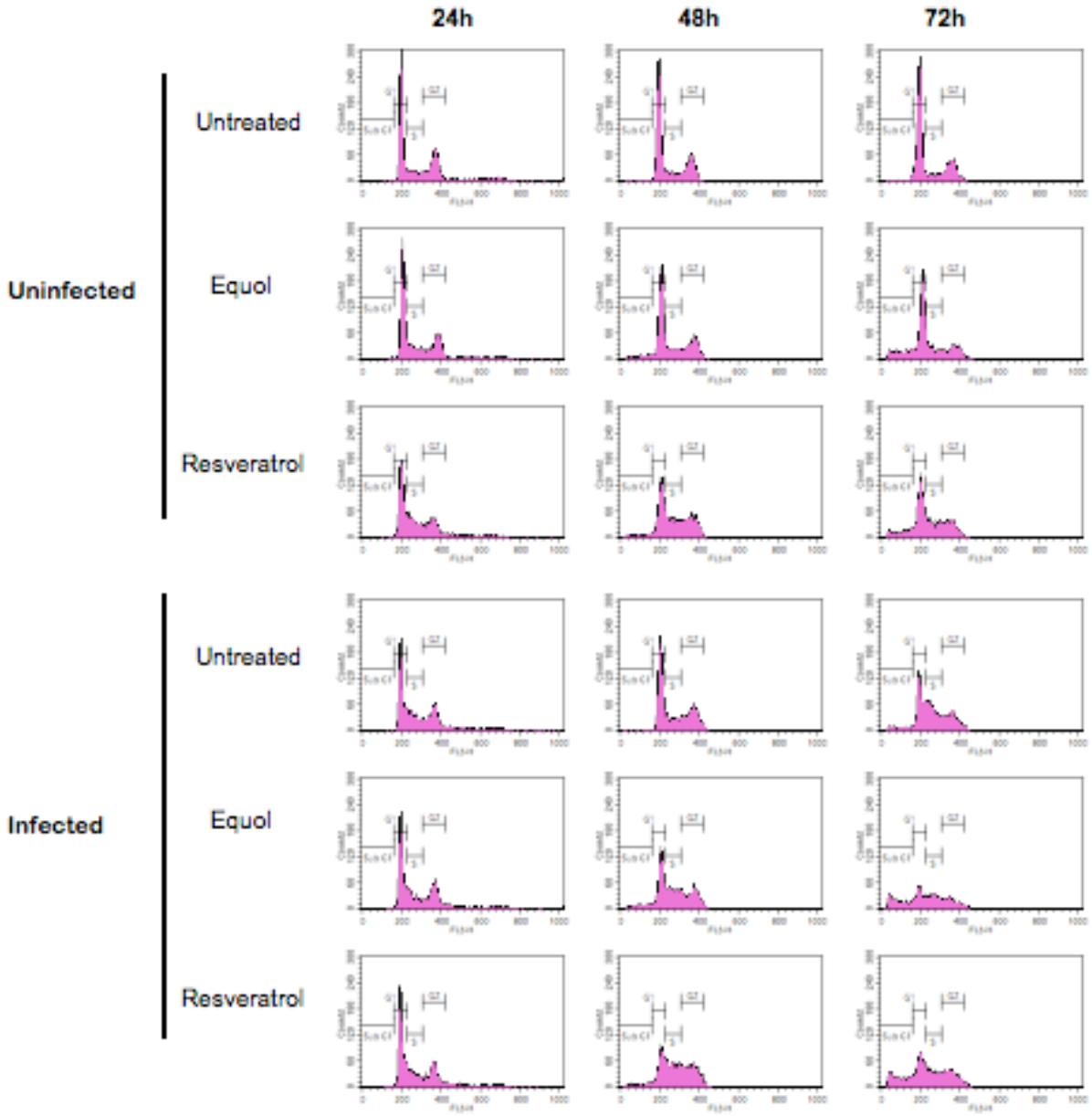

Figure 38 The effect of equol and resveratrol on cell cycle progression in DU145 cells

Cells were infected with Ad5 (100ppc) or mock infected. After 2h the infection medium was removed and replaced with 2% FCS medium with or without phytochemicals (equol, 100μM or resveratrol, 10μM). Cell cycle analysis was performed at 24-72h post-infection by flow cytometry. One experiment representative of two.

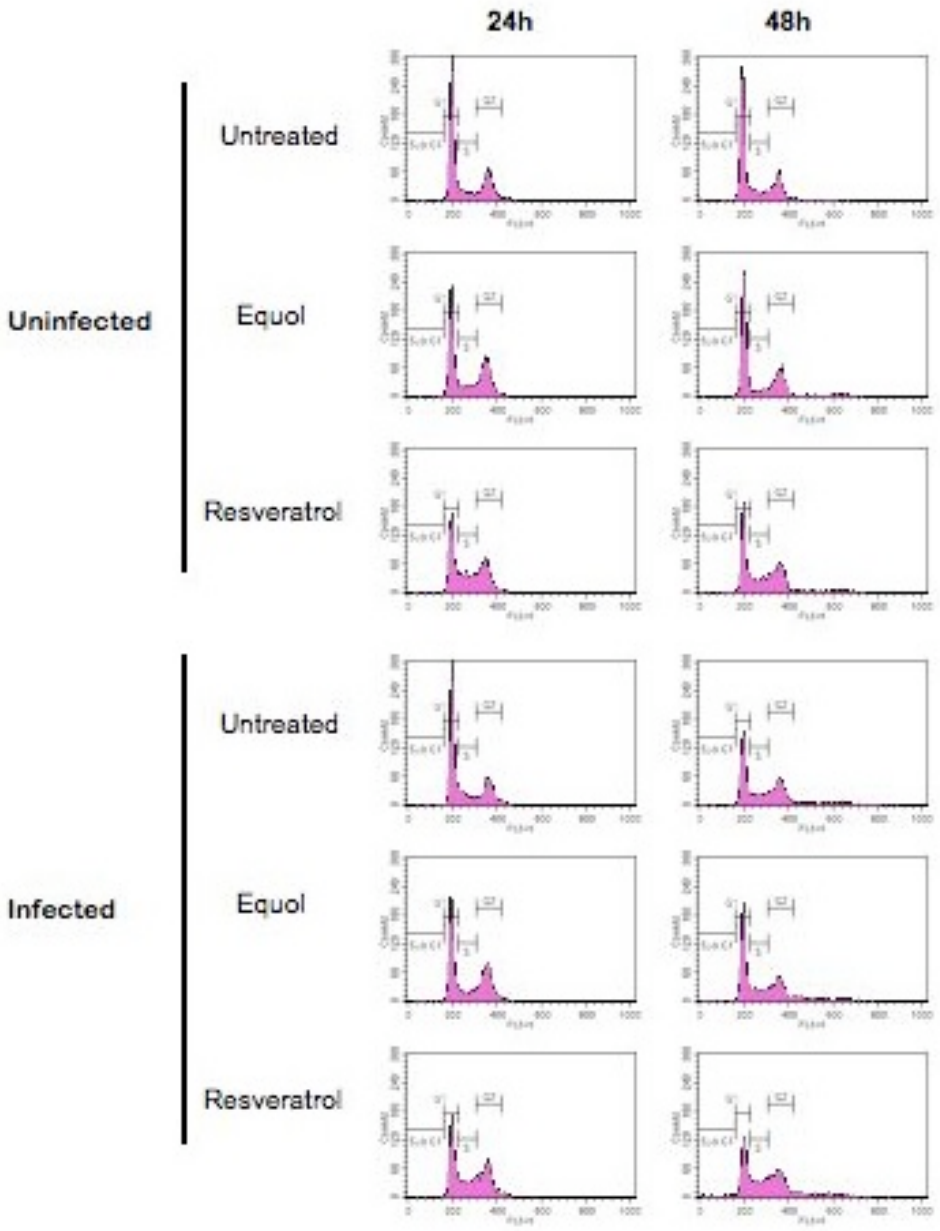

Figure 39 The effect of equol and resveratrol on cell cycle progression in PC-3 cells

Cells were infected with Ad5 (100ppc) or mock infected. After 2h the infection medium was removed and replaced with 2% FCS medium with or without phytochemicals (equol, 100μM or resveratrol, 10μM). Cell cycle analysis was performed at 24h post-infection by flow cytometry. One experiment representative of two.

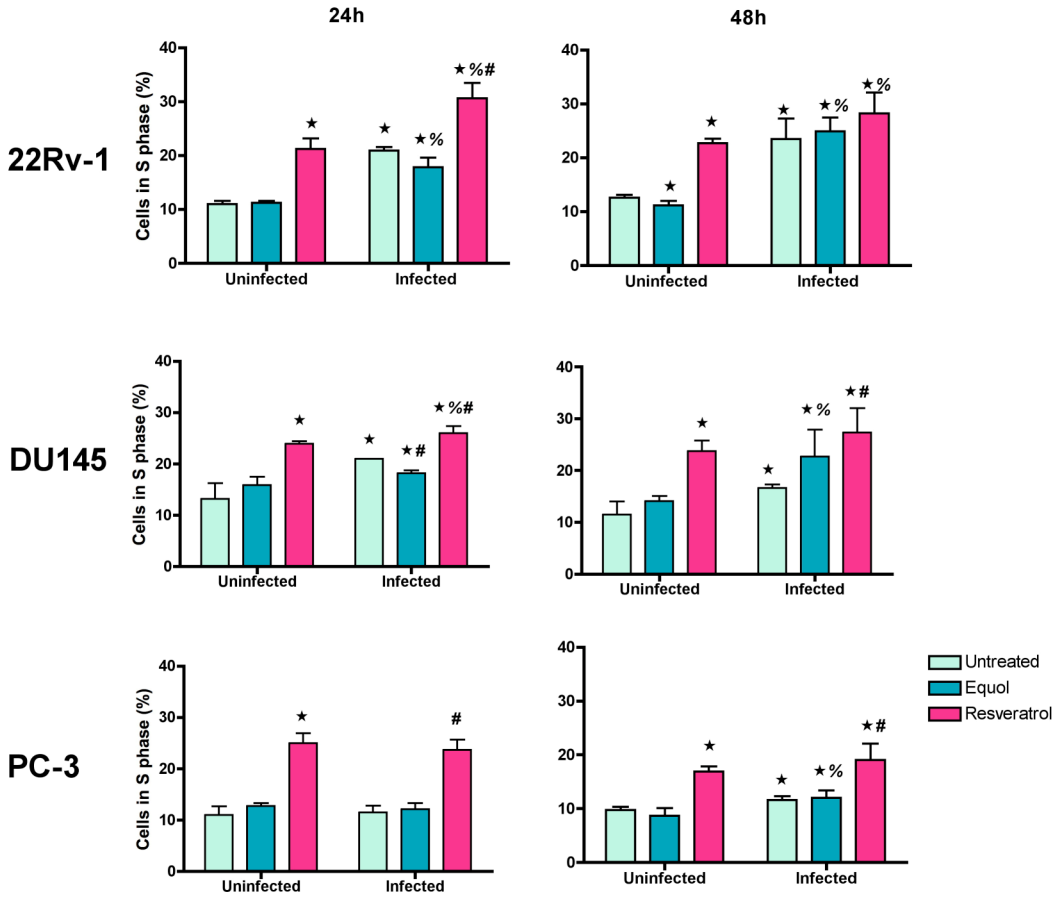

Figure 40 Proportion of cells in S phase in response to Ad5 infection and phytochemical treatment

Cells were infected with Ad5 (100ppc) or mock infected. After 2h the infection medium was removed and replaced with 2% FCS medium with or without phytochemicals (equol, 100μM or resveratrol, 10μM). Cell cycle analysis was performed at 24h post-infection by flow cytometry. Results are shown as the mean of duplicates in two experiments ± SD. * = p <0.05 compared to uninfected and untreated cells, # = p< 0.05 compared to infected and untreated cells, % = p <0.05 compared to uninfected treated cells.

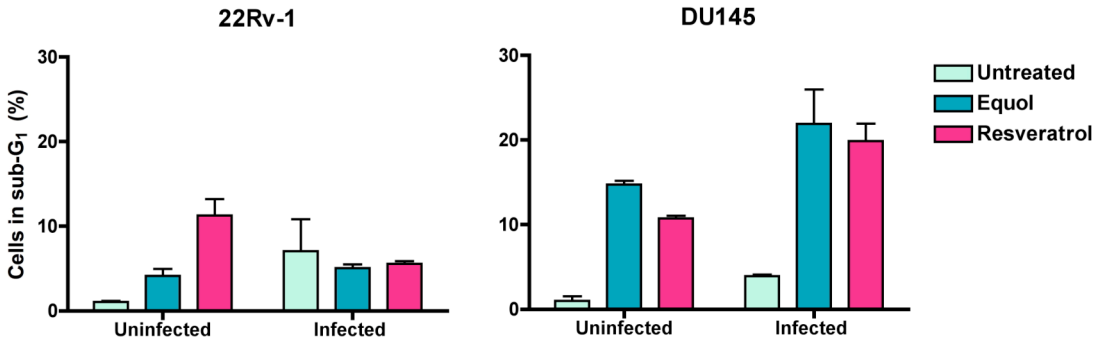

Figure 41 Proportion of cells in sub-G_1 after 72h treatments

Data from Figure 37 and Figure 38. Average of duplicates from one experiment ± SD.

Table 18 Percentage (%) of cells in sub-G_1 after 72h treatments

	22Rv1	DU145
Untreated	1.1	1.0
Equol	4.2	14.8
Resveratrol	11.3	10.8
Ad5	7.1	3.9
Ad5 Equol	5.1	21.9
Ad5 Resveratrol	5.6	19.9

Data from Figure 37 and Figure 38. Average of duplicates from one experiment ± SD.

			sub-G1		G1		S		G2/M	
			Mean	SD	Mean	SD	Mean	SD	Mean	SD
22Rv-1	24h	Untreated	0.3	0.2	63.4	4.3	11.0	0.6	22.9	1.9
		Equol	0.7	0.7	62.6	5.8	11.2	0.4	23.4	4.1
		Resveratrol	0.6	0.4	57.9	6.9	21.3	1.9	17.3	3.0
		Ad5	0.2	0.2	57.5	11.1	16.4	5.3	22.4	2.7
		Ad5 + equol	0.3	0.2	59.0	8.3	14.1	4.6	24.3	2.0
		Ad5 + res	0.4	0.3	52.7	11.2	25.5	6.2	18.8	3.3
	48h	Untreated	1.0	0.3	61.3	1.3	12.7	0.5	24.3	1.0
		Equol	2.0	0.8	61.1	2.1	11.2	0.9	24.9	0.6
		Resveratrol	5.6	2.9	46.4	4.2	22.7	0.8	24.1	0.6
		Ad5	1.0	0.5	40.9	9.4	23.6	3.8	31.0	3.5
		Ad5 + equol	1.2	0.6	42.8	2.9	25.0	2.5	27.7	1.0
		Ad5 + res	1.9	0.2	31.4	5.1	28.3	3.9	34.8	0.7
DU145	24h	Untreated	0.1	0.1	52.4	0.5	13.4	2.9	31.3	0.4
		Equol	0.3	0.1	53.0	2.7	15.4	0.8	28.1	0.4
		Resveratrol	0.2	0.1	46.5	0.9	23.9	0.5	25.9	2.9
		Ad5	0.1	0.1	46.5	3.3	20.9	0.1	27.9	0.9
		Ad5 + equol	0.2	0.0	50.5	1.9	18.3	0.5	26.9	1.1
		Ad5 + res	0.2	0.1	42.7	1.1	26.0	1.7	27.1	2.3
	48h	Untreated	0.4	0.2	60.8	4.0	11.5	2.5	26.8	1.5
		Equol	2.4	2.0	54.8	1.3	14.1	1.0	28.0	0.8
		Resveratrol	2.0	1.5	44.9	5.4	23.7	2.0	28.4	2.2
		Ad5	0.6	0.3	50.8	0.5	16.6	0.7	30.8	1.3
		Ad5 + equol	2.8	2.3	44.2	7.4	22.7	5.2	29.0	0.8
		Ad5 + res	2.2	1.7	32.5	8.1	27.3	4.7	36.1	2.5
PC-3	24h	Untreated	0.2	0.1	61.4	2.2	11.0	1.7	25.7	1.2
		Equol	0.2	0.1	55.1	2.9	12.7	0.6	30.1	4.7
		Resveratrol	0.4	0.1	45.1	2.7	25.0	1.9	27.3	5.8
		Ad5	0.3	0.1	62.1	1.9	11.6	1.3	24.1	2.0
		Ad5 + equol	0.3	0.1	55.0	3.8	12.2	1.2	30.8	5.6
		Ad5 + res	0.5	0.3	43.8	3.2	23.7	2.0	29.8	6.6
	48h	Untreated	0.4	0.1	64.2	0.6	9.8	0.6	24.3	1.4
		Equol	0.3	0.1	61.7	1.9	8.7	1.4	27.9	1.6
		Resveratrol	0.5	0.1	50.8	4.4	16.9	1.0	29.4	1.8
		Ad5	0.4	0.2	57.6	3.8	11.7	0.7	27.1	0.6
		Ad5 + equol	0.5	0.2	58.0	2.3	12.1	1.4	26.2	1.5
		Ad5 + res	1.6	0.5	45.3	9.1	19.1	3.0	30.2	2.7

Table 19 Cell cycle distribution in treated and infected PCa cells

Data from Figure 37, Figure 38 and Figure 39. Results are shown as mean of duplicates in two experiments ± SD. Changes in the proportion of cells in S phase are highlighted in blue (uninfected cells) and red (infected cells). Changes in the proportion of cells in G_2/M are highlighted in green.

3.3 The role of apoptosis in cell death induced by phytochemicals

We next sought to determine whether the synergistic interactions between Ad5 and the phytochemicals could be due to the induction of apoptosis. Although viral cell death is non-apoptotic (Abou El Hassan *et al.*, 2004; Baird *et al.*, 2008), chemotherapeutic drugs, such as docetaxel, mitoxantrone and cisplatin, cause toxicity by apoptosis. Combinations of apoptosis-inducing chemodrugs with oncolytic adenoviral mutants have been shown to improve anticancer potency both *in vitro* and *in vivo* and potentiate drug-induced cell death (Heise *et al.*, 2000b; Heise *et al.*, 1997; Leitner *et al.*, 2009; Yoon *et al.*, 2006; Yu *et al.*, 2001). Equol and resveratrol have also been reported to induce apoptosis in certain cell types (Choi *et al.*, 2009; Mahyar-Roemer *et al.*, 2001; Mohan *et al.*, 2006). We therefore hypothesised that the synergistic enhancement of cell death by the phytochemicals and Ad5 might be due to the induction of apoptosis.

3.3.1 Depolarization of the mitochondrial membrane

One of the characteristics of apoptosis is a loss in mitochondrial membrane polarity, accompanied by release of cytochrome *c* into the cytoplasm. We therefore determined changes in mitochondrial membrane polarization ($\Delta\varphi_m$) in response to virus, phytochemicals and combination treatments.

In DU145, Ad5 alone did not affect $\Delta\varphi_m$ (Figure 42), indicating that adenoviral cell death was not apoptotic, in agreement with previous reports. Decreases in $\Delta\varphi_m$ were observed in response to all other treatments in DU145 cells from 48h to 96h. By 96h, in uninfected cells treated with phytochemicals, the proportion of cells with intact $\Delta\varphi_m$ was lowered from 80% (untreated cells) to 26% by equol and 31% by resveratrol. Infection of phytochemical-treated cells with Ad5 reduced the proportion of cells with intact $\Delta\varphi_m$ further to 19% by equol and 15% by resveratrol. These effects were greater than those observed in uninfected cells treated with phytochemicals although the differences were not statistically significant.

In PC-3 cells, exposure to phytochemicals depolarized the mitochondrial membrane after 72h but the largest differences between different treatments were observed after 96h incubation. At this time-point, $\Delta\varphi_m$ was intact in 89% cells treated with Ad5 alone, in 57% equol-treated uninfected cells and 51% resveratrol-treated uninfected cells. When infected cells were treated

with equol or resveratrol, only 34% and 29% of cells treated displayed intact $\Delta\varphi_m$. The differences between infected and uninfected treated cells were not statistically significant.

In untreated 22Rv-1 cells, only 75% of cells had intact $\Delta\varphi_m$, indicating compromised viability, even without treatments (Figure 42). Further decreases due to treatments were observed from 48h, although differences between treatments only became apparent at 72h and 96h. Surprisingly, Ad5 in combination with equol or resveratrol caused less of a decrease in $\Delta\varphi_m$ than the phytochemicals alone. The proportion of cells with intact $\Delta\varphi_m$ at 96h was higher in cells treated with combinations of Ad5 and equol (41%) or resveratrol (52%) compared to uninfected cells treated with equol (24%) or resveratrol (28%) alone. This protective effect of Ad5 can also be seen when comparing Ad5 alone (69% cells with intact $\Delta\varphi_m$) to untreated cells (53%), the latter showing fewer live cells than Ad5 alone at 72h and 96h.

In conclusion, this study showed that mitochondrial membrane depolarization was induced by both equol and resveratrol in PCa cell lines. However, the proportion of cells with depolarized mitochondrial membrane was not significantly increased by the combination treatments compared to phytochemicals alone. Ad5 seems to have a protective effect in 22Rv-1 cells as viral infection reduced the phytochemical-induced depolarization of the mitochondrial membrane.

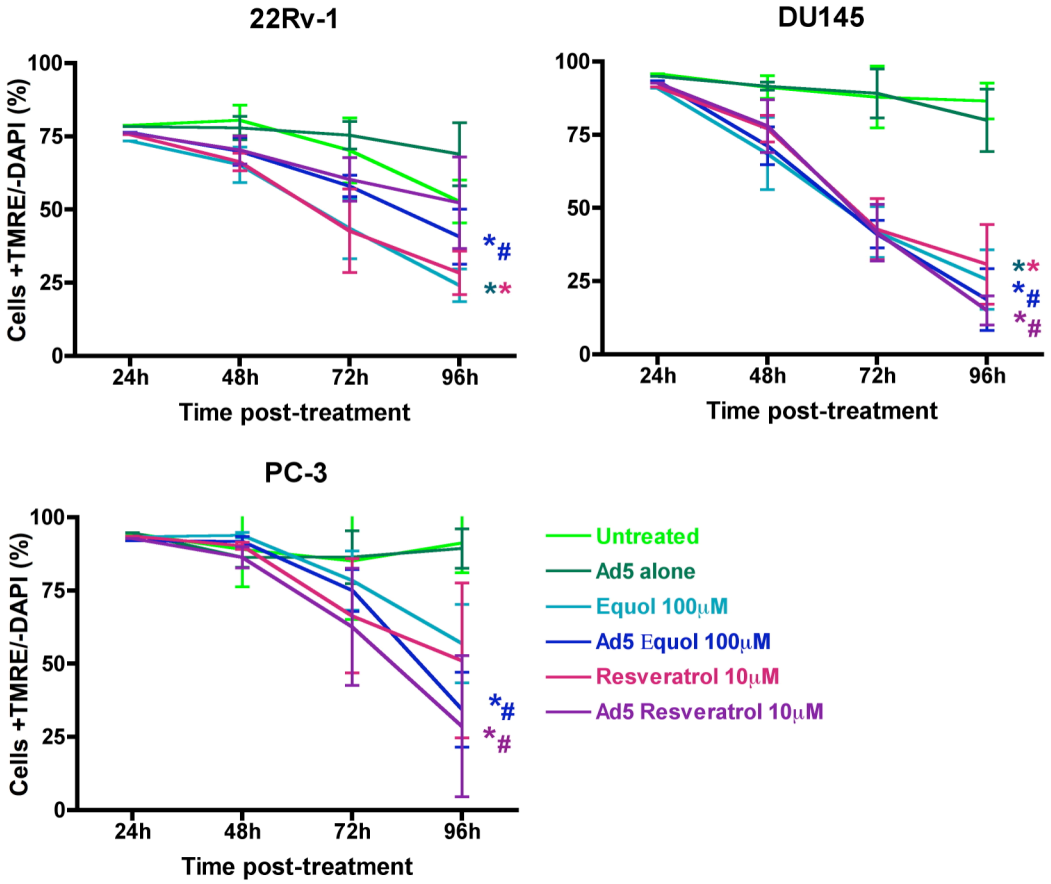

Figure 42 Changes in $\Delta\varphi_m$ in response to phytochemical treatment and Ad5 infection

Cells were infected with Ad5 (22Rv-1 and DU145: 100ppc, PC-3: 300ppc) for 2h and then incubated with normal 2% FCS medium or phytochemical-containing medium. Cells were harvested for flow cytometry analysis after 24-96h as indicated. Cells were stained with TMRE and DAPI and analysed by flow cytometry as described in Methods Section 2.5.4. Cells that retained TMRE staining (i.e. intact, active mitochondria) whilst remaining negative for DAPI (i.e. intact cellular membrane) were considered 'live'. Results are shown as the means of duplicates from three separate experiments ± SD. * = $p < 0.05$ compared to uninfected and untreated cells, # = $p < 0.05$ compared to infected and untreated cells, % = $p < 0.05$ compared to uninfected treated cells. Statistical significance was calculated for the 96h time-point.

3.3.2 Activation of caspase-3

To characterise the apoptotic response further, the activation of caspase-3, which is downstream of mitochondrial changes, was also monitored. The relative activation levels of caspase-3 varied between cell lines.

Although PC-3 cells seemed to undergo mitochondrial membrane depolarization readily in response to phytochemical and combination stimuli, active caspase-3 levels remained quite low (Figure 43). As expected, Ad5 alone did not induce activation of caspase-3 (maximum 4% of cells at 96h post-infection). Equol alone at the highest dose (100μM) induced caspase-3 activation in 7.7% of uninfected cells and in 11.7% infected cells. Treatment of PC-3 cells

with resveratrol caused slightly higher levels of caspase-3 activation compared to equol. In addition, the induction peaked earlier, at 72h. At 96h however, the differences between resveratrol-treated uninfected and infected cells were greater. At this time-point, 9.0% of uninfected cells treated with 5μM resveratrol had activated caspase-3, while up to 13.3% infected cells had active caspase-3.

Caspase-3 activation in DU145 cells was induced to higher levels than in PC-3 cells. Ad5 alone did not induce a significant degree of apoptosis until 96h infection when 28% cells had active caspase-3. The phytochemicals induced caspase-3 activation from 72h after treatment. At 96h, 41.6% cells treated with equol and 55% cells treated with resveratrol had active caspase-3. By 96h, there were notable differences between uninfected and infected cells exposed to phytochemicals. Surprisingly, the largest differences were between combinations with the lower doses of phytochemicals. While 18.5% cells treated with 50μM equol had active caspase-3, this was increased to 66.8% in infected cells exposed to equol. Similarly, 35% uninfected cells exposed to 5μM resveratrol for 96h had active caspase-3 and this was increased to 70% of cells in those also infected with Ad5.

The proportion of 22Rv-1 cells with active caspase 3 was very low. The maximum percentage of cells with active caspase-3 was 9.7% in cells treated with Ad5 and resveratrol 96h post-infection. This reluctance to undergo apoptosis might explain why 22Rv-1 cells were the least sensitive to phytochemical cytotoxicity (Figure 21). After 96h infection, Ad5 caused caspase-3 activation in 10.1% cells but the addition of 100μM equol reduced this to 5.9%. This protective effect was similar to the results observed in TMRE-stained cells (Figure 42). Treatment of infected cells with 10μM resveratrol caused caspase-3 activation in 9.7% cells and had no effect on the proportion of cells with active caspase-3 compared to single treatments.

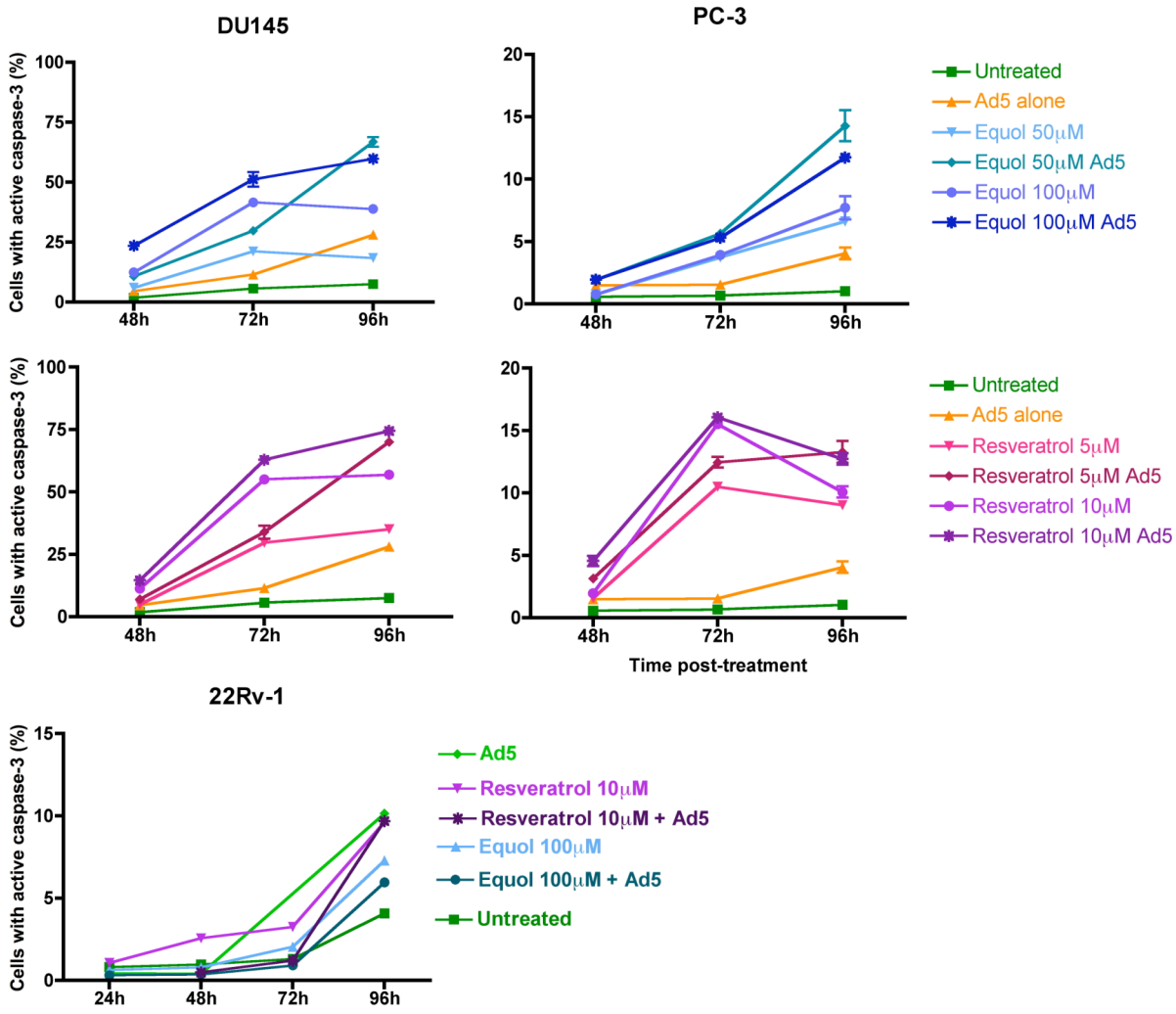

Figure 43 Active caspase-3 in PCa cells treated with phytochemicals and Ad5

Cells were infected with Ad5 (22Rv-1 and DU145: 100ppc, PC-3: 300ppc) for 2h and then incubated with normal 2% FCS medium or phytochemical-containing medium. Cells were harvested for flow cytometry analysis after 24-96h as indicated. Cells were permeabilized and incubated with a FITC-tagged antibody specific for activated caspase-3. Results shown are averages (±SD) of one experiment representative of 3 independent experiments showing the same trend.

3.3.3 Loss of cellular membrane phospholipid asymmetry

The exposure of phosphatidylserine (PS) on the outer leaflet of the cellular membrane is a characteristic feature of apoptosis downstream of mitochondrial depolarization and caspase activation. Exposed PS acts as a tag for recognition by macrophages phagocytosing apoptotic bodies. PS exposure can be detected by staining with Annexin V, which is membrane impermeable and has a high affinity for PS in the presence of calcium. PS exposure was monitored in DU145 and PC-3 cells but it could not be assessed in 22Rv-1 cells due to cytotoxicity of the calcium-binding buffer in this cell line.

Cells were co-stained with FITC-labelled annexin V (to label apoptotic cells) and the membrane-impermeable DNA dye propidium iodide (to detect cells with compromised membranes, indicating necrotic or advanced apoptotic death). Cells were analysed by flow cytometry and those negative for both dyes were determined as live cells. The results obtained were similar to the patterns observed for caspase-3 activation, with a delay of about 24h.

Ad5 infection did not induce PS exposure except in DU145 cells at the final 120h time-point (Figure 44). At this time point, 59% cells demonstrated PS exposure. In DU145 cells, equol and resveratrol alone did not increase the proportion of cells with exposed PS, except at the highest concentrations (100μM equol, 10μM resveratrol) between 72-120h. At these higher doses, the phytochemicals in combination with Ad5 did not increase the proportion of cells with PS exposure above that caused by single agent treatments. However, in combination with Ad5, 50μM equol decreased live cells from 86.5% (equol alone) and 82.7% (Ad5 alone) to 46.7% at 96h post-infection. In combination with 5μM resveratrol Ad5 did not increase the proportion of cells with exposed PS further than Ad5 alone.

In PC-3 cells, equol (50μM and 100μM) and resveratrol (5μM) in combination with Ad5 did trigger PS exposure in a higher proportion of infected cells compared to uninfected treated cells. After 120h, the percentage live cells dropped from 73.4% and 69.5% (equol 50μM and 100μM alone) to 52.9% and 40.7% (equol 50μM and 100μM with Ad5). Resveratrol at the highest dose (10μM) caused a significant drop in live cells from 72h. The combination at this dose with Ad5 did not further decrease live cells until 120h post-infection where live cells dropped from 22.8% (resveratrol 10μM alone) to 11.5% (resveratrol 10μM with Ad5).

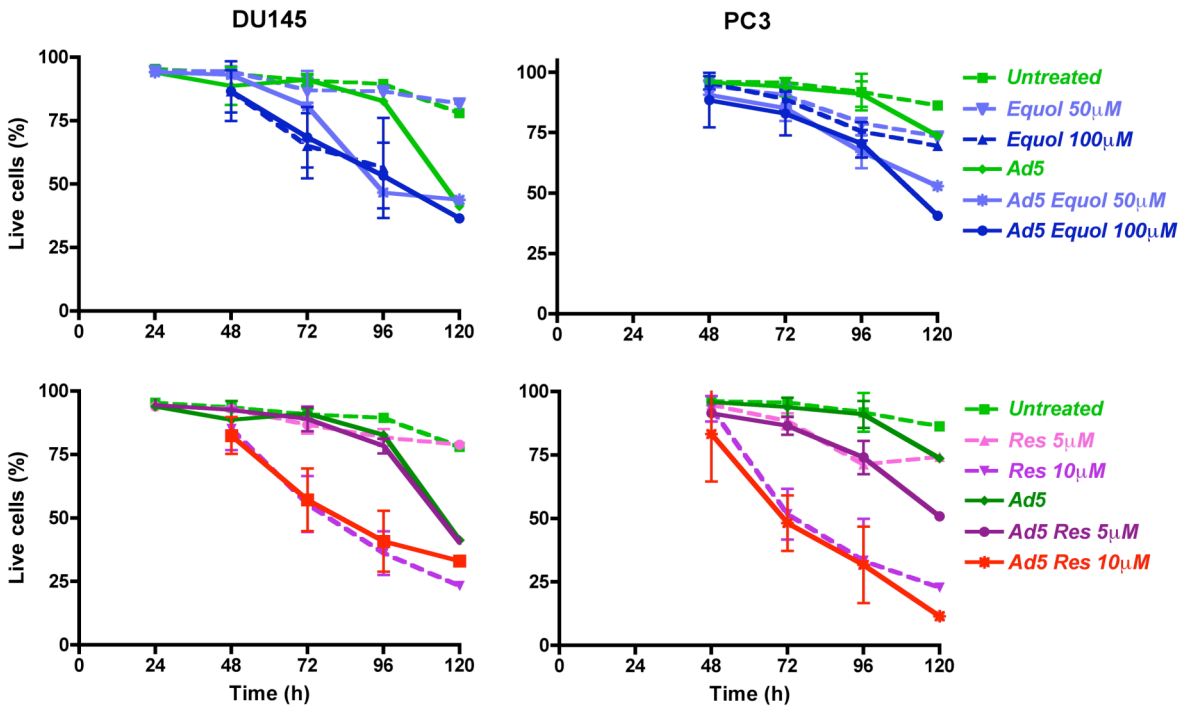

Figure 44 Exposure of phosphatidylserine (PS) in dying cells exposed to combination treatments

Cells were infected with Ad5 (22Rv-1 and DU145: 100ppc, PC-3: 300ppc) for 2h and then incubated with normal 2% FCS medium or phytochemical-containing medium. Cells were harvested for flow cytometry analysis after 24-96h as indicated. Cells were stained with Alexa fluor 488-conjugated annexin V and propidium iodide. Annexin-V negative and PI-negative cells were plotted as live cells under each condition. Results are means of duplicates from 1-4 experiments ± SD.

3.3.4 Inhibition of apoptosis reduced phytochemical-induced cell death

To evaluate the role of apoptosis in cell death induced by equol and resveratrol with and without Ad5, a pan-caspase-inhibitor, zVAD-fmk, was used in cell viability assays. Cell death was evaluated six days post-treatment with 50-100µM equol or 5-10µM resveratrol. These doses were found to initiate apoptosis at 48h-120h in previous experiments (Figure 42, Figure 43 and Figure 44), although treatments did not cause cytotoxicity before 72-96h, depending on the cell line (Figure 33). The dose of zVAD-fmk was selected based on previous experiments in our lab, although it could have been optimized for PC-3 cells which showed 15% cell death in response to treatment with 25µM zVAd-fmk alone.

The lower dose of equol (50µM) did not cause any cytotoxicity in DU145 cells at any time-point, but 100µM equol caused cell death that was reduced by the addition of the caspase inhibitor from 52.2% to 21.7% (Figure 45). Similarly, no cell death induction was observed in

response to 5μM resveratrol, while exposure of DU145 cells to 10μM resveratrol resulted in 58% cell death which was reduced by zVAD-fmk to 20.9%.

Lower levels of cytotoxicity were seen in 22Rv-1 cells and the reductions by caspase inhibition were also less in this cell line. The addition of zVAD-fmk to cells treated with 100μM equol reduced cell death from 33% to 27% respectively (Figure 45). At a lower dose, equol (50μM) induced 10.7% cell death and this was decreased by caspase inhibition to 5.8%. The lower dose of resveratrol (5μM) did not cause any cytotoxicity, but at the higher dose (10μM), 17.2% cell death was reduced by zVAD-fmk to 8.2%.

PC-3 cells were more sensitive to treatment with the pan-caspase inhibitor which caused 6.7% (5μM) and 15.3% (25μM) cell death respectively. Surprisingly, the addition of zVAD-fmk to the phytochemicals increased cytotoxicity additively, except for equol at 50μM which did not induce cell death alone or in combination with the inhibitor. The highest dose of equol (100μM), caused <5% cell death, but in combination with zVAD-fmk, cell death increased to 20.1%. When resveratrol was combined with zVAD-fmk, cell death was increased from 4.7% to 15.9% (5μM) and from 16.7% to 28.9% (10μM). This could be due to an enhancement of alternative cell death pathways, such as necrosis.

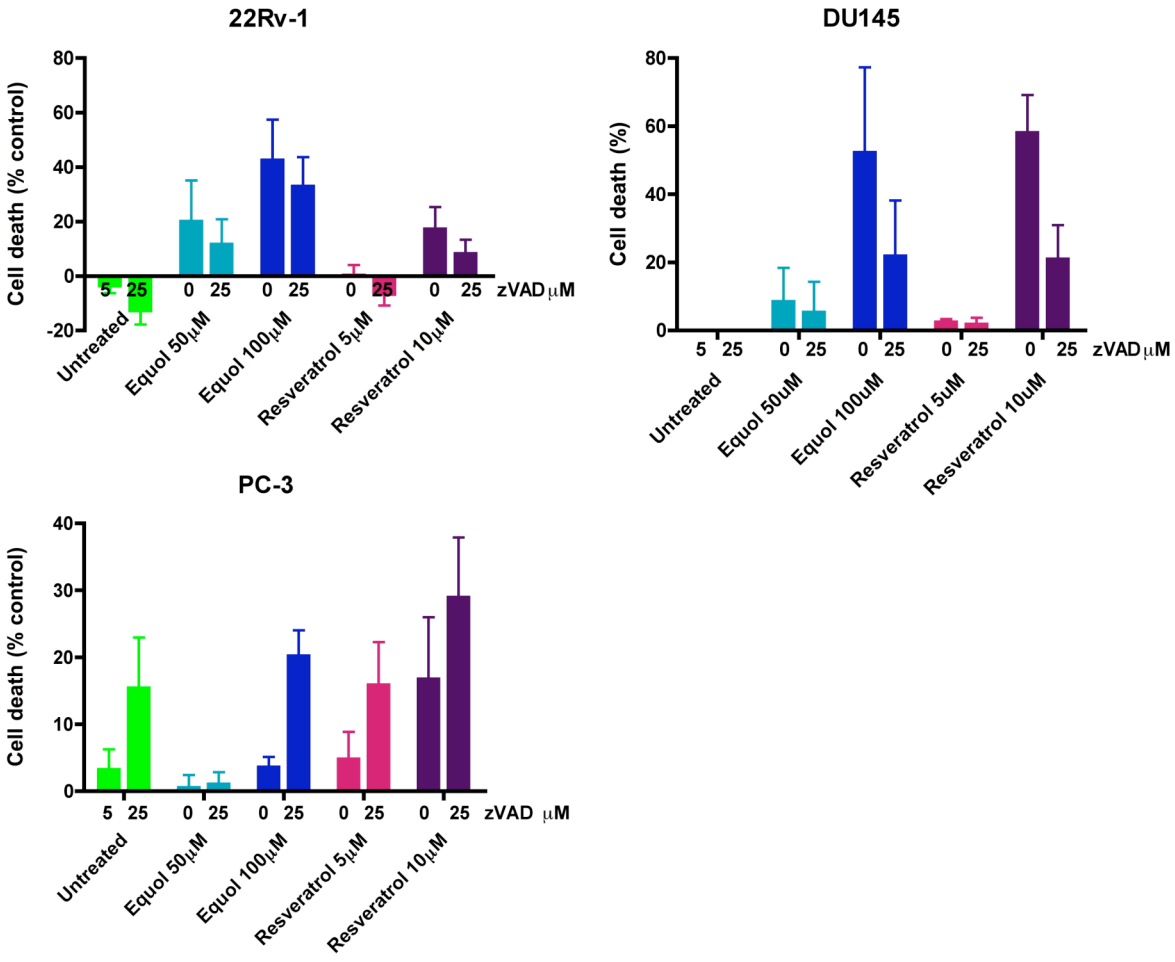

Figure 45 Effect of the pan-caspase inhibitor zVAD-fmk on phytochemical-induced cell death

Cells were treated with equol (50μM or 100μM) or resveratrol (5μM or 10μM), with or without zVAD-fmk at two concentrations (5μM or 25μM). Cell viability was assessed 6 days post-treatment by MTS assay. Results are shown as means of triplicates in one experiment ± SD.

Cell death induced by Ad5 infection was not significantly affected by caspase inhibition in DU145 cells, as is demonstrated by the overlapping dose-response curves (Figure 46). Nevertheless, there was a reduction in the Ad5 EC_{50} value with the highest dose of zVAD-fmk (25μM), from 10.6ppc to 6.7ppc, indicating a slight sensitization effect in the presence of zVAD-fmk (Table 20). The pan-caspase inhibitor had little effect on cell death induced by Ad5 in combination with 50μM equol in DU145 cells and in combinations with equol 100μM cell death was only slightly decreased by zVAD-fmk (Figure 45). A greater yet still modest protective effect was observed with resveratrol when combined with Ad5 and the caspase inhibitor. The Ad5 EC_{50} value increased from 3.4ppc to 5.3ppc (1.4-fold) in cells treated with a combination of 5μM resveratrol and Ad5, with and without the caspase inhibitor. In cells treated with combinations of Ad5 and the higher dose of resveratrol (10μM) zVAD-fmk also appeared to have a small protective effect.

In 22Rv-1 cells, there was a small decrease in the Ad5 EC_{50} value, from 14.8ppc to 9.6ppc, by the addition of zVAD-fmk at the highest concentration (Figure 47). Caspase-inhibition had a sensitising effect in infected 22Rv-1 cells treated with equol. With the highest dose of caspase inhibitor (25μM), the Ad5 EC_{50} values were reduced from 5.2ppc to 3ppc (equol 50μM) and from 3.7ppc to 0.8ppc (equol 100μM) (Table 20). In resveratrol-treated 22Rv-1 cells infected with Ad5, zVAD-fmk had opposite effects depending on the dose of phytochemical. With 5μM resveratrol, Ad5 EC_{50} was increased 1.7-fold from 9ppc to 15.8ppc. However, at a higher dose (10μM) the inhibition of caspases had a sensitising effect, with Ad5 EC_{50} value reduced by 40% from 16ppc to 9.7ppc.

Caspase inhibition also had a sensitising effect in PC-3 cells where the Ad5 EC_{50} value for Ad5 alone was reduced 2-fold from 1167ppc to 560.2ppc by 5μM zVAD-fmk (Figure 48 and Table 20). The inhibition of caspases in infected PC-3 cells treated with equol was highly protective. Cell death was clearly decreased, resulting in a shift of dose-response curves to the right. Cells treated with Ad5 and equol showed increases in Ad5 EC_{50} values from 165.5ppc to 505.2ppc (equol 50μM) and from 57.6ppc to 197ppc (equol 100μM). Caspase inhibition also protected resveratrol-treated PC-3 cells from Ad5-induced cell death (Figure 48). The highest dose of zVAD-fmk increased Ad5 EC_{50} values 1.6-fold, from 344ppc to 553ppc with 5μM resveratrol, and 8-fold from 83ppc to 662ppc with 10μM resveratrol.

These results indicate that the role of apoptotic cell death in combination treatments with phytochemicals may be cell line- and dose-dependent. A requirement for apoptosis and caspase-3 activation was most obvious in PC-3 cells, despite these cells showing significant increased cell death in response to addition of zVAD-fmk to equol- or resveratrol-treated uninfected cells.

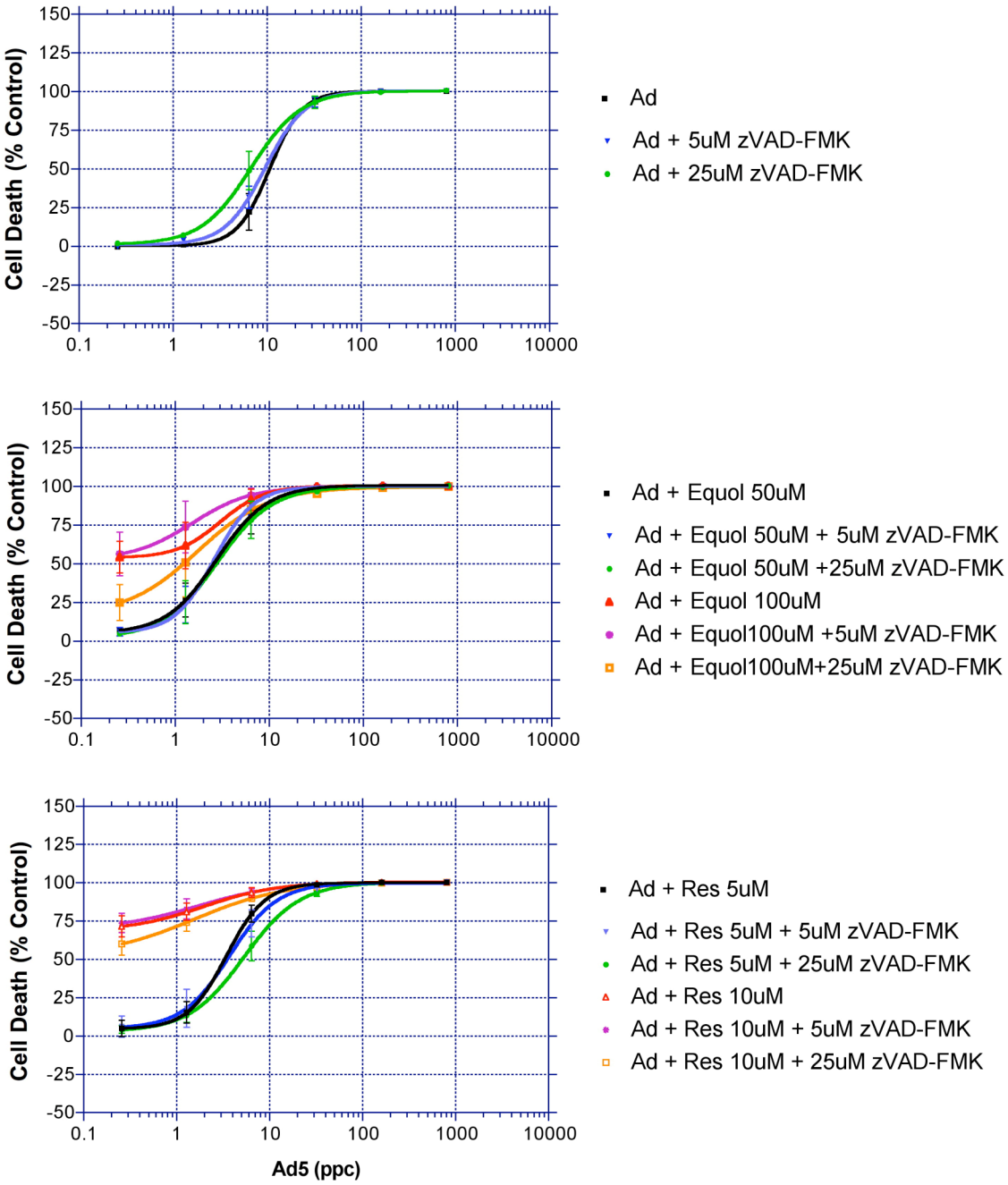

Figure 46 Effects of apoptosis inhibition on cell death in DU145 cells

Cells were infected with 5-fold serially diluted Ad5 (0.256-800ppc), with or without zVAD-FMK at two concentrations (5μM or 25μM), with or without equol (50μM or 100μM) or resveratrol (5μM or 10μM). Cell viability was assessed 6 days post-infection by MTS assay. Results are shown as means of triplicates from three independent experiments ± SD.

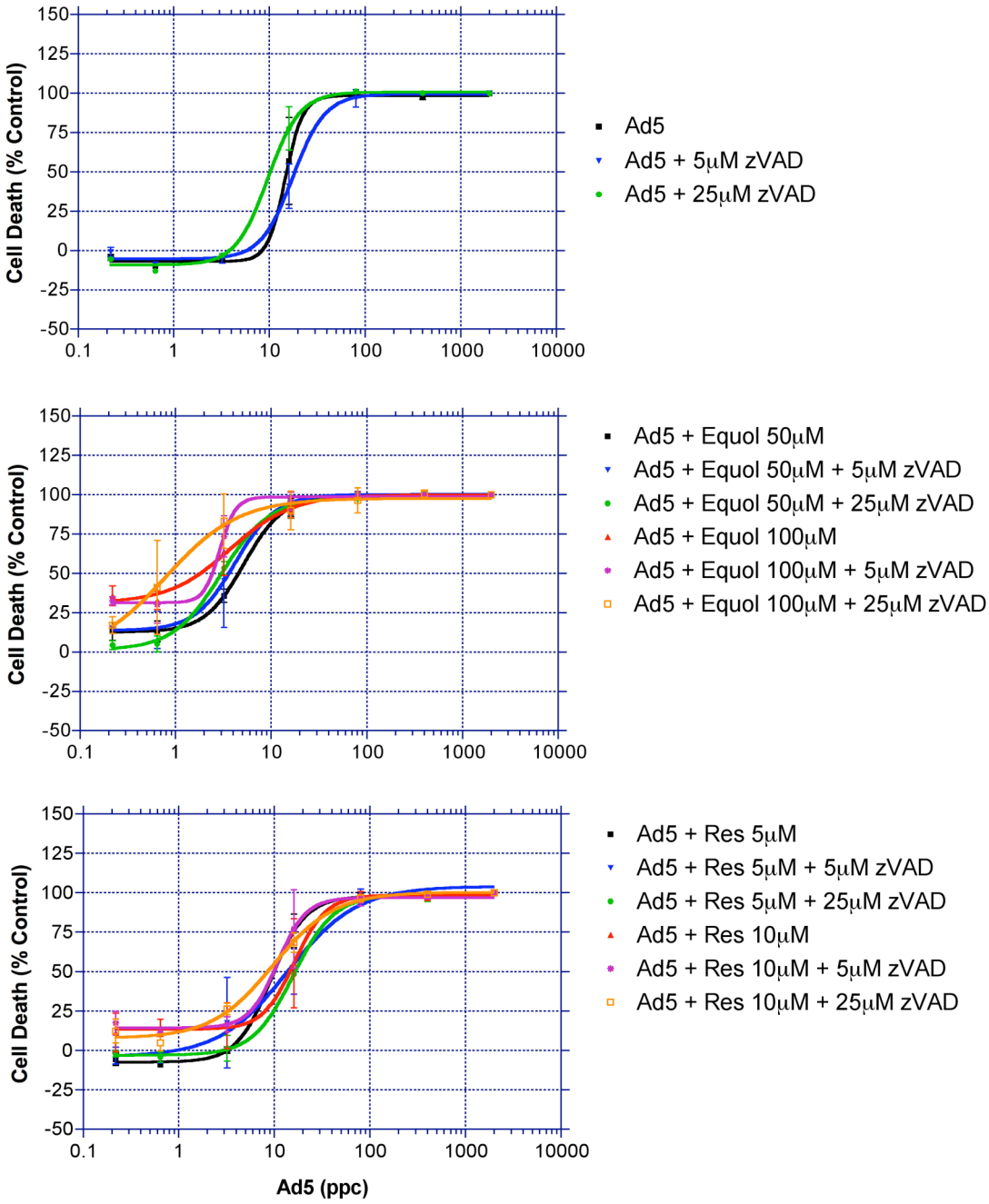

Figure 47 Effects of apoptosis inhibition on cell death in 22Rv-1 cells

Cells were infected with 5-fold serially diluted Ad5 (0.128-400ppc), with or without zVAD-fmk at two concentrations (5μM or 25μM), with or without equol (50μM or 100μM) or resveratrol (5μM or 10μM) in a final volume of 100μl/well. Cell viability was assessed 6 days post-infection by MTS assay. Results are shown as means triplicates from one experiment ± SD.

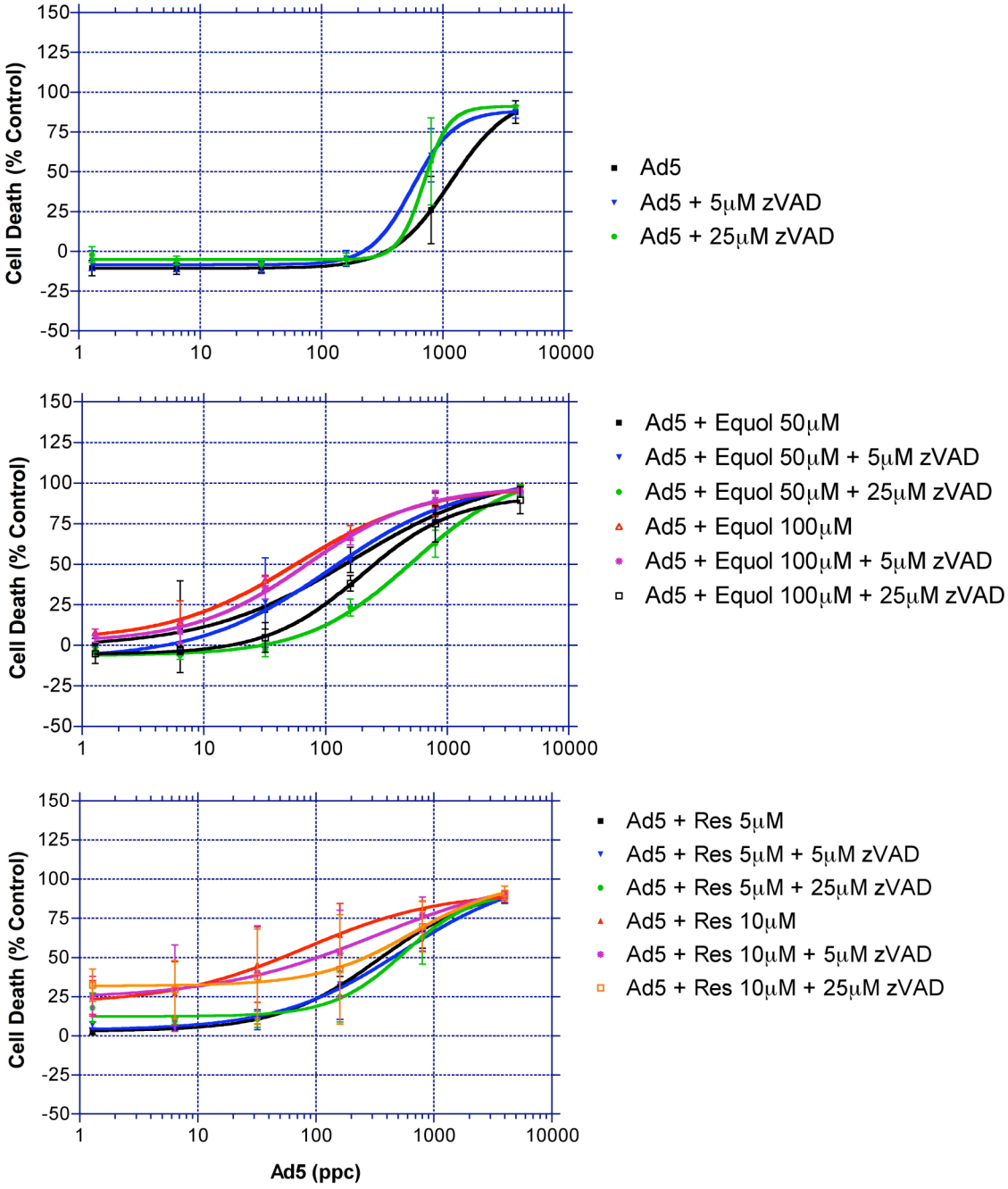

Figure 48 Effect of apoptosis inhibition on cell death in PC-3 cells

Cells were infected with 5-fold serially diluted Ad5 (0.256-800ppc), with or without zVAD-fmk at two concentrations (5μM or 25μM), with or without equol (50μM or 100μM) or resveratrol (5μM or 10μM). Cell viability was assessed six days post-infection by MTS assay. Results were corrected for cell death caused by the caspase inhibitor alone (Figure 45). Results are shown as means of triplicates ± SD from one experiment representative of two.

Table 20 Ad5 EC_{50} values for combination-treated cells with and without caspase inhibitor

Treatments	22Rv-1	DU145	PC-3
Ad5	**14.81**	**10.6**	**1167**
Ad5 + 5μM zVAD	17.54	9.5	560.2
Ad5 + 25μM zVAD	9.6	6.7	695.6
Ad5 + Equol 50μM	**5.16**	**2.75**	**165.5**
Ad5 + Equol 50μM + 5μM zVAD	4.22	2.57	109.8
Ad5 + Equol 50μM + 25μM zVAD	2.99	2.78	505.2
Ad5 + Equol 100μM	**3.71**		**57.55**
Ad5 + Equol 100μM + 5μM zVAD	2.9		69.95
Ad5 + Equol 100μM + 25μM zVAD	0.81		197
Ad5 + Res 5μM	**9.16**	**3.41**	**343.9**
Ad5 + Res 5μM + 5μM zVAD	14.02	3.69	536
Ad5 + Res 5μM + 25μM zVAD	15.75	5.26	552.9
Ad5 + Res 10μM	**16.11**		**82.67**
Ad5 + Res 10μM + 5μM zVAD	10.75		324.1
Ad5 + Res 10μM + 25μM zVAD	9.65		661.9

Data from experiments shown in Figure 46, Figure 47 and Figure 48. Reductions are shown in green, increases in red. Ad5 EC_{50} values could not be determined for combinations with the highest doses of equol (100μM) and resveratrol (10μM) in DU145 cells due to high levels of cell death.

3.3.5 Summary of apoptotic cell death studies

Taken together, these results indicate that the level of apoptosis induced by the phytochemicals and by the combinations with Ad5 is cell line-dependent. Both equol and resveratrol induced apoptosis in a dose-responsive manner, as detected by mitochondrial membrane depolarization, caspase-3 activation and externalization of PS on the cell membrane. The strongest responses were in DU145 cells. Cell death caused by equol or resveratrol alone was reduced using a pan-caspase inhibitor, except in PC-3 cells where zVAD-fmk unexpectedly increased phytochemical cytotoxicity in an additive fashion.

Ad5 alone did not cause any of the classical features of apoptosis, although low levels of active caspase-3 and PS externalization were detected 96-120h post-infection in DU145 cells. This may indicate an indirect effect of Ad5 infection that results in a general stress response in these cells at late time-points. Caspase-inhibition in Ad5-infected cells caused a small sensitising effect, suggesting cross-talk between apoptosis and the viral-induced mode of cell death.

Combination treatments of phytochemicals with Ad5 in DU145 and PC-3 cells induced higher levels of caspase-3 activation and PS externalization, but differences between combination and single treatments on mitochondrial membrane depolarization could only be seen in PC-3 cells. Caspase inhibition was protective against combination-induced cell death in DU145 and PC-3 cells, confirming the involvement of an apoptotic mechanism of cell death in these cell lines in response to combination treatment. The strong effect of zVAD-fmk in PC-3 cells is surprising, considering this cell line lacks p53 and it did not exhibit high levels of active caspase-3.

In contrast, the percentages of combination-treated 22Rv-1 cells with active caspase-3 and depolarized mitochondrial membrane were lower compared to cells exposed to single agents. Ad5 appears to have a protective effect in this cell line, reducing apoptosis induction by the phytochemicals despite clear sensitization at specific Ad5-phytochemical ratios. Caspase-inhibition sensitised 22Rv-1 cells to combinations of equol and Ad5, although zVAD-fmk was protective against combinations of resveratrol with Ad5.

In conclusion, apoptosis seemed to play a significant role in cell death caused by combinations of Ad5 and phytochemicals in DU145 and PC-3 cells. However, apoptosis remained very low in 22Rv-1 cells, despite evidence of strong synergistic induction of cell death by combinations of Ad5 and phytochemicals (Figure 25).

3.4 Autophagy is a survival mechanism induced by combination treatments

Although apoptosis seemed to be induced and play a role in cell death induced by combinations of phytochemicals with Ad5 in DU145 and PC-3 cells, additional mechanisms must play a role in 22Rv-1 cells to cause the supra-additive effects in this cell line. Furthermore, the protective effect of zVAD-fmk in DU145 and PC-3 cells did not completely desensitise cells to the synergistic combination-induced cell death.

Autophagy induction in response to Ad5 has been reported in some cell lines (Ito *et al.*, 2006; Jiang *et al.*, 2007), and by resveratrol in ovarian (Kueck *et al.*, 2007), breast (Scarlatti *et al.*, 2008) and lung (Ohshiro *et al.*, 2007) cancer cells. As discussed in Section 1.4.3.2.2, autophagy can serve as both a survival and a cell death mechanism.

Autophagy induction was evaluated in 22Rv-1 to determine whether this pathway might be functioning as a cell death mechanism in this cell line in response to combination treatment. PC-3 cells were used as a comparative cell line in which zVAD-fmk was protective against combination-induced cell death and autophagy was therefore expected to have less involvement in the cell death mechanism.

3.4.1 Expression levels of LC3: a protein marker of autophagy

Autophagy induction was assessed by monitoring LC3 expression in cells treated with the autophagy inducer rapamycin (Kabeya *et al.*, 2000). LC3-II is an essential structural protein of the autophagosome membrane and is normally localized to the cytoplasm in its precusor form, LC3-I. Upon autophagy induction, LC3-I (18kDa) is converted to LC3-II (16kDa) by post-translational modification. LC3-II is incorporated in the autophagosome membrane and the amount present correlates with the extent of autophagosome formation. After 48h treatments, the induction of LC3-II was detected in response to 1nM (PC-3 cells) and 10nM (22Rv-1 cells) rapamycin (Figure 49). Untreated PC-3 cells also expressed LC3-II, indicating that autophagy might be induced under regular cell culture conditions (2% FCS medium) in these cells. However, the level of LC3-II expression in untreated cells varied since only LC3-I was detected in a subsequent experiment (Figure 51). This variability was also noted in untreated 22Rv-1 cells (Figure 50 and Figure 51).

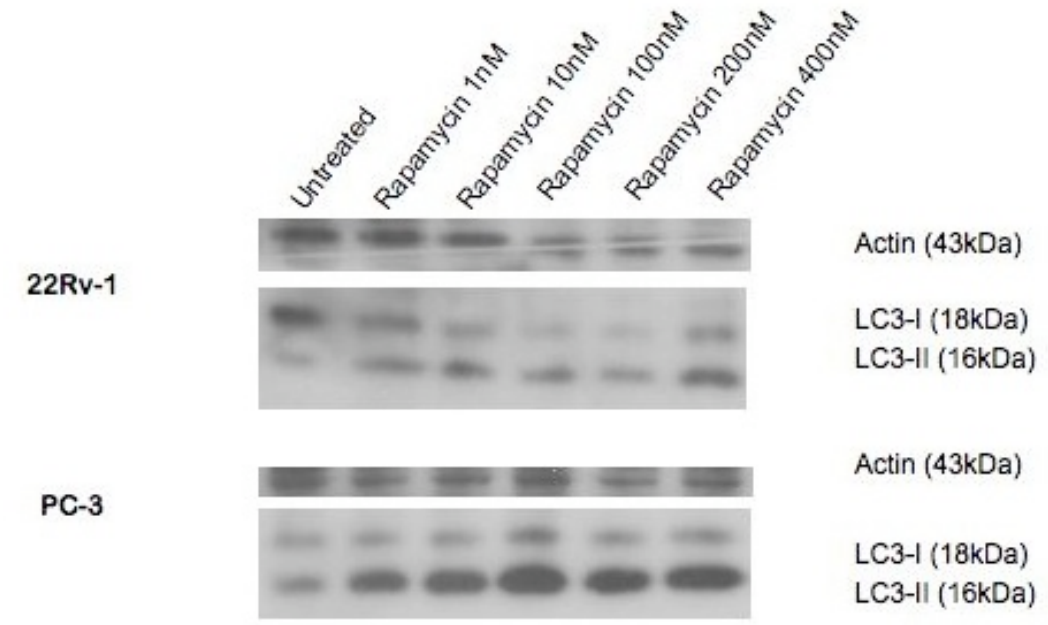

Figure 49 Induction of LC3 expression by rapamycin

22Rv-1 and PC-3 cells were treated with increasing doses of rapamycin (1nM-400nM) for 48h. Lysates were harvested and blotted for LC3 expression as detailed in Methods Section 2.7. Actin was used as a loading control. N=1.

Western blot analysis of phytochemical-treated cells showed that equol induced LC3-II expression in both 22Rv-1 and PC-3 cells (Figure 50). This effect was strongest with 100μM equol and appears to be dose-dependent. Both concentrations of resveratrol also induced LC3-II expression, especially in PC-3 cells. A decrease was observed in rapamycin-treated cells with 100μM equol in both cell lines and with 10μM resveratrol in PC-3 cells. Ad5 infection seemed to repress LC3-II expression in 22Rv-1 cells, but this was overcome by the addition of either equol or resveratrol (Figure 51). The trend was similar in PC-3 cells except Ad5 seemed to repress resveratrol-induced LC3-II expression.

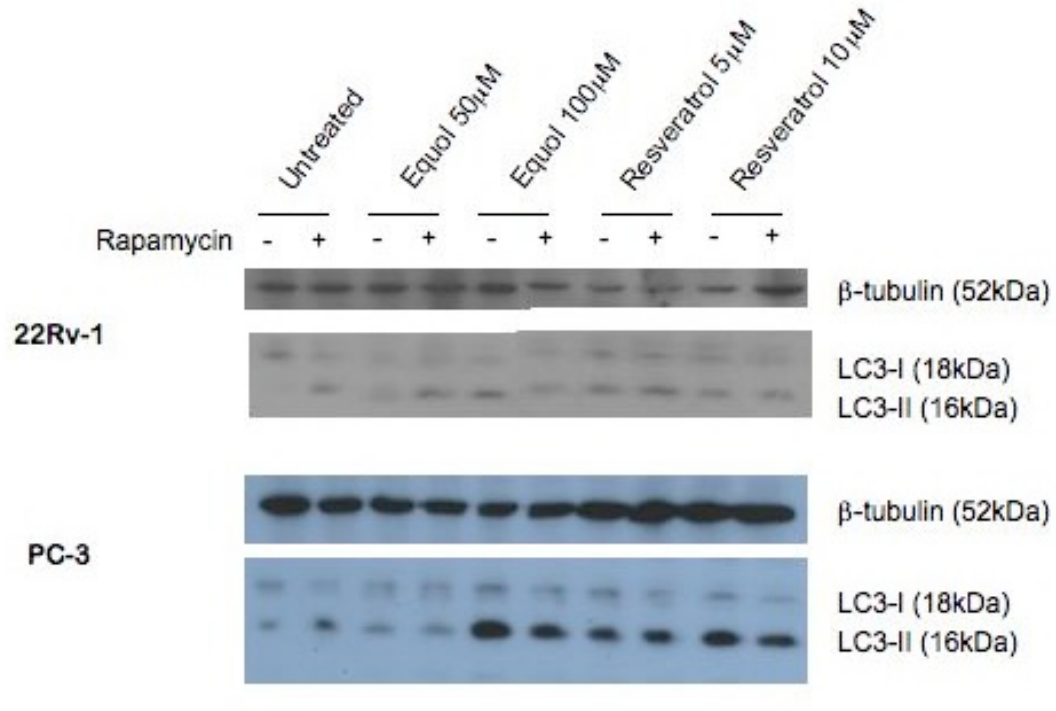

Figure 50 LC3 expression in phytochemical-treated cells with and without rapamycin

Cells were treated with equol (50μM or 100μM) or resveratrol (5μM or 10μM) and with or without rapamycin (100nM). Cell lysates were harvest 48h post-treatment and LC3 detected by western blotting as described in Methods Section 2.7.

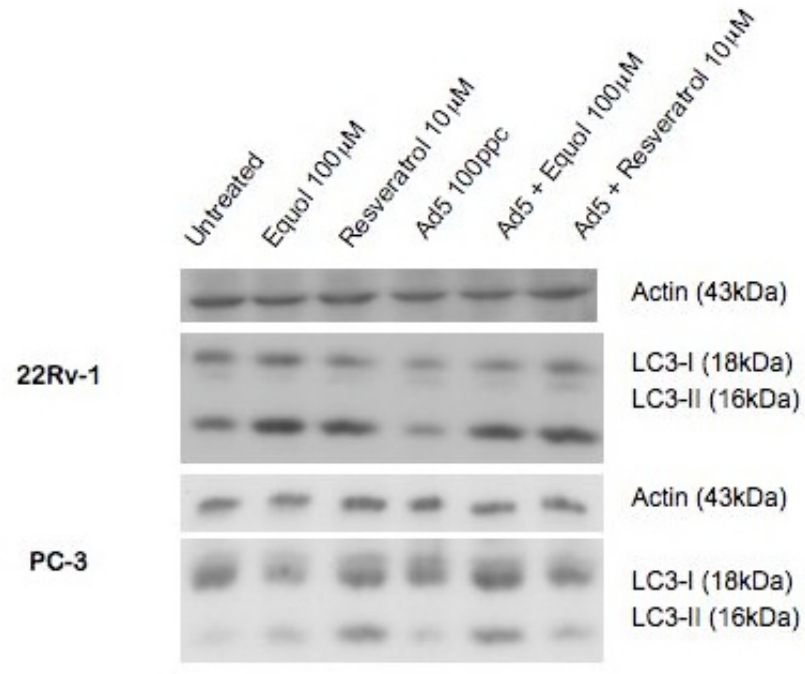

Figure 51 LC3 expression in Ad5-infected cells with and without phytochemicals

Cells were infected with Ad5 (100ppc) or left uninfected. After 2h, the medium was removed and replaced with normal or phytochemical-containing 2% FCS medium (equol 50μM, resveratrol 5μM). Lysates were harvested 48h post-infection and blotted for LC3 and actin as described in Methods Section 2.7.

3.4.2 Subcellular localization of LC3

Autophagy was also assessed by monitoring the cellular localization of LC3 in phytochemical-treated cells. This was done by creating stably transfected cells expressing GFP-tagged LC3, as described in Methods Section 2.8.1, and determining the localization of this protein by confocal microscopy.

In untreated, stably transfected 22Rv-1-LC3-GFP cells, LC3 remained cytosolic and the cells therefore appear homogeneously and diffusely green (Figure 52 A and B). A few cells in untreated samples displayed signs of autophagy. This correlates with the Western blot analyses which indicated basal levels of autophagy in untreated cells. Cells undergoing autophagy should display a punctate pattern of green, indicating relocalisation of LC3 to autophagosomes. Cells were treated with rapamycin (up to 400nM for 48h) or were serum-starved to obtain a positive control (Figure 52 C and D). A proportion of these cells did show a punctate green appearance although the phenotype was not as striking as expected. This was surprising since LC3-II expression was highly upregulated in 22Rv-1 cells treated with rapamycin, as determined by Western blotting (Figure 50).

Ad5 alone did not induce relocalization of LC3 to autophagosomes (Figure 53 B). This is consistent with LC3-II expression detected by Western blot (Figure 51). Cells treated with equol showed punctate patterns of green in some cells that were reduced by Ad5 (Figure 53 C and D). A trend towards autophagy was also observed in resveratrol-treated 22Rv-1 cells that was not prevented by Ad5 (Figure 53 E and F). LC3-GFP localization to autophagosomes was also visible in cells exposed to resveratrol after shorter treatments of 3-6h (Figure 54).

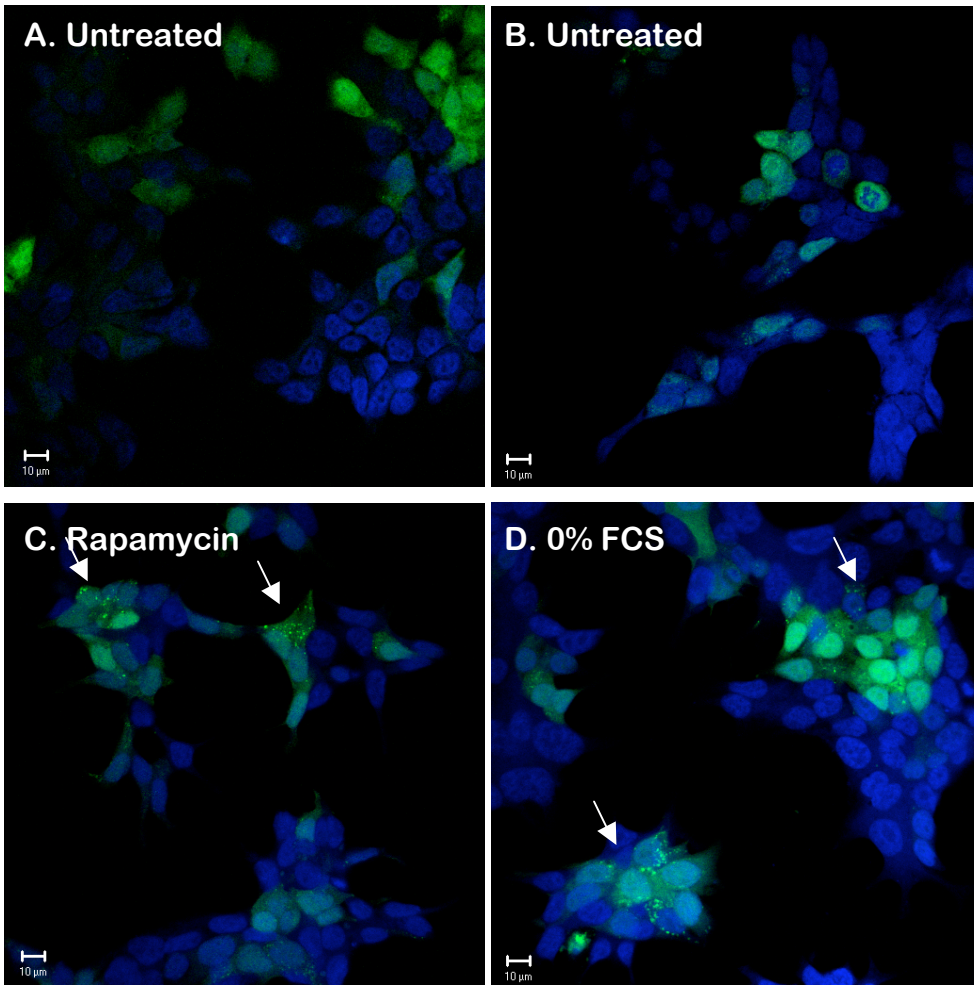

Figure 52 Autophagy-induced localization of LC3-GFP in 22Rv-1-LC3 -GFP cells viewed by confocal microscopy

Stably transfected 22Rv-1-LC3-GFP cells were seeded on glass coverslips in duplicate 6-well plates and allowed to adhere overnight. Cells were incubated for 48h with 2% FCS medium (A and B), with rapamycin (400nM, C) or with 0% FCS (D). Cells were fixed, permeabilised and mounted as described in Methods Section 2.8.2 for viewing by confocal microscopy. Arrows indicate cells with punctate green indicating LC3 localization to autophagosomes. Images are of representative fields of cells viewed on duplicate coverslips. Scale bars, 10μM. N=2.

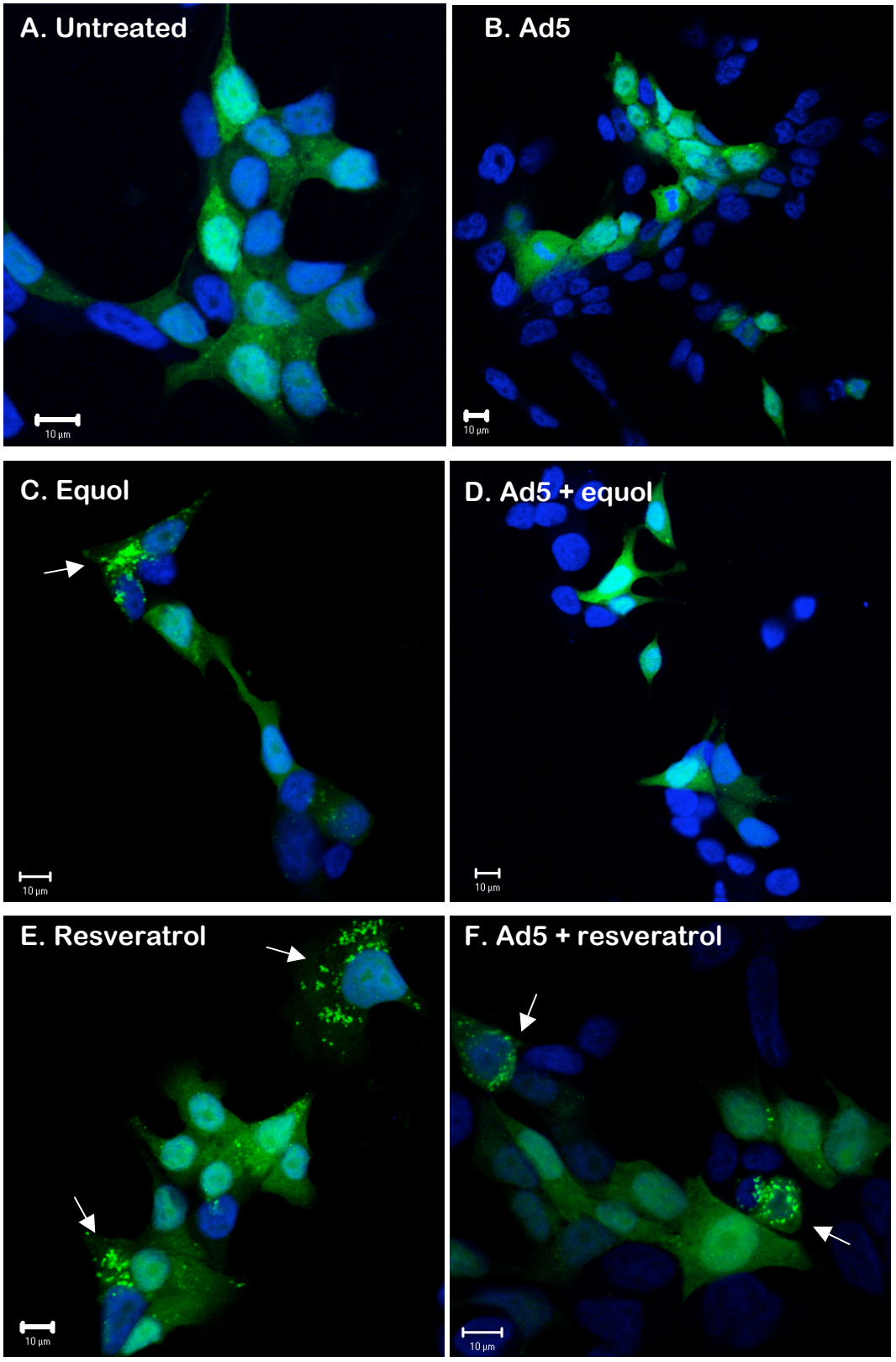

Figure 53 LC3 localization in phytochemical-treated 22Rv-1-LC3-GFP cells

Stably transfected 22Rv-1-LC3-GFP cells were seeded on glass coverslips in duplicate 6-well plates and allowed to adhere overnight. Cells were left uninfected or infected with Ad5 (100ppc) for two hours, then incubated with equol (100µM) or resveratrol (10µM) in 2% FCS. Cells were fixed, permeabilised and mounted as described in Methods Section 2.8.2 48h post-infection. A, Uninfected, untreated; B, Ad5; C, Equol; D, Ad5 and equol; E, Resveratrol; F, Ad5 and resveratrol. Images are of representative fields of cells viewed on duplicate coverslips. Scale bars, 10µM. N=2.

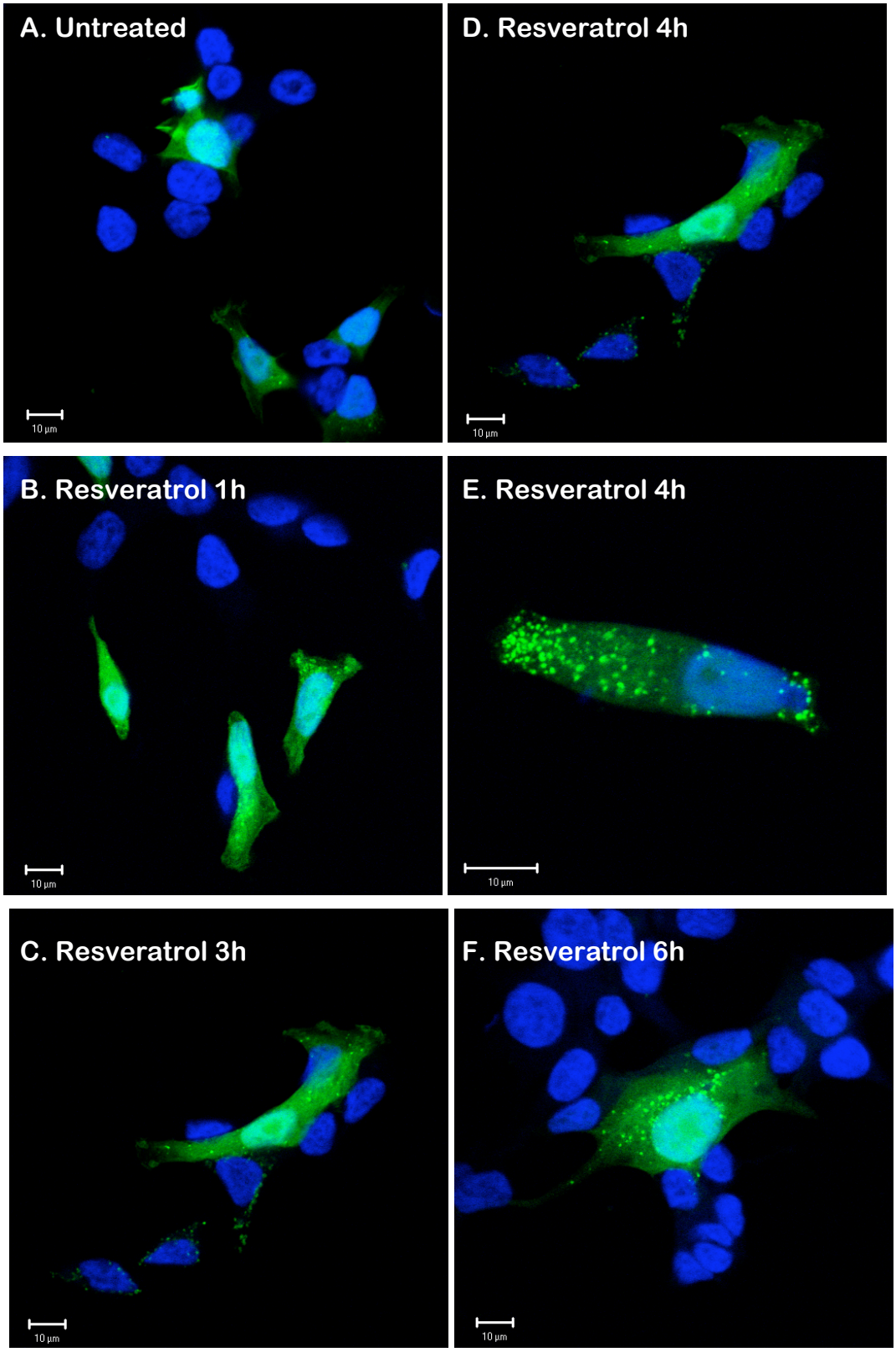

Figure 54 LC3 localisation in 22Rv-1-LC3-GFP cells treated with resveratrol at early time-points

Stably transfected 22Rv-1-LC3-GFP cells were seeded on glass coverslips in duplicate 6-well plates. The following day cells were treated with resveratrol (10μM) in 2% FCS or left untreated (A). Cells were fixed, permeabilised and mounted as described in Methods Section 2.8.2 after 1h (B), 3h (C), 4h (D and E) and 6h (F). Images are of representative fields of cells viewed on duplicate coverslips. Scale bars, 10μM. N=1.

3.4.3 Inhibition of autophagy enhances cell death

To determine whether the observed induction of autophagy might play a role in the synergistic enhancement of cell death in response to the combination treatments of Ad5 with phytochemicals, two autophagy inhibitors were used in MTS cell viability assays. 3-methyladenine (3-MA) inhibits autophagy induction by binding to class III PI3K (Petiot *et al.*, 2000; Seglen & Gordon, 1982), whereas bafilomycin A1 inhibits autophagy further downstream by preventing the fusion of the autophagosomes with lysosomes (Yamamoto *et al.*, 1998).

In cells treated with phytochemicals alone, the inhibition of autophagy increased cell death, although the effect was mostly additive (Figure 55). For example, in 22Rv-1 cells, cytotoxicity due to equol 50μM was increased from 38.6% to 47.7% by bafilomycin A1 and to 56.1% by 3-MA. Similarly, resveratrol-induced (10μM) cell death increased from 27.3% to 40.7% with bafilomycin A1 and to 44.6% 3-MA. In DU145 cells 3-MA increased cell death in response to 100μM equol from 44.8% to 65.9% and in response to 10μM resveratrol from 16.6% to 60.9%. In PC-3 cells, 3-MA increased cell death induced by 5μM resveratrol from 9.8% to 21.8%, although there was little effect on equol-induced cell death. However, there was a striking induction of cell death by the combination of equol with bafilomycin A1, cell death levels reaching 74.9% (equol 50μM) and 85.4% (equol 100μM).

In PC-3 cells, rapamycin alone caused 47.9% cell death. This was not affected by the addition of resveratrol, however, equol reduced rapamycin-induced cytotoxicity to less than 2% cell death. The induction of autophagy by rapamycin in DU145 reduced cell death caused by the highest concentrations of phytocehmicals from 44.8% (equol 100μM) and 16.7% (resveratrol 10μM) to less than 2%. In contrast to the AR-negative cell lines, in 22Rv-1 cells, rapamycin in combination with the phytochemicals induced higher cytotoxicity levels additively. With 100μM equol, rapamycin increased cell death from 61.6% to 76.3% and with 10μM, from 27.3% to 47.4%. Rapamycin alone caused 14.7% cell death in this cell line.

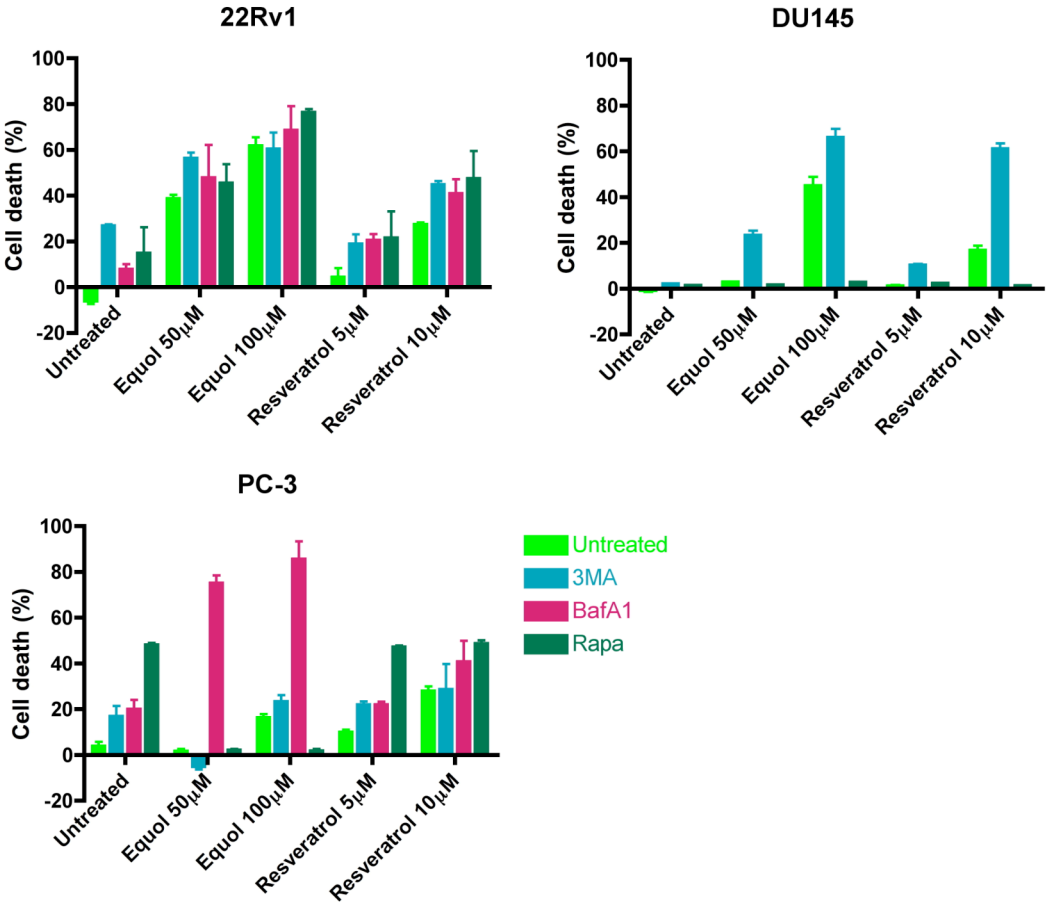

Figure 55 The effect of autophagy inhibitors on phytochemical-treated cells

Cells were treated in triplicate with phytochemicals (equol 50μM or 100μM, resveratrol 5μM or 10μM) with or without the autophagy inhibitors, 3-methyladenine (3MA, 22Rv-1 and PC-3: 2mM, DU145: 10mM) or bafilomycin-A1 (BafA1, 22Rv-1: 0.5nM, PC-3: 2nM), or with the autophagy inducer, rapamycin (Rapa, 10nM). Cell viability was determined 6 days post-treatments by MTS assay. Results show as the average percentages of cell death for triplicates from one experiment ± SD, representative of 1-3 experiments.

In infected 22Rv-1 and PC-3 cells, the inhibition of autophagy induction by 3-MA had a sensitising effect while, conversely, the addition of rapamycin had a protective effect (Figure 56). The effect was most noticeable in PC-3 cells where 3-MA reduced the Ad5 EC_{50} value more than 5-fold, from 388.1ppc to 72.6ppc. On the other hand, in this cell line, rapamycin increased the Ad5 EC_{50} value 2.6-fold, to 1011.0ppc. While 10nM rapamycin caused about 50% cell death in PC-3 cells, treatment with Ad5 seemed to reduce this cytotoxicity The inhibition of autophagosome fusion with lysosomes by bafilomycin A1 did not have a significant effect in 22Rv-1 nor PC-3 cells (this inhibitor was not tested in DU145 cells). In DU145 cells, both rapamycin and 3-MA were protective, as they increased the Ad5 EC_{50} value from 12.9ppc to 33.8ppc (rapamycin) and 44.2ppc (3-MA) respectively.

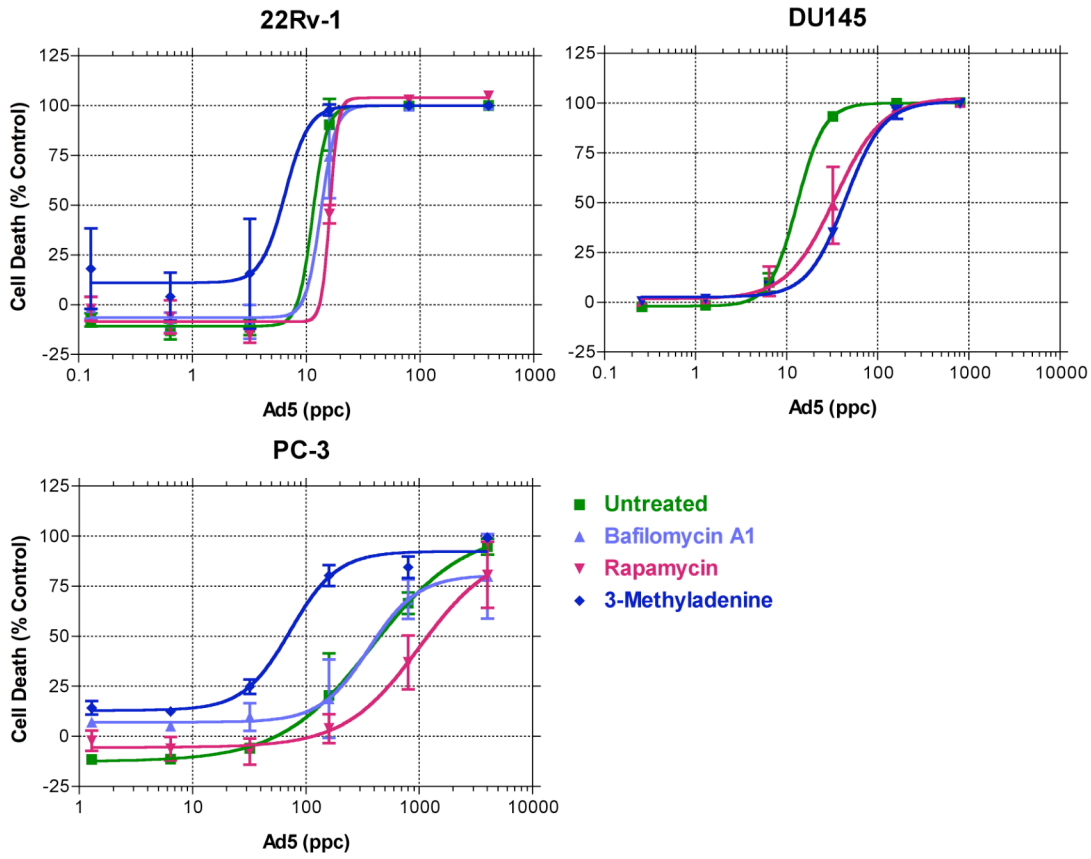

Figure 56 The effect of autophagy inhibition and stimulation on Ad5-induced cell death

Cells were infected with serially diluted Ad5 (22Rv-1, 0.128-400ppc, DU145, 0.256-800ppc, PC-3, 1.28-4000ppc) and treated with 3-methyladenine (22Rv-1 and PC-3, 0.5mM, DU145, 5mM), bafilomycin-A1 (22Rv-1, 0.5nM, PC-3, 2nM) or rapamycin (10nM). Cell viability was determined 6 days post-infection by MTS assay. Results shown as the average percentage cell death of triplicates from one experiment ± SD, representative of 2-3 experiments (except for rapamycin where N=1).

In cells treated with combinations of Ad5 and phytochemicals, 3-MA also sensitised 22Rv-1 cells to equol-induced cell death in combination with Ad5 (Figure 57), as observed when 3-MA was combined with equol (Figure 55). Inhibition of the fusion of autophagosomes with lysosomes by bafilomycin-A1 was not as potent, although Ad5 EC_{50} with equol 50μM was reduced from 2.59ppc to 1.85ppc (Table 21). 3-MA had a protective effect in PC-3 cells, where it increased Ad5 EC_{50} with 100μM equol from 8.3ppc to 22.2ppc. This is in keeping with the small protective effect of 3-MA on cell death induced by equol alone (Figure 55). Bafilomycin A1 greatly sensitised PC-3 cells to cell death induced by combinations of Ad5 and equol, similarly to its effect with equol alone in this cell line (Figure 55). 3-MA was also protective against combination-induced cell death with equol in DU145 cells, particularly at the lower concentration (50μM) of phytochemical.

The effect of rapamycin on cell death induced by Ad5 and equol was clearly protective in PC-3 cells, as in DU145 cells, although the results were less pronounced in the latter cell line. Unexpectedly, in 22Rv-1 cells, rapamycin appeared to be sensitising, particularly for combinations with equol 100μM. The induction of autophagy by rapamycin had no effect on cell death caused by combinations with resveratrol in 22Rv-1 cells, although in PC-3 cells it was clearly protective, increasing the Ad5 EC_{50} value 4.5-fold (Figure 58 and Table 21).

In DU145 cells, 3-MA was protective against combination-induced cell death with the lower dose of resveratrol (5μM) but at the higher dose (10μM), 3-MA was highly sensitising. The inhibition of autophagy signalling by 3-MA was sensitising in both 22Rv-1 and PC-3 cells treated with combinations of Ad5 and resveratrol. The effect of inhibiting autophagy at a downstream step by bafilomycin-A1 also sensitised these cell lines, although it was less potent than 3-MA.

These results showed that the modulation of autophagy using various chemical inhibitors could greatly impact the potency of combination treatments with Ad5. The induction of autophagy by rapamycin decreased Ad5-induced cell death so its stimulation may not be beneficial for adenovirus-based oncolytic virotherapy, at least in these cell lines. Rapamycin increased Ad5 EC_{50} values in combination-treated cells, except with 100μM equol in infected 22Rv-1 cells.

The inhibition of autophagy was found to sensitise the cells to combination treatments with Ad5 and phytochemicals in most instances, although the step at which autophagy was inhibited was important and the outcome varied between cell lines. The most responsive cell line to autophagy modulation was PC-3 cells.

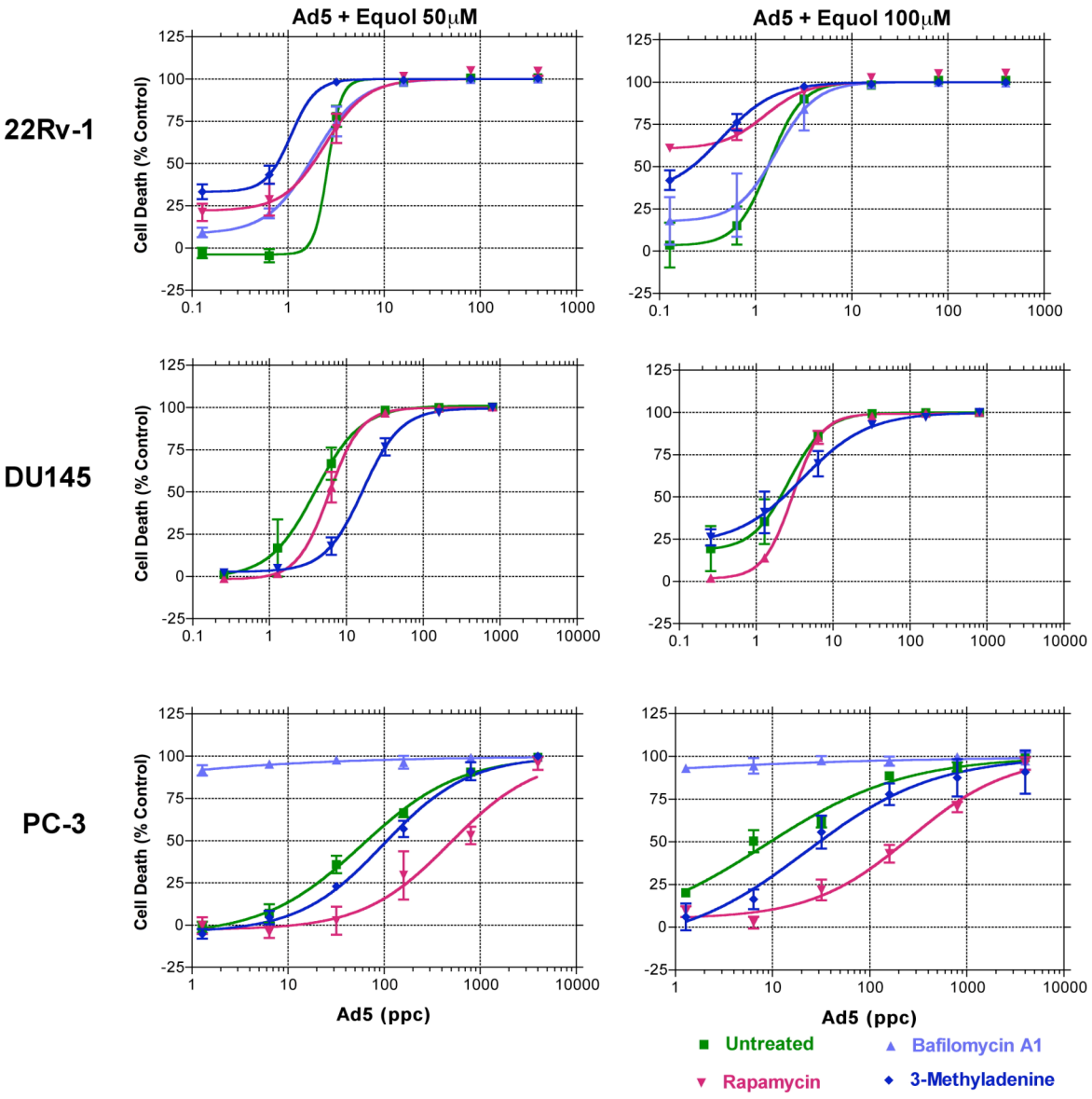

Figure 57 The effects on cell death by autophagy inhibition and stimulation when Ad5 is combined with equol

Cells were infected with serially diluted Ad5 (22Rv-1, 0.128-400ppc, DU145, 0.256-800ppc, PC-3, 1.28-4000ppc) and treated with or without equol (50μM or 100μM) and 3-methyladenine (22Rv-1 and PC-3, 0.5mM, DU145, 5mM), bafilomycin-A1 (22Rv-1, 0.5nM, PC-3, 2nM) or rapamycin (10nM). Cell viability was determined 6 days post-infection by MTS assay. Results shown as the average percentage cell death of triplicates from one experiment ± SD, representative of 2-3 experiments (except for rapamycin where N=1).

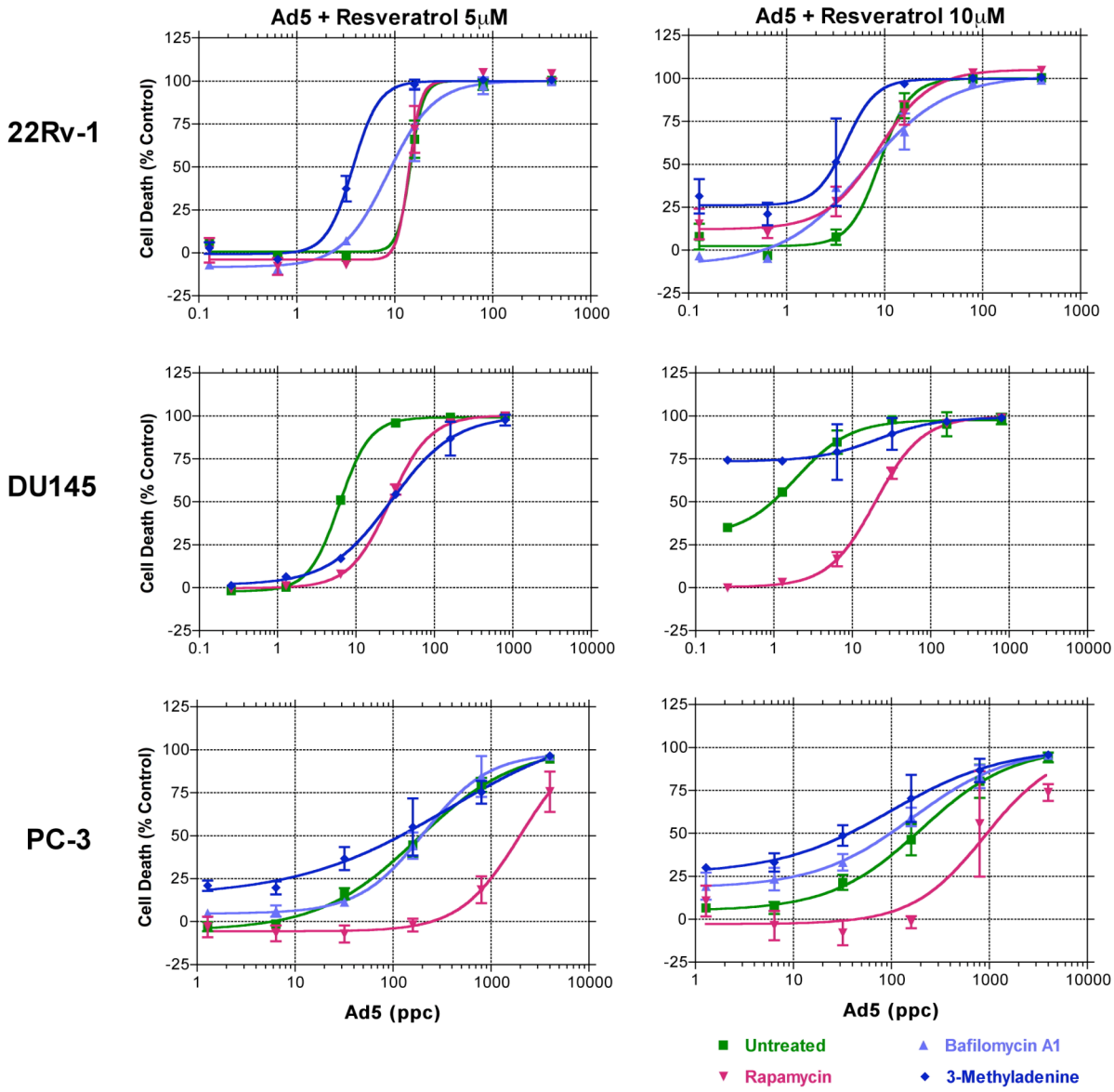

Figure 58 The effect of autophagy inhibition and stimulation on combination-induced cell death with resveratrol

Cells were infected with serially diluted Ad5 (22Rv-1, 0.128-400ppc, DU145, 0.256-800ppc, PC-3, 1.28-4000ppc) and treated with or without resveratrol (5μM or 10μM) and 3-methyladenine (22Rv-1 and PC-3, 0.5mM, DU145, 5mM), bafilomycin-A1 (22Rv-1, 0.5nM, PC-3, 2nM) or rapamycin (10nM). Cell viability was determined 6 days post-infection by MTS assay. Results shown as the average percentage cell death of triplicates from one experiment ± SD, representative of 2-3 experiments (except for rapamycin where N=1).

Table 21 Ad5 EC_{50} values in phytochemical-treated cells with two autophagy inhibitors and one inducer

22Rv1	Untreated	Bafilomycin-A1	Rapamycin	3-Methyladenine
Ad5 alone	**11.35**	**13.44**	**16.10**	**6.50**
Ad5 + Equol 50μM	2.59	1.85	2.43	1.07
Ad5 + Equol 100μM	1.38	1.65	N/A	N/A
Ad5 + Resveratrol 5μM	14.49	8.51	13.94	3.74
Ad5 + Resveratrol 10μM	8.96	6.25	8.63	4.05

DU145	Untreated	Rapamycin	3-Methyladenine
Ad5 alone	**12.90**	**33.84**	**44.15**
Ad5 + Equol 50μM	3.94	5.99	16.49
Ad5 + Equol 100μM	2.66	2.96	3.98
Ad5 + Resveratrol 5μM	6.13	27.11	28.51
Ad5 + Resveratrol 10μM	1.93	19.87	N/A

PC-3	Untreated	Bafilomycin-A1	Rapamycin	3-Methyladenine
Ad5 alone	**388.1**	**360.5**	**1011.0**	**72.6**
Ad5 + Equol 50μM	58.2	N/A	487.5	98.9
Ad5 + Equol 100μM	8.3	N/A	261.3	22.2
Ad5 + Resveratrol 5μM	172.3	214.2	1800.0	204.7
Ad5 + Resveratrol 10μM	201.9	164.4	907.0	99.6

Representative data from experiments shown in Figure 56 Figure 57 and Figure 58. Results are shown as Ad5 EC_{50} values (ppc) for each combination treatment and inhibitor/inducer. N/A = Ad5 EC_{50} value not determined due to a lack of dose response curve, resulting from high cell death.

To determine whether the inhibition of autophagy increased cell death through the apoptotic pathway, caspase-3 expression levels were verified in bafilomycin-A1-treated cells (Figure 59 and Figure 60). Caspase-3 activation was detected in both 22Rv-1 and DU145 cells treated with equol or resveratrol. Treatment with bafilomycin-A1 caused an accumulation of LC3-II, as expected since the degradation of the autophagosome is inhibited by this compound. The addition of equol or resveratrol to 22Rv-1 and DU145 cells treated with the autophagy inhibitor increased the level of LC3-II. Treatment of DU145 cells with phytochemicals and bafilomycin-A1 induced higher expression levels of caspase-3, indicating that the induction of apoptosis was enhanced by the repression of autophagy. In both 22Rv-1 and DU145 cells, caspase-3 activation was abrogated by Ad5, although combination-treated cells expressed low levels of cleaved caspase-3. In 22Rv-1 cells bafilomycin-A1 had little effect on caspase-3 activation in Ad5-infected cell, indicating that the enhanced cell death detected in combination-treated cells when autophagy is inhibited may not be due to apoptosis. However, th**ese** data correlate with the limited changes in Ad5 EC_{50} caused by bafilomycin A1 detected in this cell line (Table 21). Use of the more potent autophagy inhibitor, 3-MA, could reveal differential caspase-3 expression. In combination-treated DU145 cells exposed to bafilomycin-A1, there was a small level of active caspase-3 expression, indicating that apoptosis might play a role in combination-induced cell death when autophagy is inhibited in this cell line. The effect of bafilomycin-A1 on combination-induced cell death in DU145 cells remains to be determined.

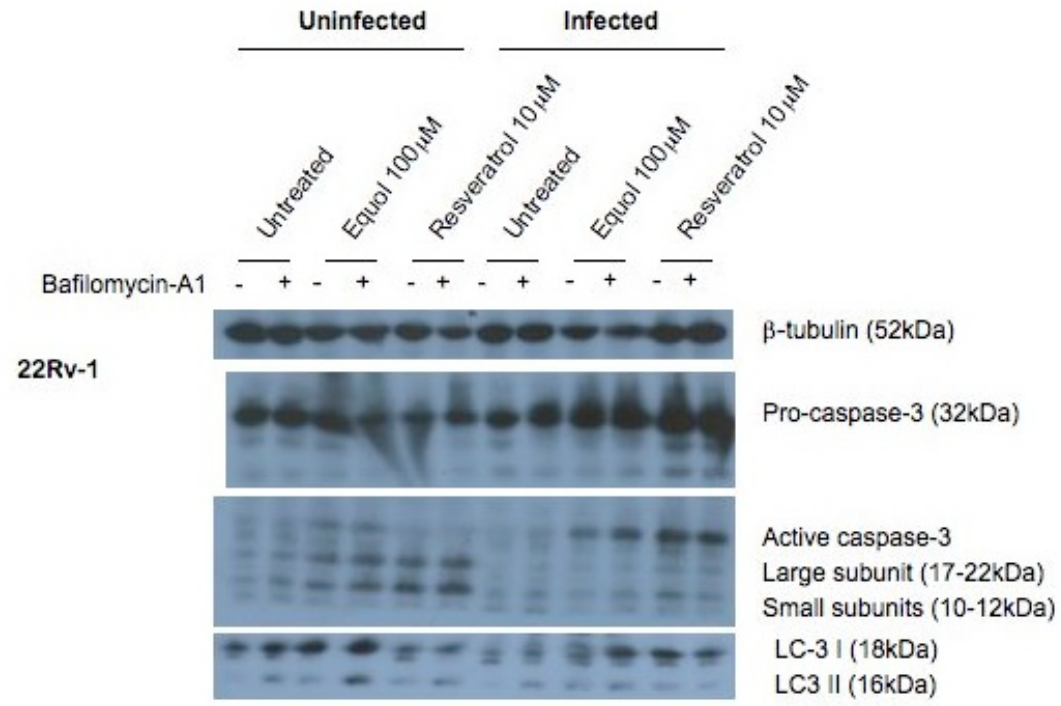

Figure 59 Caspase-3 expression in bafilomycin-A1-treated 22Rv-1 cells

Cells were infected with Ad5 (100ppc) for 2h or left uninfected. Cells were then treated with equol 100μM or resveratrol 5μM), with or without bafilomycin-A1 (1nM). Cell lysates were harvested 48h after nfection and used for western blot detection of capase-3 as detailed in Methods Section 2.7.2. Blots shown are representative of two independent experiments.

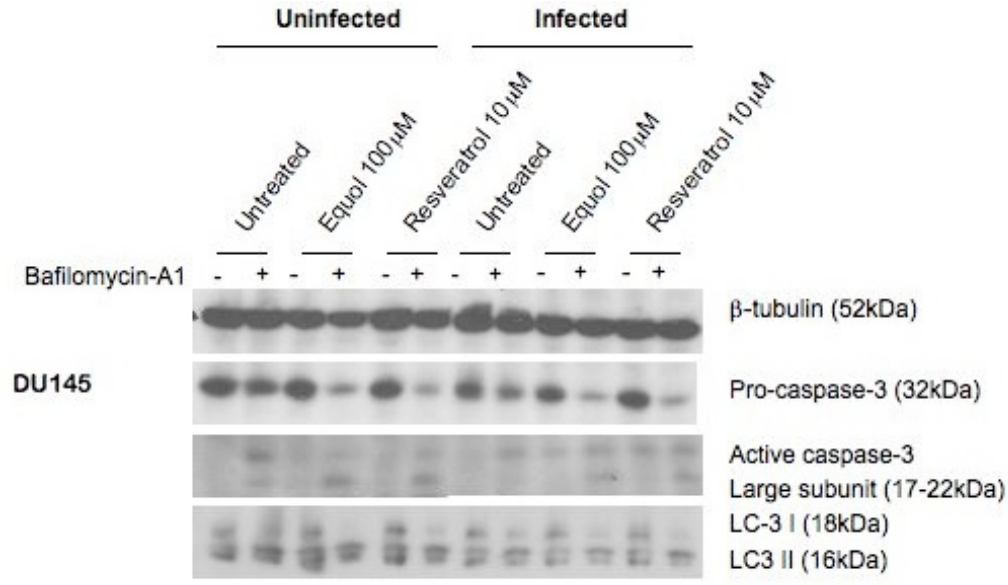

Figure 60 Caspase-3 expression in bafilomycin-A1-treated DU145 cells

Cells were infected with Ad5 (100ppc) for 2h or left uninfected. Cells were then treated with equol 100μM or resveratrol 5μM), with or without bafilomycin-A1 (1nM). Cell lysates were harvested 48h after infection and used for Western blot detection of capase-3 as detailed in Methods Section 2.7.2. N=1.

3.5 Synergy of phytochemicals with replication-selective oncolytic Ad5 mutants

We sought to determine whether the synergistic enhancement of adenovirus-induced cell death by equol and resveratrol could also be achieved with replication-selective oncolytic deletion mutants and to further investigate the mechanisms for the enhanced cell death with the phytochemicals. We therefore tested equol and resveratrol with several Ad5 mutants designed in our lab which are currently being evaluated preclinically. This was done by screening different combination ratios of adenoviral mutants and phytochemicals. Higher combination ratios were selected since the earlier synergy study showed that they seemed to give better results (Figure 22 and Figure 23). Isobolograms were constructed from the EC_{50} doses for each combination ratio and combination indexes (CIs) were determined.

PC-3 cells, which had previously been shown to be the most resistant to Ad5-induced cell death (Figure 21), were the most responsive cells to combination treatments. This cell line showed very few antagonistic results with any of the adenoviral mutants tested (Table 22). As expected, the majority of responses with wild type virus and equol were synergistic (77% responses with Ad5, 100% responses with Ad5tg, the wild type backbone from which our other mutants are constructed; see Methods Section 2.3.1). With resveratrol, 56% of the interactions with Ad5 were found to be synergistic, the rest being additive, and with Ad5tg 80% of the responses were additive and the others were synergistic.

The other replicating adenoviral mutants also acted synergistically with equol in PC-3 cells. The best CI (0.24) was obtained with AdΔΔ at the highest ratio (1ppc:15625nM) (Table 23). However, both AdΔCR2 (best CI=0.8) and AdΔΔ (best CI=0.78) were mostly additive with resveratrol and AdΔE1B-19K was antagonistic with this phytochemical (CIs between 1.34-2.6). The non-replicating AdE1A-12S mutant, that has been shown to sensitise cells to chemotherapeutic drug-induced apoptosis, gave four out of four antagonistic responses, although the average CI was less than 1.3, indicating only mild antagonism. However, this observation supports the conclusion that the synergistic interaction of phytochemicals with adenoviruses does not solely rely on the induction of apoptosis. No effects could be determined in combination with the non-replicating *dl*312 mutant in PC-3 cells since this virus killed <10% cells (2×10^5ppc) so the EC_{50} value could not be determined.

Despite clear synergy with Ad5 in combination experiments with DU145 cells (Figure 25), Ad5 in this cell line produced 48% antagonistic responses with equol and nearly a third

interactions with resveratrol (Table 22). Average CIs showed that the antagonism occurs especially at the lowest combination ratios (1ppc:125nM and 1ppc:625nM, Table 24). The highest ratio (1ppc:15625nM) gave consistent additive results with Ad5 and synergy with Ad5tg.

The replicating deletion mutants also acted synergistically at the highest ratio with equol and additively with resveratrol in DU145 cells. The most synergistic mutant with equol was Ad5ΔE1B-19K (9/12 synergistic interactions), followed by AdΔCR2 (5/8). Surprisingly, most responses with AdΔΔ were antagonistic (5/8), although at the highest combination ratio, it was synergistic with both equol (average CI=0.68) and resveratrol (average CI=0.8).

The non-replicating mutants showed good responses in DU145 cells, nearly all interactions being synergistic or additive. Ad5-Hey1, which expresses the AR co-repressor Hey1, produced 5 out of 8 synergistic responses with equol (CIs between 0.6-0.94) although this cell line does not express the androgen receptor. *dl*312 acted additively in DU145 cells. AdE1A-12S was synergistic with equol at the lowest ratio (average CI=0.6) and additive at other combination ratios with equol and resveratrol.

Interactions of the deletion mutants were not studied as extensively in 22Rv-1 cells since the results with wild type Ad5 were not as promising as for other cell lines. The majority of responses were only additive and for each phytochemical, 3 out of 8 interactions were found to be antagonistic (Table 25). One point of synergy was detected with Ad5 and resveratrol at the highest combination ratio (average CI=0.6, Table 25). The non-replicating Ad5-Hey1 mutant was also synergistic with equol at this ratio (average CI=0.65) although it was additive (3/8 responses) or antagonistic (5/8) with resveratrol.

Table 22 Summary of interactions between equol and resveratrol with Ad5 mutants

PC-3	Equol				Resveratrol			
	Synergistic	Additive	Antagonistic	Total	Synergistic	Additive	Antagonistic	Total
Ad5	10	3	0	13	5	4	0	9
Ad5tg	5	0	0	5	1	4	0	5
AdΔΔ	10	1	0	11	2	5	0	4
AdΔE1B-19K	9	0	0	9	1	3	0	5
AdΔCR2	5	0	0	5	1	4	0	5
AdE1A-12S	0	4	2	6	0	1	1	2
*dl*312	N/A (no EC_{50} for *dl*312 alone)				N/A (no EC_{50} for *dl*312 alone)			

DU145	Equol				Resveratrol			
	Synergistic	Additive	Antagonistic	Total	Synergistic	Additive	Antagonistic	Total
Ad5	6	5	10	21	2	9	5	16
Ad5tg	1	1	2	4	1	1	2	4
AdΔΔ	2	1	5	8	1	2	5	8
AdΔE1B-19K	9	2	1	12	4	2	2	8
AdΔCR2	5	2	1	8	0	5	3	8
AdE1A-12S	4	3	1	8	4	0	0	4
Ad5-Hey1	5	3	0	8	1	7	0	8
*dl*312	1	3	0	4	1	3	0	4

22Rv1	Equol				Resveratrol			
	Synergistic	Additive	Antagonistic	Total	Synergistic	Additive	Antagonistic	Total
Ad5	0	5	3	8	1	4	3	8
Ad5tg	0	1	0	1	1	0	0	1
AdΔΔ	0	1	0	1	0	1	0	1
AdE1A-12S	0	1	0	1	0	1	1	1
Ad5-Hey1	2	5	1	8	0	3	5	8

Synergy assays were performed with replicating and non-replicating Ad5 mutants with equol and resveratrol. The interactions were analysed by constructing isobolograms and determining combination indices (CIs) for combination ratios of each mutant and phytochemicals, as described in Methods Section **Error! Reference source not found.**. The results were summarized by counting the number of synergistic (CI≤0.8), additive (CI 0.8-1.2) and antagonistic (CI≥1.2) ratios from independent experiments repeated >2 times. Results for the double-deleted AdΔΔ mutant are shown in red. Results for non-replicating mutants are shown in green.

Table 23 Combination indices for adenoviral mutants with equol or resveratrol in PC-3 cells

PC-3	Ad5		pTG3602		AdΔE1B-19K		AdΔCR2		AdΔΔ	
	Equol	Resveratrol	Equol	Resveratrol	Equol	Resveratrol	Equol	Resveratrol	Equol	Resveratrol
1:125	**0.35**	**0.43**	*0.34*	*0.89*	**0.39**	*2.59*	*0.49*	*0.87*	**0.49**	*1.03*
1:625	**0.27**	**0.46**	*0.28*	*0.77*	**0.30**	*1.34*	*0.48*	*0.83*	**0.32**	*0.85*
1:3125	**0.82**	**0.48**	*0.31*	*1.04*	**0.35**	*1.55*	*0.47*	*0.83*	**0.27**	*0.83*
1:15625	**0.92**	**0.54**	0.34	1.04	**0.39**	**1.49**	*0.52*	*0.85*	**0.24**	**0.78**

AdE1A-12S		*dl*312	
Equol	Resveratrol	Equol	Resveratrol
1.18		N/A	N/A
1.03		N/A	N/A
1.95		N/A	N/A
1.30	**1.33**	N/A	N/A

Average combination indices from >2 experiments (except where N=1, numbers in italics) shown in Table 22. The most effective ratio indices are highlighted in purple.

Table 24 Combination indices for adenoviral mutants with equol or resveratrol in DU145 cells

DU145	Ad5		Ad5tg		AdΔE1B-19K		AdΔCR2		AdΔΔ	
	Equol	Resveratrol	Equol	Resveratrol	Equol	Resveratrol	Equol	Resveratrol	Equol	Resveratrol
1:125	**1.34**	**1.35**	*2.13*	*2.56*	**0.90**	**1.27**	**0.88**	**1.40**	**1.71**	**1.60**
1:625	**1.02**	**1.39**	*2.15*	*1.80*	**0.82**	**1.14**	**0.72**	**2.24**	**1.67**	**1.56**
1:3125	**0.93**	**1.14**	*0.91*	*1.16*	**0.56**	**0.91**	**0.63**	**1.12**	**1.28**	**1.18**
1:15625	**0.90**	**1.08**	*0.69*	*0.71*	**0.53**	**0.90**	**0.43**	**1.01**	**0.68**	**0.80**

AdE1A-12S		*d*l312		Ad5-Hey1	
Equol	Resveratrol	Equol	Resveratrol	Equol	Resveratrol
0.88	*0.91*	*0.82*	*1.04*	**0.94**	**0.99**
0.80	*0.88*	*0.74*	*0.93*	**0.66**	**0.84**
1.03	*0.94*	*1.01*	*0.93*	**0.60**	**0.96**
0.59	*0.84*	*1.05*	*0.96*	**0.79**	**1.07**

Average combination indices from >2 experiments (except where N=1, numbers in italics) shown in Table 22. The most effective ratio indices are highlighted in purple.

Table 25 Combination indices for adenoviral mutants with equol or resveratrol in 22Rv-1 cells

22Rv-1	Ad5		Ad5tg		AdΔΔ		AdE1A-12S		Ad5-Hey1	
	Equol	Resveratrol	Equol	Resveratrol	Equol	Resveratrol	Equol	Resveratrol	Equol	Resveratrol
1:250	**1.81**	**1.25**							**1.06**	**1.20**
1:1250	**1.24**	**1.23**							**1.05**	**1.23**
1:6250	**0.95**	**1.16**							**1.14**	**1.26**
1:31250	**0.84**	**0.60**	*0.97*	*0.77*	*1.14*	*0.85*	*1.19*	*0.83*	**0.65**	**1.26**

Average combination indices from >2 experiments (except where N=1, numbers in italics) shown in Table 22. The most effective ratio indices are highlighted in purple.

In conclusion, these synergy studies highlighted that PC-3 cells were the most easily sensitised, as they produced the most synergistic interactions, compared to 22Rv-1 and DU145 cells. The lowest average CI was obtained in PC-3 cells with AdΔΔ (ratio 1ppc:15625nM, CI=0.24). Equol induced a greater number of synergistic responses compared to resveratrol. Most notably, equol acted synergistically with the non-replicative mutant Ad5-Hey1 in both 22Rv-1 and DU145 (not tested in PC-3 cells).

4 Discussion

Selectively replicating Ad5 mutants are attractive anti-cancer therapeutics currently being developed for use in the clinic. However, their efficacy as a single modality has been limited. Combining Ad5 oncolytic vectors with chemotherapeutic drugs, as well as radiation, has proven successful in enhancing the anti-tumour potency, whilst still retaining cancer selectivity.

In view of the demonstrated anticancer benefits of phytochemicals, we hypothesized that these non-toxic compounds might also enhance tumour cell killing in combination with Ad5. This could pave the way for the development of therapeutic phytochemicals for oral administration to patients treated with oncolytic adenoviruses, avoiding systemic side-effects from non-targeted chemo- and radiotherapies. Specifically, we conceived that phytochemicals which inhibit the MAPK pathway might be able to enhance the expression of CAR, a well-known Ad5 receptor, enabling greater adenoviral infectability and enhancing cell death. We found an increase in viral uptake and a striking synergistic induction of cell death in cells treated with equol or resveratrol and Ad5. Curcumin, EGCG and genistein could also sensitise PCa cells to Ad5-induced cell death although the effects were more modest. We therefore decided to focus on equol and resveratrol to determine the underlying mechanism for synergy with Ad5.

We found that equol and resveratrol induced apoptosis in DU145 cells, and to a lower extent in PC-3 cells, and that the addition of Ad5 enhanced the apoptotic response in these cell lines. Apoptosis levels in 22Rv-1 cells remained very low, so we considered whether additional cell death mechanisms might be involved in combination-induced cell death. Equol and resveratrol alone induced autophagy in 22Rv-1 and PC-3 cells, while Ad5 alone seemed to repress autophagy. Cell viability data using pharmacological autophagy modulators suggest that autophagy may perform a survival function in these cells rather than acting as a cell death mechanism. The execution of cell death in response to combination treatments is cell line-dependent and appears to involve apoptotic, autophagic and most certainly additional pathways.

Synergy studies with replication-selective mutants demonstrated the *in vitro* potential of using equol and resveratrol for specific targeting of cancer cells. Combinations with equol demonstrated the most encouraging results in DU145 cells with AdΔE1B-19K and with AdΔΔ in PC-3 cells. The potency of these combinations remains to be verified *in vivo*.

4.1 Curcumin, EGCG and genistein are antagonistic with Ad5 under certain conditions

Combination assays showed that curcumin and EGCG treatment could enhance, but also decrease, cell death with Ad5. Ad5 EC_{50} values were increased more than 6-fold in PC-3 cells pretreated with EGCG, and to a lesser extent when the phytochemical was added simultaneously or 24h after infection. One reason for this could be the reported inhibitory effect of EGCG on the adenoviral protease (Weber *et al.*, 2003). As described in Section 1.2.3.8, the viral protease is instrumental in allowing Ad5 escape from the endosome and delivery to the nucleus, as well as for viral packaging later in the viral life-cycle. EGCG-mediated inhibition of the viral protease could therefore contribute to the antagonistic effect observed with Ad5, although the IC_{50} for the protease was reported to be 109μM which is higher than any of the concentrations used in our combination assays (<25μM).

EGCG was also the most cytotoxic phytochemical out of the five tested in this study. We observed the largest antagonistic effects with Ad5 when cells were pre-treated for 24h before infection. EGCG may therefore induce apoptosis which could block cell cycle progression, preventing viral replication and causing cell death before the virus is able to hijack the cellular machinery and express viral proteins required for the synergistic effect.

Although we found few synergistic interactions between Ad5 and EGCG, this phytochemical has previously been found to enhance cell death in PCa cells synergistically with other cytotoxic agents such as TRAIL (Siddiqui *et al.*, 2008). LNCaP cells, which are naturally resistant to TRAIL, were shown to be sensitised by EGCG-mediated Akt inhibition that blocks prosurvival signalling, lowering the sensitivity threshold of the cells for TRAIL and inducing apoptosis. This may indicate that combining EGCG with Ad5 causes a different response in the cells compared to death-inducing TRAIL.

Curcumin also antagonised cell death with Ad5 in cells treated both 24h before or after infection. There were fewer antagonistic responses in 22Rv-1 cells, but none of the conditions could significantly enhance cell death. Li *et al*. showed that curcumin induces apoptosis via the inhibition of Akt and the downregulation of the MDM2 oncogene in PCa and breast cancer cell lines (Li *et al.*, 2007). Furthermore, in LNCaP and PC-3 cells, curcumin has been found to cause growth arrest, blocking the cell cycle by preventing the G_1/S transition by upregulating p21 and p27 expression and inhibiting the expression of cyclins D and E (Srivastava *et al.*, 2007). This inhibition of cell cycle progression beyond G_1, in addition to the premature induction of apoptotic cell death, could explain the negative effects of curcumin we observed

with Ad5 on cell death since the prevention of S-phase induction would block viral gene expression and subsequent viral replication. In addition, it is well known that cyclin E is required for efficient viral replication (Zheng *et al.*, 2008).

We also chose to discard genistein as a potential enhancer of cell death with Ad5 because although this phytochemical showed some potent reductions in Ad5 EC_{50} values, the responses were not dose-dependent: the higher doses of genistein tested actually caused antagonism in both 22Rv-1 and PC-3 cells. A number of epidemiological and *in vivo* studies suggest that genistein consumption may be chemopreventive (Magee & Rowland, 2004). However, a biphasic effect on cell growth by this phytochemical has been observed in a number of breast cancer cell lines and immortalized nontumorigenic prostate epithelial cells (Wang *et al.*, 2006). Furthermore, transgenic adenocarcinoma of the mouse prostate (TRAMP) mice which consumed low doses of genistein suffered from an aggressive progression of PCa (El Touny & Banerjee, 2009). *In vitro*, El Touny *et al*. found that the equivalent concentration of genistein increased PC-3 cell proliferation and invasion via estrogen and PI3K signalling. These observations highlight the potential risk of detrimental effects by genistein. The situation *in vivo* in combination with Ad5 might be different, depending on the balance of beneficial and unfavourable systemic effects, but this was beyond the scope of the project.

4.2 Equol and resveratrol act synergistically with Ad5

Equol and resveratrol were found to act synergistically with Ad5 on cell death in both AR-positive and negative cell lines. Ad5 EC_{50} values were reduced 9-fold by equol and 17-fold by resveratrol in PC-3 cells which are the most resistant to the virus. In more permissive cell lines, equol reduced Ad5 EC_{50} values 6-fold (22Rv-1) and 5-fold (DU145), while resveratrol reduced Ad5 EC_{50} values 3-fold (22Rv-1) and 8-fold (DU145). The largest reductions in Ad5 EC_{50} values were observed in cells treated simultaneously with phytochemical and Ad5.

4.2.1 Equol and resveratrol enhance the permissivity of PCa cells to Ad5 infection

Equol and resveratrol enhanced the infectability of the cell lines, both in terms of the percentage of cells infected and the average viral load per cell. However, the increase in viral uptake was not reflected in the levels of viral replication. In fact, both phytochemicals repressed viral replication in DU145 and PC-3 cells. No major effects on viral replication were detected in 22Rv-1 cells that were the least sensitive to the phytochemicals. The mechanism behind the decrease in viral replication does not involve phytochemical-mediated cell cycle arrest, since equol and resveratrol allowed and even enhanced the induction of S phase which is required for viral replication.

We deduced that the synergy observed between Ad5 and these phytochemicals could be due to greater permissivity of the cell lines to viral infection, perhaps enhancing early viral gene expression and thereby increasing the sensitivity of cells to combination-induced cell death. The synergistic interaction is likely to require E1A to transactivate the expression of other viral proteins that might be involved in combination-induced cell death. For example, E4-orf4 has been proposed to induce cell death via mitotic arrest and remodelling of the actin cytoskeleton (Robert *et al.*, 2006). E3-11.6K encodes the adenovirus death protein (ADP) which could also be involved in the combination-induced cell death mechanism (Tollefson *et al.*, 1996). The involement of these proteins in combination-induced cell death could be investigated further by characterising their expression. The adenoviral cell death mechanism is discussed futher in Section 4.3.

Based on our findings, a key factor in the synergistic enhancement of cell death appears to be the permissivity of cells to Ad5 infection, which was enhanced by equol and resveratrol. It has

been recognised that insufficient tumour transduction by oncolytic adenoviruses is an important factor limiting the antitumoral efficacy of therapeutic mutants (Krasnykh *et al.*, 2000; Kruyt & Curiel, 2002). Efforts to improve transduction have centred on retargeting mutants to alternative receptors, such as α_V integrins, or enhancing the expression of the adenoviral receptor, CAR (Glasgow *et al.*, 2006; Mathis *et al.*, 2005).

A number of chemotherapeutic drugs, in particular histone deacetylase (HDAC) inhibitors, were reported to enhance CAR expression, enabling improved transduction of a variety of cancer cell types (Goldsmith *et al.*, 2003; Hemminki *et al.*, 2003; Kitazono *et al.*, 2002; Okegawa *et al.*, 2005). A subsequent investigation also identified phytochemicals which upregulate CAR expression in human bladder cancer cells (Pong *et al.*, 2006). Most notably, this study identified genistein as the most potent CAR inducer out of a screen of 58 phytochemicals. Genistein was also found to dramatically synergise with the HDAC inhibitor FR901228 to heighten CAR expression. Pong *et al.*'s study demonstrated the potential of phytochemicals to induce viral uptake although their study did not include equol or resveratrol.

We monitored Ad5 transduction of cells using a replication-defective mutant expressing GFP from a CMV promoter replacing the *E1* genes. Kim *et al.* recently showed that the cytotoxic drug doxorubicin could enhance transgene expression from the CMV promoter by upregulating the NFκB transcription factor that binds to and transactivates the CMV promoter (Kim *et al.*, 2007). CMV promoter activity has also been demonstrated to be increased by DNA-damaging agents such as cisplatin and by UV exposure in the context of adenoviral-mediated transgene delivery (Zacal *et al.*, 2005). Despite these considerations, we are confident that the increase in GFP-positive cells and the median fluorescence observed were not simply due to enhanced transcription from the CMV promoter as the increased infectability was also observed in phytochemical-treated cells by qPCR measuring viral genome copy numbers 3h post-infection. In addition, we can probably rule out effects via NFκB since both equol and resveratrol have been reported to inhibit NFκB activation (Estrov *et al.*, 2003; Kang *et al.*, 2005). Finally, equol and resveratrol do not induce DNA-damage at the low concentrations used in our studies, so would not function in a similar way to cisplatin or UV.

Initially we hypothesised that the phytochemicals might be able to mediate enhanced cellular infectability by inhibiting the MAPK pathway, leading to an increase in CAR expression. This has been demonstrated in a panel of cell lines using pharmacological inhibitors (Anders *et al.*, 2003a). Although statistically significant increases in CAR cell surface expression were detected in 22Rv-1 cells treated with phytochemicals, the increases were small. In PC-3 cells,

CAR levels remained extremely low while CAR expression was already maximal in DU145 cells. Consequently, the increases in viral uptake and enhanced cytotoxicity could not be explained by increased cell surface expression levels of CAR alone.

CAR expression was also monitored in LNCaP cells where resveratrol had no effect and equol actually reduced the percentage of cells expressing the receptor. The use of this cell line in further studies was hampered by difficulties in growing these cells and their variability between different clones, passages and source. Nevertheless, it would have been interesting to analyse the infectability of LNCaP cells in response to phytochemical treatment to determine whether the decreased CAR expression in response to equol also reduced permissivity to Ad5 infection.

Nevertheless, our results support the notion that the infectability of cell lines is not determined solely by CAR expression, but also internalization receptors (integrins $\alpha_V\beta_3$ and $\alpha_V\beta_5$), alternative receptors such as HS-GAGs, and additional unidentified factors (Dechecchi *et al.*, 2001). The expression of HS-GAGs in untreated and phytochemical-treated PCa cells is unknown. It is possible that other unidentified adenoviral receptors might also be present that could be upregulated by equol and resveratrol.

Furthermore, based on the analysis of $\alpha_V\beta3$ and $\alpha_V\beta5$ integrins and CAR expression, DU145 cells would be expected to be the most permissive cell line to Ad5 infectability. However, instead, we found that both 22Rv-1 and LNCaP cells were more infectable than DU145 cells, although the former two cell lines showed low levels of integrins and high (but lower than DU145!) levels of CAR. This suggests that there may be additional receptors present on 22Rv-1 and LNCaP cells which render these cells more permissive to Ad5 infection.

In accordance with our data, Okegawa *et al*. detected the highest levels of CAR in DU145 (82% cells CAR-positive), intermediate levels in LNCaP (63% cells CAR-positive) and the lowest levels in PC-3 (35% cells CAR-positive) (Okegawa *et al.*, 2000). However, in contrast to our observations, using a replication deficient adenovirus expressing CMV-βgal, they found that DU145 cells were the most infectible. Another study found that at an MOI of 30, only 24% of DU145 cells were infected with a non-replicating GFP-expressing virus, while 78% of LNCaP cells and 5% of PC-3 cells were GFP-positive (Pandha *et al.*, 2003). These results correlate better with our results. Although our data clearly showed a correlation between the levels of expression of CAR and both α_V-integrins in PC-3 cells and the low transduction rate

of these cells, no clear correlation was observed in DU145, 22Rv-1 and LNCaP cells. This suggests that additional adenoviral receptors are likely to be involved in the infection process.

Whether the increased infectability imparted by phytochemical treatment *in vitro* can also be observed *in vivo* remains to be determined. *In vivo* biodistribution following systemic administration of Ad5 vectors is reported to be independent of CAR expression on target tissues (Alemany & Curiel, 2001; Fechner *et al.*, 1999). As described in Section 1.3.2.3, in humans, Ad5 binds to erythrocytes in the blood via CAR or CR1 (Carlisle *et al.*, 2009). This interaction is absent in mice, since murine erythrocytes lack CAR. In these animals, i.v. injection of Ad5 results in liver infection mediated via binding of Ad5 hexon with blood coagulation factors, in particular Factor X (Waddington *et al.*, 2008). In addition, the specific interaction of Ad5 with Kupffer cells has recently been suggested to be mediated via Scavenger Receptor-A (SR-A) (Xu *et al.*, 2008). These macrophage receptors function as part of the immune system and recognise conserved motifs on pathogens and negatively-charged material, including the Ad5 capsid. Haisma *et al.* demonstrated that Ad5-resistant Chinese Hamster Ovary (CHO) cells could be transduced by transfecting them with SR-A and that this interaction can be abolished by polyinosinic acid, an SR-A ligand (Haisma *et al.*, 2009). The authors suggest that SR-A binding of Ad5 could trigger a defense mechanism, as they noted that Ad5 is sequestered in autophagosome-like vesicles in these cells, which subsequently fused with lysosomes. This pathway could therefore represent another route for degradation of Ad5. To avoid these 'Ad5 traps', we plan to first conduct *in vivo* experiments delivering Ad5 i.t. in mouse xenograft models.

4.2.2 Equol and resveratrol-induced cell death

Equol and resveratrol lowered Ad5 EC_{50} values in three PCa cell-lines, independently of their AR status. We observed an enhanced induction of apoptosis in DU145 and PC-3 cells infected with Ad5 and treated with phytochemicals. Inhibition of the caspases using the pharmacological inhibitor zVAD-fmk reduced phytochemical-induced cytotoxicity in DU145 cells by about 50%. However, in PC-3 cells, caspase inhibition did not decrease cell death caused by equol and resveratrol alone. In 22Rv-1 cells, the phytochemicals alone induced a modest apoptotic response which was slightly decreased by zVAD-fmk.

Both PC-3 and DU145 cell lines have defective apoptotic signalling. PC-3 cells have a homozygous mutation in *p53* which generates a premature stop codon so the cells lack p53, and DU145 cells harbour a mutated form of p53 (Isaacs *et al.*, 1991). 22Rv-1 cells express wild type p53 although immunohistochemistry staining has shown that its expression is

restricted to only 10% cells (van Bokhoven *et al.*, 2003). However, members of our lab have detected strong p53 expression in this cell line by Western blot.

Marcelli *et al.* saw that there was a loss in mitochondrial membrane potential in both DU145 and PC-3 cells in response to the apoptosis inducer staurosporine (STS) although downstream events including caspase activation and PARP cleaveage were absent in PC-3 cells and delayed in DU145 cells (Marcelli *et al.*, 2000b). These findings correlate with our observations that both cell lines display loss of mitochondrial membrane potential in response to phytochemical treatment and only DU145 cells showed significant levels of caspase-3 activation. Marcelli *et al.* propose that STS-treated DU145 and PC-3 cells die by a necrotic-like process, based mostly on morphological studies.

The PCa cell lines also exhibit enhanced activation of antiapoptotic and cell survival pathways which might contribute to resistance to chemotherapy. For instance, DU145 and PC-3 cells express the inhibitor of apoptosis protein (IAP) survivin (Tamm *et al.*, 1998). Bcl-X_L is present in both cell lines, at higher levels in PC-3 cells, and both DU145 and PC-3 cell lines appear to express Bcl-2, while DU145 cells lack proapoptotic Bax (Marcelli *et al.*, 2000b; Skjoth & Issinger, 2006). 22Rv-1 cells also have high levels of Bcl-2 (Skjoth & Issinger, 2006). These aberrations might explain the resistance of these cells to some chemotherapeutic drugs, as well as to phytochemical-induced cytotoxicity.

Resveratrol influences a variety of genes and proteins involved in cell cycle control and apoptosis, as described in Section 1.4. However, its ability to trigger apoptosis alone is reported to be modest, although it can potentiate the induction of apoptotsis by cytokines and chemotherapeutic agents (Gatz & Wiesmuller, 2008). Resveratrol has been shown to sensitise DU145 and PC-3 cells to cell death induced by death receptor-targeting agents, such as TRAIL, Fas and TNFα, but was less effective with compounds inducing apoptosis via alternative signalling pathways, such as etoposide, paclitaxel, *etc.* (Gill *et al.*, 2007; Shankar *et al.*, 2007). Gill *et al.* found that PC-3 cells may be less sensitive to resveratrol than DU145 cells due to the constitutively active status of Akt in PC-3 cells which promotes survival. Fulda *et al.* identified cell cycle arrest in S-phase and survivin upregulation as key mechanisms by which resveratrol could sensitise a panel of carcinoma cell lines to chemodrug-induced apotosis, independently of p53 status (Fulda & Debatin, 2004). We also observed an increase in the proportion of cells in S phase in response to resveratrol treatment in all three PCa cell lines tested. This may enhance Ad5 gene expression and play a role in combination-induced cell death.

Intruigingly, one study has shown that the induction of apoptosis mediated by resveratrol in colorectal cancer cells was autophagy-dependent (Trincheri *et al.*, 2008). The authors suggest that autophagy is initially rapidly and reversibly induced as a survival response, but that prolonged exposure to resveratrol triggers a switch to apoptotic cell death. A panel of ovarian cancer cell lines were also found to undergo a mixed type of cell death in response to resveratrol, regardless of the levels of Bcl-2 and Bcl-X_L proteins they harboured (Opipari *et al.*, 2004). Cells showed characteristic features of apoptosis, including release of cytochrome *c* and caspase activation, but ultrastructural changes were indicative of autophagic cell death. Our results are in agreement with the involvement of both apoptotic and autophagic pathways observed in PCa cells treated with resveratrol alone and in combination with Ad5, since caspase inhibition reduced resveratrol-induced cytotoxicity by half, and resveratrol activated LC3 and caused its relocation to autophagosomes. To further investigate the requirement of autophagy in resveratrol-mediated cytotoxicity we used the pharmacological inhibitors 3-MA and bafilomycin-A although the results did not provide clear evidence to elucidate this problem. Additional insights might be gained by interfering with autophagy using a more direct approach, such as with siRNA targeting of Atg5.

The mechanisms responsible for equol-induced cytotoxicity are less well known. Hedlund *et al.* found that equol causes benign human prostatic epithelial cells (PrEC) to arrest in G_1, but cell cycle progression in malignant PCa cell lines was not investigated, although their sensitivity to equol was established (Hedlund *et al.*, 2003). A recent study found that equol induced cytochrome *c* release and downstream activation of caspase-3, -6, -7 and -9 in human breast cancer cells, supporting a role for apoptotis in equol-induced cell death (Choi *et al.*, 2009). The effect of equol on autophagy has not been reported.

We did not find a significant effect on cell cycle progression in PCa cells after 24-48h treatments with equol, although we did observe an increase in the proportion of cells in sub-G_1 after 72h indicative of apoptosis. Equol also caused decreased mitochondrial membrane potential, caspase-3 activation and PS externalization, and caspase inhibition by zVAD-fmk protected PCa cells from equol-induced cytotoxicity. Our results therefore provide evidence of an induction of apoptosis, the level of which varied with the ability of each cell lines to undergo apoptosis. Autophagy was induced by equol but, similarly to resveratrol, its involvement in cell death remains unclear.

Additional cell death mechanism may also be involved in phytochemical-induced cell death. For instance, it is possible that our inhibition of caspases using zVAD-fmk depresses necrotic cell death which contributes to phytochemical-induced cell death. Apoptosis has been found to

have a negative feedback on necrois, possibly via caspase-8 which has been shown to cleave the necrosis mediator RIP-1 (Vandenabeele *et al.*, 2006). RIP1 is a serine/threonine kinase downstream of death receptors, such as TNF-R and TRAIL, and is thought to regulate necrosis (Festjens *et al.*, 2007).

4.3 Ad5 induced cell death is neither apoptotic nor autophagic

Although determining the adenoviral-induced mechanism of cell death was not an aim of this project, our experimental results allow us to confirm previously established findings and draw a number of additional conclusions described below.

4.3.1 Ad5-infected cells are not rescued by caspase-inhibition

Pan-caspase inhibition using the pharmacological inhibitor zVAD-fmk did not decrease Ad5-induced cell death. This observation confirms the non-apoptotic nature of cell death induced by Ad5 (Abou El Hassan *et al.*, 2004; Baird *et al.*, 2008; Ito *et al.*, 2006). However, surprisingly, at the highest dose, zVAD-fmk actually increased cell death with Ad5 in all three PCa cell lines while the inhibitor alone did not cause significant cell death, indicating sensitisation to non-apoptotic cell death. This has also been reported in other models where cell death is caused by autophagy or necrosis (Vandenabeele *et al.*, 2006). The possible role of these pathways in Ad5-induced cell death is discussed below.

4.3.2 Ad5 represses autophagy

We found no evidence that adenoviral-induced cell death was autophagy-dependent in our studies with 22Rv-1, DU145 and PC-3 cells. Confocal microscopy showed that Ad5 did not cause relocalization of GFP-LC3 to autophagosomes and expression of the activated form of LC-3 (LC3-II), detected by Western blotting, was not induced by adenoviral infection. In fact, Ad5 reduced LC3-II expression induced by the phytochemicals.

These results suggest that Ad5 might be able to repress the induction of autophagy. One possibility is that Ad5 mediates this through the activation of mTOR which has previously been reported to be induced (and necessary) during viral replication (O'Shea *et al.*, 2005a). O'Shea *et al.* found that PI3K inhibition using the pharmacological inhibitor LY294002 or blocking mTOR directly by rapamycin abolished the activation of the mTOR effector p70S6K and decreased viral replication. p70S6K initiates translation by recruiting eIF4B to the pre-initiation complex and enhances the RNA helicase acitivty of eIF4A which facilitates 40S ribosomal binding for translation initiation (Ma & Blenis, 2009). O'Shea *et al.* also found that another downstream target of mTOR, 4EBP1, was inactivated by Ad5, allowing eIF4E and

eIF4G translation initiation. The activation of mTOR was found to be mediated by E4-orf4, in cooperation with E4-orf1, which activates PI3K (O'Shea *et al.*, 2005a). The expression and functioning of these viral proteins was postulated to mimic growth signals, maintaining mTOR activation, even under nutrient-poor conditions, to ensure the translation of viral proteins.

This hypothesis is supported by earlier observations that 4EBP1 and 4EBP2 were hyperphosphorylated as early as 30min post-infection with wild-type Ad5 (Gingras & Sonenberg, 1997). 4EBP1 binds to and prevents the activity of eIF4E, a core-component of the eIF4F cap-binding protein complex required for translation initiation. In its hyperphosphorylated state, 4EBP1 cannot bind eIF4E and is therefore unable to inhibit cap-dependent translation initiation. This is probably beneficial for Ad5 since early genes are translated in a cap-dependent fashion. The upregulation of cap-dependent translation during the early stage of infection is mediated by E1A-CR1 and it has been shown to be inhibited by rapamycin (Feigenblum & Schneider, 1996). During the late stage of the adenoviral infection, cap-dependent translation is inhibited by L4-100K to selectively repress cellular mRNA translation while ribosome shunting allows the translation of viral mRNAs containing a tripartite leader sequence (see Introduction Section 1.2.3.8).

As discussed in Section 1.4.3.2.2, mTOR is also a major modulator of autophagy. In *Saccharomyces cerevisiae*, active TOR represses autophagy by preventing the initiation of autophagosome formation via Atg13 phosphorylation (Chang & Neufeld, 2009). Our finding that Ad5 seems to repress autophagy could therefore be a side-effect of viral mTOR activation. We also found that the autophagy inhibitor bafilomycin-A1 had no effect on the level of viral-induced cell death. Since this inhibitor blocks the fusion of the autophagosome with the lysosome downstream of mTOR, this suggests that the modulation of signalling upstream of autophagy may be more important to Ad5 than the final stage of autophagy. Another inhibitor of the fusion of the autophagosome with the lysosome, such as chloroquine, could be used to confirm this hypothesis (Boya *et al.*, 2005).

In addition to ensuring translation of viral proteins, inhibiting autophagy could protect Ad5 from the host immune system, since autophagy has been postulated to play a role in the anti-viral response, and could therefore be detrimental to Ad5. Toll-like receptors which recognise foreign genomic material have been shown to activate autophagy *in vitro*. Similarly, protein kinase R (PKR), a potent inducer of the antiviral interferon response, can induce autophagy (Talloczy *et al.*, 2002). A number of viruses have therefore evolved mechanisms counteracting the induction of autophagy and even hijacking the process to their own ends (Shoji-Kawata & Levine, 2009). For example, the herpes simplex virus (HSV)-1 infected cell protein 34.5

(ICP34.5) blocks autophagy by repressing PKR and inhibiting Beclin-1 (Talloczy *et al.*, 2006). Similarly, the adenovirus VA RNAs are known to block PKR and the interferon pathway (Ghadge *et al.*, 1994; Mathews & Shenk, 1991). Results from our lab show that VA1 can also inhibit autophagy (C. Binny *et al*, manuscript in preparation). The importance of autophagy in clearing adenoviral infections *in vivo* has not been investigated.

Ad5 may also have evolved mechanisms to block autophagy to ensure progression to S phase. Autophagy has also recently been identified as an effector mechanism triggering senescence, a stable form of cell cycle arrest that functions to limit the proliferation of damaged cells (Young *et al.*, 2009). This could be unfavourable to Ad5 as it would restrict cell cycle progression, which is necessary for productive infection.

4.3.3 The effect of autophagy modulation on Ad5 cytotoxicity

The induction of autophagy using rapamycin significantly increased Ad5 EC_{50} values in all cell lines, while, conversely, except in DU145 cells, repression of autophagy with 3-MA (an inhibitor of class III PI3K) had a sensitising effect and reduced Ad5 EC_{50} values. This indicates that, in 22RV-1 and PC-3 cells, autophagy probably functions as a protective cellular mechanism. The effect of autophagy inhibition on viral replication in these cells needs to be investigated to further characterize this protective effect.

Our conclusion that autophagy can protect PCa cells against adenoviral-induced cell death is in contrast to two other reports. These studies found that combinations of a telomerase-driven adenoviral mutant and temozolomide, an autophagy-inducing chemodrug, or an E1A-CR2 deletion mutant and RAD001, a derivative of rapamycin, induced autophagy and enhanced the anticancer effect in glioma cell lines (Alonso *et al.*, 2008; Yokoyama *et al.*, 2008).

Based on these observations, Jiang *et al* have proposed a model whereby, during the late stages of infection, autophagosomes disrupt cellular membranes and promote the release of viral progeny (Jiang *et al.*, 2008). Our data is not supportive of such a general and fundamental role for autophagy in adenoviral infection which might be cell line-specific. Nevertheless, this mechanism could possibly be occurring in our DU145 cells which were protected by 3-MA-mediated autophagy inhibition. However, we speculate that the protective effect of 3-MA observed in DU145 cells may not be due to the prevention of autophagic cell death, since the induction of autophagy by rapamycin in DU145 was also protective. We hypothesise that the increased Ad5 EC_{50} value in DU145 cells treated with 3-MA might instead be due to unidentified off-targets effects of 3-MA.

It should be noted that the observations on which Jiang's *et al*. model is based were made in glioblastoma cell lines. These cells are relatively resistant to apoptosis but readily undergo autophagic cell death (Furnari *et al.*, 2007; Lefranc *et al.*, 2007). Furthermore, E1A has been implicated in the regulation of viral protein translation, via 4EBP1 phosphorylation as well as p70S6K induction, hence its deletion in the mutants used could explain why autophagic cell death was observed under those conditions (Feigenblum & Schneider, 1996). Finally, both chemotherapeutic drugs used in combination with the adenoviral mutants have additional biological effects other than induction of autophagy which could play a role in the enhanced anticancer effects observed by the combination treatments. RAD001 is antiangiogenic and immunosuppressive, while the primary action of temozolomide is to induce DNA alkylation.

Our data from studies in three PCa cell lines suggest that combining oncolytic adenoviral mutants with chemodrugs which act only by inducing mTOR and autophagy could hamper viral replication. The use of RAD001 or similar drugs with oncolytic adenoviral mutants should be investigated further to determine their effect on a wider range of cell lines as well as *in vivo*. In fact, the immunosuppressant and antiangiogenic effects of RAD001 may delay tumour growth such that the net spread of virus throughout the tumour might be improved. Therefore, overall, combining RAD001 with adenoviral mutants may be beneficial if the timing of addition is optimized (Homicsko *et al.*, 2005).

4.3.4 Adenoviral-induced cell death: a novel mechanism

Having excluded apoptosis and autophagy as cell death pathways induced by Ad5 in PCa cell lines, we hypothesise that the adenoviral mode of cell death may involve an unidentified and mostly uncharacterised form of cell death.

The inhibition of apoptosis has been reported to result in caspase-independent modes of cell death, such as autophagy and necrosis, which may function as 'back-up' cell death mechanisms in case apoptosis fails (Vandenabeele *et al.*, 2006). Contrary to prior status as a basic, unregulated form of cell death, necrosis has recently been reclassified as a type of programmed cell death, as its regulation by specific transduction pathways is gradually being uncovered (Kroemer *et al.*, 2009). Necrosis, now also known as necroptosis, is characterised by morphological features, such as cell swelling and loss of plasma membrane integrity, and the activity of receptor interactive protein 1 (RIP1). Apoptosis-deficient cells have been shown to be sensitised to metabolic stress and necrosis by the inhibition of autophagy (Degenhardt *et al.*, 2006).

Since the PCa cells used in this study have deregulated apoptotic pathways, and Ad5 can prevent apoptosis and also downregulate autophagy in these cells, adenoviral infection may be forcing cells down an alternative mode of cell death such as necrosis. Indeed, necrosis has been postulated to function as part of the innate immune response against the invasion of foreign organisms, with viral inhibition of apoptosis serving as a signal to the host of the danger of infection.

The molecular pathways involved in necrosis have recently been investigated in a genome-wide siRNA screen (Hitomi *et al.*, 2008). A key regulator of necrosis is RIP1, a serine/threonine kinase downstream of death receptors such as TNF-R and TRAIL. The TLR pathway, which has been reported to induce RIP1, was also found to be involved in necrosis signalling. Activation of RIP1 can lead to downstream inflammatory signalling, via NFκB, and cell death, perhaps by the induction of mitochondrial ROS production (Festjens *et al.*, 2007).

In contrast to apoptosis and autophagy that lead to the shutdown of protein synthesis, translation of mRNAs is allowed to proceed during necrosis (Saelens *et al.*, 2005). If induced in host cells, this form of cell death would therefore not prevent Ad5 replication and would allow efficient release of progeny virions. However, investigating the involvement of necrosis in Ad5-induced cell death is hampered by the lack of specific positive markers of necrosis. Apart from distinct morphological features such as increased cell volume (oncosis) and organelle swelling, necrosis is characterised by decreased concentration of ATP, high mobility group box-1 (HMGB1) release, and the presence of an inflammatory response (Kroemer *et al.*, 2009). Although Ad5-infected cells do appear swollen, this is most likely a direct result of partial detachment and the accumulation of progeny virions due to viral replication. Furthermore, our colleagues found that ATP levels increased, rather than decreased, in response to infection with *dl*922-947 in ovarian carcinoma cells, and concluded that pure necrosis was not the Ad5-induced mode of cell death (Baird *et al.*, 2008). Necrosis may be restricted by viral TNF-inhibitory mechanisms (discussed in Section 1.2.3.6), which would preclude the activation of RIP1 by this pathway. To assess the role of necrosis in adenoviral-induced cell death under our conditions in PCa cells, the expression levels of RIP1 could be determined as a preliminary indicator of the activation of this pathway.

Perhaps a more likely cell death mechanism in response to adenoviral infection (which is not mutually exclusive with necrois) is mitotic catastrophe. Cell cycle analyses with *dl*1520 (Onyx-015, deleted in E1B-55K) determined that infected human umbilical vein endothelial cells (HUVEC) are able to overcome not only the G_1/S, but also the G_2/M checkpoint (Cherubini *et al.*, 2006). Ad5 was shown to modulate the DNA damage response by blocking

the Mre11-Rad50-NBS1 (MRN) complex and ataxia-telangectasia-mutated (ATM) protein. While Ad5-infection caused deregulation of the cell cycle and induced cell death within 72h, the E1B-55K deletion mutant accumulated cells in G_2/M, causing the generation of polyploid cells which died due to mitotic catastrophe. In addition to E1B-55K, the E4 proteins are implicated in cell cycle control beyond S phase. Cherubini *et al* showed that a mutant lacking the E4 region caused cells to accumulate in G_2/M but did not generate >4N cells. E4-orf4 has recently been shown to upregulate cyclin E, which normally induces S phase, and caused an accumulation of >4N cells in a G_1-like phase, resulting in mitotic catastrophe (Li *et al.*, 2009). To determine whether this type of cell death might be induced in our cells, the expression levels of cyclin E could be monitored at late time-points as an indicator of unrestricted cell cycle progression beyond M, although we did not observe any significant >4N cell population 24-72h post-infection.

4.4 Combination-induced cell death is cell line-dependent

4.4.1 The response of AR-negative cell lines may differ according to PI3K/Akt/mTOR activation

PC-3 cells were particularly sensitive to treatment with rapamycin, whereas no cytotoxicity was detected in DU145 cells, although exact EC_{50} values were not determined. Rapamycin blocks protein translation and cell growth, causing G_1 cell cycle arrest and apoptosis. The sensitivity of different tumours to CCI-779, an ester of rapamycin, has previously been shown to be related to PTEN status (Neshat *et al.*, 2001). PTEN is a tumour suppressive lipid phosphatase which modulates Akt activation and has a negative effect on mTOR. As discussed in Section 1.1.5, the loss of PTEN is critical in PCa tumorigenesis. Acquired mutations in *PTEN* have been found in 30-60% PCa tumours and correlate with advanced tumour stage and chemotherapeutic resistance (McMenamin *et al.*, 1999). The action of PTEN in the PI3K pathway is illustrated in Figure 13.

A number of studies have demonstrated that PC-3 cells are PTEN-null, whereas DU145 cells have retained PTEN expression (Grunwald *et al.*, 2002; McMenamin *et al.*, 1999; Neshat *et al.*, 2001). The lack of PTEN in PC-3 cells may have led to the evolution of hyperactive mTOR and 'addiction' to activation of the PI3K pathway for growth, rendering PC-3 cells vulnerable to mTOR inhibition. DU145 cells may not be as sensitive to rapamycin since they are PTEN-positive and do not have constitutively activated Akt (Nakatani *et al.*, 1999). DU145 cells are probably not as dependent on the PI3K pathway and may instead require alternative proliferation pathways, which are not blocked by rapamycin. Resistance to rapamycin has also been observed in tumours where negative feedback loops involving the activation of MAPK and PI3K signalling cascades (Carracedo *et al.*, 2008). This could be occurring in DU145 cells. However, Neshat *et al.* have found that, in comparison to other cell lines expressing intact PTEN, the IC_{50} of DU145 cells for CCI-779 is still relatively low (Neshat *et al.*, 2001). DU145 cells have been shown to have an activated mTOR, which could explain why this cell line shows some sensitivity to rapamycin, despite its independence from PI3K pathway activation (Sekulic *et al.*, 2000). These observations and hypotheses are somewhat speculative since our results are based on experiments which need to be repeated to demonstrate reproducibility. The activation of upstream signalling proteins such as Akt and PI3K also needs to be examined.

We observed no further sensitisation of (uninfected) PC-3 cells by rapamycin to resveratrol-induced cell death, and co-treatment with equol actually repressed rapamycin cytotoxicity. This is in contrast to findings by Gründwald *et al*. who showed that resistance of PC-3 cells to

the topoisomerase II inhibitor doxorubicin can be reversed by rapamycin-mediated mTOR inhibition (Grunwald *et al.*, 2002). Similarly, Wu *et al.* found that sensitivity to mitoxantrone or docetaxel could be increased additively by CCI-779 in DU145 and PC-3 xenograft experiments (Wu *et al.*, 2005). The mTOR inhibitor RAD001 has also been shown to sensitise PCa cells to radiotherapy and induce autophagy, particularly in PTEN-null cells (Cao *et al.*, 2006). The discrepancy of our data with these studies highlights the need for others to repeat these experiments. Nevertheless, if proven reproducible, these results would indicate that the phytochemicals in combination with rapamycin function differently to highly cytotoxic agents such as DNA-damaging chemodrugs and radiation. Equol could be counteracting rapamycin-mediated cytotoxicity directly, by enabling mTOR activation, or indirectly, but maintaining PI3K pathway activation, but this has not yet been shown.

In Ad5-infected cells, rapamycin treatment was highly protective, with and without phytochemicals, in both DU145 and especially in PC-3 cells. The highest Ad5 EC_{50} values were obtained in rapamycin-treated infected cells with the lower doses of phytochemcials, rather than higher doses which are apoptosis-inducing. The protective effect of rapamycin in combination-treated cells could be due to the viral inhibitory effect of rapamycin discussed in Section 4.3.3. This could be studied by assaying viral replication in combination-treated cells with and without rapamycin, and by monitoring upstream signalling mediators such as Akt, mTOR and p70S6K. Another possibility is that the protective effect of rapamycin is viral-replication independent, and rather delays onset of death by inducting autophagy which functions as a cell survival mechanism.

In PC-3 cells, the inhibition of apoptosis using the pan-caspase inhibitor zVAD-fmk also imparted significant protection against combination-induced cell death, increasing Ad5 EC_{50} values. PC-3 cells showed moderate levels of apoptosis induction in response to combination treatments in a phytochemical dose-responsive manner. This suggests that apoptosis may play a role in the cytotoxicity caused by the highest doses of phytochemicals in Ad5-infected cells. DU145 cells showed stronger induction of apoptosis but inhibition of caspase activity in this cell line had a smaller protective effect.

Overall, cell death in DU145 and PC-3 cells is therefore probably due to a combination of pathways induced by Ad5 and the phytochemicals which results in overwhelming stress and cellular death. Further investigation into the expression and activation levels of upstream signalling proteins and cell death modulators is required to understand the mechanism in greater detail.

4.4.2 The sensitivity of 22Rv-1 cells to autophagy modulation may be AR-dependent

In contrast to the other two PCa cell lines, we found that the effect of rapamycin in 22Rv-1 cells treated with combinations of Ad5 and phytochemicals was not protective. Rapamycin had no effect on Ad5 EC_{50} values except in infected cells treated with 100μM equol where it increased cell death (Figure 57 and Table 21). This sensitising effect was similar to the higher cytotoxicity observed in uninfected cells treated with rapamycin and equol (Figure 55). This effect, which was not observed in DU145 nor PC-3 cells, could be due to modulation of AR signalling by rapamycin.

Rapamycin has been reported to stimulate AR expression and transcriptional activity via Akt and mTOR, enabling AR-positive cells to develop resistance and escape the growth-inhibitory effects of rapamycin (Wang *et al.*, 2008b). However, the authors of this study also demonstrate that bicalutamide, a competitive inhibitor of AR ligand binding commonly used in the clinic (see Introduction Section 1.1.4), can sensitise AR-positive cells to rapamycin-induced cytotoxicity and overcome resistance. Wang *et al.* demonstrate that bicalutamide causes apoptosis by preventing the induction of the AR cell survival pathway, which is triggered by rapamycin.

In our system, the enhanced cytotoxicity observed in 22Rv-1 cells treated with both equol and rapamycin could be due to the anti-androgenic effect of equol sensitising the cells to rapamycin-induced cytotoxicity. Equol has been reported to inhibit DHT, sequestering the ligand from the AR (Lund *et al.*, 2004). Equol could therefore be acting similarly to bicalutamide and sensitising these cells to rapamycin. We are currently verifying whether, as in Wang *et al.*'s model, 22Rv-1 cells treated with equol and rapamycin undergo apoptosis.

Resveratrol has also been shown to have a negative effect on AR signalling (Mitchell *et al.*, 1999). Resveratrol is thought to block AR signalling by inhibition of MEK which activates the AR by phosphorylation (Gao *et al.*, 2004). Resveratrol may also be inhibiting AR signalling via the upregulation of Sirt1 which represses AR activity (Fu *et al.*, 2006; Howitz *et al.*, 2003). The different AR inhibitory mechanism of the phytochemicals may explain why the combination of rapamycin with resveratrol in Ad5-infected 22Rv-1 cells was not as sensitising as the combination with equol, although resveratrol was sufficient to prevent the protective effect of rapamycin.

Ad5 has been reported to down-regulate AR expression and transcriptional activity, an effect that has also been observed by us (S. Cheong *et al*., manuscript in preparation) and others (Hoti *et al.*, 2007). Höti *et al.* suggest that the effect of Ad5 on AR is mediated by E1A competition for common transcriptional coactivators, although the region of E1A required for this response has not yet been identified. The suppression of AR by Ad5 and downstream survival pathways could explain why the effect of rapamycin in infected cells is not as protective as in AR-negative cell lines. Furthermore, the addition of two AR-repressive agents, Ad5 and equol, could act synergistically in sensitising cells to rapamycin-induced cell death.

In AR-negative cell lines, this effect obviously does not occur, since DU145 and PC-3 cells lack the AR and are insensitive to growth stimulation by androgens. Rapamycin therefore principally acts as an autophagy-inducer in these cells. As discussed in Section 4.3.3, this is probably detrimental to Ad5 since rapamycin can abolish translation and induce senescence. This could explain the protective effect of rapamycin in DU145 and PC-3 cells infected with Ad5, with and without phytochemicals. This hypothesis will be verified by determining whether rapamycin also blocks viral replication in these cells.

4.5 Future directions

Oncolytic adenoviral mutants are currently being developed and tested in the clinic for PCa (Freytag *et al.*, 2007). It has been established that the anti-cancer effect of replication-selective Ad5 vectors can be significantly enhanced by multimodal treatments with chemo- or radiotherapy (Heise *et al.*, 2000b; Kirn, 2001). However, these agents can lead to tumour resistance, and also cause significant side-effects. The work described in this thesis presents an alternative, novel and promising stategy to improve oncolytic efficacy in PCa cells using non-toxic phytochemicals.

In the future, we plan to verify the efficacy of combining equol and resveratrol with replication-selective Ad5 mutants *in vivo* using mouse xenograft models. We have developed suitable *in vivo* mouse xenograft models for all three PCa cell lines used in this thesis. Initial experiments to validate the concept will be performed using i.p. delivery of the phytochemicals and i.t. delivery of the virus. Once proof of concept is established, we hope to extend the studies using oral delivery of the phytochemicals, with the caveat that mouse metabolism of phytochemicals differs from human metabolism.

The molecular interactions of the AdΔΔ mutant in combination with equol and resveratrol are currently being characterized. A number of encouraging *in vivo* studies have been conducted in our lab demonstrating the efficacy of this virus in both PCa and pancreatic cancer models (Öberg *et al*., submitted; Cherubini *et al*, unpublished data). Additional synergy assays will be performed to verify the supra-additive interaction between AdΔΔ and equol and resveratrol in PCa cells. The effect of combining phytochemicals with the non-replicating Ad5-Hey1 mutant, which expresses the AR co-repressor Hey1 under the control of the CMV promoter will also be tested, since combination treatment of both AR-positive and -negative cells *in vitro* has shown promising results.

The selectivity of phytochemical enhancement of cell death with Ad5 also remains to be examined. We observed an increased viral uptake in cells treated with equol or resveratrol but we anticipate that this will not occur in non-tumourigenic cells and that tumour selectivity will be maintained in the presence of phytochemicals. The sensitivity of normal PrEC cells to combination treatments will be tested *in vitro* by assaying cell viability, viral uptake and viral replication. The selectivity and biodistribution of oncolytic mutants will be determined *in vivo*.

We established that equol and resveratrol can act synergistically with Ad5 to enhance PCa cell death, despite decreasing viral replication in DU145 and PC-3 cells. This is counter-intuitive. To understand the mechanisms responsible for the inhibition of viral progeny production in phytochemical-treated cells, the expression of E1A and additional viral proteins, such as hexon, protease or L4-100K, could be characterized, both in terms of expression levels and the timing of their expression. This could help identify which step of the viral replication cycle is blocked by the phytochemicals, causing decreased viral titres. The effect of rapamycin on Ad5 replication in PCa cell lines will also be determined.

A more in-depth study of changes in cell cycle progression in response to combination treatments is also warranted. This will be done by staining cells with bromodeoxyuridine (BrdU) to distinguish between cell populations in G_2 and M. The expression patterns of cell cycle proteins, including cyclins B and E and cdc25a will be analysed.

Further investigations into the combination-induced cell death mechanism are needed to gain a greater understanding of the synergy observed between Ad5 and equol and resveratrol. As discussed in Section 4.2, viral proteins such as E1A, ADP and E4-orf4 could be involved. Additional insights might also be gained from observing cellular morphology at the ultrastructural level. The expression of LC3-II and caspase-3 will be verified under the conditions tested.

Currently, our observations suggest that autophagy functions as a survival mechanism in response to combination treatments. The autophagic response will be quantified in combination-treated cells by flow cytometry on cells stained with acridine orange, a dye specific for acidic cellular compartments. The expression of upstream signalling proteins involved in regulating the induction of autophagy, including Akt, PI3K and mTOR, will be analysed. Clarification of the role of autophagy in phytochemical-, Ad5- and combination-induced cell death will be sought by determining the effect of specific inhibition of autophagy using siRNA to knock down the essential autophagy protein Atg5.

The differential response observed in 22Rv-1 cells treated with rapamycin compared to the protective effect seen in DU145 and PC-3 cells will also be elucidated. The effect of rapamycin on autophagy and AR signalling, with and without phytochemicals, will be delineated by detecting the expression levels of LC3 and AR activity. Upstream signalling via Akt and the PI3K pathway will be analysed and the effect of inducting autophagy in combination-treated 22Rv-1 cells will be verified using alternative autophagy inducers to rapamycin.

Finally, the cross-talk between apoptosis, autophagy and necrosis will be explored by examining the role of caspase-8 and RIP1 which are thought to be at the interface of the two pathways (Vandenabeele *et al.*, 2006). A greater understanding of cell death mechanisms induced by Ad5 and phytochemicals will pave the way to designing improved anticancer therapeutic options.

5 References

Abou El Hassan, M. A., van der Meulen-Muileman, I., Abbas, S. & Kruyt, F. A. (2004). Conditionally replicating adenoviruses kill tumor cells via a basic apoptotic machinery-independent mechanism that resembles necrosis-like programmed cell death. *J Virol* **78**, 12243-12251.

Aghi, M., Hochberg, F. & Breakefield, X. O. (2000). Prodrug activation enzymes in cancer gene therapy. *J Gene Med* **2**, 148-164.

Akusjärvi (1986). Structure and function of the adenovirus-2 genome. In *Adenovirus DNA*. Edited by D. W. Boston: Martinus Nijhoff.

Alemany, R. & Curiel, D. T. (2001). CAR-binding ablation does not change biodistribution and toxicity of adenoviral vectors. *Gene Ther* **8**, 1347-1353.

Alonso, M. M., Jiang, H., Yokoyama, T., Xu, J., Bekele, N. B., Lang, F. F., Kondo, S., Gomez-Manzano, C. & Fueyo, J. (2008). Delta-24-RGD in combination with RAD001 induces enhanced anti-glioma effect via autophagic cell death. *Mol Ther* **16**, 487-493.

Anders, M., Christian, C., McMahon, M., McCormick, F. & Korn, W. M. (2003a). Inhibition of the Raf/MEK/ERK pathway up-regulates expression of the coxsackievirus and adenovirus receptor in cancer cells. *Cancer Res* **63**, 2088-2095.

Anders, M., Hansen, R., Ding, R. X., Rauen, K. A., Bissell, M. J. & Korn, W. M. (2003b). Disruption of 3D tissue integrity facilitates adenovirus infection by deregulating the coxsackievirus and adenovirus receptor. *Proc Natl Acad Sci U S A* **100**, 1943-1948.

Anders, M., Vieth, M., Rocken, C., Ebert, M., Pross, M., Gretschel, S., Schlag, P. M., Wiedenmann, B., Kemmner, W. & Hocker, M. (2009). Loss of the coxsackie and adenovirus receptor contributes to gastric cancer progression. *Br J Cancer* **100**, 352-359.

Athar, M., Back, J. H., Tang, X., Kim, K. H., Kopelovich, L., Bickers, D. R. & Kim, A. L. (2007). Resveratrol: a review of preclinical studies for human cancer prevention. *Toxicol Appl Pharmacol* **224**, 274-283.

Baird, S. K., Aerts, J. L., Eddaoudi, A., Lockley, M., Lemoine, N. R. & McNeish, I. A. (2008). Oncolytic adenoviral mutants induce a novel mode of programmed cell death in ovarian cancer. *Oncogene* **27**, 3081-3090.

Baker, A. H., McVey, J. H., Waddington, S. N., Di Paolo, N. C. & Shayakhmetov, D. M. (2007). The influence of blood on in vivo adenovirus bio-distribution and transduction. *Mol Ther* **15**, 1410-1416.

Banerjee, S., Li, Y., Wang, Z. & Sarkar, F. H. (2008). Multi-targeted therapy of cancer by genistein. *Cancer Lett* **269**, 226-242.

Bao, Y., Peng, W., Verbitsky, A., Chen, J., Wu, L., Rauen, K. A. & Sawicki, J. A. (2005). Human coxsackie adenovirus receptor (CAR) expression in transgenic mouse prostate tumors enhances adenoviral delivery of genes. *Prostate* **64**, 401-407.

Baur, J. A., Pearson, K. J., Price, N. L., Jamieson, H. A., Lerin, C., Kalra, A., Prabhu, V. V., Allard, J. S., Lopez-Lluch, G., Lewis, K., Pistell, P. J., Poosala, S., Becker, K. G., Boss, O., Gwinn, D., Wang, M., Ramaswamy, S., Fishbein, K. W., Spencer, R. G., Lakatta, E. G., Le Couteur, D., Shaw, R. J., Navas, P., Puigserver, P., Ingram, D. K., de Cabo, R. & Sinclair, D. A. (2006). Resveratrol improves health and survival of mice on a high-calorie diet. *Nature* **444**, 337-342.

Baur, J. A. & Sinclair, D. A. (2006). Therapeutic potential of resveratrol: the in vivo evidence. *Nat Rev Drug Discov* **5**, 493-506.

Bektic, J., Berger, A. P., Pfeil, K., Dobler, G., Bartsch, G. & Klocker, H. (2004). Androgen receptor regulation by physiological concentrations of the isoflavonoid genistein in androgen-dependent LNCaP cells is mediated by estrogen receptor beta. *Eur Urol* **45**, 245-251; discussion 251.

Belandia, B., Powell, S. M., Garcia-Pedrero, J. M., Walker, M. M., Bevan, C. L. & Parker, M. G. (2005). Hey1, a mediator of notch signaling, is an androgen receptor corepressor. *Mol Cell Biol* **25**, 1425-1436.

Berenbaum, M. C. (1989). What is synergy? *Pharmacol Rev* **41**, 93-141.

Bergelson, J. M., Cunningham, J. A., Droguett, G., Kurt-Jones, E. A., Krithivas, A., Hong, J. S., Horwitz, M. S., Crowell, R. L. & Finberg, R. W. (1997). Isolation of a common receptor for Coxsackie B viruses and adenoviruses 2 and 5. *Science* **275**, 1320-1323.

Berk, A. J. (2005). Recent lessons in gene expression, cell cycle control, and cell biology from adenovirus. *Oncogene* **24**, 7673-7685.

Bewley, M. C., Springer, K., Zhang, Y. B., Freimuth, P. & Flanagan, J. M. (1999). Structural analysis of the mechanism of adenovirus binding to its human cellular receptor, CAR. *Science* **286**, 1579-1583.

Bischoff, J. R., Kirn, D. H., Williams, A., Heise, C., Horn, S., Muna, M., Ng, L., Nye, J. A., Sampson-Johannes, A., Fattaey, A. & McCormick, F. (1996). An adenovirus mutant that replicates selectively in p53-deficient human tumor cells. *Science* **274**, 373-376.

Boya, P., Gonzalez-Polo, R. A., Casares, N., Perfettini, J. L., Dessen, P., Larochette, N., Metivier, D., Meley, D., Souquere, S., Yoshimori, T., Pierron, G., Codogno, P. & Kroemer, G. (2005). Inhibition of macroautophagy triggers apoptosis. *Mol Cell Biol* **25**, 1025-1040.

Brader, K. R., Wolf, J. K., Hung, M. C., Yu, D., Crispens, M. A., van Golen, K. L. & Price, J. E. (1997). Adenovirus E1A expression enhances the sensitivity of an ovarian cancer cell line to multiple cytotoxic agents through an apoptotic mechanism. *Clin Cancer Res* **3**, 2017-2024.

Braithwaite, A. W. & Russell, I. A. (2001). Induction of cell death by adenoviruses. *Apoptosis* **6**, 359-370.

Breidenbach, M., Rein, D. T., Wang, M., Nettelbeck, D. M., Hemminki, A., Ulasov, I., Rivera, A. R., Everts, M., Alvarez, R. D., Douglas, J. T. & Curiel, D. T. (2004). Genetic replacement of the adenovirus shaft fiber reduces liver tropism in ovarian cancer gene therapy. *Hum Gene Ther* **15**, 509-518.

Breslow, N., Chan, C. W., Dhom, G., Drury, R. A., Franks, L. M., Gellei, B., Lee, Y. S., Lundberg, S., Sparke, B., Sternby, N. H. & Tulinius, H. (1977). Latent carcinoma of prostate at autopsy in seven areas. The International Agency for Research on Cancer, Lyons, France. *Int J Cancer* **20**, 680-688.

Brown, L., Kroon, P. A., Das, D. K., Das, S., Tosaki, A., Chan, V., Singer, M. V. & Feick, P. (2009). The Biological Responses to Resveratrol and Other Polyphenols From Alcoholic Beverages. *Alcohol Clin Exp Res*.

Bruning, A. & Runnebaum, I. B. (2003). CAR is a cell-cell adhesion protein in human cancer cells and is expressionally modulated by dexamethasone, TNFalpha, and TGFbeta. *Gene Ther* **10**, 198-205.

Bruning, A. & Runnebaum, I. B. (2004). The coxsackie adenovirus receptor inhibits cancer cell migration. *Exp Cell Res* **298**, 624-631.

Burmeister, W. P., Guilligay, D., Cusack, S., Wadell, G. & Arnberg, N. (2004). Crystal structure of species D adenovirus fiber knobs and their sialic acid binding sites. *J Virol* **78**, 7727-7736.

Bursch, W., Ellinger, A., Kienzl, H., Torok, L., Pandey, S., Sikorska, M., Walker, R. & Hermann, R. S. (1996). Active cell death induced by the anti-estrogens tamoxifen and ICI 164 384 in human mammary carcinoma cells (MCF-7) in culture: the role of autophagy. *Carcinogenesis* **17**, 1595-1607.

Cairns, P., Okami, K., Halachmi, S., Halachmi, N., Esteller, M., Herman, J. G., Jen, J., Isaacs, W. B., Bova, G. S. & Sidransky, D. (1997). Frequent inactivation of PTEN/MMAC1 in primary prostate cancer. *Cancer Res* **57**, 4997-5000.

Campbell, E. M. & Hope, T. J. (2005). Gene therapy progress and prospects: viral trafficking during infection. *Gene Ther* **12**, 1353-1359.

Cao, C., Subhawong, T., Albert, J. M., Kim, K. W., Geng, L., Sekhar, K. R., Gi, Y. J. & Lu, B. (2006). Inhibition of mammalian target of rapamycin or apoptotic pathway induces autophagy and radiosensitizes PTEN null prostate cancer cells. *Cancer Res* **66**, 10040-10047.

Carlisle, R. C., Di, Y., Cerny, A. M., Sonnen, A. F., Sim, R. B., Green, N. K., Subr, V., Ulbrich, K., Gilbert, R. J., Fisher, K. D., Finberg, R. W. & Seymour, L. W. (2009). Human erythrocytes bind and inactivate type 5 adenovirus by presenting Coxsackie virus-adenovirus receptor and complement receptor 1. *Blood* **113**, 1909-1918.

Carracedo, A., Ma, L., Teruya-Feldstein, J., Rojo, F., Salmena, L., Alimonti, A., Egia, A., Sasaki, A. T., Thomas, G., Kozma, S. C., Papa, A., Nardella, C., Cantley, L. C., Baselga, J. & Pandolfi, P. P. (2008). Inhibition of mTORC1 leads to MAPK pathway activation through a PI3K-dependent feedback loop in human cancer. *J Clin Invest* **118**, 3065-3074.

Castilla, C., Congregado, B., Chinchon, D., Torrubia, F. J., Japon, M. A. & Saez, C. (2006). Bcl-xL is overexpressed in hormone-resistant prostate cancer and promotes survival of LNCaP cells via interaction with proapoptotic Bak. *Endocrinology* **147**, 4960-4967.

Chang, S. S. & Kibel, A. S. (2009). The role of systemic cytotoxic therapy for prostate cancer. *BJU Int* **103**, 8-17.

Chang, Y. Y. & Neufeld, T. P. (2009). An Atg1/Atg13 complex with multiple roles in TOR-mediated autophagy regulation. *Mol Biol Cell* **20**, 2004-2014.

Chartier, C., Degryse, E., Gantzer, M., Dieterle, A., Pavirani, A. & Mehtali, M. (1996). Efficient generation of recombinant adenovirus vectors by homologous recombination in Escherichia coli. *J Virol* **70**, 4805-4810.

Chen, Y., DeWeese, T., Dilley, J., Zhang, Y., Li, Y., Ramesh, N., Lee, J., Pennathur-Das, R., Radzyminski, J., Wypych, J., Brignetti, D., Scott, S., Stephens, J., Karpf, D. B., Henderson, D. R. & Yu, D. C. (2001). CV706, a prostate cancer-specific adenovirus variant, in combination with radiotherapy produces synergistic antitumor efficacy without increasing toxicity. *Cancer Res* **61**, 5453-5460.

Chendil, D., Ranga, R. S., Meigooni, D., Sathishkumar, S. & Ahmed, M. M. (2004). Curcumin confers radiosensitizing effect in prostate cancer cell line PC-3. *Oncogene* **23**, 1599-1607.

Cherubini, G., Petouchoff, T., Grossi, M., Piersanti, S., Cundari, E. & Saggio, I. (2006). E1B55K-deleted adenovirus (ONYX-015) overrides G1/S and G2/M checkpoints and causes mitotic catastrophe and endoreduplication in p53-proficient normal cells. *Cell Cycle* **5**, 2244-2252.

Choi, E. J., Ahn, W. S. & Bae, S. M. (2009). Equol induces apoptosis through cytochrome c-mediated caspases cascade in human breast cancer MDA-MB-453 cells. *Chem Biol Interact* **177**, 7-11.

Chou, T. C. (2006). Theoretical basis, experimental design, and computerized simulation of synergism and antagonism in drug combination studies. *Pharmacol Rev* **58**, 621-681.

Chou, T. C., Hayball (1997). CalcuSyn for Windows: Multiple-Drug Dose-Effect Analyzer and Manual. Edited by Biosoft. Cambridge, UK.

Chou, T. C., Martin, N. (2005). CompuSyn for Drug Combinations: PC Software and User's Guide. Edited by ComboSyn. NJ, USA: Paramus.

Chou, T. C. & Talalay, P. (1984). Quantitative analysis of dose-effect relationships: the combined effects of multiple drugs or enzyme inhibitors. *Adv Enzyme Regul* **22**, 27-55.

Chroboczek, J., Bieber, F. & Jacrot, B. (1992). The sequence of the genome of adenovirus type 5 and its comparison with the genome of adenovirus type 2. *Virology* **186**, 280-285.

Chu, R. L., Post, D. E., Khuri, F. R. & Van Meir, E. G. (2004). Use of replicating oncolytic adenoviruses in combination therapy for cancer. *Clin Cancer Res* **10**, 5299-5312.

Codogno, P. & Meijer, A. J. (2005). Autophagy and signaling: their role in cell survival and cell death. *Cell Death Differ* **12 Suppl 2**, 1509-1518.

Cohen, C. J., Shieh, J. T., Pickles, R. J., Okegawa, T., Hsieh, J. T. & Bergelson, J. M. (2001). The coxsackievirus and adenovirus receptor is a transmembrane component of the tight junction. *Proc Natl Acad Sci U S A* **98**, 15191-15196.

Coyne, C. B. & Bergelson, J. M. (2005). CAR: a virus receptor within the tight junction. *Adv Drug Deliv Rev* **57**, 869-882.

Craft, N., Chhor, C., Tran, C., Belldegrun, A., DeKernion, J., Witte, O. N., Said, J., Reiter, R. E. & Sawyers, C. L. (1999). Evidence for clonal outgrowth of androgen-independent prostate cancer cells from androgen-dependent tumors through a two-step process. *Cancer Res* **59**, 5030-5036.

Cripe, T. P., Dunphy, E. J., Holub, A. D., Saini, A., Vasi, N. H., Mahller, Y. Y., Collins, M. H., Snyder, J. D., Krasnykh, V., Curiel, D. T., Wickham, T. J., DeGregori, J., Bergelson, J. M. & Currier, M. A. (2001). Fiber knob modifications overcome low, heterogeneous expression of the coxsackievirus-adenovirus receptor that limits adenovirus gene transfer and oncolysis for human rhabdomyosarcoma cells. *Cancer Res* **61**, 2953-2960.

Cuconati, A., Degenhardt, K., Sundararajan, R., Anschel, A. & White, E. (2002). Bak and Bax function to limit adenovirus replication through apoptosis induction. *J Virol* **76**, 4547-4558.

Damber, J. E. & Aus, G. (2008). Prostate cancer. *Lancet* **371**, 1710-1721.

de la Lastra, C. A. & Villegas, I. (2005). Resveratrol as an anti-inflammatory and anti-aging agent: mechanisms and clinical implications. *Mol Nutr Food Res* **49**, 405-430.

Dechecchi, M. C., Melotti, P., Bonizzato, A., Santacatterina, M., Chilosi, M. & Cabrini, G. (2001). Heparan sulfate glycosaminoglycans are receptors sufficient to mediate the initial binding of adenovirus types 2 and 5. *J Virol* **75**, 8772-8780.

Dechecchi, M. C., Tamanini, A., Bonizzato, A. & Cabrini, G. (2000). Heparan sulfate glycosaminoglycans are involved in adenovirus type 5 and 2-host cell interactions. *Virology* **268**, 382-390.

Deeb, D., Jiang, H., Gao, X., Hafner, M. S., Wong, H., Divine, G., Chapman, R. A., Dulchavsky, S. A. & Gautam, S. C. (2004). Curcumin sensitizes prostate cancer cells to tumor necrosis factor-related apoptosis-inducing ligand/Apo2L by inhibiting nuclear factor-kappaB through suppression of IkappaBalpha phosphorylation. *Mol Cancer Ther* **3**, 803-812.

Degenhardt, K., Mathew, R., Beaudoin, B., Bray, K., Anderson, D., Chen, G., Mukherjee, C., Shi, Y., Gelinas, C., Fan, Y., Nelson, D. A., Jin, S. & White, E. (2006). Autophagy promotes tumor cell survival and restricts necrosis, inflammation, and tumorigenesis. *Cancer Cell* **10**, 51-64.

Degterev, A. & Yuan, J. (2008). Expansion and evolution of cell death programmes. *Nat Rev Mol Cell Biol* **9**, 378-390.

Dewailly, E., Mulvad, G., Sloth Pedersen, H., Hansen, J. C., Behrendt, N. & Hart Hansen, J. P. (2003). Inuit are protected against prostate cancer. *Cancer Epidemiol Biomarkers Prev* **12**, 926-927.

DeWeese, T. L., van der Poel, H., Li, S., Mikhak, B., Drew, R., Goemann, M., Hamper, U., DeJong, R., Detorie, N., Rodriguez, R., Haulk, T., DeMarzo, A. M., Piantadosi, S., Yu, D. C., Chen, Y., Henderson, D. R., Carducci, M. A., Nelson, W. G. & Simons, J. W. (2001). A phase I trial of CV706, a replication-competent, PSA selective oncolytic adenovirus, for the treatment of locally recurrent prostate cancer following radiation therapy. *Cancer Res* **61**, 7464-7472.

Dhillon, N., Aggarwal, B. B., Newman, R. A., Wolff, R. A., Kunnumakkara, A. B., Abbruzzese, J. L., Ng, C. S., Badmaev, V. & Kurzrock, R. (2008). Phase II trial of curcumin in patients with advanced pancreatic cancer. *Clin Cancer Res* **14**, 4491-4499.

Dixon, R. A. & Ferreira, D. (2002). Genistein. *Phytochemistry* **60**, 205-211.

Doll, R. & Peto, R. (1981). The causes of cancer: quantitative estimates of avoidable risks of cancer in the United States today. *J Natl Cancer Inst* **66**, 1191-1308.

Dorai, T. & Aggarwal, B. B. (2004). Role of chemopreventive agents in cancer therapy. *Cancer Lett* **215**, 129-140.

Douglas, J. T., Kim, M., Sumerel, L. A., Carey, D. E. & Curiel, D. T. (2001). Efficient oncolysis by a replicating adenovirus (ad) in vivo is critically dependent on tumor expression of primary ad receptors. *Cancer Res* **61**, 813-817.

El Touny, L. H. & Banerjee, P. P. (2009). Identification of a biphasic role for genistein in the regulation of prostate cancer growth and metastasis. *Cancer Res* **69**, 3695-3703.

Elshami, A. A., Saavedra, A., Zhang, H., Kucharczuk, J. C., Spray, D. C., Fishman, G. I., Amin, K. M., Kaiser, L. R. & Albelda, S. M. (1996). Gap junctions play a role in the 'bystander effect' of the herpes simplex virus thymidine kinase/ganciclovir system in vitro. *Gene Ther* **3**, 85-92.

Estrov, Z., Shishodia, S., Faderl, S., Harris, D., Van, Q., Kantarjian, H. M., Talpaz, M. & Aggarwal, B. B. (2003). Resveratrol blocks interleukin-1beta-induced activation of the nuclear transcription factor NF-kappaB, inhibits proliferation, causes S-phase arrest, and induces apoptosis of acute myeloid leukemia cells. *Blood* **102**, 987-995.

Fechner, H., Haack, A., Wang, H., Wang, X., Eizema, K., Pauschinger, M., Schoemaker, R., Veghel, R., Houtsmuller, A., Schultheiss, H. P., Lamers, J. & Poller, W. (1999). Expression of coxsackie adenovirus receptor and alphav-integrin does not correlate with adenovector targeting in vivo indicating anatomical vector barriers. *Gene Ther* **6**, 1520-1535.

Feigenblum, D. & Schneider, R. J. (1996). Cap-binding protein (eukaryotic initiation factor 4E) and 4E-inactivating protein BP-1 independently regulate cap-dependent translation. *Mol Cell Biol* **16**, 5450-5457.

Ferley, J., Bray, F., Pisani, P. & Parkin, D. M. (2004). GLOBOCAN 2002: Cancer Incidence, Mortality and Prevalence Worldwide: IARC*Press*

Festjens, N., Vanden Berghe, T., Cornelis, S. & Vandenabeele, P. (2007). RIP1, a kinase on the crossroads of a cell's decision to live or die. *Cell Death Differ* **14**, 400-410.

Finkel, T. & Holbrook, N. J. (2000). Oxidants, oxidative stress and the biology of ageing. *Nature* **408**, 239-247.

Fitzpatrick, D. F., Hirschfield, S. L. & Coffey, R. G. (1993). Endothelium-dependent vasorelaxing activity of wine and other grape products. *Am J Physiol* **265**, H774-778.

Freytag, S. O., Khil, M., Stricker, H., Peabody, J., Menon, M., DePeralta-Venturina, M., Nafziger, D., Pegg, J., Paielli, D., Brown, S., Barton, K., Lu, M., Aguilar-Cordova, E. & Kim, J. H. (2002). Phase I study of replication-competent adenovirus-mediated double suicide gene therapy for the treatment of locally recurrent prostate cancer. *Cancer Res* **62**, 4968-4976.

Freytag, S. O., Rogulski, K. R., Paielli, D. L., Gilbert, J. D. & Kim, J. H. (1998). A novel three-pronged approach to kill cancer cells selectively: concomitant viral, double suicide gene, and radiotherapy. *Hum Gene Ther* **9**, 1323-1333.

Freytag, S. O., Stricker, H., Peabody, J., Pegg, J., Paielli, D., Movsas, B., Barton, K. N., Brown, S. L., Lu, M. & Kim, J. H. (2007). Five-year Follow-up of Trial of Replication-competent Adenovirus-mediated Suicide Gene Therapy for Treatment of Prostate Cancer. *Mol Ther*.

Freytag, S. O., Stricker, H., Pegg, J., Paielli, D., Pradhan, D. G., Peabody, J., DePeralta-Venturina, M., Xia, X., Brown, S., Lu, M. & Kim, J. H. (2003). Phase I study of replication-competent adenovirus-mediated double-suicide gene therapy in combination with conventional-dose three-dimensional conformal radiation therapy for the treatment of newly diagnosed, intermediate- to high-risk prostate cancer. *Cancer Res* **63**, 7497-7506.

Frisch, S. M. & Mymryk, J. S. (2002). Adenovirus-5 E1A: paradox and paradigm. *Nat Rev Mol Cell Biol* **3**, 441-452.

Fu, M., Liu, M., Sauve, A. A., Jiao, X., Zhang, X., Wu, X., Powell, M. J., Yang, T., Gu, W., Avantaggiati, M. L., Pattabiraman, N., Pestell, T. G., Wang, F., Quong, A. A.,

Wang, C. & Pestell, R. G. (2006). Hormonal control of androgen receptor function through SIRT1. *Mol Cell Biol* **26**, 8122-8135.

Fujimoto, N., Mizokami, A., Harada, S. & Matsumoto, T. (2001). Different expression of androgen receptor coactivators in human prostate. *Urology* **58**, 289-294.

Fulda, S. & Debatin, K. M. (2004). Sensitization for anticancer drug-induced apoptosis by the chemopreventive agent resveratrol. *Oncogene* **23**, 6702-6711.

Furnari, F. B., Fenton, T., Bachoo, R. M., Mukasa, A., Stommel, J. M., Stegh, A., Hahn, W. C., Ligon, K. L., Louis, D. N., Brennan, C., Chin, L., DePinho, R. A. & Cavenee, W. K. (2007). Malignant astrocytic glioma: genetics, biology, and paths to treatment. *Genes Dev* **21**, 2683-2710.

Gao, N., Zhang, Z., Jiang, B. H. & Shi, X. (2003). Role of PI3K/AKT/mTOR signaling in the cell cycle progression of human prostate cancer. *Biochem Biophys Res Commun* **310**, 1124-1132.

Gao, S., Liu, G. Z. & Wang, Z. (2004). Modulation of androgen receptor-dependent transcription by resveratrol and genistein in prostate cancer cells. *Prostate* **59**, 214-225.

Garber, K. (2006). China approves world's first oncolytic virus therapy for cancer treatment. *J Natl Cancer Inst* **98**, 298-300.

Gatz, S. A. & Wiesmuller, L. (2008). Take a break--resveratrol in action on DNA. *Carcinogenesis* **29**, 321-332.

Gehm, B. D., McAndrews, J. M., Chien, P. Y. & Jameson, J. L. (1997). Resveratrol, a polyphenolic compound found in grapes and wine, is an agonist for the estrogen receptor. *Proc Natl Acad Sci U S A* **94**, 14138-14143.

Geoerger, B., Grill, J., Opolon, P., Morizet, J., Aubert, G., Terrier-Lacombe, M. J., Bressac De-Paillerets, B., Barrois, M., Feunteun, J., Kirn, D. H. & Vassal, G. (2002). Oncolytic activity of the E1B-55 kDa-deleted adenovirus ONYX-015 is independent of cellular p53 status in human malignant glioma xenografts. *Cancer Res* **62**, 764-772.

Ghadge, G. D., Malhotra, P., Furtado, M. R., Dhar, R. & Thimmapaya, B. (1994). In vitro analysis of virus-associated RNA I (VAI RNA): inhibition of the double-stranded RNA-activated protein kinase PKR by VAI RNA mutants correlates with the in vivo phenotype and the structural integrity of the central domain. *J Virol* **68**, 4137-4151.

Gill, C., Walsh, S. E., Morrissey, C., Fitzpatrick, J. M. & Watson, R. W. (2007). Resveratrol sensitizes androgen independent prostate cancer cells to death-receptor mediated apoptosis through multiple mechanisms. *Prostate* **67**, 1641-1653.

Gingras, A. C. & Sonenberg, N. (1997). Adenovirus infection inactivates the translational inhibitors 4E-BP1 and 4E-BP2. *Virology* **237**, 182-186.

Glasgow, J. N., Everts, M. & Curiel, D. T. (2006). Transductional targeting of adenovirus vectors for gene therapy. *Cancer Gene Ther* **13**, 830-844.

Goldsmith, M. E., Kitazono, M., Fok, P., Aikou, T., Bates, S. & Fojo, T. (2003). The histone deacetylase inhibitor FK228 preferentially enhances adenovirus transgene expression in malignant cells. *Clin Cancer Res* **9**, 5394-5401.

Gossner, G., Choi, M., Tan, L., Fogoros, S., Griffith, K. A., Kuenker, M. & Liu, J. R. (2007). Genistein-induced apoptosis and autophagocytosis in ovarian cancer cells. *Gynecol Oncol* **105**, 23-30.

Gowardhan, B., Douglas, D. A., Mathers, M. E., McKie, A. B., McCracken, S. R., Robson, C. N. & Leung, H. Y. (2005). Evaluation of the fibroblast growth factor system as a potential target for therapy in human prostate cancer. *Br J Cancer* **92**, 320-327.

Greco, O. & Dachs, G. U. (2001). Gene directed enzyme/prodrug therapy of cancer: historical appraisal and future prospectives. *J Cell Physiol* **187**, 22-36.

Greco, W. R., Bravo, G. & Parsons, J. C. (1995). The search for synergy: a critical review from a response surface perspective. *Pharmacol Rev* **47**, 331-385.

Green, N. K., Morrison, J., Hale, S., Briggs, S. S., Stevenson, M., Subr, V., Ulbrich, K., Chandler, L., Mautner, V., Seymour, L. W. & Fisher, K. D. (2008). Retargeting

polymer-coated adenovirus to the FGF receptor allows productive infection and mediates efficacy in a peritoneal model of human ovarian cancer. *J Gene Med* **10**, 280-289.

Gregory, C. W., He, B., Johnson, R. T., Ford, O. H., Mohler, J. L., French, F. S. & Wilson, E. M. (2001). A mechanism for androgen receptor-mediated prostate cancer recurrence after androgen deprivation therapy. *Cancer Res* **61**, 4315-4319.

Grunwald, V., DeGraffenried, L., Russel, D., Friedrichs, W. E., Ray, R. B. & Hidalgo, M. (2002). Inhibitors of mTOR reverse doxorubicin resistance conferred by PTEN status in prostate cancer cells. *Cancer Res* **62**, 6141-6145.

Gudmundsson, J., Sulem, P., Manolescu, A., Amundadottir, L. T., Gudbjartsson, D., Helgason, A., Rafnar, T., Bergthorsson, J. T., Agnarsson, B. A., Baker, A., Sigurdsson, A., Benediktsdottir, K. R., Jakobsdottir, M., Xu, J., Blondal, T., Kostic, J., Sun, J., Ghosh, S., Stacey, S. N., Mouy, M., Saemundsdottir, J., Backman, V. M., Kristjansson, K., Tres, A., Partin, A. W., Albers-Akkers, M. T., Godino-Ivan Marcos, J., Walsh, P. C., Swinkels, D. W., Navarrete, S., Isaacs, S. D., Aben, K. K., Graif, T., Cashy, J., Ruiz-Echarri, M., Wiley, K. E., Suarez, B. K., Witjes, J. A., Frigge, M., Ober, C., Jonsson, E., Einarsson, G. V., Mayordomo, J. I., Kiemeney, L. A., Isaacs, W. B., Catalona, W. J., Barkardottir, R. B., Gulcher, J. R., Thorsteinsdottir, U., Kong, A. & Stefansson, K. (2007). Genome-wide association study identifies a second prostate cancer susceptibility variant at 8q24. *Nat Genet* **39**, 631-637.

Gupta, S., Hussain, T. & Mukhtar, H. (2003). Molecular pathway for (-)-epigallocatechin-3-gallate-induced cell cycle arrest and apoptosis of human prostate carcinoma cells. *Arch Biochem Biophys* **410**, 177-185.

Haisma, H. J., Boesjes, M., Beerens, A. M., van der Strate, B. W., Curiel, D. T., Pluddemann, A., Gordon, S. & Bellu, A. R. (2009). Scavenger Receptor A: A New Route for Adenovirus 5. *Mol Pharm* **6**, 366-374.

Hallden, G., Thorne, S., Yang, J. & Kirn, D. (2004). Replication-selective oncolytic adenoviruses. In *Methods in Molecular Medicine*, pp. 71-90. Edited by C. J. Springer. Totowa, NJ, USA: Humana Press Inc.

Hamdy, F. C. & Thomas, B. G. (2001). New therapeutic concepts in prostate cancer. *BJU Int* **88 Suppl 2**, 43-48; discussion 49-50.

Harper, C. E., Patel, B. B., Wang, J., Arabshahi, A., Eltoum, I. A. & Lamartiniere, C. A. (2007). Resveratrol suppresses prostate cancer progression in transgenic mice. *Carcinogenesis* **28**, 1946-1953.

Hastak, K., Gupta, S., Ahmad, N., Agarwal, M. K., Agarwal, M. L. & Mukhtar, H. (2003). Role of p53 and NF-kappaB in epigallocatechin-3-gallate-induced apoptosis of LNCaP cells. *Oncogene* **22**, 4851-4859.

Hedlund, T. E., Johannes, W. U. & Miller, G. J. (2003). Soy isoflavonoid equol modulates the growth of benign and malignant prostatic epithelial cells in vitro. *Prostate* **54**, 68-78.

Hedlund, T. E., Maroni, P. D., Ferucci, P. G., Dayton, R., Barnes, S., Jones, K., Moore, R., Ogden, L. G., Wahala, K., Sackett, H. M. & Gray, K. J. (2005). Long-term dietary habits affect soy isoflavone metabolism and accumulation in prostatic fluid in caucasian men. *J Nutr* **135**, 1400-1406.

Heinlein, C. A. & Chang, C. (2002). Androgen receptor (AR) coregulators: an overview. *Endocr Rev* **23**, 175-200.

Heise, C., Hermiston, T., Johnson, L., Brooks, G., Sampson-Johannes, A., Williams, A., Hawkins, L. & Kirn, D. (2000a). An adenovirus E1A mutant that demonstrates potent and selective systemic anti-tumoral efficacy. *Nat Med* **6**, 1134-1139.

Heise, C., Lemmon, M. & Kirn, D. (2000b). Efficacy with a replication-selective adenovirus plus cisplatin-based chemotherapy: dependence on sequencing but not p53 functional status or route of administration. *Clin Cancer Res* **6**, 4908-4914.

Heise, C., Sampson-Johannes, A., Williams, A., McCormick, F., Von Hoff, D. D. & Kirn, D. H. (1997). ONYX-015, an E1B gene-attenuated adenovirus, causes tumor-specific

cytolysis and antitumoral efficacy that can be augmented by standard chemotherapeutic agents. *Nat Med* **3**, 639-645.

Hellerstedt, B. A. & Pienta, K. J. (2002). The current state of hormonal therapy for prostate cancer. *CA Cancer J Clin* **52**, 154-179.

Hemminki, A., Kanerva, A., Liu, B., Wang, M., Alvarez, R. D., Siegal, G. P. & Curiel, D. T. (2003). Modulation of coxsackie-adenovirus receptor expression for increased adenoviral transgene expression. *Cancer Res* **63**, 847-853.

Hinata, N., Shirakawa, T., Terao, S., Goda, K., Tanaka, K., Yamada, Y., Hara, I., Kamidono, S., Fujisawa, M. & Gotoh, A. (2006). Progress report on phase I/II clinical trial of Ad-OC-TK plus VAL therapy for metastatic or locally recurrent prostate cancer: Initial experience at Kobe University. *Int J Urol* **13**, 834-837.

Hitomi, J., Christofferson, D. E., Ng, A., Yao, J., Degterev, A., Xavier, R. J. & Yuan, J. (2008). Identification of a molecular signaling network that regulates a cellular necrotic cell death pathway. *Cell* **135**, 1311-1323.

Homicsko, K., Lukashev, A. & Iggo, R. D. (2005). RAD001 (everolimus) improves the efficacy of replicating adenoviruses that target colon cancer. *Cancer Res* **65**, 6882-6890.

Horwitz, M. S. (2004). Function of adenovirus E3 proteins and their interactions with immunoregulatory cell proteins. *J Gene Med* **6 Suppl 1**, S172-183.

Hoti, N., Li, Y., Chen, C. L., Chowdhury, W. H., Johns, D. C., Xia, Q., Kabul, A., Hsieh, J. T., Berg, M., Ketner, G., Lupold, S. E. & Rodriguez, R. (2007). Androgen receptor attenuation of Ad5 replication: implications for the development of conditionally replication competent adenoviruses. *Mol Ther* **15**, 1495-1503.

Howitz, K. T., Bitterman, K. J., Cohen, H. Y., Lamming, D. W., Lavu, S., Wood, J. G., Zipkin, R. E., Chung, P., Kisielewski, A., Zhang, L. L., Scherer, B. & Sinclair, D. A. (2003). Small molecule activators of sirtuins extend Saccharomyces cerevisiae lifespan. *Nature* **425**, 191-196.

Huang, X., Chen, S., Xu, L., Liu, Y., Deb, D. K., Platanias, L. C. & Bergan, R. C. (2005). Genistein inhibits p38 map kinase activation, matrix metalloproteinase type 2, and cell invasion in human prostate epithelial cells. *Cancer Res* **65**, 3470-3478.

Hwang, C. S., Kwak, H. S., Lim, H. J., Lee, S. H., Kang, Y. S., Choe, T. B., Hur, H. G. & Han, K. O. (2006). Isoflavone metabolites and their in vitro dual functions: they can act as an estrogenic agonist or antagonist depending on the estrogen concentration. *J Steroid Biochem Mol Biol* **101**, 246-253.

Isaacs, W. B., Carter, B. S. & Ewing, C. M. (1991). Wild-type p53 suppresses growth of human prostate cancer cells containing mutant p53 alleles. *Cancer Res* **51**, 4716-4720.

Ito, H., Aoki, H., Kuhnel, F., Kondo, Y., Kubicka, S., Wirth, T., Iwado, E., Iwamaru, A., Fujiwara, K., Hess, K. R., Lang, F. F., Sawaya, R. & Kondo, S. (2006). Autophagic cell death of malignant glioma cells induced by a conditionally replicating adenovirus. *J Natl Cancer Inst* **98**, 625-636.

Jang, M., Cai, L., Udeani, G. O., Slowing, K. V., Thomas, C. F., Beecher, C. W., Fong, H. H., Farnsworth, N. R., Kinghorn, A. D., Mehta, R. G., Moon, R. C. & Pezzuto, J. M. (1997). Cancer chemopreventive activity of resveratrol, a natural product derived from grapes. *Science* **275**, 218-220.

Jiang, H., Gomez-Manzano, C., Aoki, H., Alonso, M. M., Kondo, S., McCormick, F., Xu, J., Kondo, Y., Bekele, B. N., Colman, H., Lang, F. F. & Fueyo, J. (2007). Examination of the therapeutic potential of Delta-24-RGD in brain tumor stem cells: role of autophagic cell death. *J Natl Cancer Inst* **99**, 1410-1414.

Jiang, H., White, E. J., Gomez-Manzano, C. & Fueyo, J. (2008). Adenovirus's last trick: you say lysis, we say autophagy. *Autophagy* **4**, 118-120.

Jin, F., Kretschmer, P. J. & Hermiston, T. W. (2005). Identification of novel insertion sites in the Ad5 genome that utilize the Ad splicing machinery for therapeutic gene expression. *Mol Ther* **12**, 1052-1063.

Jolly, C. & Morimoto, R. I. (2000). Role of the heat shock response and molecular chaperones in oncogenesis and cell death. *J Natl Cancer Inst* **92**, 1564-1572.

Jones, N. & Shenk, T. (1979). An adenovirus type 5 early gene function regulates expression of other early viral genes. *Proc Natl Acad Sci U S A* **76**, 3665-3669.

Kabeya, Y., Mizushima, N., Ueno, T., Yamamoto, A., Kirisako, T., Noda, T., Kominami, E., Ohsumi, Y. & Yoshimori, T. (2000). LC3, a mammalian homologue of yeast Apg8p, is localized in autophagosome membranes after processing. *EMBO J* **19**, 5720-5728.

Kaner, R. J., Worgall, S., Leopold, P. L., Stolze, E., Milano, E., Hidaka, C., Ramalingam, R., Hackett, N. R., Singh, R., Bergelson, J., Finberg, R., Falck-Pedersen, E. & Crystal, R. G. (1999). Modification of the genetic program of human alveolar macrophages by adenovirus vectors in vitro is feasible but inefficient, limited in part by the low level of expression of the coxsackie/adenovirus receptor. *Am J Respir Cell Mol Biol* **20**, 361-370.

Kang, J. S., Yoon, Y. D., Han, M. H., Han, S. B., Lee, K., Kang, M. R., Moon, E. Y., Jeon, Y. J., Park, S. K. & Kim, H. M. (2005). Estrogen receptor-independent inhibition of tumor necrosis factor-alpha gene expression by phytoestrogen equol is mediated by blocking nuclear factor-kappaB activation in mouse macrophages. *Biochem Pharmacol* **71**, 136-143.

Kang, M. R., Kim, M. S., Oh, J. E., Kim, Y. R., Song, S. Y., Kim, S. S., Ahn, C. H., Yoo, N. J. & Lee, S. H. (2009). Frameshift mutations of autophagy-related genes ATG2B, ATG5, ATG9B and ATG12 in gastric and colorectal cancers with microsatellite instability. *J Pathol* **217**, 702-706.

Kanzawa, T., Germano, I. M., Komata, T., Ito, H., Kondo, Y. & Kondo, S. (2004). Role of autophagy in temozolomide-induced cytotoxicity for malignant glioma cells. *Cell Death Differ* **11**, 448-457.

Kawakami, Y., Li, H., Lam, J. T., Krasnykh, V., Curiel, D. T. & Blackwell, J. L. (2003). Substitution of the adenovirus serotype 5 knob with a serotype 3 knob enhances multiple steps in virus replication. *Cancer Res* **63**, 1262-1269.

Kelkar, S., De, B. P., Gao, G., Wilson, J. M., Crystal, R. G. & Leopold, P. L. (2006). A common mechanism for cytoplasmic dynein-dependent microtubule binding shared among adeno-associated virus and adenovirus serotypes. *J Virol* **80**, 7781-7785.

Kelkar, S. A., Pfister, K. K., Crystal, R. G. & Leopold, P. L. (2004). Cytoplasmic dynein mediates adenovirus binding to microtubules. *J Virol* **78**, 10122-10132.

Khan, N., Afaq, F., Saleem, M., Ahmad, N. & Mukhtar, H. (2006). Targeting multiple signaling pathways by green tea polyphenol (-)-epigallocatechin-3-gallate. *Cancer Res* **66**, 2500-2505.

Kim, K. I., Kang, J. H., Chung, J. K., Lee, Y. J., Jeong, J. M., Lee, D. S. & Lee, M. C. (2007). Doxorubicin enhances the expression of transgene under control of the CMV promoter in anaplastic thyroid carcinoma cells. *J Nucl Med* **48**, 1553-1561.

Kirn, D. (2001). Clinical research results with dl1520 (Onyx-015), a replication-selective adenovirus for the treatment of cancer: what have we learned? *Gene Ther* **8**, 89-98.

Kirn, D., Niculescu-Duvaz, I., Hallden, G. & Springer, C. J. (2002). The emerging fields of suicide gene therapy and virotherapy. *Trends Mol Med* **8**, S68-73.

Kitazono, M., Goldsmith, M. E., Aikou, T., Bates, S. & Fojo, T. (2001). Enhanced adenovirus transgene expression in malignant cells treated with the histone deacetylase inhibitor FR901228. *Cancer Res* **61**, 6328-6330.

Kitazono, M., Rao, V. K., Robey, R., Aikou, T., Bates, S., Fojo, T. & Goldsmith, M. E. (2002). Histone deacetylase inhibitor FR901228 enhances adenovirus infection of hematopoietic cells. *Blood* **99**, 2248-2251.

Kolonel, L. N., Altshuler, D. & Henderson, B. E. (2004). The multiethnic cohort study: exploring genes, lifestyle and cancer risk. *Nat Rev Cancer* **4**, 519-527.

Kondo, Y., Kanzawa, T., Sawaya, R. & Kondo, S. (2005). The role of autophagy in cancer development and response to therapy. *Nat Rev Cancer* **5**, 726-734.

Krasnykh, V., Dmitriev, I., Navarro, J. G., Belousova, N., Kashentseva, E., Xiang, J., Douglas, J. T. & Curiel, D. T. (2000). Advanced generation adenoviral vectors

possess augmented gene transfer efficiency based upon coxsackie adenovirus receptor-independent cellular entry capacity. *Cancer Res* **60**, 6784-6787.

Kreppel, F. & Kochanek, S. (2008). Modification of adenovirus gene transfer vectors with synthetic polymers: a scientific review and technical guide. *Mol Ther* **16**, 16-29.

Kroemer, G., Galluzzi, L., Vandenabeele, P., Abrams, J., Alnemri, E. S., Baehrecke, E. H., Blagosklonny, M. V., El-Deiry, W. S., Golstein, P., Green, D. R., Hengartner, M., Knight, R. A., Kumar, S., Lipton, S. A., Malorni, W., Nunez, G., Peter, M. E., Tschopp, J., Yuan, J., Piacentini, M., Zhivotovsky, B. & Melino, G. (2009). Classification of cell death: recommendations of the Nomenclature Committee on Cell Death 2009. *Cell Death Differ* **16**, 3-11.

Kruyt, F. A. & Curiel, D. T. (2002). Toward a new generation of conditionally replicating adenoviruses: pairing tumor selectivity with maximal oncolysis. *Hum Gene Ther* **13**, 485-495.

Kueck, A., Opipari, A. W., Jr., Griffith, K. A., Tan, L., Choi, M., Huang, J., Wahl, H. & Liu, J. R. (2007). Resveratrol inhibits glucose metabolism in human ovarian cancer cells. *Gynecol Oncol* **107**, 450-457.

Kuiper, G. G., Lemmen, J. G., Carlsson, B., Corton, J. C., Safe, S. H., van der Saag, P. T., van der Burg, B. & Gustafsson, J. A. (1998). Interaction of estrogenic chemicals and phytoestrogens with estrogen receptor beta. *Endocrinology* **139**, 4252-4263.

Kumar, B., Koul, S., Khandrika, L., Meacham, R. B. & Koul, H. K. (2008). Oxidative stress is inherent in prostate cancer cells and is required for aggressive phenotype. *Cancer Res* **68**, 1777-1785.

Kundu, J. K. & Surh, Y. J. (2004). Molecular basis of chemoprevention by resveratrol: NF-kappaB and AP-1 as potential targets. *Mutat Res* **555**, 65-80.

Kurahashi, N., Iwasaki, M., Sasazuki, S., Otani, T., Inoue, M. & Tsugane, S. (2007). Soy product and isoflavone consumption in relation to prostate cancer in Japanese men. *Cancer Epidemiol Biomarkers Prev* **16**, 538-545.

Lacher, M. D., Tiirikainen, M. I., Saunier, E. F., Christian, C., Anders, M., Oft, M., Balmain, A., Akhurst, R. J. & Korn, W. M. (2006). Transforming growth factor-beta receptor inhibition enhances adenoviral infectability of carcinoma cells via up-regulation of Coxsackie and Adenovirus Receptor in conjunction with reversal of epithelial-mesenchymal transition. *Cancer Res* **66**, 1648-1657.

Lefranc, F., Facchini, V. & Kiss, R. (2007). Proautophagic drugs: a novel means to combat apoptosis-resistant cancers, with a special emphasis on glioblastomas. *Oncologist* **12**, 1395-1403.

Leitner, S., Sweeney, K., Oberg, D., Davies, D., Miranda, E., Lemoine, N. R. & Hallden, G. (2009). Oncolytic adenoviral mutants with E1B19K gene deletions enhance gemcitabine-induced apoptosis in pancreatic carcinoma cells and anti-tumor efficacy in vivo. *Clin Cancer Res* **15**, 1730-1740.

Lenaerts, L., De Clercq, E. & Naesens, L. (2008). Clinical features and treatment of adenovirus infections. *Rev Med Virol* **18**, 357-374.

Leopold, P. L., Ferris, B., Grinberg, I., Worgall, S., Hackett, N. R. & Crystal, R. G. (1998). Fluorescent virions: dynamic tracking of the pathway of adenoviral gene transfer vectors in living cells. *Hum Gene Ther* **9**, 367-378.

Leopold, P. L., Kreitzer, G., Miyazawa, N., Rempel, S., Pfister, K. K., Rodriguez-Boulan, E. & Crystal, R. G. (2000). Dynein- and microtubule-mediated translocation of adenovirus serotype 5 occurs after endosomal lysis. *Hum Gene Ther* **11**, 151-165.

Levine, B. & Kroemer, G. (2008). Autophagy in the pathogenesis of disease. *Cell* **132**, 27-42.

Li, E., Stupack, D., Bokoch, G. M. & Nemerow, G. R. (1998). Adenovirus endocytosis requires actin cytoskeleton reorganization mediated by Rho family GTPases. *J Virol* **72**, 8806-8812.

Li, M., Zhang, Z., Hill, D. L., Wang, H. & Zhang, R. (2007). Curcumin, a dietary component, has anticancer, chemosensitization, and radiosensitization effects by down-regulating the MDM2 oncogene through the PI3K/mTOR/ETS2 pathway. *Cancer Res* **67**, 1988-1996.

Li, P., Nicosia, S. V. & Bai, W. (2001). Antagonism between PTEN/MMAC1/TEP-1 and androgen receptor in growth and apoptosis of prostatic cancer cells. *J Biol Chem* **276**, 20444-20450.

Li, S., Szymborski, A., Miron, M. J., Marcellus, R., Binda, O., Lavoie, J. N. & Branton, P. E. (2009). The adenovirus E4orf4 protein induces growth arrest and mitotic catastrophe in H1299 human lung carcinoma cells. *Oncogene* **28**, 390-400.

Li, Y., Ahmed, F., Ali, S., Philip, P. A., Kucuk, O. & Sarkar, F. H. (2005). Inactivation of nuclear factor kappaB by soy isoflavone genistein contributes to increased apoptosis induced by chemotherapeutic agents in human cancer cells. *Cancer Res* **65**, 6934-6942.

Lin, E. & Nemunaitis, J. (2004). Oncolytic viral therapies. *Cancer Gene Ther* **11**, 643-664.

Linja, M. J., Savinainen, K. J., Saramaki, O. R., Tammela, T. L., Vessella, R. L. & Visakorpi, T. (2001). Amplification and overexpression of androgen receptor gene in hormone-refractory prostate cancer. *Cancer Res* **61**, 3550-3555.

Liu, R. H. (2004). Potential synergy of phytochemicals in cancer prevention: mechanism of action. *J Nutr* **134**, 3479S-3485S.

Lund, T. D., Munson, D. J., Haldy, M. E., Setchell, K. D., Lephart, E. D. & Handa, R. J. (2004). Equol is a novel anti-androgen that inhibits prostate growth and hormone feedback. *Biol Reprod* **70**, 1188-1195.

Ma, X. M. & Blenis, J. (2009). Molecular mechanisms of mTOR-mediated translational control. *Nat Rev Mol Cell Biol* **10**, 307-318.

Magee, P. J. & Rowland, I. R. (2004). Phyto-oestrogens, their mechanism of action: current evidence for a role in breast and prostate cancer. *Br J Nutr* **91**, 513-531.

Maheshwari, R. K., Singh, A. K., Gaddipati, J. & Srimal, R. C. (2006). Multiple biological activities of curcumin: a short review. *Life Sci* **78**, 2081-2087.

Mahyar-Roemer, M., Katsen, A., Mestres, P. & Roemer, K. (2001). Resveratrol induces colon tumor cell apoptosis independently of p53 and precede by epithelial differentiation, mitochondrial proliferation and membrane potential collapse. *Int J Cancer* **94**, 615-622.

Maiuri, M. C., Zalckvar, E., Kimchi, A. & Kroemer, G. (2007). Self-eating and self-killing: crosstalk between autophagy and apoptosis. *Nat Rev Mol Cell Biol* **8**, 741-752.

Maizel, J. V., Jr., White, D. O. & Scharff, M. D. (1968). The polypeptides of adenovirus. I. Evidence for multiple protein components in the virion and a comparison of types 2, 7A, and 12. *Virology* **36**, 115-125.

Marcelli, M., Ittmann, M., Mariani, S., Sutherland, R., Nigam, R., Murthy, L., Zhao, Y., DiConcini, D., Puxeddu, E., Esen, A., Eastham, J., Weigel, N. L. & Lamb, D. J. (2000a). Androgen receptor mutations in prostate cancer. *Cancer Res* **60**, 944-949.

Marcelli, M., Marani, M., Li, X., Sturgis, L., Haidacher, S. J., Trial, J. A., Mannucci, R., Nicoletti, I. & Denner, L. (2000b). Heterogeneous apoptotic responses of prostate cancer cell lines identify an association between sensitivity to staurosporine-induced apoptosis, expression of Bcl-2 family members, and caspase activation. *Prostate* **42**, 260-273.

Markovits, J., Linassier, C., Fosse, P., Couprie, J., Pierre, J., Jacquemin-Sablon, A., Saucier, J. M., Le Pecq, J. B. & Larsen, A. K. (1989). Inhibitory effects of the tyrosine kinase inhibitor genistein on mammalian DNA topoisomerase II. *Cancer Res* **49**, 5111-5117.

Maruo, T., Sakamoto, M., Ito, C., Toda, T. & Benno, Y. (2008). Adlercreutzia equolifaciens gen. nov., sp. nov., an equol-producing bacterium isolated from human faeces, and emended description of the genus Eggerthella. *Int J Syst Evol Microbiol* **58**, 1221-1227.

Mathew, R., Karantza-Wadsworth, V. & White, E. (2007). Role of autophagy in cancer. *Nat Rev Cancer* **7**, 961-967.

Mathews, M. B. & Shenk, T. (1991). Adenovirus virus-associated RNA and translation control. *J Virol* **65**, 5657-5662.

Mathis, J. M., Stoff-Khalili, M. A. & Curiel, D. T. (2005). Oncolytic adenoviruses - selective retargeting to tumor cells. *Oncogene* **24**, 7775-7791.

Matsubara, S., Wada, Y., Gardner, T. A., Egawa, M., Park, M. S., Hsieh, C. L., Zhau, H. E., Kao, C., Kamidono, S., Gillenwater, J. Y. & Chung, L. W. (2001). A conditional replication-competent adenoviral vector, Ad-OC-E1a, to cotarget prostate cancer and bone stroma in an experimental model of androgen-independent prostate cancer bone metastasis. *Cancer Res* **61**, 6012-6019.

Matthies, A., Blaut, M. & Braune, A. (2009). Isolation of a human intestinal bacterium capable of daidzein and genistein conversion. *Appl Environ Microbiol* **75**, 1740-1744.

McCormick, F. (2001). Cancer gene therapy: fringe or cutting edge? *Nat Rev Cancer* **1**, 130-141.

McMenamin, M. E., Soung, P., Perera, S., Kaplan, I., Loda, M. & Sellers, W. R. (1999). Loss of PTEN expression in paraffin-embedded primary prostate cancer correlates with high Gleason score and advanced stage. *Cancer Res* **59**, 4291-4296.

Meeran, S. M. & Katiyar, S. K. (2008). Cell cycle control as a basis for cancer chemoprevention through dietary agents. *Front Biosci* **13**, 2191-2202.

Meinbach, D. S. & Lokeshwar, B. L. (2006). Insulin-like growth factors and their binding proteins in prostate cancer: cause or consequence? *Urol Oncol* **24**, 294-306.

Meyskens, F. L., Jr. & Szabo, E. (2005). Diet and cancer: the disconnect between epidemiology and randomized clinical trials. *Cancer Epidemiol Biomarkers Prev* **14**, 1366-1369.

Michishita, E., Park, J. Y., Burneskis, J. M., Barrett, J. C. & Horikawa, I. (2005). Evolutionarily conserved and nonconserved cellular localizations and functions of human SIRT proteins. *Mol Biol Cell* **16**, 4623-4635.

Miller, K., Anderson, J. & Abrahamsson, P. A. (2009). Treatment of prostate cancer with hormonal therapy in Europe. *BJU Int* **103 Suppl 2**, 2-6.

Mitchell, S. H., Zhu, W. & Young, C. Y. (1999). Resveratrol inhibits the expression and function of the androgen receptor in LNCaP prostate cancer cells. *Cancer Res* **59**, 5892-5895.

Mittereder, N., March, K. L. & Trapnell, B. C. (1996). Evaluation of the concentration and bioactivity of adenovirus vectors for gene therapy. *J Virol* **70**, 7498-7509.

Miyake, H., Hara, I., Fujisawa, M. & Gleave, M. E. (2006). The potential of clusterin inhibiting antisense oligodeoxynucleotide therapy for prostate cancer. *Expert Opin Investig Drugs* **15**, 507-517.

Miyamoto, H., Messing, E. M. & Chang, C. (2004). Androgen deprivation therapy for prostate cancer: current status and future prospects. *Prostate* **61**, 332-353.

Mohan, J., Gandhi, A. A., Bhavya, B. C., Rashmi, R., Karunagaran, D., Indu, R. & Santhoshkumar, T. R. (2006). Caspase-2 triggers Bax-Bak-dependent and -independent cell death in colon cancer cells treated with resveratrol. *J Biol Chem* **281**, 17599-17611.

Mukhopadhyay, A., Bueso-Ramos, C., Chatterjee, D., Pantazis, P. & Aggarwal, B. B. (2001). Curcumin downregulates cell survival mechanisms in human prostate cancer cell lines. *Oncogene* **20**, 7597-7609.

Murillo, H., Huang, H., Schmidt, L. J., Smith, D. I. & Tindall, D. J. (2001). Role of PI3K signaling in survival and progression of LNCaP prostate cancer cells to the androgen refractory state. *Endocrinology* **142**, 4795-4805.

Nakatani, K., Thompson, D. A., Barthel, A., Sakaue, H., Liu, W., Weigel, R. J. & Roth, R. A. (1999). Up-regulation of Akt3 in estrogen receptor-deficient breast cancers and androgen-independent prostate cancer lines. *J Biol Chem* **274**, 21528-21532.

Nelson, P. S. & Montgomery, B. (2003). Unconventional therapy for prostate cancer: good, bad or questionable? *Nat Rev Cancer* **3**, 845-858.

Nemerow, G. R., Pache, L., Reddy, V. & Stewart, P. L. (2009). Insights into adenovirus host cell interactions from structural studies. *Virology* **384**, 380-388.

Nemerow, G. R. & Stewart, P. L. (1999). Role of alpha(v) integrins in adenovirus cell entry and gene delivery. *Microbiol Mol Biol Rev* **63**, 725-734.

Nemunaitis, J., Ganly, I., Khuri, F., Arseneau, J., Kuhn, J., McCarty, T., Landers, S., Maples, P., Romel, L., Randlev, B., Reid, T., Kaye, S. & Kirn, D. (2000). Selective replication and oncolysis in p53 mutant tumors with ONYX-015, an E1B-55kD gene-deleted adenovirus, in patients with advanced head and neck cancer: a phase II trial. *Cancer Res* **60**, 6359-6366.

Neshat, M. S., Mellinghoff, I. K., Tran, C., Stiles, B., Thomas, G., Petersen, R., Frost, P., Gibbons, J. J., Wu, H. & Sawyers, C. L. (2001). Enhanced sensitivity of PTEN-deficient tumors to inhibition of FRAP/mTOR. *Proc Natl Acad Sci U S A* **98**, 10314-10319.

O'Reilly, D., Muller, L. & Luckow, V. (1994). Virus Methods, pp. 132-134. Oxford: Oxford University Press.

O'Shea, C., Klupsch, K., Choi, S., Bagus, B., Soria, C., Shen, J., McCormick, F. & Stokoe, D. (2005a). Adenoviral proteins mimic nutrient/growth signals to activate the mTOR pathway for viral replication. *Embo J* **24**, 1211-1221.

O'Shea, C. C., Johnson, L., Bagus, B., Choi, S., Nicholas, C., Shen, A., Boyle, L., Pandey, K., Soria, C., Kunich, J., Shen, Y., Habets, G., Ginzinger, D. & McCormick, F. (2004). Late viral RNA export, rather than p53 inactivation, determines ONYX-015 tumor selectivity. *Cancer Cell* **6**, 611-623.

O'Shea, C. C., Soria, C., Bagus, B. & McCormick, F. (2005b). Heat shock phenocopies E1B-55K late functions and selectively sensitizes refractory tumor cells to ONYX-015 oncolytic viral therapy. *Cancer Cell* **8**, 61-74.

Oefelein, M. G., Agarwal, P. K. & Resnick, M. I. (2004). Survival of patients with hormone refractory prostate cancer in the prostate specific antigen era. *J Urol* **171**, 1525-1528.

Ohshiro, K., Rayala, S. K., Kondo, S., Gaur, A., Vadlamudi, R. K., El-Naggar, A. K. & Kumar, R. (2007). Identifying the estrogen receptor coactivator PELP1 in autophagosomes. *Cancer Res* **67**, 8164-8171.

Oka, H., Chatani, Y., Kohno, M., Kawakita, M. & Ogawa, O. (2005). Constitutive activation of the 41- and 43-kDa mitogen-activated protein (MAP) kinases in the progression of prostate cancer to an androgen-independent state. *Int J Urol* **12**, 899-905.

Okegawa, T., Li, Y., Pong, R. C., Bergelson, J. M., Zhou, J. & Hsieh, J. T. (2000). The dual impact of coxsackie and adenovirus receptor expression on human prostate cancer gene therapy. *Cancer Res* **60**, 5031-5036.

Okegawa, T., Nutahara, K., Pong, R. C., Higashihara, E. & Hsieh, J. T. (2005). Enhanced transgene expression in urothelial cancer gene therapy with histone deacetylase inhibitor. *J Urol* **174**, 747-752.

Opipari, A. W., Jr., Tan, L., Boitano, A. E., Sorenson, D. R., Aurora, A. & Liu, J. R. (2004). Resveratrol-induced autophagocytosis in ovarian cancer cells. *Cancer Res* **64**, 696-703.

Ostapchuk, P. & Hearing, P. (2005). Control of adenovirus packaging. *J Cell Biochem* **96**, 25-35.

Pandha, H. S., Stockwin, L. H., Eaton, J., Clarke, I. A., Dalgleish, A. G., Todryk, S. M. & Blair, G. E. (2003). Coxsackie B and adenovirus receptor, integrin and major histocompatibility complex class I expression in human prostate cancer cell lines: implications for gene therapy strategies. *Prostate Cancer Prostatic Dis* **6**, 6-11.

Papatsoris, A. G., Karamouzis, M. V. & Papavassiliou, A. G. (2007). The power and promise of "rewiring" the mitogen-activated protein kinase network in prostate cancer therapeutics. *Mol Cancer Ther* **6**, 811-819.

Parker, A. L., Waddington, S. N., Nicol, C. G., Shayakhmetov, D. M., Buckley, S. M., Denby, L., Kemball-Cook, G., Ni, S., Lieber, A., McVey, J. H., Nicklin, S. A. & Baker, A. H. (2006). Multiple vitamin K-dependent coagulation zymogens promote adenovirus-mediated gene delivery to hepatocytes. *Blood* **108**, 2554-2561.

Pattingre, S., Espert, L., Biard-Piechaczyk, M. & Codogno, P. (2008). Regulation of macroautophagy by mTOR and Beclin 1 complexes. *Biochimie* **90**, 313-323.

Pattingre, S., Tassa, A., Qu, X., Garuti, R., Liang, X. H., Mizushima, N., Packer, M., Schneider, M. D. & Levine, B. (2005). Bcl-2 antiapoptotic proteins inhibit Beclin 1-dependent autophagy. *Cell* **122**, 927-939.

Petiot, A., Ogier-Denis, E., Blommaart, E. F., Meijer, A. J. & Codogno, P. (2000). Distinct classes of phosphatidylinositol 3'-kinases are involved in signaling pathways that control macroautophagy in HT-29 cells. *J Biol Chem* **275**, 992-998.

Pong, R. C., Lai, Y. J., Chen, H., Okegawa, T., Frenkel, E., Sagalowsky, A. & Hsieh, J. T. (2003). Epigenetic regulation of coxsackie and adenovirus receptor (CAR) gene promoter in urogenital cancer cells. *Cancer Res* **63**, 8680-8686.

Pong, R. C., Roark, R., Ou, J. Y., Fan, J., Stanfield, J., Frenkel, E., Sagalowsky, A. & Hsieh, J. T. (2006). Mechanism of increased coxsackie and adenovirus receptor gene expression and adenovirus uptake by phytoestrogen and histone deacetylase inhibitor in human bladder cancer cells and the potential clinical application. *Cancer Res* **66**, 8822-8828.

Prins, G. S. & Korach, K. S. (2008). The role of estrogens and estrogen receptors in normal prostate growth and disease. *Steroids* **73**, 233-244.

Qu, X., Yu, J., Bhagat, G., Furuya, N., Hibshoosh, H., Troxel, A., Rosen, J., Eskelinen, E. L., Mizushima, N., Ohsumi, Y., Cattoretti, G. & Levine, B. (2003). Promotion of tumorigenesis by heterozygous disruption of the beclin 1 autophagy gene. *J Clin Invest* **112**, 1809-1820.

Raffo, A. J., Perlman, H., Chen, M. W., Day, M. L., Streitman, J. S. & Buttyan, R. (1995). Overexpression of bcl-2 protects prostate cancer cells from apoptosis in vitro and confers resistance to androgen depletion in vivo. *Cancer Res* **55**, 4438-4445.

Ramos, S. (2008). Cancer chemoprevention and chemotherapy: dietary polyphenols and signalling pathways. *Mol Nutr Food Res* **52**, 507-526.

Rauen, K. A., Sudilovsky, D., Le, J. L., Chew, K. L., Hann, B., Weinberg, V., Schmitt, L. D. & McCormick, F. (2002). Expression of the coxsackie adenovirus receptor in normal prostate and in primary and metastatic prostate carcinoma: potential relevance to gene therapy. *Cancer Res* **62**, 3812-3818.

Reid, T., Warren, R. & Kirn, D. (2002). Intravascular adenoviral agents in cancer patients: lessons from clinical trials. *Cancer Gene Ther* **9**, 979-986.

Research, W. C. R. F. A. I. f. C. (2007). Food, Nutrition, Physical Activity, and the Prevention of Cancer: a Global Perspective. Washington DC: World Cancer Research Fund / American Institute for Cancer Research.

Robert, A., Smadja-Lamere, N., Landry, M. C., Champagne, C., Petrie, R., Lamarche-Vane, N., Hosoya, H. & Lavoie, J. N. (2006). Adenovirus E4orf4 hijacks rho GTPase-dependent actin dynamics to kill cells: a role for endosome-associated actin assembly. *Mol Biol Cell* **17**, 3329-3344.

Rocchi, P., Beraldi, E., Ettinger, S., Fazli, L., Vessella, R. L., Nelson, C. & Gleave, M. (2005). Increased Hsp27 after androgen ablation facilitates androgen-independent progression in prostate cancer via signal transducers and activators of transcription 3-mediated suppression of apoptosis. *Cancer Res* **65**, 11083-11093.

Rosenberg Zand, R. S., Jenkins, D. J. & Diamandis, E. P. (2002). Flavonoids and steroid hormone-dependent cancers. *J Chromatogr B Analyt Technol Biomed Life Sci* **777**, 219-232.

Russell, W. C. (2009). Adenoviruses: update on structure and function. *J Gen Virol* **90**, 1-20.

Russo, G. L. (2007). Ins and outs of dietary phytochemicals in cancer chemoprevention. *Biochem Pharmacol* **74**, 533-544.

Sachs, M. D., Ramamurthy, M., Poel, H., Wickham, T. J., Lamfers, M., Gerritsen, W., Chowdhury, W., Li, Y., Schoenberg, M. P. & Rodriguez, R. (2004). Histone deacetylase inhibitors upregulate expression of the coxsackie adenovirus receptor (CAR) preferentially in bladder cancer cells. *Cancer Gene Ther* **11**, 477-486.

Saelens, X., Festjens, N., Parthoens, E., Vanoverberghe, I., Kalai, M., van Kuppeveld, F. & Vandenabeele, P. (2005). Protein synthesis persists during necrotic cell death. *J Cell Biol* **168**, 545-551.

Salti, G. I., Grewal, S., Mehta, R. R., Das Gupta, T. K., Boddie, A. W., Jr. & Constantinou, A. I. (2000). Genistein induces apoptosis and topoisomerase II-mediated DNA breakage in colon cancer cells. *Eur J Cancer* **36**, 796-802.

Sanchez-Prieto, R., Quintanilla, M., Cano, A., Leonart, M. L., Martin, P., Anaya, A. & Ramon y Cajal, S. (1996). Carcinoma cell lines become sensitive to DNA-damaging agents by the expression of the adenovirus E1A gene. *Oncogene* **13**, 1083-1092.

Scarlatti, F., Bauvy, C., Ventruti, A., Sala, G., Cluzeaud, F., Vandewalle, A., Ghidoni, R. & Codogno, P. (2004). Ceramide-mediated macroautophagy involves inhibition of protein kinase B and up-regulation of beclin 1. *J Biol Chem* **279**, 18384-18391.

Scarlatti, F., Granata, R., Meijer, A. J. & Codogno, P. (2009). Does autophagy have a license to kill mammalian cells? *Cell Death Differ* **16**, 12-20.

Scarlatti, F., Maffei, R., Beau, I., Codogno, P. & Ghidoni, R. (2008). Role of non-canonical Beclin 1-independent autophagy in cell death induced by resveratrol in human breast cancer cells. *Cell Death Differ* **15**, 1318-1329.

Seglen, P. O. & Gordon, P. B. (1982). 3-Methyladenine: specific inhibitor of autophagic/lysosomal protein degradation in isolated rat hepatocytes. *Proc Natl Acad Sci U S A* **79**, 1889-1892.

Sekulic, A., Hudson, C. C., Homme, J. L., Yin, P., Otterness, D. M., Karnitz, L. M. & Abraham, R. T. (2000). A direct linkage between the phosphoinositide 3-kinase-AKT signaling pathway and the mammalian target of rapamycin in mitogen-stimulated and transformed cells. *Cancer Res* **60**, 3504-3513.

Setchell, K. D., Brown, N. M. & Lydeking-Olsen, E. (2002). The clinical importance of the metabolite equol-a clue to the effectiveness of soy and its isoflavones. *J Nutr* **132**, 3577-3584.

Setchell, K. D., Clerici, C., Lephart, E. D., Cole, S. J., Heenan, C., Castellani, D., Wolfe, B. E., Nechemias-Zimmer, L., Brown, N. M., Lund, T. D., Handa, R. J. & Heubi, J. E. (2005). S-equol, a potent ligand for estrogen receptor beta, is the exclusive enantiomeric form of the soy isoflavone metabolite produced by human intestinal bacterial flora. *Am J Clin Nutr* **81**, 1072-1079.

Shah, R. B., Ghosh, D. & Elder, J. T. (2006). Epidermal growth factor receptor (ErbB1) expression in prostate cancer progression: correlation with androgen independence. *Prostate* **66**, 1437-1444.

Shand, R. L. & Gelmann, E. P. (2006). Molecular biology of prostate-cancer pathogenesis. *Curr Opin Urol* **16**, 123-131.

Shankar, S., Siddiqui, I. & Srivastava, R. K. (2007). Molecular mechanisms of resveratrol (3,4,5-trihydroxy-trans-stilbene) and its interaction with TNF-related apoptosis inducing ligand (TRAIL) in androgen-insensitive prostate cancer cells. *Mol Cell Biochem* **304**, 273-285.

Shenk, T. E. (2001). *Adenoviridae*: The Viruses and Their Replication. In *Fields Virology*, pp. 2265-2300. Edited by P. M. H. David M. Knipe. Philadelphia: Lippincott Williams & Wilkins.

Shoji-Kawata, S. & Levine, B. (2009). Autophagy, antiviral immunity, and viral countermeasures. *Biochim Biophys Acta*.

Short, J. J., Pereboev, A. V., Kawakami, Y., Vasu, C., Holterman, M. J. & Curiel, D. T. (2004). Adenovirus serotype 3 utilizes CD80 (B7.1) and CD86 (B7.2) as cellular attachment receptors. *Virology* **322**, 349-359.

Siddiqui, I. A., Adhami, V. M., Saleem, M. & Mukhtar, H. (2006). Beneficial effects of tea and its polyphenols against prostate cancer. *Mol Nutr Food Res* **50**, 130-143.

Siddiqui, I. A., Malik, A., Adhami, V. M., Asim, M., Hafeez, B. B., Sarfaraz, S. & Mukhtar, H. (2008). Green tea polyphenol EGCG sensitizes human prostate carcinoma LNCaP cells to TRAIL-mediated apoptosis and synergistically inhibits biomarkers associated with angiogenesis and metastasis. *Oncogene* **27**, 2055-2063.

Signorelli, P. & Ghidoni, R. (2005). Resveratrol as an anticancer nutrient: molecular basis, open questions and promises. *J Nutr Biochem* **16**, 449-466.

Sim, H. G. & Cheng, C. W. (2005). Changing demography of prostate cancer in Asia. *Eur J Cancer* **41**, 834-845.

Singletary, K. & Milner, J. (2008). Diet, autophagy, and cancer: a review. *Cancer Epidemiol Biomarkers Prev* **17**, 1596-1610.

Skjoth, I. H. & Issinger, O. G. (2006). Profiling of signaling molecules in four different human prostate carcinoma cell lines before and after induction of apoptosis. *Int J Oncol* **28**, 217-229.

Sonn, G. A., Aronson, W. & Litwin, M. S. (2005). Impact of diet on prostate cancer: a review. *Prostate Cancer Prostatic Dis* **8**, 304-310.

Srivastava, R. K., Chen, Q., Siddiqui, I., Sarva, K. & Shankar, S. (2007). Linkage of curcumin-induced cell cycle arrest and apoptosis by cyclin-dependent kinase inhibitor p21(/WAF1/CIP1). *Cell Cycle* **6**, 2953-2961.

Strunze, S., Trotman, L. C., Boucke, K. & Greber, U. F. (2005). Nuclear targeting of adenovirus type 2 requires CRM1-mediated nuclear export. *Mol Biol Cell* **16**, 2999-3009.

Subr, V., Kostka, L., Selby-Milic, T., Fisher, K., Ulbrich, K., Seymour, L. W. & Carlisle, R. C. (2009). Coating of adenovirus type 5 with polymers containing quaternary amines prevents binding to blood components. *J Control Release* **135**, 152-158.

Suomalainen, M., Nakano, M. Y., Boucke, K., Keller, S. & Greber, U. F. (2001). Adenovirus-activated PKA and p38/MAPK pathways boost microtubule-mediated nuclear targeting of virus. *Embo J* **20**, 1310-1319.

Surh, Y. J. (2003). Cancer chemoprevention with dietary phytochemicals. *Nat Rev Cancer* **3**, 768-780.

Suzuki, H., Sato, N., Watabe, Y., Masai, M., Seino, S. & Shimazaki, J. (1993). Androgen receptor gene mutations in human prostate cancer. *J Steroid Biochem Mol Biol* **46**, 759-765.

Takahashi, Y., Hursting, S. D., Perkins, S. N., Wang, T. C. & Wang, T. T. (2006). Genistein affects androgen-responsive genes through both androgen- and estrogen-induced signaling pathways. *Mol Carcinog* **45**, 18-25.

Talloczy, Z., Jiang, W., Virgin, H. W. t., Leib, D. A., Scheuner, D., Kaufman, R. J., Eskelinen, E. L. & Levine, B. (2002). Regulation of starvation- and virus-induced autophagy by the eIF2alpha kinase signaling pathway. *Proc Natl Acad Sci U S A* **99**, 190-195.

Talloczy, Z., Virgin, H. W. t. & Levine, B. (2006). PKR-dependent autophagic degradation of herpes simplex virus type 1. *Autophagy* **2**, 24-29.

Tamm, I., Wang, Y., Sausville, E., Scudiero, D. A., Vigna, N., Oltersdorf, T. & Reed, J. C. (1998). IAP-family protein survivin inhibits caspase activity and apoptosis induced by Fas (CD95), Bax, caspases, and anticancer drugs. *Cancer Res* **58**, 5315-5320.

Taplin, M. E., Bubley, G. J., Ko, Y. J., Small, E. J., Upton, M., Rajeshkumar, B. & Balk, S. P. (1999). Selection for androgen receptor mutations in prostate cancers treated with androgen antagonist. *Cancer Res* **59**, 2511-2515.

Taylor, R. C., Cullen, S. P. & Martin, S. J. (2008). Apoptosis: controlled demolition at the cellular level. *Nat Rev Mol Cell Biol* **9**, 231-241.

Thomasset, S. C., Berry, D. P., Garcea, G., Marczylo, T., Steward, W. P. & Gescher, A. J. (2007). Dietary polyphenolic phytochemicals--promising cancer chemopreventive agents in humans? A review of their clinical properties. *Int J Cancer* **120**, 451-458.

Tollefson, A. E., Scaria, A., Hermiston, T. W., Ryerse, J. S., Wold, L. J. & Wold, W. S. (1996). The adenovirus death protein (E3-11.6K) is required at very late stages of infection for efficient cell lysis and release of adenovirus from infected cells. *J Virol* **70**, 2296-2306.

Tomko, R. P., Xu, R. & Philipson, L. (1997). HCAR and MCAR: the human and mouse cellular receptors for subgroup C adenoviruses and group B coxsackieviruses. *Proc Natl Acad Sci U S A* **94**, 3352-3356.

Trincheri, N. F., Follo, C., Nicotra, G., Peracchio, C., Castino, R. & Isidoro, C. (2008). Resveratrol-induced apoptosis depends on the lipid kinase activity of Vps34 and on the formation of autophagolysosomes. *Carcinogenesis* **29**, 381-389.

Tso, C. L., McBride, W. H., Sun, J., Patel, B., Tsui, K. H., Paik, S. H., Gitlitz, B., Caliliw, R., van Ophoven, A., Wu, L., deKernion, J. & Belldegrun, A. (2000). Androgen deprivation induces selective outgrowth of aggressive hormone-refractory prostate cancer clones expressing distinct cellular and molecular properties not present in parental androgen-dependent cancer cells. *Cancer J* **6**, 220-233.

Tuve, S., Wang, H., Jacobs, J. D., Yumul, R. C., Smith, D. F. & Lieber, A. (2008). Role of cellular heparan sulfate proteoglycans in infection of human adenovirus serotype 3 and 35. *PLoS Pathog* **4**, e1000189.

Udenigwe, C. C., Ramprasath, V. R., Aluko, R. E. & Jones, P. J. (2008). Potential of resveratrol in anticancer and anti-inflammatory therapy. *Nutr Rev* **66**, 445-454.

Ulrich, S., Wolter, F. & Stein, J. M. (2005). Molecular mechanisms of the chemopreventive effects of resveratrol and its analogs in carcinogenesis. *Mol Nutr Food Res* **49**, 452-461.

van Bokhoven, A., Varella-Garcia, M., Korch, C., Johannes, W. U., Smith, E. E., Miller, H. L., Nordeen, S. K., Miller, G. J. & Lucia, M. S. (2003). Molecular characterization of human prostate carcinoma cell lines. *Prostate* **57**, 205-225.

Vandenabeele, P., Vanden Berghe, T. & Festjens, N. (2006). Caspase inhibitors promote alternative cell death pathways. *Sci STKE* **2006**, pe44.

Visakorpi, T., Hyytinen, E., Koivisto, P., Tanner, M., Keinanen, R., Palmberg, C., Palotie, A., Tammela, T., Isola, J. & Kallioniemi, O. P. (1995). In vivo amplification of the androgen receptor gene and progression of human prostate cancer. *Nat Genet* **9**, 401-406.

Waddington, S. N., McVey, J. H., Bhella, D., Parker, A. L., Barker, K., Atoda, H., Pink, R., Buckley, S. M., Greig, J. A., Denby, L., Custers, J., Morita, T., Francischetti, I. M., Monteiro, R. Q., Barouch, D. H., van Rooijen, N., Napoli, C., Havenga, M. J., Nicklin, S. A. & Baker, A. H. (2008). Adenovirus serotype 5 hexon mediates liver gene transfer. *Cell* **132**, 397-409.

Wang, R. H., Sengupta, K., Li, C., Kim, H. S., Cao, L., Xiao, C., Kim, S., Xu, X., Zheng, Y., Chilton, B., Jia, R., Zheng, Z. M., Appella, E., Wang, X. W., Ried, T. & Deng, C. X. (2008a). Impaired DNA damage response, genome instability, and tumorigenesis in SIRT1 mutant mice. *Cancer Cell* **14**, 312-323.

Wang, X., Clubbs, E. A. & Bomser, J. A. (2006). Genistein modulates prostate epithelial cell proliferation via estrogen- and extracellular signal-regulated kinase-dependent pathways. *J Nutr Biochem* **17**, 204-210.

Wang, Y., Mikhailova, M., Bose, S., Pan, C. X., deVere White, R. W. & Ghosh, P. M. (2008b). Regulation of androgen receptor transcriptional activity by rapamycin in prostate cancer cell proliferation and survival. *Oncogene* **27**, 7106-7117.

Webb, J. (1963). Effect of more than one inhibitor. In *Enzyme and Metabolic Inhibitors*, pp. 66-79, 488-512. New York: Academic Press.

Webber, M. M., Bello, D. & Quader, S. (1997). Immortalized and tumorigenic adult human prostatic epithelial cell lines: characteristics and applications Part 2. Tumorigenic cell lines. *Prostate* **30**, 58-64.

Weber, J. M., Ruzindana-Umunyana, A., Imbeault, L. & Sircar, S. (2003). Inhibition of adenovirus infection and adenain by green tea catechins. *Antiviral Res* **58**, 167-173.

White, E., Cipriani, R., Sabbatini, P. & Denton, A. (1991). Adenovirus E1B 19-kilodalton protein overcomes the cytotoxicity of E1A proteins. *J Virol* **65**, 2968-2978.

Wickham, T. J., Mathias, P., Cheresh, D. A. & Nemerow, G. R. (1993). Integrins alpha v beta 3 and alpha v beta 5 promote adenovirus internalization but not virus attachment. *Cell* **73**, 309-319.

Wiethoff, C. M., Wodrich, H., Gerace, L. & Nemerow, G. R. (2005). Adenovirus protein VI mediates membrane disruption following capsid disassembly. *J Virol* **79**, 1992-2000.

Wiseman, M. (2008). The second World Cancer Research Fund/American Institute for Cancer Research expert report. Food, nutrition, physical activity, and the prevention of cancer: a global perspective. *Proc Nutr Soc* **67**, 253-256.

Wold, W. S. M. (1998). *Adenovirus Methods and Protocols*. Totowa, NJ: Humana Press.

Wu, C. & Huang, J. (2006). PI3 kinase-AKT-mTOR pathway is essential for neuroendocrine differentiation of prostate cancer. *J Biol Chem*.

Wu, J. D., Haugk, K., Woodke, L., Nelson, P., Coleman, I. & Plymate, S. R. (2006). Interaction of IGF signaling and the androgen receptor in prostate cancer progression. *J Cell Biochem* **99**, 392-401.

Wu, L., Birle, D. C. & Tannock, I. F. (2005). Effects of the mammalian target of rapamycin inhibitor CCI-779 used alone or with chemotherapy on human prostate cancer cells and xenografts. *Cancer Res* **65**, 2825-2831.

Xi, Q., Cuesta, R. & Schneider, R. J. (2005). Regulation of translation by ribosome shunting through phosphotyrosine-dependent coupling of adenovirus protein 100k to viral mRNAs. *J Virol* **79**, 5676-5683.

Xia, Z. J., Chang, J. H., Zhang, L., Jiang, W. Q., Guan, Z. Z., Liu, J. W., Zhang, Y., Hu, X. H., Wu, G. H., Wang, H. Q., Chen, Z. C., Chen, J. C., Zhou, Q. H., Lu, J. W., Fan, Q. X., Huang, J. J. & Zheng, X. (2004). [Phase III randomized clinical trial of intratumoral injection of E1B gene-deleted adenovirus (H101) combined with cisplatin-based chemotherapy in treating squamous cell cancer of head and neck or esophagus.]. *Ai Zheng* **23**, 1666-1670.

Xu, Z., Tian, J., Smith, J. S. & Byrnes, A. P. (2008). Clearance of adenovirus by Kupffer cells is mediated by scavenger receptors, natural antibodies, and complement. *J Virol* **82**, 11705-11713.

Yamamoto, A., Tagawa, Y., Yoshimori, T., Moriyama, Y., Masaki, R. & Tashiro, Y. (1998). Bafilomycin A1 prevents maturation of autophagic vacuoles by inhibiting fusion between autophagosomes and lysosomes in rat hepatoma cell line, H-4-II-E cells. *Cell Struct Funct* **23**, 33-42.

Yang, C. S., Sang, S., Lambert, J. D., Hou, Z., Ju, J. & Lu, G. (2006). Possible mechanisms of the cancer-preventive activities of green tea. *Mol Nutr Food Res* **50**, 170-175.

Yokoyama, T., Iwado, E., Kondo, Y., Aoki, H., Hayashi, Y., Georgescu, M. M., Sawaya, R., Hess, K. R., Mills, G. B., Kawamura, H., Hashimoto, Y., Urata, Y., Fujiwara, T. & Kondo, S. (2008). Autophagy-inducing agents augment the antitumor effect of telerase-selve oncolytic adenovirus OBP-405 on glioblastoma cells. *Gene Ther* **15**, 1233-1239.

Yoon, A. R., Kim, J. H., Lee, Y. S., Kim, H., Yoo, J. Y., Sohn, J. H., Park, B. W. & Yun, C. O. (2006). Markedly enhanced cytolysis by E1B-19kD-deleted oncolytic adenovirus in combination with cisplatin. *Hum Gene Ther* **17**, 379-390.

Youn, H. S., Saitoh, S. I., Miyake, K. & Hwang, D. H. (2006). Inhibition of homodimerization of Toll-like receptor 4 by curcumin. *Biochem Pharmacol* **72**, 62-69.

Young, A. R., Narita, M., Ferreira, M., Kirschner, K., Sadaie, M., Darot, J. F., Tavare, S., Arakawa, S., Shimizu, S. & Watt, F. M. (2009). Autophagy mediates the mitotic senescence transition. *Genes Dev* **23**, 798-803.

Yu, D. C., Chen, Y., Dilley, J., Li, Y., Embry, M., Zhang, H., Nguyen, N., Amin, P., Oh, J. & Henderson, D. R. (2001). Antitumor synergy of CV787, a prostate cancer-specific adenovirus, and paclitaxel and docetaxel. *Cancer Res* **61**, 517-525.

Yu, D. C., Chen, Y., Seng, M., Dilley, J. & Henderson, D. R. (1999). The addition of adenovirus type 5 region E3 enables calydon virus 787 to eliminate distant prostate tumor xenografts. *Cancer Res* **59**, 4200-4203.

Yuan, J. P., Wang, J. H. & Liu, X. (2007). Metabolism of dietary soy isoflavones to equol by human intestinal microflora--implications for health. *Mol Nutr Food Res* **51**, 765-781.

Zacal, N. J., Francis, M. A. & Rainbow, A. J. (2005). Enhanced expression from the human cytomegalovirus immediate-early promoter in a non-replicating adenovirus encoded reporter gene following cellular exposure to chemical DNA damaging agents. *Biochem Biophys Res Commun* **332**, 441-449.

Zhang, Y. & Bergelson, J. M. (2005). Adenovirus receptors. *J Virol* **79**, 12125-12131.

Zhang, Y. & Schneider, R. J. (1994). Adenovirus inhibition of cell translation facilitates release of virus particles and enhances degradation of the cytokeratin network. *J Virol* **68**, 2544-2555.

Zhao, H., Granberg, F. & Pettersson, U. (2007). How adenovirus strives to control cellular gene expression. *Virology* **363**, 357-375.

Zheng, X., Rao, X. M., Gomez-Gutierrez, J. G., Hao, H., McMasters, K. M. & Zhou, H. S. (2008). Adenovirus E1B55K region is required to enhance cyclin E expression for efficient viral DNA replication. *J Virol* **82**, 3415-3427.